

**A Study of Frost Heave-related
Exposure Risk to Abandoned
Transmission Pipelines in
Cropland Areas of Southern
Canada**

**Stage 1 (Literature Search and
Numerical Modeling)**

Volume 2 (Appendices)



Prepared for:

Petroleum Technology Alliance
Canada
Pipeline Abandonment Research
Steering Committee
500 Fifth Avenue, S.W., Suite 400
Calgary, AB T2P 3L5


Prepared by:

Stantec Consulting Ltd.
70 Southgate Drive, Suite 1
Guelph, ON N1G 4P5
T: 519-836-6050
F: 519-836-2493

File No. 160960891
FRP No. PARSC 003
November 3, 2014

Sign-off Sheet

This document entitled 'A Study of Frost Heave-related Exposure Risk to Abandoned Transmission Pipelines in Cropland Areas of Southern Canada: Stage 1 (Literature Search and Numerical Modeling): Volume 2 (Appendices)' was prepared by Stantec Consulting Ltd. ("Stantec") for the account of Petroleum Technology Alliance Canada (the "Client"). Any reliance on this document by any third party is strictly prohibited. The material in it reflects Stantec's professional judgment in light of the scope, schedule and other limitations stated in the document and in the contract between Stantec and the Client. The opinions in the document are based on conditions and information existing at the time the document was published and do not take into account any subsequent changes. In preparing the document, Stantec did not verify information supplied to it by others. Any use which a third party makes of this document is the responsibility of such third party. Such third party agrees that Stantec shall not be responsible for costs or damages of any kind, if any, suffered by it or any other third party as a result of decisions made or actions taken based on this document.

Prepared by 
(signature)

Ray McBride, Ph.D., P.Ag.
Principal Investigator

Reviewed by 
(signature)

Steve Thurtell, M.Sc., P.Ag., CISEC
Project Manager



TABLE OF CONTENTS

A Study of Frost Heave-related Exposure Risk to Abandoned Transmission Pipelines in Cropland Areas of Southern Canada (Project: PARSC-003)

Stage 1 (Literature Search and Numerical Modeling)

Volume 2 (Appendices)

APPENDICES	<u>Pg.</u>
Appendix A ('Segregation Potential' and 'Heave Index' Concepts).....	1
<hr style="border-top: 1px dashed black;"/>	
● LitRev1 (Numerical Models of Frost Heaving in Soils)	
Appendix B (Narrative Paper on Frost Heave Models).....	5
Appendix C (Annotated Bibliography on Frost Heave Models).....	26
● LitRev2	
Appendix D (Frost Penetration Depth in Soils).....	55
● LitRev3	
Appendix E (Pipeline Depth).....	72
● LitRev4	
Appendix F (Soil Structure and Strength of Frozen Soils).....	82
● LitRev5	
Appendix G (Water and Wind Erosion within Transmission Pipeline ROWs).....	105
● LitRev6	
Appendix H (Update DNV [2010] Report Literature Review on Frost Heaving).....	115
<hr style="border-top: 1px dashed black;"/>	
● NumMod (Numerical Modeling)	
Appendix I (Programming Code for the <i>Konrad_SP1.0</i> Frost Heave Model [Mathcad version]).....	120
Appendix J (Example Output from the <i>Konrad_SP1.0</i> Frost Heave Model).....	143
<hr style="border-top: 1px dashed black;"/>	
● PTFDev (Pedotransfer Function Development)	
Appendix K (Estimation of the Consistency [Atterberg] Limits of Southern Ontario Soils).....	149
Appendix L (Estimation of the Specific Surface Area of Soils).....	156
Appendix M (Estimation of the Compression Index of Southern Ontario Soils).....	164
Appendix N (Estimation of the Standard Proctor Density Test Indices of Southern Ontario Soils).....	171
Appendix O (Five Municipality Soil Data Set for Southern Ontario).....	180
Appendix P ($d_{50[FF]}$ soil particle-size distribution parameter).....	188
<hr style="border-top: 1px dashed black;"/>	
Appendix Q (Relationships between Internal Soil Drainage Class and Seasonal Groundwater Table Depth).....	196
Appendix R (Soil Landscapes of Canada [SLC3.2]).....	209
Appendix S (Variation of Regional Geoclimatic Conditions across Southern Canada).....	218
Appendix T (Pipeline Segments Abandoned-in-Place [Variable Diameter & Length])..	225

Acknowledgments

Stantec Consulting Ltd. would like to thank Petroleum Technology Alliance Canada (PTAC) for providing funding for this study, as well as the Pipeline Abandonment Research Steering Committee (PARSC) for their guidance during the preparation of this report.

Abbreviations

The entries in each of the following six abbreviation lists are arranged in alphabetical order

1. Terms / phrases / acronyms

AEI	agri-environmental indicator
AEIs	agri-environmental indicators
A/G	above-ground
CESI	Canadian Environmental Sustainability Indicators
CLI	Canada Land Inventory
CMP	component tables
CPESC	Certified Professional in Erosion and Sediment Control
DBMS	data base management system
DOC	depth of (soil) cover
EDP	excavation damage prevention
ELC	Ecological Land Classification
FDD	freezing degree-day
FDDs	freezing degree-days
FI	freezing index
GDD	growing degree-day
GDDs	growing degree-days
GIS	geographic information system
GPS	global positioning system
GWT	groundwater table
HI	heave index
n	number of observations
NAHARP	National Agri-Environmental Health Analysis and Reporting Program
PAT	polygon attribute tables
PTF	pedotransfer function
PTFs	pedotransfer functions
r (or R)	coefficient of simple (or multiple) correlation
r ² (or R ²)	coefficient of simple (or multiple) determination
RMSE	root mean square error
ROW	right-of-way
ROWs	rights-of-way
s.e.e.	standard error of estimate
SLT	soil layer tables
SNT	soil name tables
SP	segregation potential
TDD	thawing degree-day
TDDs	thawing degree-days
U/G	under-ground
1D	one-dimensional
2D	two-dimensional

2. Soil property (and other) variables

BET	Brunauer, Emmett and Teller
C _c	compression index
d ₅₀ (FF)	average size of the fines fraction
D _b	dry bulk density
D _p	particle density
EGME	ethylene glycol monomethyl ether
L	length (when expressing dimensions)

K	hydraulic conductivity of soil
MDD	maximum dry density
NCL	normal consolidation line
OWC	optimum water content
P	maximum depth of frost penetration
PI	plasticity index
SOC	soil organic carbon content
SOM	soil organic matter content
SSA	specific surface area
t	time (when expressing dimensions)
T	temperature (when expressing dimensions)
w	gravimetric soil water content
w _{wp}	gravimetric soil water content at the permanent wilting point
w _L	liquid limit
w _P	plastic limit
σ _c '	preconsolidation stress

3. Computer-based systems

CanSIS	Canada Soil Information System
CSV	'comma- (or character-) separated values' file type
<i>Groenevelt_HI1.0</i>	Groenevelt & Grant (2013) <u>H</u> eave <u>I</u> ndex model (version 1.0)
HYDRUS 2D	soil heat and water flux model (two-dimensional)
<i>Konrad_SP1.0</i>	Konrad (1999; 2005) <u>S</u> egregation <u>P</u> otential model (version 1.0)
RUSLE	Revised Universal Soil Loss Equation
RUSLE2	Revised Universal Soil Loss Equation (version 2)
SHAW 1D	<u>S</u> imultaneous <u>H</u> eat <u>a</u> nd <u>W</u> ater model (one-dimensional)
SLC	Soil Landscapes of Canada
SLC1.0	Soil Landscapes of Canada (version 1.0)
SLC3.2	Soil Landscapes of Canada (version 3.2)
SOIL	Soil water and heat model
USLE	Universal Soil Loss Equation
WEPS	Wind Erosion Prediction System

4. Reference list abbreviations

AAFC	Agriculture and Agri-Food Canada
ALA	American Lifelines Alliance
ASCE	American Society of Civil Engineers
ASME	American Society of Mechanical Engineers
ASTM	American Society for Testing and Materials
CEPA	Canadian Energy Pipeline Association
DNV	Det Norske Veritas
IRWA	International Right of Way Association
MOT	Ontario Ministry of Transportation
MTC	Ontario Ministry of Transportation and Communications
NEB	National Energy Board
OCSRE	Ontario Centre for Soil Resource Evaluation
OEB	Ontario Energy Board
OIP	Ontario Institute of Pedology
OMAF	Ontario Ministry of Agriculture and Food
OMAFRA	Ontario Ministry of Agriculture, Food and Rural Affairs
PARSC	Pipeline Abandonment Research Steering Committee
PASC	Pipeline Abandonment Steering Committee

USDA United States Department of Agriculture
USDA-ARS United States Department of Agriculture - Agricultural Research Services

5. Canadian provinces and territories

AB Alberta
BC British Columbia
MB Manitoba
NB New Brunswick
NL Newfoundland/Labrador
NS Nova Scotia
NT Northwest Territories
NU Nunavut
ON Ontario
PE Prince Edward Island
QC Quebec
SK Saskatchewan
YT Yukon Territories

6. U.S. states

AL	Alabama	MT	Montana
AK	Alaska	NE	Nebraska
AZ	Arizona	NV	Nevada
AR	Arkansas	NH	New Hampshire
CA	California	NJ	New Jersey
CO	Colorado	NM	New Mexico
CT	Connecticut	NY	New York
DE	Delaware	NC	North Carolina
FL	Florida	ND	North Dakota
GA	Georgia	OH	Ohio
HI	Hawaii	OK	Oklahoma
ID	Idaho	OR	Oregon
IL	Illinois	PA	Pennsylvania
IN	Indiana	RI	Rhode Island
IA	Iowa	SC	South Carolina
KS	Kansas	SD	South Dakota
KY	Kentucky	TN	Tennessee
LA	Louisiana	TX	Texas
ME	Maine	UT	Utah
MD	Maryland	VT	Vermont
MA	Massachusetts	VA	Virginia
MI	Michigan	WA	Washington
MN	Minnesota	WV	West Virginia
MS	Mississippi	WI	Wisconsin
MO	Missouri	WY	Wyoming

APPENDIX A

'Segregation Potential' and 'Heave Index' Concepts



'Segregation Potential' and 'Heave Index' Concepts

1. Segregation Potential (SP)

The modeling of frost heave-induced interactions between buried pipelines and the surrounding soil is a complex, time-dependent thermo-hydro-mechanical process (Hawladar *et al.*, 2006; Henry, 2000; O'Neill, 1983; Yang *et al.*, 2006). Existing published models of 'secondary' frost heave range from i) process-based thermodynamic simulation models (e.g., Selvadurai *et al.*, 1999), to ii) more simplified semi-analytical models (e.g., Hawladar *et al.*, 2006), to iii) even more practical empirical models based on laboratory and/or field observations (e.g., Konrad, 1999). The information/data requirements of process-based simulation models are much greater than for simpler empirical models (e.g., soil thermal properties vs. soil test index properties, respectively). The use of finite difference or finite element analysis in 2-dimensional space also adds to the computational complexity of simulation models.

Over the last 30 years, the 'segregation potential' (SP) concept introduced by Konrad and Morgenstern (1983) has gained wide acceptance among cold region design engineers for estimating the susceptibility of soils to frost heave. The SP parameter can be determined from laboratory step-freezing tests (Konrad, 1993) or from field observations, but more recently it has been shown that reliable empirical relationships exist between the SP parameter and basic geotechnical soil index properties (Fig. A-1). Indeed, Konrad (1999) argues that the determination of the SP parameter from laboratory freezing tests or field observations may be too costly to consider as part of the design approach for linear facilities such as pipelines. Once the SP parameter has been determined, it is possible to estimate the frost heave rate (Fig. A-2).

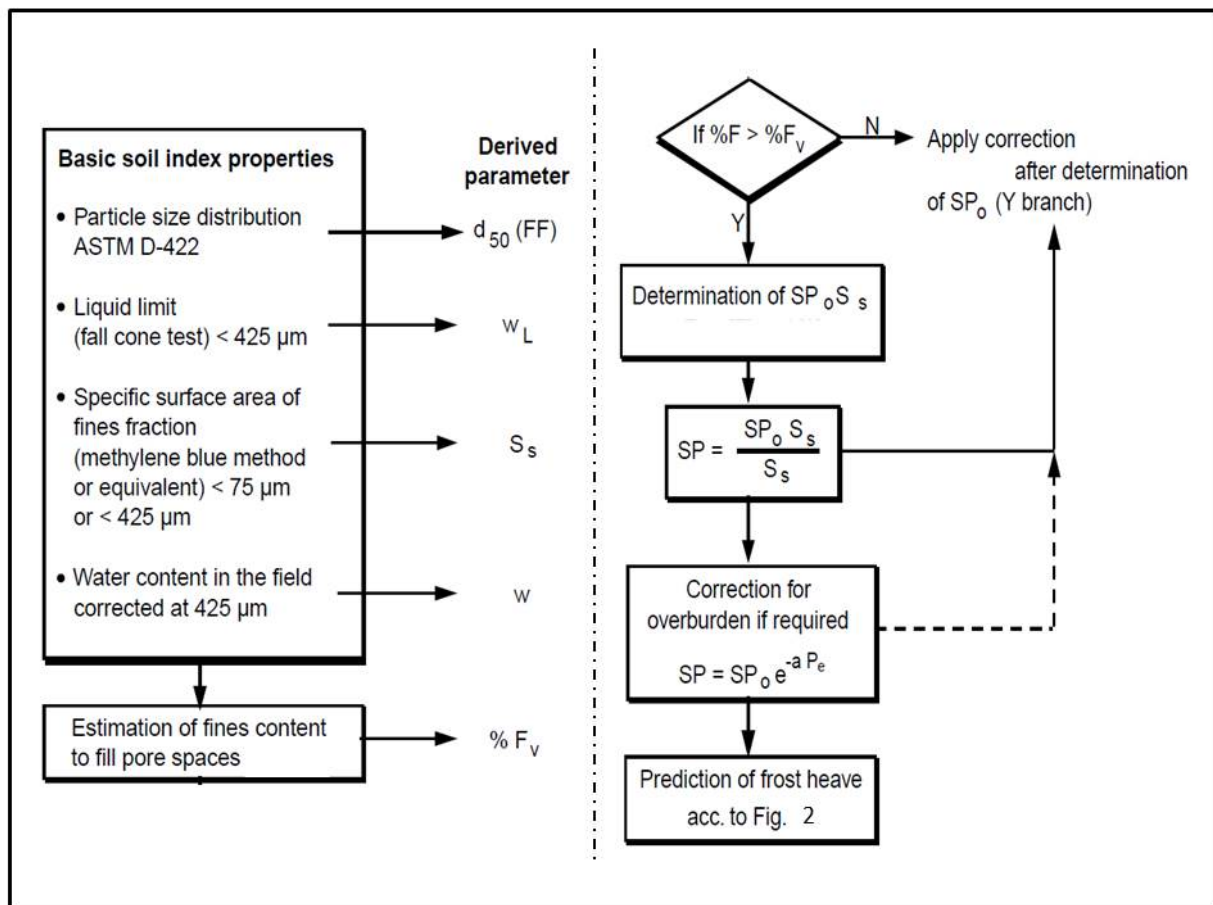


Figure A-1. Flow chart of methodology for frost susceptibility assessment. (after Konrad, 1999).

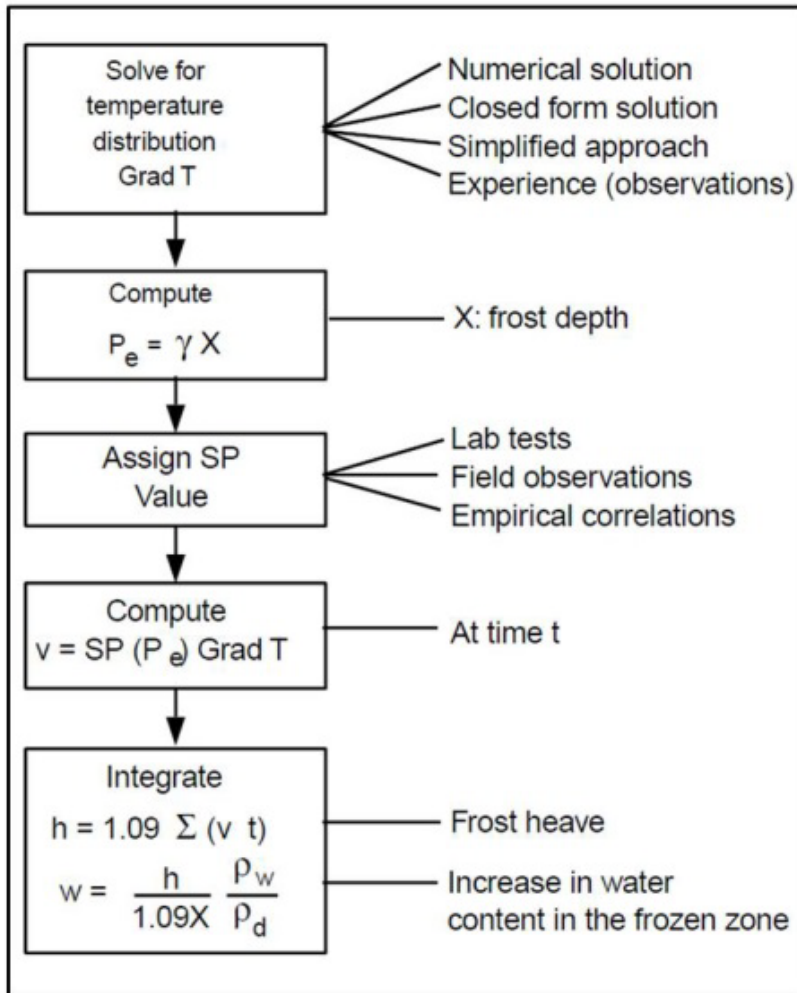


Figure A-2. Flow chart of methodology for frost heave estimation. (after Konrad, 1999).

Konrad published a subsequent paper in 2005 that extended the concepts put forth in Konrad (1999). Essentially, Konrad (2005) presents 'correction' algorithms that allow the original 'test index' approach to SP estimation to be extended to soils where the clay fraction is made up dominantly of primary minerals ('rock powder') rather than secondary minerals (phyllosilicates). Konrad (2005) is aimed at engineers involved in building road beds out of crushed aggregate where there may be a significant <2 μm component (rock powder) in the particle-size distribution. There are no known natural soils in Canada that have large amounts of rock powder in the clay fraction.

2. Heave Index (HI)

A new unifying theory for the process of heave in freezing soils has recently emerged (Groenevelt & Grant, 2013), and through the re-examination of previous work (including the SP parameter), a new 'heave index' (HI) was devised. Even though the dimensions ($L^2 t^{-1} T^{-1}$) and units ($mm^2 s^{-1} ^\circ C^{-1}$, or $m^2 s^{-1} K^{-1}$) for the SP and HI parameters are the same, the physical meaning of each is explained somewhat differently by the authors. The SP parameter is described as the 'ratio of the water intake flux to the temperature gradient' across the frozen fringe (Konrad & Morgenstern, 1983). Similarly, the equation defining the HI parameter is described as containing two terms as follows (Groenevelt & Grant, 2013):

- i) one representing the heat of fusion, which is relatively constant
- ii) one obtained by substituting the Darcy equation, which suggests that the hydraulic conductivity (saturated or unsaturated) of the unfrozen soil (beneath the frozen fringe) primarily determines soil susceptibility to frost heave

Further, the temperature gradient is determined over the entire depth range from the soil surface to the 0°C isotherm when calculating the HI parameter (unlike the SP parameter).

3. Summary (Appendix A)

In the field of frost heave estimation, the SP parameter is 'time-tested and proven', while the much newer HI parameter is derived from sound thermodynamic principles but is largely untested. It is interesting that the SP and HI parameters were arrived at independently from very different perspectives on the frost heave process. Nevertheless, both parameters have essentially the same physical meaning (i.e., the absolute value of the ratio of the Darcy [water] flux and the temperature gradient). It is for these reasons that this study attempts to use elements of both the Konrad (1999; 2005) and Groenevelt & Grant (2013) approaches in achieving the overall study goal and research objectives 2 and 3 (see Section 3).

References (Appendix A)

Groenevelt, P.H. and C.D. Grant. 2013. Heave and heaving pressure in freezing soils: A unifying theory. *Vadose Zone J.* 12(1). 11 pp.

Hawlder, B.C., V. Morgan and J.I. Clark. 2006. Modelling of pipeline under differential frost heave considering post-peak reduction of uplift resistance in frozen soil. *Can. Geotech. J.* 43:282-293.

Henry, K.S. 2000. A review of the thermodynamics of frost heave. Technical Report, Engineer Research and Development Centre, Hanover, NH (CRREL). 26 pp.

Konrad, J.-M. 1993. Frost heave potential. p. 797-806. *In* M.R. Carter (ed.) *Soil Sampling and Methods of Analysis*. Canadian Society of Soil Science. CRC Press, Lewis Publishers, Boca Raton, FL.

Konrad, J.-M. 1999. Frost susceptibility related to soil index properties. *Can. Geotech. J.* 36:403-417.

Konrad, J.-M. 2005. Estimation of the segregation potential of fine-grained soils using the frost heave response of two reference soils. *Can. Geotech. J.* 42:38-50.

Konrad, J.-M. and N.R. Morgenstern. 1983. Frost susceptibility of soils in terms of their segregation potential. p. 660-665. *In Proc. 4th Int'l. Conf. on Permafrost*, Fairbanks, AK. National Academy Press, Washington, DC.

O'Neill, K. 1983. The physics of mathematical frost heave models: A review. *Cold Regions Sci. and Tech.* 6(3):275-291.

Selvadurai, A.P.S., J. Hu and I. Konuk. 1999. Computational modeling of frost heave induced soil-pipeline interaction: I. Modelling of frost heave. *Cold Regions Sci. and Tech.* 29(3):215-228.

Yang, P., J. Ke, J.G. Wang, Y.K. Chow and F. Zhu. 2006. Numerical simulation of frost heave with coupled water freezing, temperature and stress fields in tunnel excavation. *Computers and Geotechnics* 33(6-7):330-340.

APPENDIX B

Narrative Paper on Frost Heave Models



Narrative Paper on Frost Heave Models

1. Preface

This narrative paper presents an overview of the published literature on processes that occur in frozen and freezing soils. For example, it is known that the two most essential driving forces leading to heave and heaving pressures in soils are i) the water intake rate, or the upward Darcy flux, and ii) the heat extraction rate at the soil surface. This narrative paper goes on i) to review the divergent 'schools of thought' among research groups, and ii) to reconcile the different approaches to the study of frost heave that exist in the science and engineering fields.

2. Overview of key mechanical aspects of frozen and freezing soils

2.1 Ice and ice pressure in soils

Ice exists in frozen soil in different forms and formations. There may be ice lenses and solid chunks of ice in plate-like form. There may be pore ice, brittle conglomerations of crystalline ice, ice needles and separate crystals of ice. During dynamic processes in field soils, the ice phase behaves neither as a solid, nor as a liquid. As for its mobility, it behaves like a very viscous quasi-liquid. As for its bearing strength, it behaves like an unstable and unreliable solid, somewhat like wet clay. Differences in temperature and liquid pressure (over time and space) cause H₂O molecules to change from the liquid to the solid phase and vice versa. Heat extraction causes local H₂O molecules to turn to ice, a process that is often accompanied by an increase in the local mechanical ice pressure. However, ice tries to avoid being under pressure. Hence, if there is an opportunity for the recently formed ice to relocate to a more favourable position (e.g., in a large pore or in an air-filled crack), it will migrate there by first turning to liquid, then moving in the liquid phase and subsequently refreezing (a process called 'regelation'). Even ice lenses can relocate themselves or grow or shrink by the process of regelation.

Ice lenses themselves do not always consist of solid ice. Because of their columnar structure (Volger, 1854), the spaces between the columns probably contain liquid water, which makes the ice lens permeable to liquid water. Taber (1929) writes: "Excessive heaving, in the laboratory, is always accompanied by the introduction of additional water and the segregation of some water to form masses or layers of more or less pure ice. Such ice, while usually solid and transparent, has a satiny luster and fibrous structure because of the orientation of the tiny ice prisms normal to the cooling surface." Therefore, on a micro-scale (on the grain or crystal scale [mm²]), the mechanical ice pressure has little meaning for the prediction of frost heave. On a meso-scale (Darcy-scale [cm²]), the equilibrium ice pressure (p_i) should be measurable just as the equilibrium liquid pressure (p_l) is measurable with a tensiometer-like instrument suitable for sub-zero (°C) conditions. Just as the Darcy liquid flux is driven by the gradient of the equilibrium liquid pressure, so is the Darcy-scale ice flux driven by the gradient of the equilibrium ice pressure. However, this equilibrium ice pressure also has little predictive power with respect to the process of heaving. Even if the Darcy-scale ice pressure is proper for a representative volume element in the frozen soil, i) non-homogeneity (in particular the presence of macro-pores or cracks) in the vicinity of the volume element, plus ii) dissipation of the ice pressure by regelation, will make the equilibrium ice pressure a poor predictor of the process of heaving. On a macro-scale (m²), the regelation process is probably too slow to undermine the predictive power of the equilibrium ice pressure. Thus, when dealing with the "heaving pressure", we will think of the force on a large enough unit area (m²), so that the regelation effect along the edges of the area is negligible.

2.2 The heaving pressure

Although heave can occur in non-vertical directions, for the present purpose we define the heaving pressure as the minimum, downward, vertical force per unit horizontal area, required to prevent upward movement, at the soil surface, of soil or ice. The unit horizontal area must be quite large (m²), such that regelation effects around the edges are negligible. The tendency for

upward movement is caused by the upward movement of liquid water in the underlying unfrozen soil towards the frozen fringe and the ice lenses above the frozen fringe. The supply of liquid water is usually from a groundwater table or any source of free water in the proximity where $p_i = 0$. The source of free water cannot be too deep or too far away. If that is the case, the upward liquid flux from the groundwater table will be too small or the supply of the unsaturated zone below the frozen fringe will be too small to cause a heaving pressure. Taber (1991a, pg.19) used loads of 6 kPa and 16 kPa with considerable amounts of heaving observed. Later (pg. 21) he writes: "The determination of the maximum force that may be exerted by growing ice crystals is an interesting but difficult problem. The clay, containing 20% water as it came from the mine, had a crushing strength of 200 lb/in² ... Therefore, the maximum pressure developed by growing ice crystals in these experiments must have been well over 1400 kPa." Such a pressure could lift a 70-m tall concrete building. Later (pg. 25) Taber writes: "The maximum pressure that may be developed as a direct result of ice segregation in the materials used in these experiments is probably not much above 1500 kPa. This limit is not due to the inability of ice crystals to grow under higher pressure, but to the failure of the water supply when the tensile strength of the water is exceeded. Water under such high tensile strength is superheated, even below 0°C, and the formation of vapor would immediately interrupt the supply."

2.3 The rate of heat extraction

Heat extraction at the soil surface and its rate dictate the processes of soil freezing, water migration, regelation and the Darcy flux in the surrounding unfrozen soil. Heat extraction at the soil surface causes temperature gradients in the frozen soil and in the frozen fringe. There will also be temperature gradients in the unfrozen soil below the frozen fringe, but those gradients are mostly irrelevant with respect to the process of frost heave. The temperature gradients in the frozen zone and the frozen fringe are determined by the most favourable locations where heat can be "created". Most of the heat extracted from the soil surface comes from the heat "created" by the freezing of liquid water. The heat of fusion (freezing) is large in comparison to the heat capacity of the soil and the existing ice. The location or locations where the transition from liquid water to ice occurs is largely dependent on the rate of heat extraction. When the heat extraction rate is small, the heat "creation" will occur at the bottom of an existing ice lens. However, when the heat extraction rate is so large that not enough heat can be "created" at the surface of an existing ice lens, because the Darcy flux is too small to supply enough water to the surface of the ice lens for freezing, a new ice lens will form at greater depth. Within the frozen fringe, it is the hydraulic conductivity of the frozen fringe which dictates where the water will freeze. This, in turn, dictates the temperature gradients in the frozen fringe.

During heat extraction, there is a constant interaction between the heat fluxes and the regelation fluxes in the frozen zone and the frozen fringe, both influenced by the constantly changing heat conductivities of the two zones. When the heat extraction rate is quite small, the soil tries to deliver the heat at a location as close to the soil surface as possible. The upward Darcy flux, which is also relatively small, will try to deliver liquid water to a point as close to the soil surface as possible. However, the presence of an already existing ice lens will block the Darcy flux (i.e., make the hydraulic conductivity very low, certainly in comparison to the hydraulic conductivity of the frozen fringe). Thus, the upward moving liquid water will freeze at the bottom of the deepest ice lens and that lens will get thicker. A quote from Taber (1991a, pg.17): "The formation of segregated ice layers during the freezing of soils is favored by a very slow lowering of the freezing isotherm; therefore, the most favorable places for the development of ice layers are close to the surface and near the lower limit of frost penetration. Needle ice, or frost columns, develop at the surface of moist, clayey soils when the temperature of the ground immediately below the surface remains above freezing, while the air temperature is below freezing. They do not form when previously chilled soils are rapidly frozen during a sudden drop in temperature." There is another reason why ice tends to sit above the soil surface: ice tries to

avoid having to carry a load, even if the load is very small. So, it tries to creep from under the soil surface to above it. The reason why this above surface ice (needles) can only be observed early in the morning is that the above surface ice easily and quickly sublimates.

2.4 The Darcy flux

The Darcy flux, driven by the temperature gradient, is the major contributor to frost heave. When there is a constant groundwater table, at not too great a depth below the frozen fringe, a sustained Darcy flux can cause considerable amounts of frost heave. When the soil between the frozen zone and the groundwater table is saturated, the classical law of Darcy relates the water flux to the driving force via the saturated hydraulic conductivity. In many cases, however, the soil below the frozen fringe is unsaturated. Darcy's Law then relates the flux to the driving force via a weighted integrated unsaturated hydraulic conductivity function. When there is no groundwater table at all, the soil below the frozen fringe dries out and the role of the unsaturated hydraulic conductivity function becomes more complicated. In the absence of a groundwater table, the frozen zone will pull up water from the unfrozen soil below the frozen fringe. Eventually the upward movement of water will come to a halt.

In Table B-1 below (Table 1 in Taber [1991a]), Taber (1991a) presents data for seven identical columns filled with powdered clay, brought to different initial, homogeneous water contents. The columns were subjected to the same rate of heat extraction, and the tops and bottoms of the columns were sealed. The columns were frozen from the top. After a certain time of freezing, the water contents of the unfrozen soil at the bottom of the columns were measured.

Table B-1. Gravimetric soil water content (kg kg^{-1}) at the bottom of Each of seven soil columns, and the difference between water contents before and after freezing. (after Taber, 1991a).

Cylindrical Column No.	Gravimetric water content of unfrozen soil at the bottom of each cylinder		Difference (before - after)
	Before freezing	After freezing	
1	0.290	0.208	0.082
2	0.258	0.199	0.059
3	0.242	0.183	0.059
4	0.232	0.183	0.049
5	0.199	0.168	0.031
6	0.168	0.123	0.045
7	0.095	0.077	0.018

Ice lenses formed in Columns 1-4, but not in Columns 5-7. Thus, in absolute terms, the upward Darcy flux is larger in columns of higher initial water content. The driving force in Darcy's equation is the same for all columns, but the unsaturated hydraulic conductivity is much smaller for lower initial water contents. If the strongly water content-dependent hydraulic conductivity function were the only factor in determining the upward delivery from the unfrozen zone to the frozen zone, the differences listed in Table B-1 would drop off much faster. However, the wetter columns have, at the top, more water available for freezing. Therefore, at a constant rate of heat extraction, in order to satisfy the demand for heat, the drier columns will start the upward suction from the unfrozen soil much earlier than the wetter columns.

3. 'Schools of thought' on frost heave

3.1 Preface

After the pioneering work by Taber (1929, 1930) and Beskow (1935), groups of researchers have studied the intricacies of the processes occurring in frozen and freezing soils (Fig. B-1). These

groups can be thought of as “Schools”, which have used different concepts and different methods of analysis. In this narrative paper, we will focus on two of these Schools and try to reconcile their different approaches. The first is the School of Dr. Duwayne (D.M.) Anderson of the Cold Regions Research and Engineering Laboratory (CRREL), located in Hanover, NH. The second is the School of Dr. Bob (R.D.) Miller, Professor of Soil Physics at Cornell University, Ithaca, NY. The reader is referred to the following references (Beskow, 1991a, 1991b; Black, 1991; Black & Hardenberg, 1991; Taber, 1991a, 1991b) for further historical and background information.

In the Anderson School, we find the names of Morgenstern and Konrad (e.g., Anderson & Morgenstern, 1973; Konrad & Morgenstern, 1980, 1981, 1982; Konrad, 1987, 1993, 1999, 2005).

In the Miller School, we find the names of Koopmans, Hoekstra, Loch, Kay, Perfect, Van Loon and Groenevelt (e.g., Miller *et al.*, 1960; Koopmans & Miller, 1966; Miller, 1972, 1973, 1978; Hoekstra, 1966; Hoekstra & Miller, 1967; Loch & Miller, 1975; Loch & Kay, 1978; Groenevelt & Kay, 1980; Kay & Groenevelt, 1974; Kay & Perfect, 1988; Perfect *et al.*, 1990, 1991; Perfect & Kay, 1993; Van Loon, 1991; Van Loon *et al.*, 1991).



Figure B-1. Frost heave on roadways in a) Montana, USA, and b) Norway.

In this narrative paper, the attempt at reconciliation between the two 'schools of thought' will be made by focussing on one publication from each of the two Schools:

From the **Anderson School**:

Konrad, J.-M. 1993. Frost Heave Potential (Chapter 74). p. 797-806. In M.R. Carter (ed.). *Soil Sampling and Methods of Analysis*. Canadian Society of Soil Science. Lewis Publishers. Boca Raton, FL.

From the **Miller School**:

Van Loon, W.K.P. 1991. *Heat and Mass Transfer in Frozen Porous Media*. Ph.D. Thesis. University of Wageningen, The Netherlands.

First, a broad outline of the content of these two works will be presented, focussing on the concepts, the methods of analysis, and some of the results. While doing so, we will provide some **comments** and **notes**, relevant to the development of a 'unifying theory' on the thermodynamic process of frost heave in soil (Groenevelt & Grant, 2013).

3.2 The Anderson School: Konrad (1993)

Clearly, Dr. J.-M. Konrad belongs to the Anderson School. Konrad (1993) starts off with the definition of the *Segregation Potential (SP)*:

$$SP = v(\text{Grad } T_f)^{-1} \quad (\text{Equation 74.1 in Konrad [1993]}) \quad \text{Eqn. B-1}$$

where: SP = Segregation Potential ($\text{m}^2 \text{s}^{-1} \text{K}^{-1}$)

v = upward Darcy flux of liquid water from the groundwater table to the frost front [m^3 (water) m^{-2} (bulk space) s^{-1}]

(Grad T_f) = temperature gradient in the frozen fringe (K)

Clearly, there was an unfortunate printing error made in this equation (i.e., '-1' should read '-1'). The definition was meant to be:

$$SP \equiv v(\text{Grad } T_f)^{-1} \quad \text{Eqn. B-2}$$

Based on this concept, "the chapter describes a simple laboratory frost heave test referred to as step freezing, which provides the basic frost heave parameter of a given soil" (Konrad, 1993, pg. 797):

Comments on the definition of the "Segregation Potential" in Konrad (1993):

1. In science, the word "potential" is usually reserved for "energy per unit mass" [$\text{m}^2 \text{s}^{-2}$]. Obviously, in the definition of "Segregation Potential", the word "potential" has the more general meaning of "capability" or "tendency". For soil physicists, the introduction of a "Segregation Potential" suggests that there is an additional component potential of the water in frozen soils. This is not so. A similar situation occurred when Dr. John Philip (Philip, 1969) introduced the "Overburden Potential" (cf. Grant *et al.*, 2002, pg. 98). Philip (1969) suggested that there is an additional component potential of the water in swelling soils. That too is not so, but his suggestion caused much confusion.

2. The Segregation Potential is a parameter meant to quantify the heaving characteristics of freezing soils while in a transient thermal state, with the frost front advancing into the unfrozen soil below. It is preferable that this parameter has a positive value. In Fig. B-2 (or Fig. 74.4 in Konrad [1993]), positive values are indeed reported. If the Darcy flux is taken to be positive (upwards), then the vertical co-ordinate (x) is positive upwards. At the same time, (Grad T_f) is then negative. This causes the parameter SP to have a negative value.

The theory starts with the formulation of the total heave rate:

$$dh/dt = 1.09 v + 0.09 n dX/dt \quad (\text{Equation 74.4 in Konrad [1993]}) \quad \text{Eqn. B-3}$$

where: h = height of the soil surface above a reference level

v = Darcy flux [m^3 (water) m^{-2} (bulk space) s^{-1}]

dX/dt = "the rate of frost front advance"

n = "the porosity of the unfrozen soil, reduced to account for the percentage of *in situ* pore water that will not freeze"

Note: It is not unambiguously clear what 'X' is. Later in Konrad (1993), it is identified as "the frozen soil thickness $X(t)$ "

Comment: The term ' $1.09 v$ ' represents the heave rate caused by the transformation of all of the imported water by means of the Darcy flux, but this is only so when all the imported water ends up in an air-free environment. The term ' $0.09 n dX/dt$ ' is troublesome. It is meant to represent the expansion of water in the frozen fringe upon freezing. This is only correct when the frozen fringe is constantly air-free (saturated). Most field soils drain during the period of freezing, whether a groundwater table is present or not. Thus the soil below the frozen fringe contains air and the 9% expansion of the water that freezes can easily be accommodated in the air space and will therefore not contribute to frost heave. When there is no source of free water (e.g., groundwater table is very deep; no lateral water flow), the freezing of (unsaturated) soils usually exhibits very little frost heave.

Konrad (1993) subsequently describes the laboratory equipment and procedure for the determination of the Segregation Potential parameter by the step freezing test. Some of the data presented in Fig. B-2 (i.e., or Fig. 74.4 in Konrad [1993]) will be used in the attempt to reconcile Konrad (1993) with Van Loon (1991) later in this narrative paper.

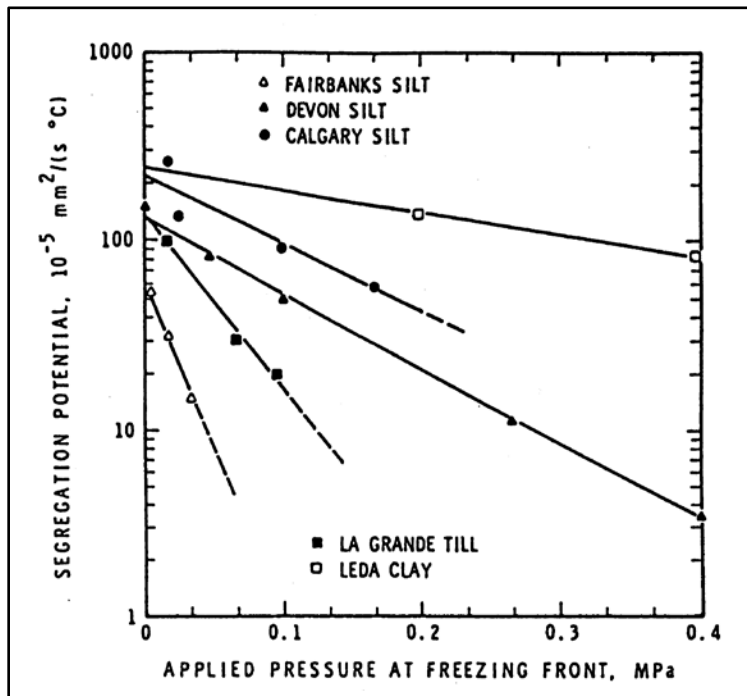


Figure B-2. Summary of data for SP parameter. (after Konrad, 1993).

3.3 The Miller School: *Van Loon (1991)*

3.3.1 Overview

Clearly, Dr. W.K.P. Van Loon belongs to the Miller School. In his Ph.D. thesis, however, he frequently refers to Konrad's Segregation Potential. In the 'Abstract' of his thesis, Van Loon writes: "For some of the materials studied, a minimum temperature gradient has been observed at which heave starts. From this and other results, an effort was made to come to a synthesis of the rigid ice concept and the segregation potential concept". Here, obviously, the "rigid ice concept" represents the Miller School, and the "segregation potential concept" represents the Anderson School.

Note: Later in this paper, we will comment extensively on the part of the quote: "For some of the materials studied, a minimum temperature gradient has been observed at which heave starts."

The first half of the Van Loon thesis deals with the equipment and the measurements of the temperature of the frozen and unfrozen soil in the test columns. The improvements of the latest equipment and the innovative approaches contained in Van Loon (1991) are impressive. In the second half of the thesis, Van Loon deals with the heave rate and the Segregation Potential. There, he makes an excellent attempt at reconciliation, which is also the purpose of the 'unifying theory' put forth by Groenevelt & Grant (2013) which is discussed later in this narrative paper (see Section 6 below).

In order to set the stage for this narrative paper, we present a rather long quote from the last Chapter of Van Loon's thesis (Ch. 5: Conclusions and Final Discussion, pg. 178):

"In the last two decades of frost research in porous media two major concepts have been developed to understand the observed phenomena: the rigid ice concept of Miller [1978] and the segregation concept of Konrad and Morgenstern [1980]. The latter concept formed the basis of the theory of the present thesis and has been discussed quite extensively. So we have to explain why this concept has been chosen and not the rigid ice concept. First of all we must stress that Miller developed earlier two important concepts which are the basis of any modern frost heave research: the frozen fringe and the secondary heave. These two concepts are needed to understand that ice lenses grow at temperatures below 0°C. However, from here the two earlier mentioned concepts start to deviate. Miller [1978] assumes that pore ice is rigid (i.e., it acts as one body) but not immobile. Movement of the ice phase with respect to the soil matrix occurs as a result of locally melting of ice, movement of liquid water, and subsequent refreezing (regelation). Thus, the ice body (pore ice plus ice lens) moves uniformly. Next a certain stress partition between the different constituents is assumed in order to calculate the stresses. And from there the location of a new ice lens can be predicted. However, we find the existence of the rigid ice body less attractive than the direct flow of liquid water towards the ice lens as is suggested with the segregation potential (SP) concept. The regelation concept complicates the way the water transport takes place and a model has to be as simple as possible. However, the SP concept is less clear about the stresses existing during frost heave. Because of this omission we have extended the SP concept with the minimum pressure at which heave starts and assume that this pressure is needed to create room for the new ice lens (as is suggested by Miller [1978]). In general, the major objection against the SP concept is its discontinuous character: when only one dimension is considered the heave rate is increasing and decreasing with every newly formed ice lens. However, when three dimensions are considered it is very likely that several ice lenses are growing at different heights, different temperatures and different rates at the same time. The three dimensional character will average the different heave rates and the measured heave rate will be this averaged, smoothed value. This agrees with the rather constant observed heave rates, which is mentioned by all scientists."

Later that year, Black (1991, pg. 5) wrote: "The last half of the 1970s brought about the final development of a model of frost heaving in the secondary mode. As envisioned by Miller (1978), the criterion for the initiation of a new ice lens within the frozen fringe below a growing lens was simply the same criterion for initiation of an air-filled crack in unsaturated ice-free soil used by geotechnical engineers, i.e., the condition for tensile failure of moist soils (Snyder and Miller 1985). This made it possible to compile a complete list of simultaneous equations for the conservation of mass and energy to be satisfied for a freezing front descending through an air-free, solute-free incompressible soil. This model, now known as the "rigid ice model" is hardly ready for use on practical problems. Computational difficulties are unusually formidable and, of course, it is necessary to have, as inputs, a series of functions that describe the relevant properties of a given soil. As the 1990s arrive, we find that we have no satisfactory explanation for the mechanics of frost heaving."

Following Miller, Van Loon distinguishes between "primary heave" and "secondary heave". He defines these two forms of heave as follows (pg. 28): "The formation of pure ice at the upper soil surface is called primary heave, while the formation of ice lenses inside the soil (at a certain overburden pressure) is called secondary heave. Later (pg. 146, footnote) he writes: "Primary heave is the formation of pure ice at the top of the soil at zero overburden pressure". Later that year, Black (1991, pg. 4), in his discussion of Miller's observations, wrote: "...ice in the "frozen fringe" beneath an ice lens could move (by regelation) at the same velocity as the lens in a process he identified as "secondary heaving" (fringe present) as opposed to "primary heaving" (fringe absent). What had previously been regarded as a theoretical maximum for heaving pressure became the transition from primary heaving to secondary heaving as the load to be heaved was increased. This hypothesis was tested and appeared to be confirmed in experiments done at Cornell by G. Loch and Miller (1975)".

Comment on the above quotes: In this narrative paper, no distinction will be made between primary and secondary heaving.

We quote Van Loon again (pg. 799):

"The suction at the frost front is a function of the hydraulic conductivity of the unfrozen soil, K_u , and the length of flow path, l_u . It can be calculated using Darcy's law: Eqn. (74.3)". Eqn. (74.3) suggests that the suction at the frost front should be calculated from the K_u and the Darcy velocity.

Comment on the above quote:

Here we have the horse behind the cart. It is the First Law of Thermodynamics that dictates the value of the suction at the frost front. The depressed liquid pressure (suction) then causes the Darcy flux, which, in magnitude, depends on the unsaturated hydraulic conductivity, $K_u(\theta)$, which is a function of the liquid water content. The liquid water content is dependent upon the depth below the frost front, or upon the height above the groundwater table.

On pg. 28, Van Loon writes: "The freezing soil can now be divided in three zones: The unfrozen zone, the frozen fringe and the frozen zone. In the latter, absence of transport of liquid water is assumed"

Comment on the above quote:

The assumption that liquid water transport in the frozen zone is absent is unnecessary and incorrect. If the assumption was correct, pure ice formation on the soil surface ("primary heave"), by the freezing of liquid water that comes from the groundwater table below the frost front, would be impossible.

On pg. 28, Van Loon writes: "If a groundwater table with external water supply is situated not far from the frost front, the unfrozen zone in the soil is saturated with water. Therefore, the hydraulic conductivity can be considered constant at $T > 0^{\circ}\text{C}$."

Comment on the above quote:

This statement is not necessarily correct. It is the suction at the frost front (which can be very large) which pulls up the water against the force of gravity. This suction can cause the soil just below the frost front to be unsaturated. Thus, just below the frost front, air can be present and ice can then grow into the air-filled pores at atmospheric pressure.

At the start of his section 4.3 on "Moisture Transfer", Van Loon states (pg. 146):

"As has been shown in section 2.3.1, the heave rate is proportional to the temperature gradient over the frozen fringe under equilibrium conditions. The coupling constant is called the segregation potential (SP). In this paragraph, the SP of the different materials is calculated by analysing the heave measurements (section 4.3.1)."

Comments on the above quote:

1. The use of the word "coupling" in this context is unwise. That word belongs to the discipline of Non-Equilibrium Thermodynamics.
2. It is not so that the Segregation Potential is the ratio between the heave rate and the temperature gradient over the frozen fringe. It is, by definition, the absolute value of the ratio of the Darcy flux and the temperature gradient over the frozen fringe. It is regrettable that Van Loon did not measure the Darcy flux by observing the intake rate of water at the bottom of the soil columns.

We continue to quote Van Loon (pg. 146): "Since we did not measure the water intake rate, we have to calculate v from the secondary heave rate":

$$v = (\rho_i/\rho_w) (dh_{\text{sec}}/dt) \quad (\text{Equation 4.3.2 in Van Loon [1991]}) \quad \text{Eqn. B-4}$$

where: ρ_i and ρ_w = density of ice and water, respectively
 h_{sec} = "height of secondary heave"

Comment on the above quote:

It is the intake rate, or the upward Darcy flux, which is one of the most essential driving forces (together with the heat extraction rate at the soil surface) leading to heave and heaving pressures. Moreover, in the laboratory, the intake rate is quite easy to measure.

Van Loon clearly shows (Fig. 4.3.1 on pg. 147 of his thesis, here presented as Fig. B-3) that the temperature gradient in the frozen fringe is not equal to the overall temperature gradient. The temperature gradient in the frozen fringe can be considerably larger or considerably smaller than the overall temperature gradient.

In the discussion below, we will analyze the data in Fig. B-3 for loamy sand (solid circles), sandy loam (open squares) and crushed concrete (solid stars). The data for river basin clay (open stars) are too few (only 2) and too erratic for analysis. In order to be able to switch the independent variable from $(\text{Grad } T)_{\text{ff}}$ in the frozen fringe to $(\text{Grad } T)_{\text{oa}}$ overall, we present here the coordinates which were extracted from the graph.

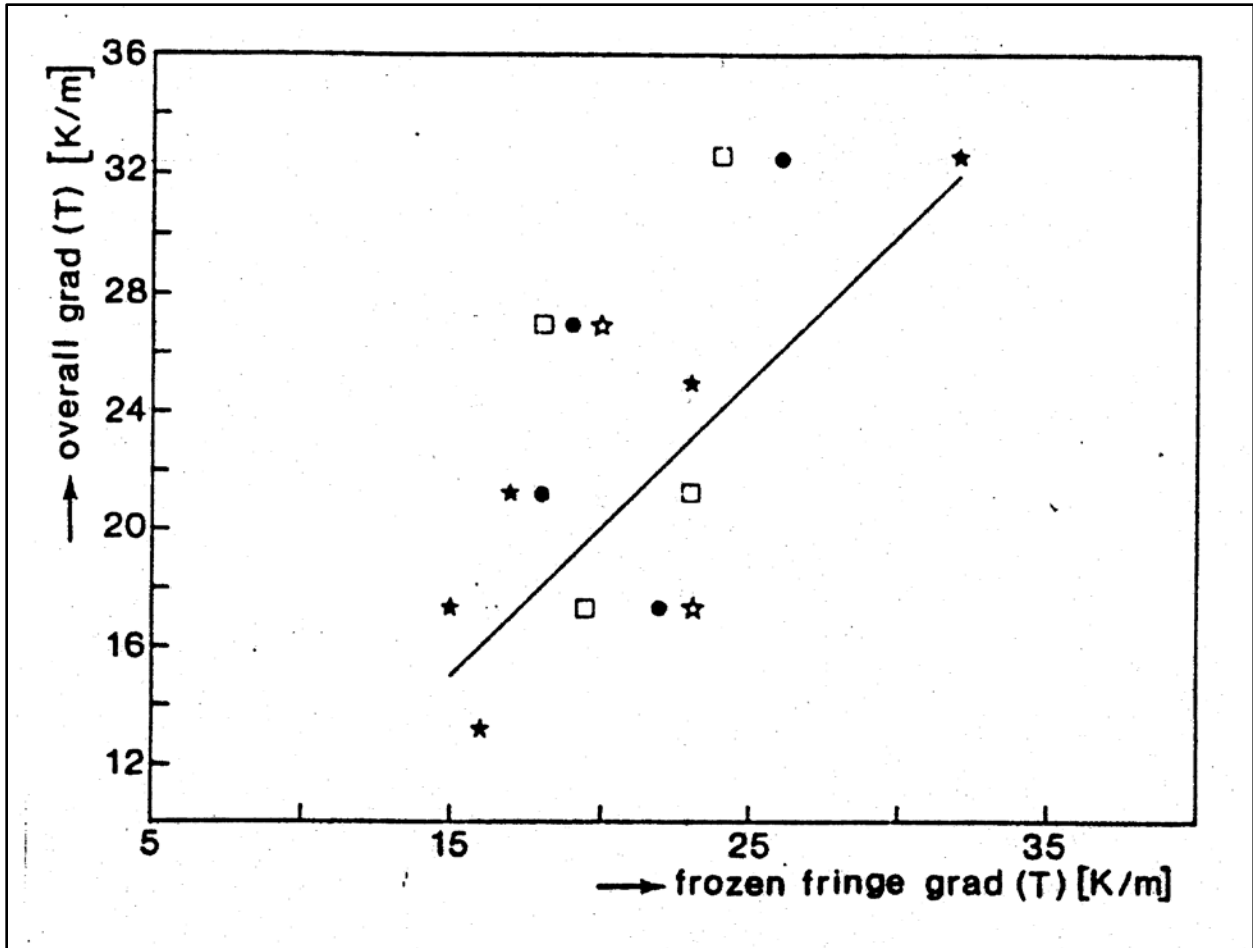


Figure B-3. Measured overall temperature gradients (K m^{-1}) as a function of the gradient of the temperature in the frozen fringe (K m^{-1}). (after Van Loon, 1991).

Loamy sand (solid circles in Fig. B-3):

$$\text{GradT}_{\text{ff}} := \begin{pmatrix} 18.0 \\ 19.1 \\ 22.0 \\ 26.0 \end{pmatrix} \quad \text{GradT}_{\text{oa}} := \begin{pmatrix} 21.1 \\ 26.8 \\ 17.3 \\ 32.4 \end{pmatrix}$$

Sandy loam (open squares in Fig. B-3):

$$\text{GradT}_{\text{ff}} := \begin{pmatrix} 18.0 \\ 19.5 \\ 23.0 \\ 24.0 \end{pmatrix} \quad \text{GradT}_{\text{oa}} := \begin{pmatrix} 26.8 \\ 17.3 \\ 21.2 \\ 32.5 \end{pmatrix}$$

Crushed concrete (solid stars in Fig. B-3):

$$\text{GradT}_{\text{ff}} := \begin{pmatrix} 15.0 \\ 16.0 \\ 17.0 \\ 23.0 \\ 32.0 \end{pmatrix} \quad \text{GradT}_{\text{oa}} := \begin{pmatrix} 17.3 \\ 13.2 \\ 21.2 \\ 24.8 \\ 32.5 \end{pmatrix}$$

Comment: Both Konrad and Van Loon use the temperature gradient in the frozen fringe as the driving force causing heave. The origin of this concept probably lies in the general belief that liquid water does not move in the frozen zone. As will be discussed below, local temperature gradients and magnitudes of the Darcy flux (both in the frozen fringe and in the overall frozen zone) may vary considerably, both in space and in time. This may cause erratic measurement results. It can be argued that the overall temperature gradient should be considered as the driving force. The overall temperature gradient is easy to measure: one determines the temperature at the soil surface and the depth of the 0°C isotherm. All the internal fluctuations of the temperature gradient are then taken into account. In contrast, the temperature gradient over the frozen fringe is very difficult to measure. Van Loon mentions in his thesis that the frozen fringe is only 15 mm thick on average. In addition, the location of the frozen fringe is constantly changing under field conditions.

In Fig. B-4 (or Fig. 4.3.2 on pg. 148 in Van Loon [1991]), Van Loon presents measured heave rate data as a function of the temperature gradient in the frozen fringe.

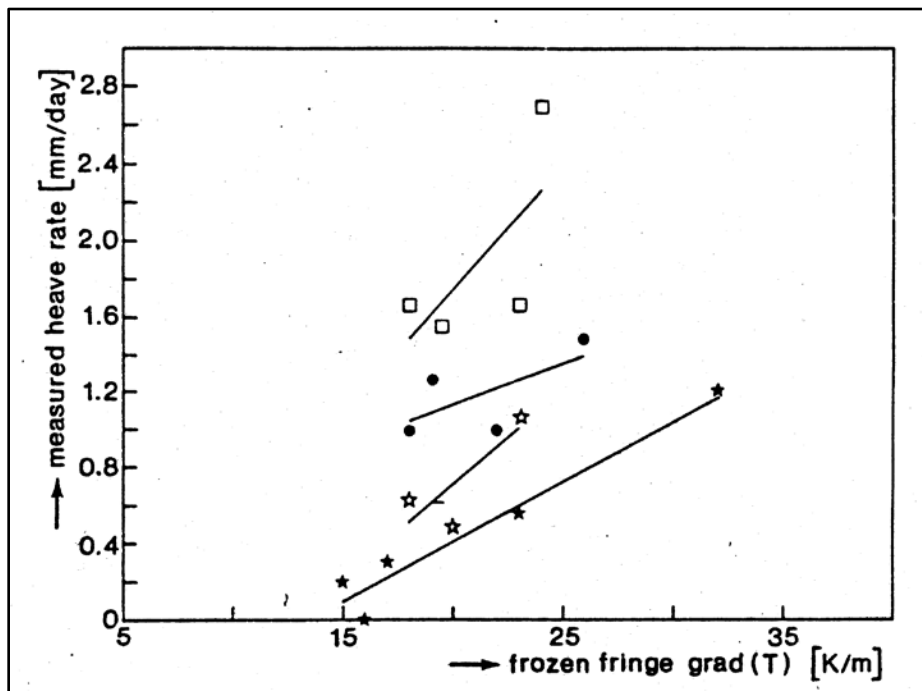


Figure B-4. Measured heave rates (mm day^{-1}) as a function of Grad T (K m^{-1}) in the frozen fringe for: loamy sand (solid circles); sandy loam (open squares); river basin clay (open stars); crushed concrete (solid stars). (after Van Loon, 1991).

We extract the co-ordinates of the data points in Fig. B-4 as follows:

Loamy sand (solid circles in Fig. B-4):

$$\text{GradT}_{\text{ff}} := \begin{pmatrix} 18.0 \\ 19.1 \\ 22.0 \\ 26.0 \end{pmatrix} \quad \text{LSAHR} := \begin{pmatrix} 0.99 \\ 1.25 \\ 0.99 \\ 1.47 \end{pmatrix}$$

Sandy loam (open squares in Fig. B-4):

$$\text{GradT}_{\text{ff}} := \begin{pmatrix} 18.0 \\ 19.5 \\ 23.0 \\ 24.0 \end{pmatrix} \quad \text{SLOHR} := \begin{pmatrix} 1.64 \\ 1.54 \\ 1.65 \\ 2.68 \end{pmatrix}$$

Crushed concrete (solid stars in Fig. B-4):

$$\text{GradT}_{\text{ff}} := \begin{pmatrix} 15.0 \\ 16.0 \\ 17.0 \\ 23.0 \\ 32.0 \end{pmatrix} \quad \text{CCHR} := \begin{pmatrix} 0.19 \\ 0.00 \\ 0.30 \\ 0.55 \\ 1.20 \end{pmatrix}$$

These data will be used for calculations of the Segregation Potential and for comparisons with Konrad's data.

3.3.2 Van Loon's extension of the theory

While Konrad focuses on the deduction of a parameter most promising for the prediction of the heave sensitivity of soils (Eqn. B-2), Van Loon focuses on the prediction of the heave rate, using a model that incorporates the Segregation Potential:

$$dh_{\text{sec}}/dt = A + B(\partial T/\partial z)_{\text{ff}} \quad (\text{Equation 4.3.3 in Van Loon [1991]}) \quad \text{Eqn. B-5}$$

where: dh_{sec}/dt = heave rate

$$B = SP(\rho_w / \rho_i) \quad \text{Eqn. B-6}$$

Thus, Van Loon assumes a linear relationship between the two variables in Fig. B-4 and presents the values of the intercept (A) and the slope (B) of the lines drawn in Fig. B-4 as follows:

Loamy sand (solid circles in Fig. B-4): $A = +0.2 \times 10^{-8} \text{ m s}^{-1}$ $B = 0.05 \times 10^{-10} \text{ m}^2 \text{ s}^{-1} \text{ K}^{-1}$

Sandy loam (open squares in Fig. B-4): $A = -0.9 \times 10^{-8} \text{ m s}^{-1}$ $B = 0.13 \times 10^{-10} \text{ m}^2 \text{ s}^{-1} \text{ K}^{-1}$

Crushed concrete (solid stars in Fig. B-4): $A = -0.8 \times 10^{-8} \text{ m s}^{-1}$ $B = 0.06 \times 10^{-10} \text{ m}^2 \text{ s}^{-1} \text{ K}^{-1}$

The remaining part of Van Loon's thesis is devoted to a discussion of the slope (B) and the intercept (A) of the best-fit lines in Fig. B-4. The data in Fig. B-4 will be analyzed in Section 4 (Discussion) below.

3.3.3 Van Loon's 'minimum (absolute) temperature gradient' required for frost heave to start

In the 'Abstract' of his thesis, Van Loon writes: "For some of the materials studied, a minimum temperature gradient has been observed at which heave starts."

Comment on the above quote: On pg. 16, while discussing Darcy's law, Van Loon writes "z is the gravitational head". That means that z is positive upwards, and that the temperature gradients are negative. Obviously, Van Loon meant that the absolute value was observed to have a minimum.

4. Discussion

4.1 Heave rate vs. temperature gradient

Both Konrad and Van Loon use the temperature gradient in the frozen fringe (ff) as the driving force for heave. This concept obviously stems from the time that both Schools believed that there is no water movement in the frozen zone (fz) above the frozen fringe. This leads to all kinds of problems. In the first place, the measurement of the temperature gradient over the frozen fringe is difficult. Van Loon states that, in his experiments, the frozen fringe was only 15 mm thick. In addition the spatial and temporal variability of the temperature gradient in both the frozen fringe and the frozen zone are very large due to the constantly changing demand for, and delivery of, heat and the constantly changing hydraulic conductivity. We are of the opinion that water is as mobile in the frozen zone as it is in the frozen fringe, and that the magnitude of the flux is solely dependent on the hydraulic conductivity. It can be seen from Fig. B-3 that the correlation between the temperature gradient in the frozen fringe and the overall temperature gradient is very poor. This is a clear indication of the variability of both. We suggest that the choice of the overall temperature as the driving force is far superior from a physical point of view, and is much easier and much more accurately measured (i.e., the temperature at the soil surface divided by the distance between the soil surface and the 0°C isotherm).

4.2 Van Loon's extension of the theory

Van Loon's extension of the existing theory is the introduction of an intercept in the relation between the heave rate and the gradient of the temperature (Eqn. B-5). Even though the data points in Fig. B-4 are quite scattered, Van Loon assumes that they are linear in nature, which can be described by Eqn. B-5. In Van Loon's work, the vertical coordinate z is positive upwards, so that the gradient of the temperature T is negative. In Fig. B-4, he plots Grad T as positive. Therefore, we re-write Eqn. B-5 as:

$$dh_{sec}/dt = A + B(\partial/\partial z)_{ff} (-T) \quad \text{Eqn. B-7}$$

where: $(\partial/\partial z)_{ff} (-T)$ is positive in the positive direction of the horizontal axis and B is positive

We also re-write Eqn. B-6 as:

$$B = (\rho_w / \rho_i) |SP| \quad \text{Eqn. B-8}$$

4.3 Analysis of the heave rate data

4.3.1 Loamy sand (solid circles)

Loamy sand (Fig. B-5) is the only soil for which Van Loon found a positive value for the intercept (A). A positive value for A is physically unacceptable. It would mean that the soil is heaving while there is no temperature gradient. After plotting the heave rate data as a function of the overall temperature gradient (solid red circles), the points are better aligned and there is no need for a positive intercept (nor a negative intercept).

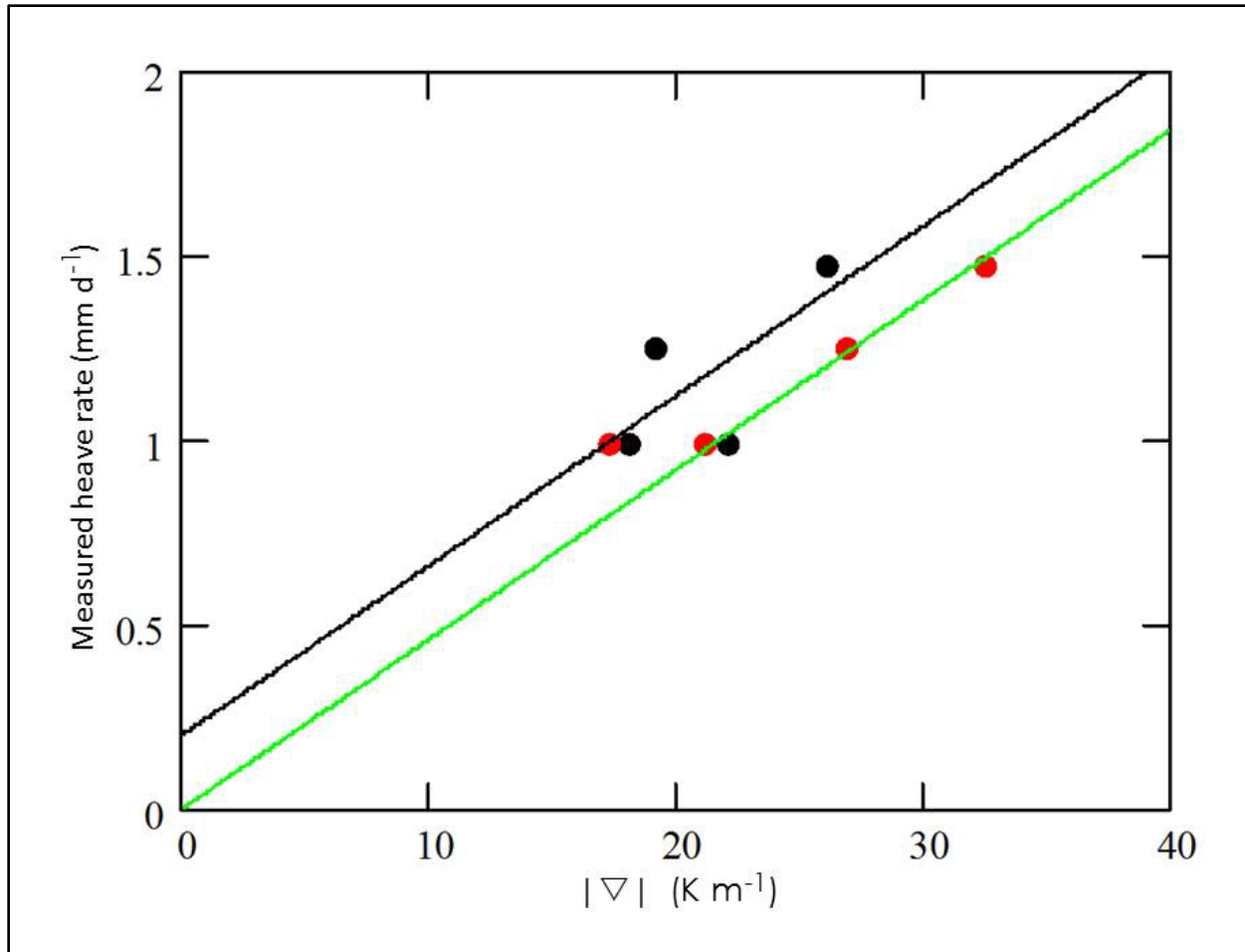


Figure B-5. Heave rate as a function of the temperature gradient for loamy sand when ∇T is calculated i) either across the frozen fringe (solid black circles, solid black line), or ii) between the soil surface and the 0°C isotherm, that is, the overall temperature gradient (solid red circles, solid green line). (after Groenevelt & Grant, 2013).

4.3.2 Sandy loam (open squares)

For sandy loam (Fig. B-6), Van Loon found a negative value for the intercept (A). That would mean that a minimum absolute value of the temperature gradient is required (here 7°C m⁻¹) to first observe a heave rate. This is a tenuous conclusion in view of the scatter in the data points. When the data are plotted as a function of the overall temperature gradient (open red squares), the points are better aligned, there is less scatter, and there seems to be no need for an intercept.

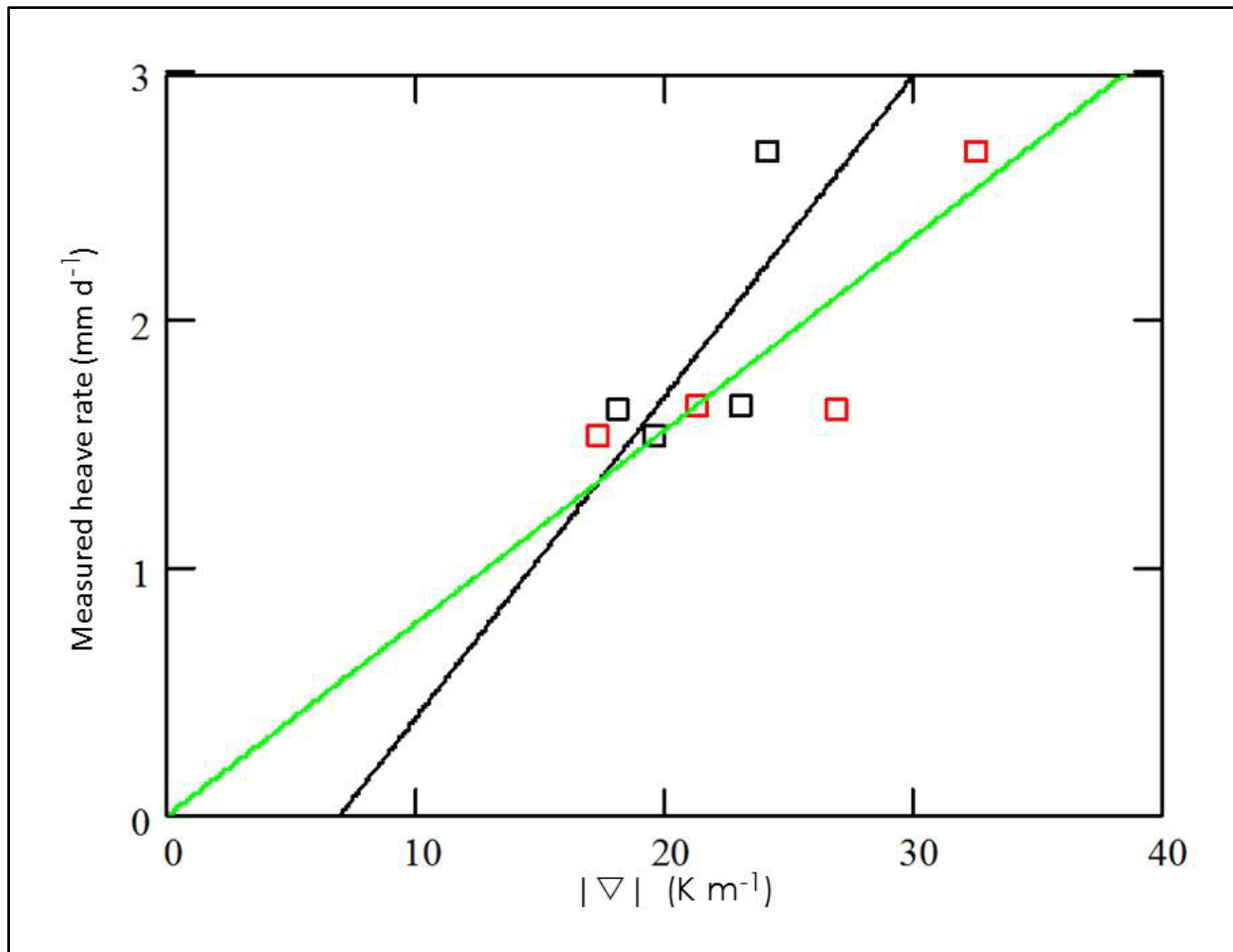


Figure B-6. Heave rate as a function of the temperature gradient for sandy loam when ∇T is calculated i) either across the frozen fringe (open black squares, solid black line), or ii) between the soil surface and the 0°C isotherm, that is, the overall temperature gradient (open red squares, solid green line). (after Groenevelt & Grant, 2013).

4.3.3 Crushed concrete (open circles)

For crushed concrete (Fig. B-7), a sizable negative intercept is reported (i.e., 13°C m⁻¹). When the data are plotted as a function of the overall temperature gradient (open red circles), the points are better aligned. In particular, the data point for which the heave rate is zero, is now at the lowest (absolute) temperature gradient of all the data. Except for river basin clay (for which the data are quite unreliable), this is the only soil for which a negative intercept is strongly indicated statistically. Physically, such a negative intercept is not unacceptable. Further research is needed.

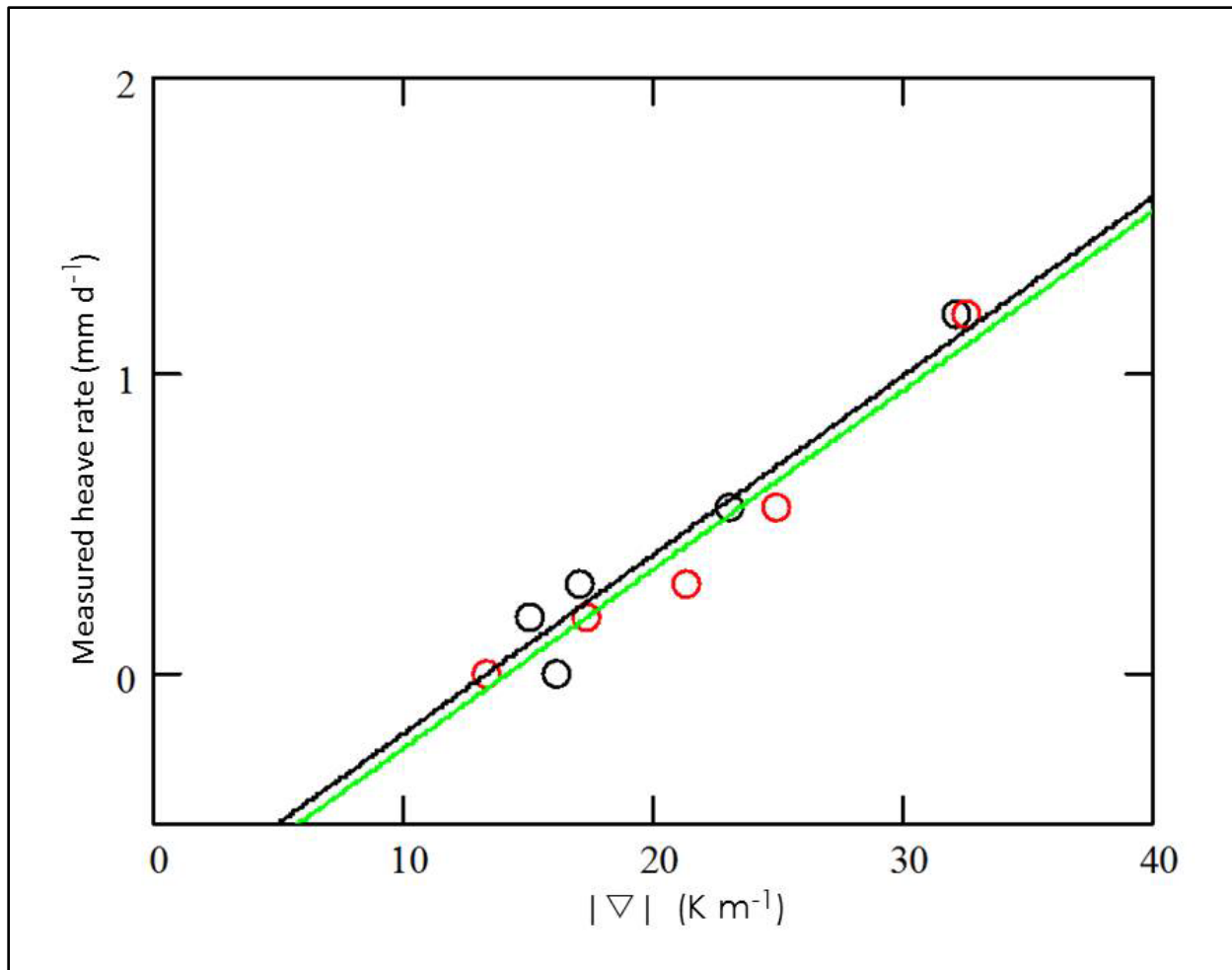


Figure B-7. Heave rate as a function of the temperature gradient for crushed concrete when ∇T is calculated i) either across the frozen fringe (open black circles, solid black line), or ii) between the soil surface and the 0°C isotherm, that is, the overall temperature gradient (open red circles, solid green line). (after Groenevelt & Grant, 2013).

5. Reported values for the segregation potential

In Fig. B-2 (or Fig 74.4 in Konrad [1993]), Konrad reports values for the Segregation Potential under unloaded conditions that are in the order of $100 \times 10^{-5} \text{ mm}^2 \text{ s}^{-1} \text{ C}^{-1}$ (or $10^{-9} \text{ m}^2 \text{ s}^{-1} \text{ K}^{-1}$). Van Loon reports the following values for B (Eqn. B-6):

Loamy sand	$0.05 (\pm 0.04) \times 10^{-8} \text{ m}^2 \text{ s}^{-1} \text{ K}^{-1}$
Sandy loam	$0.13 (\pm 0.10) \times 10^{-8} \text{ m}^2 \text{ s}^{-1} \text{ K}^{-1}$
Crushed concrete	$0.06 (\pm 0.01) \times 10^{-8} \text{ m}^2 \text{ s}^{-1} \text{ K}^{-1}$

It should be noted that the exponent (or power) appearing in the three lines above (10^{-8}) is different from the exponent actually published in Van Loon's original thesis (10^{-10}). The exponent that was published in 1991 (10^{-10}) was clearly a typographical error, which has since been confirmed by Dr. Van Loon himself (W. Van Loon, per. comm., 2012). Thus, the values for the Segregation Potential reported by Van Loon are of the same order of magnitude as those reported by Konrad, which is $10^{-9} \text{ m}^2 \text{ s}^{-1} \text{ K}^{-1}$.

6. Unifying theory of Groenevelt & Grant (2013)

As noted in Section 3.3.1 (above), Van Loon made an excellent attempt at reconciliation between the two 'Schools' in his Ph.D. thesis. More recently, Groenevelt & Grant (2013) introduced a 'unifying theory', also with a view to reconciling the two 'Schools'. The following is an overview of that 'unifying theory'.

The 'unifying theory' recognizes straight from the start that the process of heave in freezing soil cannot be treated satisfactorily by 'mechanical' formulations alone. For that, there is too much heat involved. The treatment needs the tools provided by classical (equilibrium) thermodynamics first, and ultimately the tools provided by non-equilibrium (irreversible) thermodynamics. At the outset, Groenevelt & Grant (2013) does away with the idea that the driving force for heave is the temperature gradient in the frozen fringe. This idea was conceived in the Miller School and adopted by the Anderson School. It was brought about by the unfortunate phenomenon that ice lenses in columns in the laboratory grow wall-to-wall, preventing liquid water from flowing around them and rendering the frozen zone above the warmest lens as "passive". In the field, ice lenses are finite in all directions and liquid water flows around them to replenish the liquid water that is "absorbed" and frozen on the cold side of the lenses.

Fundamental thermodynamics (i.e., the First Law and the Gibbs-Duhem equation) lead to the generalized Clapeyron equations (see Groenevelt & Kay, 1974), which arrive in differential form, and do not require integration. One of these equations relates the liquid pressure to the ice pressure and the temperature. In order to classify soils in terms of their sensitivity to heaving, it is advisable to first exclude mechanical, or "external", pressures on the ice, such as the overburden pressure and any external pressures (e.g., buildings, machinery) on the surface of the soil. This allows the ice lenses to form freely and readjust themselves (regelation) in order to avoid any positive pressure. The consequence of this is that the ice pressure is zero (atmospheric) and that the differential of the ice pressure in the Clapeyron equation can be deleted. This leaves two terms in the Clapeyron equation. The differentials are subsequently replaced by gradients and one finds a relationship between the liquid pressure gradient and the temperature gradient. The slope of this relationship is equal to the product of the latent heat of freezing and the hydraulic conductivity, divided by the partial specific volume of liquid water times the absolute temperature. If one now uses the Darcy equation to replace the liquid pressure gradient, one finds a relationship between the Darcy flux and the temperature gradient. For saturated soils (such as those used by Konrad in his step freezing laboratory tests), with the saturated hydraulic conductivity being constant, one finds a linear relationship between the Darcy flux and the temperature gradient. This is what Konrad found experimentally. In the field, where the source of liquid water is usually a groundwater table at some depth, the soil below the warmest ice lenses is usually unsaturated. One then has to deal with the unsaturated hydraulic conductivity which is dependent on the water content, a relationship which is strongly non-linear.

7. Summary (Appendix B)

Frost heave and heaving pressures occur in frozen soils and are caused by a temperature gradient in the presence of a supply of free water. Usually this water supply is a shallow groundwater table or a perched water table. In sloping terrain, the water is often supplied by lateral flow underneath the frozen layer. For homogeneous soil profiles, the dominant soil characteristic is the hydraulic conductivity function of the soil. For stratified soils, the layer of soil between the water supply and the frozen fringe that is the least conductive determines the severity of heaving. The least conductive layer may be a band of heavy clay, which, even when saturated, has a low hydraulic conductivity. It may also be a band of sand or gravel, for which

the unsaturated hydraulic conductivity is usually very low. In all cases, consideration should be given to the possibility of lateral water flow below the frozen zone.

References (Appendix B)

- Anderson, D.M. and N.R. Morgenstern. 1973. Physics, chemistry and mechanics of frozen ground. p. 257-288. *In Permafrost: 2nd Int'l. Conference*, National Academy Press, Washington DC.
- Beskow, G. 1935. Soil Freezing and Frost Heaving with Special Application to Roads and Railroads. The Swedish Geological Society, C, no. 375, Year Book no. 3 (Translated by J.O. Osterberg). Technological Institute, Northwestern University.
- Beskow, G. 1991a. Soil Freezing and Frost Heaving with Special Applications to Roads and Railroads. p. 37-157. *In Special Report 91-23*, Cold Regions Research & Engineering Laboratory (CRREL), Hanover, NH.
- Beskow, G. 1991b. Progress of Scandinavian Soil Frost Research from 1935 to 1946. p. 159-169. *In Special Report 91-23*, Cold Regions Research & Engineering Laboratory (CRREL), Hanover, NH.
- Black, P.B. 1991. Historical Perspective of Frost Heave Research. p. 1-7. *In Special Report 91-23*, Cold Regions Research & Engineering Laboratory (CRREL), Hanover, NH.
- Black, P.B. and M.J. Hardenberg (eds.). 1991. Historical Perspectives in Frost Heave Research. The Early Works of S. Taber and G. Beskow. Special Report 91-23, Cold Regions Research & Engineering Laboratory (CRREL), Hanover, NH.
- Grant, C.D., P.H. Groenevelt and G.H. Bolt. 2002. On Hydrostatics and Matristatics of Swelling Soils. p. 95-105. *In P.A.C. Raats, D. Smiles and A.W. Warrick (eds.) Environmental Mechanics*. Am. Geophysical Union, Washington, DC.
- Groenevelt, P.H. and C.D. Grant. 2013. Heave and heaving pressure in freezing soils: A unifying theory. *Vadose Zone J.* 12(1). 11 pp.
- Groenevelt, P.H. and B.D. Kay. 1974. On the interaction of water and heat transport in frozen and unfrozen soils: II The liquid phase. *Soil Sci. Soc. Amer. Proc.* 38: 400-404.
- Groenevelt, P.H. and B.D. Kay. 1980. Pressure distribution and effective stress in frozen soils. *Proc. 2nd Int'l. Symposium on Ground Freezing*, Norwegian Inst. of Technology, Trondheim. pp. 597-610.
- Hoekstra, P. 1966. Moisture movement in soils under temperature gradients with the cold-side temperature below freezing. *Water Resources Research* 2:241-250.
- Hoekstra, P. and R.D. Miller. 1967. On the mobility of water molecules in the transition layer between ice and solid surface. *Journal of Colloid Interface Science* 25:166-173.
- Kay, B.D. and P.H. Groenevelt. 1974. On the interaction of water and heat transport in frozen and unfrozen soils: I. Basic theory: the vapor phase. *Soil Sci. Soc. Amer. Proc.* 38:395-400.
- Kay, B.D. and E. Perfect. 1988. State of the art: Heat and mass transfer in freezing soils. *Proc. 5th Int'l. Symposium on Ground Freezing*, Vol. 1. Balkema, Rotterdam. pp. 3-21.

- Konrad, J.-M. 1987. Procedure for determining the segregation potential of freezing soils. *Geotech. Test. J.* 10:51-58.
- Konrad, J.-M. 1993. Frost Heave Potential (Chapter 74). p. 797-806. *In* M.R. Carter (ed.). *Soil Sampling and Methods of Analysis*. Canadian Society of Soil Science. Lewis Publishers. Boca Raton, FL.
- Konrad, J.-M. 1999. Frost susceptibility related to soil index properties. *Can. Geotech. J.* 36:403-417.
- Konrad, J.-M. 2005. Estimation of the segregation potential of fine-grained soils using the frost heave response of two reference soils. *Can. Geotech. J.* 42:38-50.
- Konrad, J.-M. and N.R. Morgenstern. 1980. A mechanistic theory of ice lens formation in fine grained soils. *Can. Geotech. J.* 17:473-486.
- Konrad, J.-M. and N.R. Morgenstern. 1981. The segregation potential of a freezing soil. *Can. Geotech. J.* 18:482-491.
- Konrad, J.-M. and N.R. Morgenstern. 1982. Prediction of frost heave in the laboratory during transient freezing. *Can. Geotech. J.* 19:250-259.
- Koopmans, R.W.R. and R.D. Miller. 1966. Soil freezing and soil water characteristic curves. *Soil Sci. Soc. Amer. Proc.* 30:680-685.
- Loch, J.P.G. and B.D. Kay. 1978. Water redistribution in partially frozen, saturated silt under several temperature gradients and overburden loads. *Soil Sci. Soc. Amer. J.* 42:400-406.
- Loch, J.P.G. and R.D. Miller. 1975. Test of the concept of secondary frost heaving. *Soil Sci. Soc. Am. Proc.* 39:1036-1041.
- Miller, R.D. 1972. Freezing and heaving of saturated and unsaturated soils. *Highway Res. Rec.* 393. pp. 1-11.
- Miller, R.D. 1973. Soil freezing in relation to pore water pressure and temperature. p. 344-352. *In* *Permafrost: 2nd Int'l. Conference*, National Academy Press, Washington DC.
- Miller, R.D. 1978. Frost heaving in non-colloidal soils. *In* *Proceedings, 3rd Int'l. Conference on Permafrost*, Edmonton, AB. National Research Council of Canada.
- Miller, R.D., J.H. Baker and J.H. Kolaian. 1960. Particle size, overburden pressure, pore water pressure and freezing temperature of ice lenses in soil. *7th International Congress of Soil Science*, Transactions 1:122-129.
- Perfect, E., P.H. Groenevelt and B.D. Kay. 1991. Transport phenomena in frozen porous media. p. 243-270. *In* J. Bear and M.Y. Corapcioglu (eds.). *Transport Processes in Porous Media*. Kluwer Academic Publishers.
- Perfect, E. and B.D. Kay. 1993. Hydrological Properties of Frozen Soil (Chapter 72). p. 767-781. *In* M.R. Carter (ed.). *Soil Sampling and Methods of Analysis*. Canadian Society of Soil Science. Lewis Publishers. Boca Raton, FL.

Perfect, E., W.K.P. Van Loon, P.H. Groenevelt and B.D. Kay. 1990. Influence of ice segregation and solutes on soil structural stability. *Can. J. Soil Sci.* 70:571-581.

Philip, J.R. 1969. Moisture equilibrium in the vertical in swelling soils. 1. Basic theory. *Australian J. Soil Res.* 7:99-120.

Taber, S. 1929. Frost heaving. *Journal of Geology* 37:428-461

Taber, S. 1930. The mechanics of frost heaving. *Journal of Geology* 38:303-317.

Taber, S. 1991a. Frost Heaving. p. 9-26. *In* Special Report 91-23, Cold Regions Research & Engineering Laboratory (CRREL), Hanover, NH.

Taber, S. 1991b. The Mechanics of Frost Heaving. p. 27-35. *In* Special Report 91-23, Cold Regions Research & Engineering Laboratory (CRREL), Hanover, NH.

Van Loon, W.K.P. 1991. Heat and Mass Transfer in Frozen Porous Media. Ph.D. Thesis. University of Wageningen, The Netherlands.

Van Loon, W.K.P. (Wilko). 2012. Program Manager, Agrotechnology & Food Sciences Group, Wageningen UR, Wageningen, The Netherlands. (personal communication).

Van Loon, W.K.P., I.A. van Haneghem, E. Perfect and B.D. Kay. 1991. Thermal Properties of Frozen Soils (Chapter 73). p. 797-806. *In* M.R. Carter (ed.). *Soil Sampling and Methods of Analysis*. Canadian Society of Soil Science. Lewis Publishers, Boca Raton, FL.

Volger, G.H.O. 1854. *Über die Volumveränderungen, welche durch die Krystallisation hervorgerufen werden*. *Annalen der Physik and Chemie, Vierte Reihe*. Published by Poggendorff, Berlin, 1854, Band XCIII, p. 232-237.

APPENDIX C

Annotated Bibliography on Frost Heave Models

Annotated Bibliography on Frost Heave Models

1. General overview

The task of assembling the most pertinent literature on numerical models of frost heaving in soils (PARSC-003 'Core Task' - **LitRev 1**) was made manageable by i) concentrating on the frost heave phenomenon in soils in temperate climate zones only, and ii) categorizing the research papers that deal with frost heave models/concepts according to their relevance to frost heave of pipelines (i.e., Category I or II).

'Category I' included research papers that were relevant to frost heave of pipelines, whereas 'Category II' included those that were not overly relevant to the current study but still contained useful information.

CATEGORY I (Papers relevant to frost heaving of pipelines)

Paper I-1

Konrad, J.-M. 1999. Frost susceptibility related to soil index properties. *Can. Geotech. J.* 36:403-417.

Published Abstract

The analysis of frost-heave data on several soils confirmed that segregation potential, hence frost susceptibility, of saturated soils was best related to the average size of the fines fraction, the specific surface area of the fines fraction, and the ratio of the material's water content to its liquid limit. The influence of overburden pressure can also be accounted for by an empirical relationship between the segregation potential, the average size of the fines fraction, and the compressibility index of the soil. The segregation potential was also proportional to the relative fines content in soils where the fines do not completely fill the voids of the coarser fraction. This study led to the development of a new frost-susceptibility assessment methodology based on simple geotechnical routine soil index testing that was validated on a highway site on frost-susceptible subgrade till.

Annotation

General:

The paper is mechanistic in nature, but, in several aspects, it is compatible with thermodynamic principles

The paper originated from the "Anderson School", but it has adopted the concept of a "frozen fringe", which originated in the "Miller School"

The author claims that the model has been adequately validated

A multitude of soil data is required

Specific:

This paper deserves extensive scrutiny as it contains the core of the work by Dr. Konrad, who is presently considered to be the authority with regard to the phenomenon of pipeline heaving in freezing soils. In this 1999 paper Konrad states (p. 403): "...there is as yet no generally accepted criterion for a qualitative assessment of frost susceptibility". He then states that present classifications of frost susceptibility are based on grain-size distribution supplemented by information about capillary rise, hydraulic conductivity of unfrozen soil, water retention curve, etc., and that "these classifications display limitations". He also states that otherwise

"assessments of frost susceptibility are based on direct observations of frost heaving in the laboratory or in the field."

In this, and subsequent papers, the author suggests that laboratory experiments are representative of field conditions. In his Fig.1 he presents a "Schematic of conditions in freezing soil", showing a column with an "Active ice lens" stretching from wall to wall. *Here, we wish to express our major criticism regarding the underlying philosophy of the author: In the field, ice lenses do not stretch from coast to coast. They are finite in all directions, giving liquid water a pathway for upward flow around the ice lenses.* In column experiments, an ice lens forms from wall to wall, obstructing all upward liquid flow. This causes the soil layer above the warmest ice lens to become "passive" during the freezing process. *In the field such a "passive" layer does not exist.* In his Fig.1 the author also shows the location of the "frozen fringe" just below the warmest ice lens. *It is our opinion that in the field "frozen fringes" are present around ice lenses in many locations.*

The author expands the work by Konrad and Morgenstern (1983), who (p404) "...suggested a new approach for estimating the relative frost susceptibility of soils using the segregation potential parameter, SP,The SP based approach allows one to predict the amount of frost heave and permits one to establish the degree of frost susceptibility by comparison of predicted heave with an acceptable frost-heave value related to the project requirement." Up to now (2014) this is the most advanced method of dealing with the problem of frost heaving. Earlier, Konrad and Morgenstern (1980, 1981) "showed that....the velocity of the pore water entering into the unfrozen soil is proportional to the temperature gradient..." *This important finding can be derived from the Clapeyron equation, which follows immediately from the First Law of Thermodynamics. The derivation leads to the conclusion that the ratio of the upward Darcy flux and $\text{Grad}(-T)$ is constant, under the conditions that the ice pressure is, and remains atmospheric, and that the hydraulic conductivity is a constant.*

The SP is defined as the ratio of "...the velocity of pore water entering into the unfrozen soil and the temperature gradient" (Eqn [1]), and is considered to be "a function of soil type, porosity, over-consolidation ratio, pore fluid, etc." (Eqn [2]).

From here on, the paper concerns itself with the determination of the SP. The primary ingredient is the grain-size distribution, followed by the influence of mineralogy, "fabric", and overburden pressure. *It should be pointed out that for all SP calculations, based on soil properties, there is still the fundamental requirement that the temperature gradient in the frozen fringe is known or set. It is also assumed that the soil is always saturated, where ever the liquid water comes from under whatever hydraulic conductivity values.*

The section "Methodology to assess the frost susceptibility of soils from index properties" is the essence of this paper (p 411): Here the idea is that the plethora of existing data for most soils should be sufficient to predict the value of SP. A "working example" includes a "flow chart of proposed methodology for frost-susceptibility assessment" (Fig 14) and a "flow chart for frost-heave prediction" (Fig 15). *It should be pointed out that the "flow chart" does not provide sufficient guidance, leading to a straightforward method for the calculation of the SP.*

In the "conclusions" the author claims that "The analysis of frost-heave data on several soils confirmed that segregation potential, hence frost susceptibility, of saturated soils was best related to the average size of the fines fraction, specific surface area of the fines fraction, and the ratio of the material's water content to its liquid limit.

At this point we wish to remind the reader that the material presented in this paper only applies to air-free soils. Here we suggest that an estimation of the hydraulic conductivity, required for the Darcy equation, is less complicated than the proposed procedure to obtain a value for SP.

Paper I-2

Konrad, J.-M. and N.R. Morgenstern. 1981. The segregation potential of a freezing soil. *Can. Geotech. J.* 18:482-491.

Published Abstract

In previous work it has been shown that when a soil sample freezes in a one-dimensional manner under different cold-side step temperatures but the same warm-side temperature, at the formation of the final ice lens the water intake flux is proportional to the temperature gradient across the frozen fringe. The constant of proportionality has been called the segregation potential and this linear relation constitutes the coupling between heat and mass flow in a general theory of frost heave. This paper shows experimentally that the segregation potential is also a function of the average suction in the frozen fringe which is readily expressed in terms of the suction at the frost front. As a result it is also shown that measured water intake flux during freezing is dependent on the freezing path used to initiate the final ice lens. A thermodynamic explanation of the dependence of segregation potential on suction in the frozen fringe is also offered.

Annotation

General:

This paper is mechanistic in concept, but it embraces several thermodynamic principles. In particular, it recognizes the fundamental importance of the Clapeyron equation, which follows immediately from the First Law of Thermodynamics. In contrast, the purely "mechanistic models" concern themselves with pore size distribution and the "Everett equation".

The paper originated from the "Anderson School", but it has "borrowed" the concept of a "frozen fringe" and the use of the Clapeyron equation from the "Miller School".

Specific:

For its time (1981), this is an advanced paper. Because this paper is based on observations in columns in the laboratory, where ice lenses grow from wall to wall, the derived relationship between the "intake" flux of liquid water and the temperature gradient in the frozen fringe, leading to a value for the Segregation Potential, is not necessarily useful under field conditions. In a laboratory column the warmest ice lens blocks all upward flow of liquid water. This causes the temperature gradient in the frozen fringe to become the dominant driving force for the upward movement of liquid water. In the field, however, ice lenses are finite in all directions, so that liquid water can flow around them. In the field therefore, it is the overall temperature gradient, from the soil surface to the 0°C depth, which is the driving force.

Although the authors recognize the fundamental importance of the Clapeyron equation, they present this equation in integral form. This form is not particularly useful and the authors do not apply the Clapeyron equation properly. The authors even go so far as to question the validity of the Clapeyron equation: (p 484, RH column) "...the validity of the Clausius-Clapeyron (CC) equation in the frozen fringe may be questioned." Also, (p 485, RH column) "... it is clear that the CC equation....does not hold in the frozen fringe.....". *Such a statement is fundamentally unacceptable. The Clapeyron equation follows directly from the First Law of Thermodynamics. It*

comes **in differential form**. In that form it can be applied directly and successfully. Integration is not needed.

A final criticism concerns the water intake rate. This is an essential component of the Segregation Potential and should be, and can be easily, measured directly, certainly in laboratory experiments. The authors did not do so. Page 490, LH column, last sentence: "The water intake rate...was inferred from the total heave versus time....". *This procedure is unacceptable. There are several reasons why the heave rate does not reflect the water intake rate proportionally.*

Paper I-3

O'Neill, K. 1983. The physics of mathematical frost heave models: A review. Cold Regions Sci. and Tech. 6(3):275-291.

Published Abstract

This paper is concerned with the physical and thermodynamical bases of frost heave modeling. An attempt is made to isolate and illuminate issues which all such models must address, at least by implication. Although numerous relevant publications are surveyed, emphasis is less on an enumeration of items in the literature, and more on the concepts themselves, and on their alternative mathematical expressions, approximations, and manners of applications. Ultimately a selection of specific mathematical models is discussed, in light of the points raised in the general discussion.

Annotation

General:

This paper comes out of the "Miller School", but is written as a publication of CRREL, the seat of the Anderson School. It provides an excellent overview of the "state-of-the-art" in 1983. It is made clear that that "state" was, at that time, still quite shaky. Statements (p 275) like: "...this is due to the lack of a common understanding of the basic phenomenon..." and "...lack of a general understanding limits our ability to extrapolate beyond the specific conditions under which any given criterion has been developed" demonstrate the absence of a coherent theory.

Specific:

Coming out of the "Miller School", this paper tends to push the train of thought in the direction of a thermodynamic theory. It does recognize the work by Konrad and Morgenstern (p. 283 and 284: "...segregation potential"...") and even mentions (p. 281) the "...pressure jump between the two phases...in a configuration with curved phase interfaces...", but otherwise it shies away from "mechanistic models".

In this paper, however, a comprehensive thermodynamic theory only lurks at the horizon. The author does mention the 1974 papers by Kay and Groenevelt in which a detailed development of the complete set of generalized Clapeyron equations in **differential form** is presented, but when it comes to dealing with the Clapeyron equation the author only presents an **integral form** (Eqn. 1) and then does not know what to do with it.

The author presents interesting observations regarding the moisture characteristics of saturated and unsaturated frozen soils (p 281-282) and excellent thoughts regarding the measurement of the hydraulic conductivity of frozen soils (p 283-284).

Paper I-4

Loch, J.P.G. 1981. State-of-the-art report - Frost action in soils. Engineering Geology 18:213-224.

Published Abstract

Several theories have been employed to describe the mechanism of frost heave and ice lens formation in soils. In the early seventies, the capillary theory, visualizing ice lens growth at the frost front in non-colloidal soils, has been invalidated by experimental evidence. This led to models in which ice lens growth takes place behind the frost front. Experimental confirmation of this concept was presented at several occasions. Simultaneously, numerical simulation of these models was attempted. In some of these, advanced finite-element and finite-difference techniques were employed.

In these recent approaches, mass movement for ice lens growth takes place in a zone of frozen soil. This movement is facilitated by the presence of liquid water films between the pore ice and the pore wall. Coupling of heat and moisture movement in this zone is achieved by employing a generalized form of the Clausius-Clapeyron equation.

Some qualitative and numerical models now include the effect of overburden load on the heaving process. Different approaches are followed to predict the effect of overburden load on the pressures in pore liquid and pore ice. In this paper various laboratory tests for frost-heave susceptibility, in use or proposed in recent years, are summarized. A major difference among them is that either a constant frost penetration rate or a step change in surface temperature is applied. In recent publications it is concluded that net rate of heat extraction is the independent variable in the frost-heave process and should be standardized in laboratory tests.

Annotation

General:

This paper is a product of the "Miller School". It presents a good overview of the state-of-the-art in 1981. The, for that time, most advanced, unexpected and surprising statement of this paper is contained in the last sentence of the Abstract: "...it is concluded that (*the*) net rate of heat extraction (*from the soil surface*) is the independent variable in the frost heave process...." . *This is indeed the fundamental driving force and it should be the starting point for a comprehensive thermodynamic theory.* In the same last sentence of the Abstract, the author commits himself to something ("...and should be standardized in laboratory tests") that is very difficult to achieve. *Other standardization criteria may turn out to be more practical.*

Specific:

The major novel aspect of this paper is the introduction of the osmotic pressure into the Clapeyron equation (see eqn. (3)). Notice that this is carried out for an **integral form** of the Clapeyron equation. *The introduction of the osmotic pressure into the **differential** form of the Clapeyron equation follows immediately from the First Law of Thermodynamics and the Gibbs-Duhem equation. That form is unambiguous and can be applied immediately and successfully. Integration of the Clapeyron equation is tricky and equation (3) requires thorough scrutiny. By the time the frost starts to penetrate into ordinary Canadian soils, the effect of the osmotic pressure is quite small. However, when seawater or salty ground water is involved, the osmotic pressure can play a major role.*

The discussion of the, in 1981 commonly used, frost-heave (*laboratory*) susceptibility tests, is interesting. The tests are classified as: "constant frost penetration rate", "constant rate of heat extraction", and "step change in surface temperature". *All these tests are **laboratory** tests, with their inherent restrictions for field application.*

Paper I-5

Loch, J.P.G. 1978. Thermodynamic equilibrium between ice and water in porous media. *Soil Science* 126(2):77-80.

Published Abstract

A derivation is given for the equation of thermodynamic equilibrium between ice and water in porous media. The equation accounts for a difference between the pressure of the ice phase and the total potential (in pressure units) of the water phase. Emphasis is laid on the distinction between the total potential and the hydrostatic pressure and osmotic pressure of the unfrozen soil solution. The difference between the hydrostatic pressure of the solution and the ice pressure is accounted for by the ice-water interfacial tension, as expressed by the generalized form of Laplace's equation. The resulting generalized form of the Clausius-Clapeyron equation is an equilibrium expression, whereas the Laplace equation only expresses a definition, valid under any circumstances. It is emphasized that all influences of the pore wall, which may or may not work via the diffuse double layer, and which cause the liquid to have lower Gibbs free energy than the equilibrium liquid at the same temperature, are collected in the osmotic pressure term.

Annotation

General:

This, rather early (1978), paper is a product of the "Miller School". It is an attempt to introduce the basic laws of thermodynamics to the dynamics of freezing soils. Everything in this paper should be consistent with the First Law of Thermodynamics and with the Clapeyron equation. Of particular interest is the introduction of the osmotic pressure. By equating the Gibbs free energy of the ice with that of the liquid water, the equilibrium osmotic pressure has to be subtracted from the equilibrium solution pressure, before it is introduced as the water pressure in the Clapeyron equation. It is not so that *The Clapeyron equation results from the Laplace equation.* (see Abstract: "The resulting generalized form of the (Clausius-) Clapeyron equation....")

The last sentence of the Abstract: "It is emphasized that all influences of the pore wall.....
....are collected in the osmotic pressure term" *is incorrect. The osmotic pressure only accounts for the free salts and does not include the effect of the counter ions.*

Specific:

There are errors in the section "Theoretical": Equation (1) is for **closed** systems and equation (2) is for **open** systems. The distinction between "mono-component" and "multi-component" systems is irrelevant. Eqn. (15) is correct and should be used for the development of a "Heave Index". The subsequent integration of equation (16) is not necessary and not necessarily correct. It is certainly not useful for the development of a "Heave Index".

The section (p. 79) "The meaning of π " is fundamentally wrong. The sentence "The adsorbed cations represent the osmotic pressure, so that....." demonstrates that the author is confused.

Paper I-6

Konrad, J.-M. and N.R. Morgenstern. 1980. A mechanistic theory of ice lens formation in fine-grained soils. *Can. Geotech. J.* 17:473-486.

Published Abstract

This study reveals that a freezing soil can be characterized by two parameters, the segregation-freezing temperature T_s and the overall permeability of the frozen fringe K_f . During unsteady heat flow, the variation of these parameters with temperature produces rhythmic ice banding in fine-grained soils. At the onset of steady-state conditions, freezing tests conducted at a fixed warm end temperature showed that T_s was independent of the cold side step temperature. In addition, a model is presented that indicates how the overall permeability of the frozen fringe can be calculated without detailed measurements at the scale of the frozen fringe. It is also constant in the tests reported here.

Annotation

General:

This paper is classic "Anderson School", and very "mechanistic".

A truly "mechanistic" aspect of laboratory experiments is described at the bottom of the LH column of page 474: "Once an ice lens is formed over the whole area of the sample, it has been shown that the ice lens acts like a cut-off with regard to water migration.....". The authors should have followed this sentence up with: "...and from that moment on, the laboratory experiment is no longer representative of field conditions."

Nevertheless, the contents of the abstract show that, from a physical point of view, the authors did identify the most essential property of wet (saturated) freezing soil regarding the heaving process, viz. "the overall permeability of the frozen fringe K_f ". Correctly, the equations [6] and [7] indicate that some form of integration of $K(z)$ is required. *It is remarkable, that in the present procedure to evaluate the Segregation Potential, this frozen fringe permeability does not appear.*

Specific:

Halfway the LH column of page 474 there is a touch of thermodynamics: "Basic thermodynamics also establishes that the thermodynamic potential or Gibb's free energy of the unfrozen water films is lower the lower the negative temperature". This attempt to describe the Clapeyron equation is not quite correct. Note that the authors, like many Americans, write **Gibb's**. The man's name was **Gibbs**. So, one should write: **Gibbs'** or **Gibbs's** or just the **Gibbs free energy**. Eqn. [8] is clearly for saturated conditions only: all the incoming liquid water freezes, expands by a factor 1.09 and contributes in full to the heave value.

The section "Experimental Procedure and Results" is based on the "formation of the final ice lens" and the establishment of a "steady state". It is likely that neither of these "concepts" is applicable in the field. It is noteworthy that the point in time of both the "Formation of Last Ice Lens" (see Fig. 11) and the "Growth of Last Ice Lens" (see Fig. 12) are insignificant.

The results presented in Fig. 13 are consistent with thermodynamic theory under the condition that there is no gradient of the ice pressure.

Paper I-7

Konrad, J.-M. 1987. The influence of heat extraction rate in freezing soils. Cold Regions Sci. and Tech. 14(2):129-137.

Published Abstract

The processes that are operative during fine grained soil freezing with no applied surcharge are described and related to the rate of net heat extraction. One-dimensional frost heave experiments were carried out on a Canadian silty soil under various freezing conditions. It was established that the segregational heave rate is strongly dependent on the rate of heat removal. No water flow was observed at heat extraction rates between 0.35 and 0.45 mW/mm². Maximum segregational heave rates occurred at rates of about 0.1 mW/mm². For the same soil, however, significant variations in segregational heave rates were measured for a given heat removal rate during transient freezing. Frost heave predictions using freezing tests at rates of heat extraction representative of field conditions are also discussed.

Annotation

General:

This paper is classic "Anderson School". Obviously, in this paper, the rate of heat extraction (to be expressed in mW mm⁻² or kJ s⁻¹m⁻²) is considered as the independent variable. This variable is the driving force and is independently adjustable, *which is not easy to achieve*. As the dependent variable one may choose the *upward liquid water flow* from a source of free liquid water. As a result of this dependent variable one usually observes heave. Heave is dependent on the dependent variable liquid flow and, in particular in saturated soil, on the expansion of water upon freezing. By choosing "**segregational heave**" as the dependent variable, the author has excluded the "expansion" component. The author reports that the value of this dependent variable (with "significant variations") rises with rising value of the independent variable up to a value at 0.1 mW/mm². But then it drops with rising value of the independent variable and reaches the value of zero at 0.35 mW/mm². This in itself is quite interesting. It is possible that, at the higher rates of heat extraction, the *in situ* freezing is so large that existing ice lenses, if any, do no longer grow and that the influx of liquid water is halted. Another explanation for this could be that, at greater heat extraction rates, the warmest (lowest) ice lens "**bites**" itself into the wall of the column and refuses the slide any further upwards. This would be an artificial laboratory effect.

Specific:

The values for "the thermal conductivities of the unfrozen and frozen silt, which were respectively 1.47 mW/(mm °C) and 1.76 mW/(mm °C)" are of interest (see p. 133, LH column, first two lines).

The **conclusion** is decisive:

1. Page 135, LH column, line 4: "Seeking a relationship between total heave rate and heat extraction rate, as done by most of the researchers, will inevitably lead to apparently contradictory results." Herewith, the author declares that the heat extraction rate is not useful as the independent variable. *This is because the heat extraction rate (like the evaporation rate) is difficult to regulate.*

2. Page 135, RH column, line 23: "Because the rate of heat extraction is dependent on the thermal conditions and the thickness of the frozen and unfrozen layers, it cannot be an independent variable in the frost heave process." *Obviously, this is for practical reasons.*

Paper I-8

Konrad, J.-M. and C. Duquennoi. 1993. A model for water transport and ice lensing in freezing soils. *Water Resources Research* 29(9):3109-3124.

Published Abstract

A one-dimensional model for water transport and ice lensing in incompressible saturated and solute-free soil specimens is proposed for the simulation of small-scale frost heave tests in the

laboratory. The model considers (1) open-system freezing in which the variables T and P_w , are independent, (2) an ice lens that continues to grow as long as enough energy is available in the frozen fringe to produce the work required for mass transfer to the ice lens, and (3) a new ice lens that forms when the vertical strain in the frozen soil reaches the instantaneous tensile failure strain. The proposed frost heave model is amenable to computer simulation procedures which provide predictions of rate of frost heave and rate of pore freezing front penetration as functions of applied load, thermal and water flow regimes, and soil properties. Position, time of initiation, and ultimate thickness of individual ice lenses emerge also as a part of the solution. A quantitative comparison of observed and simulated responses for various boundary conditions is shown for a reference soil known as Devon silt. The model was found to exhibit many of the characteristics observed in frost heave tests on Devon silt and predicted the effects of overburden pressure on frost heave rate.

Annotation

General:

The constraints of the proposed model, in particular *saturated soil* and a *column scenario*, have been discussed earlier. Only two independent variables are considered, viz. T and P_w , where T is the temperature and P_w is the pore water pressure. The condition (2) of "enough energy" for the continuation of an ice lens to grow is unworkable. The location and growth of ice lenses is dictated by the demand for heat and liquid water. The formation of a new ice lens is not based on tensile failure strain, but on the heat extraction rate and the availability of liquid water to deliver the required heat upon freezing.

Specific:

The Clapeyron equation (2) is (again) discussed in integral form. For the purpose of defining a Heave Index or a Segregation Potential, dealing with the Clapeyron equation in its original (differential) form is sufficient and avoids the problems associated with the integration process. The asterisks in eqn. (2) and (3) are unnecessary: the Clapeyron equation is not restricted to "closed system conditions".

On p 3112, RH column, line 4, the authors write: "The present model considers that the soil specimen can be separated into a **passive zone** defined as the *frozen soil* between the top surface and the base of the warmest ice lens, and an **active zone** composed of the *frozen fringe* and the unfrozen soil." *This statement demonstrates that a column study in the laboratory creates an artifact that does not occur in the field.* As the column has a finite diameter, the ice lens grows wall-to-wall. Such an ice lens then blocks all upward movement of liquid water. In the field there is no such blockage and *there is no **passive zone***. The whole soil profile, whether frozen or unfrozen is an **active zone**. That makes the designation of *the frozen fringe* pretty well useless: the whole soil profile, from the soil surface to the 0 °C depth is a "**frozen fringe**", with ice lenses of all sizes and shapes, crystals, needles and other ice fragments all over the place.

On p 3114, RH column, line 5: "...since the ice lens carries the full overburden pressure." *This is another artifact created by the finite diameter of the column with the ice lens stretching from wall-to-wall.* In the field, ice lenses maneuver themselves (partly during their formation and partly by regelation) in such a position that they have to carry the least possible amount of the overburden.

The material presented on pages 3120 – 3123 is impressive. Fig. 11 deserves careful attention. The zigzag, rhythmic, behavior of both, the ice lens temperature and the water flux (**in tandem**) demonstrates the direct link between the demand for heat and the delivery of liquid water, causing a sort of "flickering" behavior. In the laboratory set-up, where there is a single bundle of ice lenses, this (**simulated**) process is well-behaved and can be plotted easily. In the field,

however, where there are ice lenses here and there and everywhere, all with their own “mini-frozen-fringes”, the whole frozen zone appears to be one big random “flickering” heat production-delivery-transport system.

Paper I-9

Konrad, J.-M. 2005. Estimation of the segregation potential of fine-grained soils using the frost heave response of two reference soils. *Can. Geotech. J.* 42:38-50.

Published Abstract

The frost heave response of quarry fines from several locations in the Province of Quebec was studied in the laboratory using one-dimensional step-freezing tests with free access to water. Comparison of the segregation potential values obtained from these tests with available data on fine-grained soils revealed the importance of including clay mineralogy and overburden effects in any predictive empirical relationship, especially when fines are non-clays. A new approach is presented to estimate segregation potential values using the frost heave response of two reference soils. The reference characteristics consist of a relationship between segregation potential at zero overburden pressure, specific surface area, and average grain size of the fines fraction for two artificial soil mixtures in which the clay mineral is poorly crystallized kaolinite. The prediction of segregation potential values using the reference frost heave characteristics approach is more robust and reliable than other empirical approaches that do not specifically distinguish between clay and non-clay fines. Furthermore, the new approach was also efficient for the assessment of frost susceptibility of well-graded glacial tills.

Annotation

General:

Six years after his 1999 paper (**Paper I-1**), the author comes to the conclusion that the **soil index properties** required to calculate the Segregation Potential are not always sufficient. When “*fines*” are involved that are not swelling clays (“*nonclays*” such as kaolinite), the author recommends to also take “...clay mineralogy...and overburden effects...” into consideration. The author then proposes “a new approach....using the frost heave response of two reference soils”.

Assuming that **frost heave response**, measured in the laboratory, is the appropriate observation for the evaluation of the frost sensitivity of a soil, the “corrections” to calculate the Segregation Potential, as proposed in this paper, seem to drift further away from the essential characteristic, viz. the unsaturated hydraulic conductivity of the soil. *It seems that, instead of adding static properties to the list of requirements to determine the Segregation Potential, it would be better to return to the essential dynamic characteristic, i.e. the **intake rate of liquid water** upon freezing.*

Specific:

Here, we will once again address the effect of the overburden. The concept of the Segregation Potential is that it is a soil (profile) characteristic, which can be calculated from **soil index properties**. To now make this characteristic a function of the overburden pressure, P_e (cf. eqn. [3]) seems to confound the characteristics of the soil with the response of the soil to external conditions. For heave to occur there needs to be a positive ice pressure. That ice pressure must be greater than the total load the ice lens of concern has to carry. That total load is the sum of the weight of the overburden (soil) plus the external load present on top of the soil. Thus, for heave to occur, i.e. for liquid water to flow towards the ice lens, the gradient of the ice pressure, as it occurs in the Clapeyron equation should be evaluated in order to calculate what temperature gradient is required for heave to occur. Thus, instead of relating the Segregation

Potential to the total load (Eqn. [3]), one should use the SP or Heave Index to calculate the ice pressure and compare that value with the total load.

The experimental data, presented in this paper, are of little use for the purpose of the definition of a Heave Index.

Paper I-10

Henry, K.S. 2000. A review of the thermodynamics of frost heave. U.S. Army Corps of Engineers. ERDC/CRREL TR-00-16. Hanover, NH. pp. 26.

Published Abstract

Thermodynamic equilibrium requires a balance of thermal, mechanical, and chemical forces. The general equation for mechanical equilibrium between two phases describes capillary effects in porous materials, important in both unsaturated water flow and in understanding ice/water interfaces in freezing soil. The Gibbs-Duhem equation, which relates changes in chemical potential of a substance to changes in temperature, pressure, and presence of other chemicals, is of critical importance in understanding the flow of water in freezing soils. Osmotic pressure, related to the chemical potential of the substance, is useful in formulating expressions for total soil water pressure because soil water contains solutes, and the influence of soil particle surfaces can be "approximated" as solutes. It is the gradient of the total soil water pressure that drives flow to the freezing front in soils. The Clapeyron equation, based on the thermodynamic equilibrium of ice and water in soils (e.g., Loch 1978), is utilized by the thermodynamically based models of Miller (1978) and Gilpin (1980). In these models Fourier's Law and Darcy's Law describe heat and mass transfer in the frozen fringe, respectively, and mass flow and heat flow are coupled by one equation that describes heat transfer in frozen soil. Ice lenses start to grow when the effective stress in the frozen fringe becomes zero (Miller 1978, Gilpin 1980). Once an ice lens is established, liquid water is removed from the adjacent pores because of phase change, and water flows up through the soil to replenish the liquid water. If the rate of water loss caused by phase change is matched by the rate of water flow to replenish the liquid water, the ice lens will continue to grow in thickness. If the hydraulic conductivity of the soil limits the rate of water replenishment to the ice lens for the given rate of heat loss, soil water will freeze at increasing depths with associated changes in the depth and thickness of the frozen fringe.

Annotation

General:

This paper comes out of the Anderson School. It is an attempt by the engineers to embrace Thermodynamics. It is clumsy and messy. In general, there is a lot of confusion in the branch of science called "Thermodynamics" and this paper has a sizable share of it.

About the sentences in the Abstract: 1 Ok. 2 Useless. 3 Well, yes. 4 Inaccurate, messy, distorting. 5 What does "pressure" mean here? 6 Yes, but it is not used properly/effectively. 7 More or less. 8 Useless (this has nothing to do with thermodynamics). 9 This statement is clumsy. What does "removed" and "replenish" mean? 10 This criterion should be based on the rate of heat extraction together with the rate of liquid water flow. 11 This is pretty good, but the focus should not be on "changes...of the frozen fringe", but on the formation of a new ice lens.

Specific:

Page 6, last paragraph:

“Equation 38 is known as the Clapeyron equation”. This is incorrect. Eqn (38) is a rewrite of Eqn. (37). Eqn (37) is a proper differential equation (straight d's). It is then transformed into an equation that contains partial differentials (∂ 's) and step (Δ) functions. *That is unacceptable.*

Page 7, RH column, line 12: “Furthermore, the influence of soil particle surfaces on the chemical potential of the soil water can be approximated as “solute” “. This is incorrect. The influence of the particle surfaces is taken care of by the equilibrium liquid pressure.

Page 11: On this page the author presents a workout that leads to “**the generalized Clapeyron equation**”. In this workout one finds the same combination of partial differentials (∂ 's) and step (Δ) functions in the same equation (Eqn. 58). The final product comes in integral form. Thereafter, no indication is presented how this equation can be used to evaluate the frost sensitivity of a soil.

Paper I-11

Groenevelt, P.H. and C.D. Grant. 2013. Heave and heaving pressure in freezing soils: a unifying theory. *Vadose Zone J.* 12(1). 11 pp. doi:10.2136/vzj2012.0051

Published Abstract

A unifying theory is presented for the process of heave in freezing soils. Out of the Cold Regions Research and Engineering Laboratory (CRREL) school of D.M. Anderson came the concept of the *segregation potential*. Out of the Cornell school of R.D. Miller came the model for the *heave rate*. Here ideas from both schools are put on a fundamental thermodynamic footing, leading to the definition of a new *heave index*. Both schools use the temperature gradient in the frozen fringe as the driving force for heave. We argue and demonstrate that this choice leads to erratic results. The driving force should be the temperature gradient over the complete layer of soil that is at sub-zero ($^{\circ}\text{C}$) temperature, that is, the combined frozen zone plus the frozen fringe. The value of the heave index is completely dominated by the unsaturated hydraulic conductivity function of both the unfrozen soil below the frozen fringe and the soil layer at sub-zero temperature.

Annotation

General:

This paper recognizes straight from the start that the process of heave in freezing soil cannot be treated satisfactorily by mechanical formulations alone. For that, there is too much heat involved. The treatment needs the tools provided by classical (equilibrium) thermodynamics first, and ultimately the tools provided by non-equilibrium (irreversible) thermodynamics. Straight from the start the paper does away with the idea that the driving force for heave is the temperature gradient in the frozen fringe. This idea was conceived in the Miller School and adopted by the Anderson School. It was brought about by the unfortunate phenomenon that ice lenses in columns in the laboratory grow wall-to-wall, preventing liquid water to flow around them and rendering the frozen zone above the warmest lens as “passive”. In the field ice lenses are finite in all directions and liquid water flows around them to replenish the liquid water that is “absorbed” and frozen on the cold side of the lenses. Fundamental thermodynamics, the First Law and the Gibbs-Duhem equation, lead to the generalized Clapeyron equations (see Groenevelt and Kay, 1974), which arrive in differential form, and do not require integration. One of these equations relates the liquid pressure to the ice pressure and the temperature. In order to classify soils in terms of their sensitivity to heaving, it is advisable to first exclude mechanical, or “external”, pressures on the ice, such as the overburden pressure and an external pressure (buildings, machines) on the surface of the soil. This allows the ice lenses to form freely and readjust themselves (regelation) in order to avoid any positive pressure as much as possible. The

consequence of this is that the ice pressure can be set at zero (atmospheric) and that the differential of the ice pressure in the Clapeyron equation can be deleted. This leaves two terms in the Clapeyron equation. The differentials are subsequently replaced by gradients and one finds a linear relationship between the liquid pressure gradient and the temperature gradient. The slope of this relationship is equal to the latent heat of freezing divided by the partial specific volume of liquid water times the absolute temperature. If one now uses the Darcy equation to replace the liquid pressure gradient, one finds a relationship between the Darcy flux and the temperature gradient. The temperature gradient is now taken over the whole frozen zone, from the soil surface to the 0°C level. For saturated soils (such as those used by Konrad), with the saturated hydraulic conductivity being a constant, one finds a linear relationship between the Darcy flux and the temperature gradient. This is what Konrad found experimentally. If the liquid water has to flow through a frozen fringe, the Darcy flux is governed by the “unsaturated” hydraulic conductivity of the frozen fringe, where the ice plays a role similar to that played by air in unfrozen, unsaturated soils. The linearity found by Konrad then requires this “unsaturated” conductivity to be a constant. In the field, where the source of liquid water is usually a water table at some depth, the soil below the warmest ice lenses is usually unsaturated. One then also has to deal with the unsaturated hydraulic conductivity which is dependent on the water content, a relationship which is strongly non-linear. Some form of integration of the unsaturated hydraulic conductivity function will then be required.

Specific:

Equation [7]: In order to start dealing with external (or overburden) pressures, leading to the calculation of heaving pressures, one obviously has to reintroduce the ice pressure as a variable into equation [7].

Paper I-12

Derjaguin, B.V. and N.V. Churaev. 1978. The theory of frost heave. J. Colloid Interface Sci. 67: 391-396.

Published Abstract

It has been shown that the disjoining pressure contributes to the rate of thickening of ice interlayers but that the maximum pressure which can be set up owing to the crystallization of ice is determined only by the crystallization heat and the super-cooling degree, and it does not depend on the disjoining pressure.

Annotation

General:

This is an important paper. These two authors were the most eminent Russian scientists in Physical Chemistry during the 1970's. Their Institute of the Academy of Sciences in Moscow was in great esteem. The fame of these two colloid scientists was based on their publications regarding “the special structure of very thin films (*of water in proximity of charged solid surfaces*), that is very different from that of water in bulk” (page 391, RH column, middle).

Their downfall came with their publication claiming the invention of “poly-water” (water structured like a polymer).

Their definition of a **disjoining pressure Π** (page 391, LH column, last line) belongs to the theory of electrical double layers. *That element should not enter into the discussion at this point.* It leads the authors to a conundrum, and causes them to proceed with a tortuous, tormented train of thoughts (page 391, LH column), leading to a surprising conclusion **“The strict quantitative theory of the frost heaving of soil must therefore be obtained by applying the non-equilibrium**

thermodynamics to a steady-state process." *This is not so. The authors jumped straight over the branch of equilibrium thermodynamics. The steady-state process is perfectly described by something that comes out of very early **equilibrium** thermodynamics: the Clapeyron equation. This is not to say that in a later stage of development **non-equilibrium** thermodynamics will not be called upon. The authors never even mention the Clapeyron equation. This is all the more remarkable as four years before their publication a complete development of the generalized Clapeyron equations had appeared in the soil physics literature (Groenevelt and Kay, 1974).* The authors then proceed (page 392) with a "mechanical" discussion of what is captured in the Clapeyron equation. While they skip the classical **equilibrium** thermodynamics, in the end they have to rely on one of the greatest achievements of **non-equilibrium** thermodynamics: the Onsager Reciprocal Relations (page 393, below eqn. [7]). *This is odd indeed. But this does not mean that in a further advanced stage of the development of the theory of frost heave in soils, the Onsager Reciprocal Relations will not play an important role.*

There is a remarkable sentence on page 394 (RH column, middle): "Thus, the maximum pressure of frost heaving is not connected with the disjoining pressure, but is determined by some sort of thermo-osmotic pressure." *This sort of thermo-osmosis is described by the Clapeyron equation.*

Specific:

The authors never mention the Darcy equation.

Paper I-13

Gilpin, R.R. 1980. A model for the prediction of ice lensing and frost heave in soils. *Water Resources Research* 16(5): 918-930.

Published Abstract

A model of the frost heave phenomenon in soil is developed. The model predicts ice lensing and heave rates as a function of the basic soil properties (thermal conductivities and particle size) and the externally applied boundary conditions (surface temperatures and overburden pressure). The results are in general agreement with experimental observations as to the effects of the various parameters. The predicted heave rates are also of the right order of magnitude. An examination of the model equations reveals that at least four different processes may limit the heave rate of a soil. The specific process which controls the heave rate will depend on the soil properties and the applied boundary conditions. From the model it has also been possible to identify the properties of a soil that must be known in order to make an accurate prediction of heave rate in that soil.

Annotation

General:

This is a high quality paper. The physical background is excellent. The author knows about Russian publications (Derjaguin and Churaev, see Annotation I-12) and he probably can read Russian. He goes about thin films of water on a solid surface in a way similar to that of D&C, but focuses directly on soils (see title). He mentions the diffuse (or electrical) double layer (page 918, RH column, middle) and he recognizes the Clapeyron equation (8b).

In the Abstract it says: "An examination of the model equations reveals that at least four different processes may limit the heave rate of a soil." This deserves attention (see *Specific:*) The last paragraph of page 919 shows his thorough understanding: "This pressure, which has been called the disjoining pressure [Derjaginn (! this spelling shows that Gilpin is not happy with the usual transcription of Derjaguin's name from Russian (Cyrillic) into English) and Churaev, 1978], would result even if one of the surfaces is not ice. Returning again to the analogy of a fluid

in a gravitational field, the disjoining force is analogous to the buoyancy force experienced by an object with negligible density."

Pages 920-923 are "too mechanistic", although the "model" calculations of the hydraulic conductivity of the frozen fringe (Fig. 5) are interesting. Notice the number of orders of magnitude by which the hydraulic conductivity drops when the temperature drops.

Specific:

Of great interest is his equation (17), where he proposes a relationship between the hydraulic conductivity and the temperature, when ice is present. Also of interest are the values of the thermal conductivities (page 924, RH column, bottom).

Note: Page 926, LH column, 7 lines from bottom: "...; that is, heave will be limited by the permeability of the frozen fringe."

Page 927, RH column, middle: Conclusions: "A physical model based on the freezing of a **saturated matrix of uniform spheres** was found to exhibit many of the characteristics observed in the frost heave of soils."

Page 928, LH column, line 12: "The four limiting factors that were found to control the heave rate under different conditions were (1) the rate of heat conduction away from the freezing front, (2) the hydraulic resistance in the frozen fringe, (3) the hydraulic resistance at the ice lens, and (4) the hydraulic resistance in the unfrozen soil. Of these factors the first two are most likely to be the controlling factors."

Comment:

ad (1): this could be so when the soil below the warmest ice lens is very wet (saturated), so that the liquid water supply (Darcy flux to the bottom of the warmest ice lens) is plentiful, and the heat conductivity of the frozen soil above is small.

ad (2): this is probably in general the case, dependent on the ice content of the frozen fringe.

ad (3): in soils this is doubtful.

ad (4): this will be so when there is, in the unfrozen soil, a natural, or an artificial layer, with very low hydraulic conductivity, while the liquid water supply relies on a source (water table), which is situated below that particular layer.

Eqn. (A1) is interesting

Eqn. (A7) deserves ample attention.

CATEGORY II (Papers not overly relevant to the current study, but still contain useful information)

Paper II-1

Peppin, S.S.L. and R.W. Style. 2013. The physics of frost heave and ice-lens growth. *Vadose Zone J.* 12(1). 12 pp.

Published Abstract

The principle cause of frost heave is the formation of segregated ice - ice lenses - in freezing soil columns. Despite much experimental and theoretical work, there remain many questions about the fundamental process by which this occurs. Frost-heave models fall into **two main classes: capillary and frozen-fringe models**. Which model is appropriate depends on whether there is a frozen fringe; these are difficult to observe but some experimental evidence does exist. Recent advances have revitalized the capillary model, such as the engulfment model and the concept of geometrical supercooling. Key experimental and theoretical challenges remain to be resolved.

Annotation

General:

This paper is essentially "**mechanistic**" (NB: date of publication: 2013). The "**two main classes: capillary and frozen-fringe models**" are both "*beating around the bushes*" approaches. The "capillary model" treats the Clapeyron equation (presented in integral form) mechanistically and misses the essential thermodynamic content. The authors even dare to question the validity of the Clapeyron equation (Page 07, RH column: "2. Failure of the Clapeyron Equation...".) The "frozen-fringe model", borrowed from the Miller School, misses the thermodynamic boat completely.

Specific:

Page 04: Section: "Problems with the Capillary Theory, item #2":

"The Clapeyron equation breaks down outside equilibrium". ***This one sentence provides sufficient reason to send this paper to the waste basket.***

Last paragraph of this Section: "These obstacles to the capillary theory...led to the development of a radically different approach—the *frozen-fringe* model of frost heave." The "frozen-fringe model of frost heave" *is a testimonium paupertatis, concocted for laboratory experiments that are not representative of field conditions.*

Paper II-2

Selvadurai, A.P.S., J. Hu and I. Konuk. 1999. Computational modeling of frost heave induced soil-pipeline interaction: I. Modelling of frost heave. *Cold Regions Sci. and Tech.* 29(3):215-228.

Published Abstract

This research focuses on the development of a computational approach to the study of soil-pipeline interaction due to the development of discontinuous frost heave within a frozen soil region. The modelling of frost heave development within the soil is an important aspect in the computational treatment of the interaction problem. This paper deals with the calibration of a three-dimensional computational approach for the study of frost heave development, which takes into consideration the coupled effects of heat conduction and moisture migration. The results of one-dimensional frost heave tests are used to calibrate the computational approach.

Annotation

General:

In the section: **1. Introduction** (second last sentence, page 216) one finds:

“The focus of this paper is to develop a three-dimensional computational formulation of the modified hydrodynamic model of frost action in soils.....”

This paper lies outside the scope of our project. Otherwise, this paper is of high quality. The physical and mathematical content is excellent. The presentation of an extensive set of values for many physical soil properties may turn out to be quite helpful for the further development of the present project.

Specific:

The name Clapeyron is consistently spelled incorrectly (page 217, 218)

Concluding remarks (last two sentences of the paper): **“The paramedic studies conducted using this coupled model indicate(s) that the hydraulic conductivity of the soil is a key parameter which governs the rate of fluid influx and consequently the magnitude of the frost heave. The accurate determination of the hydraulic conductivity of the frost susceptible soil is regarded as an essential prerequisite for the accurate estimation of frost heave.”** *They got that right.*

Paper II-3

Shah, K.R. and G. Razaqpur. 1993. A two-dimensional frost-heave model for buried pipelines. Int'l. J. for Numerical Methods in Eng. 36:2545-2566.

Published Abstract

The rigid-ice model of frost heave is one of the most comprehensive frost-heave models but is restricted to one-dimensional cases in its present form. In this paper, the model is extended to two-dimensional problems. The complete formulation of the partial differential equations governing heat, moisture and ice transport in freezing soils is provided. The equations are subsequently solved using the Galerkin finite element method in space and the finite difference method in time. A computer program is developed for the two-dimensional rigid-ice model. A case of freezing around chilled gas pipeline is solved and the numerical results are compared with experimental values, with good agreement between the two sets of results.

Annotation

General:

This paper presents an *(old)* computer program using the Galerkin finite element method to solve the two-dimensional partial differential equations for heat and water transport in soils.

This paper is not useful for our project. Nevertheless, the presentation of data obtained by “the Caen (France) project” and the modelling of those data are interesting.

Specific:

The theory (rigid-ice model), used by these authors, is out- dated.

Introduction (first sentence): “When ground is subjected to subzero temperatures, water in the ground freezes and expands, a phenomenon known as frost heave.” **(sic!)**

Paper II-4

Krantz, W.B. and K.E. Adams. 1996. Application of a fully predictive model for secondary frost heave. *Arctic and Alpine Research* 28(3):284-293.

Published Abstract

Laboratory core freezing data for a Calgary silt are used to validate the secondary frost-heave model of Fowler and Krantz. This model is based on the model of O'Neill and Miller, but incorporates scaling and asymptotic analysis to make the complex physics of the freezing fringe more tractable and employs a more realistic thermal regelation mechanism for ice movement. Although this model does not involve any adjustable parameters, owing to insufficient soil-characterization data, it was necessary to fit one parameter in the equation describing the hydraulic conductivity of the frozen soils. However, this parameter was found to correlate very well with the porosity of the Calgary silt samples. These results were used to develop an equation for predicting the hydraulic conductivity of frozen Calgary silt as a function of soil porosity and unfrozen water volume fraction. These studies strongly support the predictive capability of the Fowler and Krantz model which because of its simplicity can be readily extended to incorporate solutal effects on freezing, soil compressibility, and differential frost heave.

Annotation

General:

This model is meant for the validation of laboratory core freezing data. *The Fowler and Krantz Model (1994), based on Fowler's (1989) model is out-dated. It is not useful for the prediction of the heaving of pipelines in the field.*

Specific:

Page 286, RH column, lines 2&3: "Water permeation can occur below ...the lowest (warmest) ice lens..., but not above it owing to the ice lenses." *This is the ever present "laboratory" problem caused by the ice lenses growing wall-to-wall.*

Paper II-5

Hawladar, B.C., V. Morgan and J.I. Clark. 2006. Modelling of pipeline under differential frost heave considering post-peak reduction of uplift resistance in frozen soil. *Can. Geotech. J.* 43:282-293.

Published Abstract

The interaction between buried chilled gas pipelines and the surrounding frozen soil subjected to differential frost heave displacements has been investigated. A simplified semi-analytical solution has been developed considering the post-peak reduction of uplift resistance in frozen soil as observed in laboratory tests. The nonlinear stress-strain behaviour of the pipeline at large strains has been incorporated in the analysis using an equivalent bending stiffness. The predicted results agree well with our finite element analysis and also with numerical predictions available in the literature, hence the simple semi-analytical solution can be considered as an alternative to numerical techniques. A parametric study has been carried out to identify the influence of key factors that can modify the uplift resistance in frozen soil. Among them, the residual uplift resistance has been found to be the important parameter for the development of stresses and strains in the pipeline.

Annotation

General:

This paper deals with chilled gas pipelines subject to differential frost heave due to discontinuous permafrost. The modelling and the calculations fall outside the scope of the present project.

Specific:

Page 283, last sentence: "Figure 1b shows the end displacements for two freezing periods in the Caen large-scale test". *Although not relevant for the present project, some of the contents of the "Database Report for the Caen Frost Heave Testing Facility (Carlson, L., 1994) could be of interest for later development of this project (see the Annotation of Paper II-3).*

Paper II-6

Yang, P., J. Ke, J.G. Wang, Y.K. Chow and F. Zhu. 2006. Numerical simulation of frost heave with coupled water freezing, temperature and stress fields in tunnel excavation. *Computers and Geotechnics* 33(6-7):330-340.

Published Abstract

Artificial ground freezing is an effective ground improvement technique to deal with diverse geotechnical construction problems as it serves to cut off the water and also improves the ground soil strength. However, ground freezing may produce frost heave and thaw settlement at the ground surface. Predicting and controlling the frost heave is a challenge to engineering construction in a heavily populated city. This paper proposes an analysis model that couples the water freezing, temperature and stress fields. This model is first applied to an underground excavation problem of a corridor where ground freezing is used. The numerical predictions are compared with field measurements. It is then applied for a model tunnel problem to study the effect of the overlying soil thickness, frozen soil wall thickness, excavation radius and brine temperature on the frost heave. It is found that the vertical component of the frost heave follows a normal distribution with a maximum at the tunnel axis, while the horizontal component reaches a maximum at a distance from the tunnel axis. This distance is directly proportional to the thickness of the overlying soil. A critical brine temperature is also found at which the frost heave at the ground surface reaches a maximum.

Annotation

General:

This paper deals with artificial ground freezing for tunnel excavation. It uses the finite element method for the calculation of frost penetration around a tunnel.

The contents of this paper fall outside the scope of the present project.

Paper II-7 a&b

a. Sheng, D., K. Axelsson and S. Knutsson. 1995a. Frost heave due to ice lens formation in freezing soils 1. Theory and verification. *Nordic Hydrology* 26:125-146.

b. Sheng, D., K. Axelsson and S. Knutsson. 1995b. Frost heave due to ice lens formation in freezing soils 2. Field application. *Nordic Hydrology* 26:147-168.

Published Abstract(s)

Part 1: Theory and verification

A frost heave model which simulates formation of ice lenses is developed for saturated salt-free soils. Quasi-steady state heat and mass flow is considered. Special attention is paid to the transmitted zone, i.e. the frozen fringe. The permeability of the frozen fringe is assumed to vary exponentially as a function of temperature. The rates of water flow in the frozen fringe and in the unfrozen soil are assumed to be constant in space but vary with time. The pore water pressure in

the frozen fringe is integrated from the Darcy law. The ice pressure in the frozen fringe is determined by the generalized Clapeyron equation. A new ice lens is assumed to form in the frozen fringe when and where the effective stress approaches zero. The neutral stress is determined as a simple function of the unfrozen water content and porosity. The model is implemented on a personal computer. The simulated heave amounts and heaving rates are compared with experimental data, which shows that the model generally gives reasonable estimation.

Part 2: Field application

An operational model for estimation of frost heave in field where stratified soil profile appears is presented. The model is developed from the research model described in part B. Soil layers are first classified into frost-susceptible layers (FSL) or non-frost-susceptible layers (NFSL). In an FSL, both heat flow and water flow are considered and ice lensing can occur. In a NFSL, only heat flow is possible and no ice lensing is allowed. The governing equations for heat and mass transfer are established for the time period when the frost front is moving within FSL. Capillarity and unsaturation are also considered. The operational model is verified by field measurements of heave amounts. Examples of application are given.

Annotation

General:

This set of large papers (44 pages) is seldom referenced (it is referenced in paper II-11), probably because *Nordic Hydrology* is not widely read. The emphasis in this paper is on **saturated** conditions and on the **frozen fringe**. This suggests that this model may not be useful for field conditions. The following sentences in the Abstract of Part 1 raise concerns: "Quasi-steady state heat and mass flow is considered." *Freezing soils, in particular under field conditions, are extremely "non-steady-state". The frozen fringe is constantly shifting in the vertical direction. In addition, in the field it is discontinuous in the horizontal direction. How does one go about measuring temperatures (leave alone permeability) in such a non-stationary layer of the soil? "The pore water pressure in the frozen fringe is integrated from the Darcy law." Here, the cart is pulling the horse. "A new ice lens is assumed to form in the frozen fringe when and where the effective stress approaches zero." Certainly for field conditions, this statement is useless. Nevertheless, the data, presented in Table 1, Fig. 5 and Table 2 are worth considering.*

Specific:

Part 2, Fig.1, page 149: *Here, the field situation is illustrated with an Ice Lens and a Frozen Fringe running from wall-to- wall. Thus, the authors are dealing with a two-dimensional, semi-infinite, stratified, system of alternating layers of ice and soil. This does not seem to represent field conditions very well.*

Paper II-8

Kay, B.D., M.I. Sheppard and J.P.G. Loch. 1977. A preliminary comparison of simulated and observed water redistribution in soils freezing under laboratory and field conditions. p. 29-41. *In Proc. Int'l. Symp. Frost Action in Soils, Vol. 1, Lulea, Sweden.*

Published Abstract

A model has been developed to simulate the flow of heat and water in a soil which is freezing with subsequent matrix deformation. The model is being tested on data generated by concurrent studies which are being carried out under both laboratory and field conditions. Preliminary tests indicate excellent agreement between the simulated and observed volumes of water transported under laboratory conditions. However, under field conditions the model

under-predicts the amount of water which is transported and also fails to accurately locate the zone of ice enrichment.

Annotation

General:

The authors used a sophisticated set of differential equations containing many parameters. They used advanced numerical solving methods to produce water profiles. For column experiments the model produces excellent results. The same model, with the same boundary conditions, applied for field conditions, however, produced very poor results. *Here again, one finds an indication that the boundary conditions for the field are not the same as those for a column in the laboratory. This paper seems to unconditionally accept the idea that the wall-to-wall conditions in a column are applicable in the field: "The boundary conditions which were used in the analysis were the same as those used in simulating the laboratory data" (page 37, line 8).* Abstract: "Preliminary tests indicate excellent agreement between the simulated and observed volumes of water transported under laboratory conditions. *This is encouraging. It indicates that the problem of the "unsaturated" hydraulic conductivity in the "frozen fringe" (Equation (7)) can be dealt with satisfactorily. This paper deserves further inspection at a later stage of the development of this project.*

Specific:

p. 33, nine lines from bottom: "...on a soil column **3 cm** in height..." *Should that be 30 cm?*

p. 34, Figure 1: *Why was the simulation halted after 21 minutes, while there are data points up to 27 minutes?*

p. 37 line 3: "In addition the model predicted only about half the heave that was recorded by the heavograph." *Why are the data points and the modelling results for the field experiment not shown in a figure like Fig. 1?*

p. 39 Discussion: "Failure of the model to accurately predict (*under field conditions*) either the quantity of water transported or the depth of ice accumulation may arise for several reasons. These include inappropriate characterization..., inappropriate adjustment of the hydraulic properties...." *Not likely. Most of the reasons given show lack of understanding. The authors then try to "adjust" the parameters to get a better fit. This is hopeless.*

*Let me start with the finding that under field conditions the upward movement of water into the upper soil layer was far greater than the model predicted. This is, most likely, because in the field each separate ice lens can suck in liquid water on both sides, the bottom (warm side) and the top (cold side). In a column experiment, with a wall-to-wall ice lens, the top is made inactive because the liquid water cannot "go around". In addition, the whole layer above the ice lens has become inactive ("passive", as Konrad calls it). So, if the model predicts well for laboratory experiments, it will not do so for field experiments. Next, the observed heave was far greater (about twice) than what the model predicted. This is, most likely, because in the field ice lenses can grow on both sides, whereas in a column the ice lens can grow only at the bottom (warm) side. **Speculation:** "The model predicted only about half the heave that was recorded by the heavograph." *If the authors had set the boundary conditions such that the ice lenses were allowed to grow on both the warm **and** the cold side, the model would have predicted twice the present value, or about the same value as recorded by the heavograph.**

Paper II-9

Konrad, J.-M. and N.R. Morgenstern. 1984. Frost heave prediction of chilled pipelines buried in unfrozen soils. *Can. Geotech. J.* 21:100-115.

Published Abstract

Frost heave is an important consideration in the design of buried chilled pipelines. A procedure for calculating the amount of heave under a chilled gas pipeline is presented based on a finite-difference formulation of the heat and mass transfer in **saturated** soils. The frost heave of the soil is characterized in terms of the segregation potential concept developed in earlier papers by the authors. Good agreement is found between the predictions of heave obtained with this procedure and that observed in long-term full-scale experiments at a test site in Calgary, Canada. Additional calculations are presented to explore the influence of pipeline temperature, pipe insulation, and ground temperature on frost heave of buried pipelines.

Annotation

General:

This paper deals with chilled pipelines and is therefore not immediately useful for our project.

Abstract: "**Good agreement is found between the predictions of heave obtained with this procedure and that observed in long-term full-scale experiments at a test site in Calgary, Canada**". *I wonder where in Calgary one can find a pipeline that is permanently submerged in **saturated** conditions.* This paper presents interesting data for Devon silt. Fig. 4 shows the relationship between the SP value and the overburden (or external) pressure, P_e .

Specific:

Page 103, RH column, end of 2nd paragraph: "If the soil is **unsaturated**, the rate of frost heave is considerably reduced." *Sooner or later, Konrad will have to come to grips with the unsaturated hydraulic conductivity.*

Page 107, RH column, 9 lines from bottom: "SP for each test is readily obtained by dividing the measured *intake* velocity by the **overall** temperature gradient near the 0 C isotherm. *What does this word **overall** mean? Konrad always insists that the SP is calculated on the basis of the temperature gradient in the frozen fringe.*

Paper II-10

Akagawa, S. 1988. Experimental study of frozen fringe characteristics. *Cold Regions Sci. and Tech.* 15:209-223.

Published Abstract

The objectives of the paper are to show the efficacy of a newly developed X-ray radiography technique for the study of frost heaving, and to discuss experimental data which reveal the characteristics of the frozen fringe.

An open-system frost heave test was conducted for about 700 hours. Lead sphere position markers, in which thermocouples are installed, were placed every 5 mm along the axis of a cylindrical 97 mm long specimen. Seventy-four X-ray radiographs were taken during the test. These X-ray radiographs show ice lenses and the lead spheres clearly. The measured coordinates and temperatures of the spheres enable precise temperature profiles to be determined for each X-ray radiograph. By referring the temperature profile to the X-ray photograph, the thickness and temperature range of the frozen fringe are determined.

The data obtained by this experiment include heave rate, water intake rate, thickness and temperature range of the frozen fringe, and strain rate distribution within the specimen. From these, the periods of in situ and/or segregation freezing and water movement are discussed.

Annotation

General:

This paper is a laboratory study. It reveals new and essential information about the formation, the location, the size, and the behaviour of ice lenses in freezing soil.

Page 219, Discussion: "The experimental results indicate that in situ freezing and segregation freezing may take place simultaneously and that water may be supplied to a growing ice (*lens*) from pore water expelled from adjacent pores by the in situ freezing within the frozen fringe, when the freezing front is advancing at a relatively high speed." *This is a useful observation. It shows that the whole process of in situ freezing and ice lens formation is a play of give and take, which, on the micro-scale, is dictated by the local availability of liquid water and the instantaneous local demand for heat.*

Specific:

Page 220, Fig 14a: Porosity is 70%. Unfrozen water content at – 5.5 C is 16%. *These are large values!* Page 222, second paragraph: "Segregation freezing is revealed at the very onset of freezing by vertical crack observation." *This must concern the formation of very small ice lenses, because for the first 5 hours of freezing ice lenses were too small for observation.*

Page 220, third paragraph: "Segregation freezing is also revealed at the very onset of freezing by the water migration observed." *This statement, together with the former one, makes the concept of "Segregation Potential", from a physical point of view, rather nebulous.*

Paper II-11

Michalowski, R.L. and M. Zhu. 2006. Frost heave modelling using porosity rate function. *Int. J. for Numerical and Analytical Methods in Geomechanics* 30(8): 703-722.

Published Abstract

Frost-susceptible soils are characterized by their sensitivity to freezing that is manifested in heaving of the ground surface. While significant contributions to explaining the nature of frost heave in soils were published in late 1920s, modelling efforts did not start until decades later. Several models describing the heaving process have been developed in the past, but none of them has been generally accepted as a tool in engineering applications. The approach explored in this paper is based on the concept of the porosity rate function dependent on two primary material parameters: the maximum rate, and the temperature at which the maximum rate occurs. The porosity rate is indicative of ice growth, and this growth is also dependent on the temperature gradient and the stress state in the freezing soil. The advantage of this approach over earlier models stems from a formulation consistent with continuum mechanics that makes it possible to generalize the model to arbitrary three-dimensional processes, and use the standard numerical techniques in solving boundary value problems. The physical premise for the model is discussed first, and the development of the constitutive model is outlined. The model is implemented in a 2-D finite element code, and the porosity rate function is calibrated and validated. Effectiveness of the model is then illustrated in an example of freezing of a vertical cut in frost-susceptible soil.

Annotation

General:

This paper is not immediately useful for our project. It contains, however, some attractive features, which may be useful, even essential, in the future development of the theory for the actual heaving process of a pipeline. This paper focuses on the "porosity (growth) rate function". An interesting feature is the definition of the POROSITY (GROWTH) RATE TENSOR (equation (4)). Such a tensor is probably required when, after the first ice has formed under the pipe, stresses and strains develop, causing the pipe to rise. The theory presented in sections 3, 4 and 5 look very attractive. Figures 8, 9 and 10 are impressive.

Last two sentences of section 3: "Consequently, the porosity (growth) rate function replaces the Darcy law for water transfer in the description of heaving soil. Owing to this formulation one does not need to make assessments of the cryogenic suction and the hydraulic conductivity in the freezing soil. The former requires making arbitrary assumptions regarding the distribution of pressure in ice, so that the (Clausius-) Clapeyron equation can be used, whereas the hydraulic conductivity changes orders of magnitude in the freezing soil, and it is not easily determined." *This sounds futuristic to me: Is this reverse thermodynamics?*

Specific:

In section 10: "FINAL REMARKS" one finds the following sentence:

"The model presented here belongs to the category of thermo-mechanic models, and makes it possible to use the continuum mechanics framework to implement it in solving boundary value problems." This seems to indicate that by means of "reverse thermodynamics", some tools in the continuum mechanics box can be brought into action.

Paper II-12

Modisette, J.P. and J.L. Modisette. 2014. Pipe line frost heave (or the lack thereof). Paper PSIG 1421. Pipeline Simulation Interest Group (PSIG) Annual Meeting, Baltimore, MD. May 6 - 9, 2014. 8 pp.

Published Abstract

The mechanism of frost heave, also known as *frost jacking*, is described as it is manifested in warm pipelines, cold pipelines, and inert objects. It is shown by both descriptions of the physical phenomena and simulations of the seasonal movement of the frost line that the transport of water in unsaturated soils dries the ground around a warm pipe so that frost heave is not expected to affect most buried pipelines.

Annotation

General:

This paper is not useful for our project. The whole paper deals with "**transport of water in unsaturated soil**". There is no mentioning of the existence of a water table or any other source of liquid water. There are disturbing sentences in this paper:

Page 1, RH column, line 2: "When water freezes it expands, by about 12% in volume (sic!).

Page 1, RH column, line 11: "Frost heave is a generic term, usually referring to any movement of the soil (is) caused by the expansion due to freezing of water in soil" *Here, the authors miss the boat completely.*

Re: Effects of Frost Jacking...: Second paragraph: "There are two mechanisms moving water in **unsaturated** ground: capillary action and differential vapor pressure". *In unsaturated soil vapour transport towards ice lenses can indeed contribute to the growth of these lenses. This is dictated*

by the Clapeyron equation. But this only happens in **very** dry soil and the effect is small. The "**capillary action**" is a cop-out. What the authors try to grasp here is the liquid transport towards the ice lens dictated by the Clapeyron equation. Here the engineers try to find a mechanistic explanation for something that is intrinsically thermodynamic. And then they say (3rd paragraph): "In frozen ground the **capillary action** stops." Herewith, they have flushed the baby down the drain.

Re: Conclusions: First paragraph: "For pipelines and rocks buried in **saturated** soil there is no transport of moisture due to temperature differences, so frost heave does **not** occur." Herewith, the authors ruined all works by Konrad.

Specific:

Section "Rocks": *This is pretty good. I like the last sentence:* "New England fields have been known for growing rocks since the time of the Pilgrims."

Paper II-13

Shen, M. and B. Ladanyi. 1987. Modelling of coupled heat, moisture and stress field in freezing soil. Cold Regions Sci. and Tech. 14: 237-246.

Published Abstract

A model for coupled heat, moisture and stress field in freezing soil is proposed. A numerical simulation for an experiment published by Penner (1986) in **saturated** soil using this model is carried out. The results of the simulation for temperature field and heave agree well with the experimental results. In addition, the stress field in freezing soil is also given by this model. The model is well adapted for solving practical frost heave problems in which the heave is coupled with deviatoric creep, such as under foundations or around chilled buried pipelines.

Annotation

General:

This paper uses the theory developed by Sheppard, Kay and Loch, 1978, which uses all the equations in Kay, Sheppard and Loch, 1977 (*Paper II-8*). It carries out a numerical simulation and finds good agreement (Fig. 3 and Fig. 4) with the experimental results of Penner (1986). Fig. 5 (page 244) shows the predicted water content as a function of the distance from the warm side at different points in time. This is of great interest. There is, however, a disturbing sentence in the write-up of this figure 5: "Discrete ice lenses cannot be predicted by the proposed model."

(page 243, RH column, line 8). The implications of this shortcoming are not clear. The soil was already saturated. So, the increase in water content must have been due to the formation of ice lenses.

Specific:

The section "Soil properties" (page 241) and the values presented in Tables 1 & 2 are of interest. In both Fig. 3 (calculated frost penetration vs. time) and Fig. 4 (calculated heave vs. time) one finds that, straight from the start, the experimental values (Penner, 1986) are larger than the calculated values. This is contrary to what is expected in light of that fact that the model does not consider a freezing point depression.

Paper II-14

Smith, M.W. and D. Onysko. 1990. Observations and significance of internal pressures in freezing soil. p. 75-81. *In Proc. 5th Canadian Permafrost Conference, Universite Laval, Collection Nordicana 54.*

Published Abstract

The development of positive internal pressures accompanying soil freezing has been observed in experiments at laboratory and field scales. The measurements are explained in terms of the pressure developed as ice grows in the soil. Prior to freezing, the measured pressure is simply indicative of the weight of the overburden, but as the freezing front advances through the soil a characteristic evolution of pressure is observed. With the passage of the freezing front there is an abrupt rise in pressure to a peak value, after which it tends to gradually fall away. This pattern appears to be temperature related. An expression is proposed based upon thermodynamic and soil mechanical considerations.

Annotation

General:

For the present project this paper is not immediately useful. **However, for the next step, the calculation of ice and heaving pressures, this paper is a must.** It is thermodynamically and mechanically sound. The calculations of the differential relations between the liquid pressure, the ice pressure and the temperature (p. 76, LH column), according to the Clapeyron equation, are correct. The data presented in Fig. 4 are extremely important. Of great interest are the links with the Caen project in France, in particular the data concerning Site1 and 2 of the Caen experiment, presented in Figs. 6 and 7. For further information about the Caen Project see the Annotations of Papers II-3 and II-5.

Specific:

Page 76, LH column, past paragraph: "...if the water phase is continuous right into the frozen ground..., then it is probable that some formation of ice lenses occurs within the frozen ground." *This is precisely why column experiments are not representative of field conditions.*

Page 78, first paragraph: "The vertical displacement of the soil associated with this is resisted by friction between the soil and the sidewall of the column". *Excellent! This makes the observation of heave in laboratory columns pretty unreliable.*

Page 78, last paragraph, and page 79: This explanation is **too mechanical**. The authors do not understand the principle of **regelation**.

Paper II-15

Black, P.B. 1995. RIGIDICE model of secondary frost heave. U.S. Army Corps of Engineers, CRREL Special Report 95-12. Hanover, NH. 33 pp.

Published Abstract

A revised version of an earlier attempt to numerically solve Miller's equations for the RIGIDICE model of frost heave is presented that corrects earlier mistakes and incorporates recent improvements in the scaling factors of ground freezing. The new version of the computer code also follows the concepts of Object Oriented Numerics (OON), which allow for easy modifications and enhancements. Analysis of the program is accomplished with the symbolic math program MathCad. A brief sensitivity analysis of the input variables indicates that those parameters that calculate the hydraulic conductivity have the greatest influence on the variability of predicted heaving pressure.

Annotation

General:

This paper is not useful for our project. What is, is the statement in the Abstract:

".....those parameters that calculate the hydraulic conductivity have the greatest influence on the variability of predicted heaving pressure." The paper uses the out-dated RIGIDICE model of frost heave. The model is designed for freezing processes in columns in the laboratory. The column must be saturated.

Specific:

Page 2, RH column, last paragraph: "The flux of water into the fringe could also be computed if the amount of heave were known." *It is remarkable how almost all researchers of the 20th century got this backwards. The upwards flux of water into the fringe (in a saturated column (sic!)) is easy to measure directly, while the relation between that flux and the heave is clouded by the friction along the inner wall of the column.*

Page 3, RH column, middle: "...the expression given by Brooks and Corey (1964)....." *The Brooks and Corey model for the water retention curve is primitive and long ago abandoned.*

Paper II-16

O'Neill, K. and R.D. Miller. 1985. Exploration of a rigid ice model of frost heave. *Water Resources Research* 21 (3): 281-296.

Published Abstract

A numerical model is explored which simulates frost heave in saturated, granular, air-free, solute-free soil. It is based on equations developed from fundamental thermo-mechanical considerations and previous laboratory investigations. Although adequate data are lacking for strict experimental verification of the model, we note that simulations produce an overall course of events together with significant specific features which are familiar from laboratory experience. Simulated heave histories show proper sensitivities in the shapes and orders of magnitude of output responses and in the relations between crucial factors such as heave rate, freezing rate, and overburden.

Annotation

General:

This paper is not immediately useful for the present project. The Rigid Ice Model is out-dated. It is meant to model the formation of ice in saturated laboratory columns. The "fundamental thermo-mechanical considerations", however, such as those exposed in the RH column of page 283 will remain quite valuable.

Specific:

Page 281, RH column, 14 lines from bottom: "The sheer number and variety of these approaches and procedures is forceful testimony to the difficulty of the problem, to the absence of any understanding of it, and to the inadequacy of any established approach for general application." (sic!)

Page 282, RH column, middle: *The comment regarding the integration of the Clapeyron equation is noteworthy.*

Page 283, RH column, top: *This is a beautiful verbalization of the processes of regelation and the upward movement of objects in freezing soil.*

Page 291, Fig. 4: *The computer results presented in Fig.4 are not useful for field conditions.*

Paper II-17

Guymon, G.L., T.V. Hromadka and R.L. Berg. 1980. A one-dimensional frost heave model based upon simulation of simultaneous heat and water flux. *Cold Regions Sci. and Tech.* 3: 253-262.

Published Abstract

A one-dimensional frost heave model is presented for unidirectional freezing in moist silts with a water table present. Frost heave is computed based upon a macro-thermodynamic model that simulates heat and moisture transfer from an element of soil undergoing freezing. It is assumed that a portion of water in the element will not freeze, and all water in addition to this amount that freezes in excess to the soil porosity results in a corresponding heave. The freezing process is assumed to be iso-thermal. Simultaneous heat and water flux are simulated by a Galerkin finite element analog of the heat equation, including convective component, and the water flux equation based upon total energy head as the state variable. The dynamic component of the problem is simulated by the Crank-Nicholson procedure, and non-linear parameters are estimated on the basis of element centered state variable values which are generated by the quadratic shape functions used. To avoid instability, the moisture sink term in the water flux equation that arises as a result of water freezing is eliminated and handled as a thermodynamic bookkeeping quantity.

Annotation

General:

This paper is useless. The abstract sounds fishy...."thermodynamic bookkeeping quantity" ? Do they mean to say "fudge factor"?

Page 260, RH column, 1st paragraph: "The proposed model was applied to a set of laboratory data as described by Berg et al. (2) with excellent results..... Table 1 shows a comparison...." *The results presented in Table 1 are so impressive, that a better model is unthinkable. Or, is all this too good to be true? There are many soil properties and fitting parameters required for the model, such as K_f and C_m in eqn. (2); the beta's in eqn. (13); and the porosity and saturated hydraulic conductivity in eqns. (19) and (20). No values for these properties and constants are presented anywhere in the paper.*

Specific:

Page 254, RH column, 10 lines from bottom: "Overburden effects are modelled by the Groenevelt and Kay (9) approximation." **What?**

APPENDIX D

Frost Penetration Depth in Soils

Frost Penetration Depth in Soils (LitRev2)

1. Climate-only models

1.1. Preface

Frost penetration in soil involves the downward movement of a 'freezing front' (or '0°C isotherm') into the ground during seasonal periods of sub-zero air temperatures in cold climate regions. The factors controlling this process (apart from climate and geographic position) include soil type, soil water content, and surface cover (vegetation, snow) (Schellekens & Williams, 1993). Figure D-1 shows a measured frost penetration profile for a bare (snow-free) roadway site in the Parry Sound District of Ontario. The frozen soil profile (denoted in blue) indicates several shallow freeze cycles through November, followed by a solid deep freeze beginning in mid-December, and a spring thaw through early April. By late February, the frost penetration depth had reached a maximum at about 140 cm. The spring thaw pattern shows that the frozen soil zone thawed from above and below, until the soil profile was completely thawed by April 25.

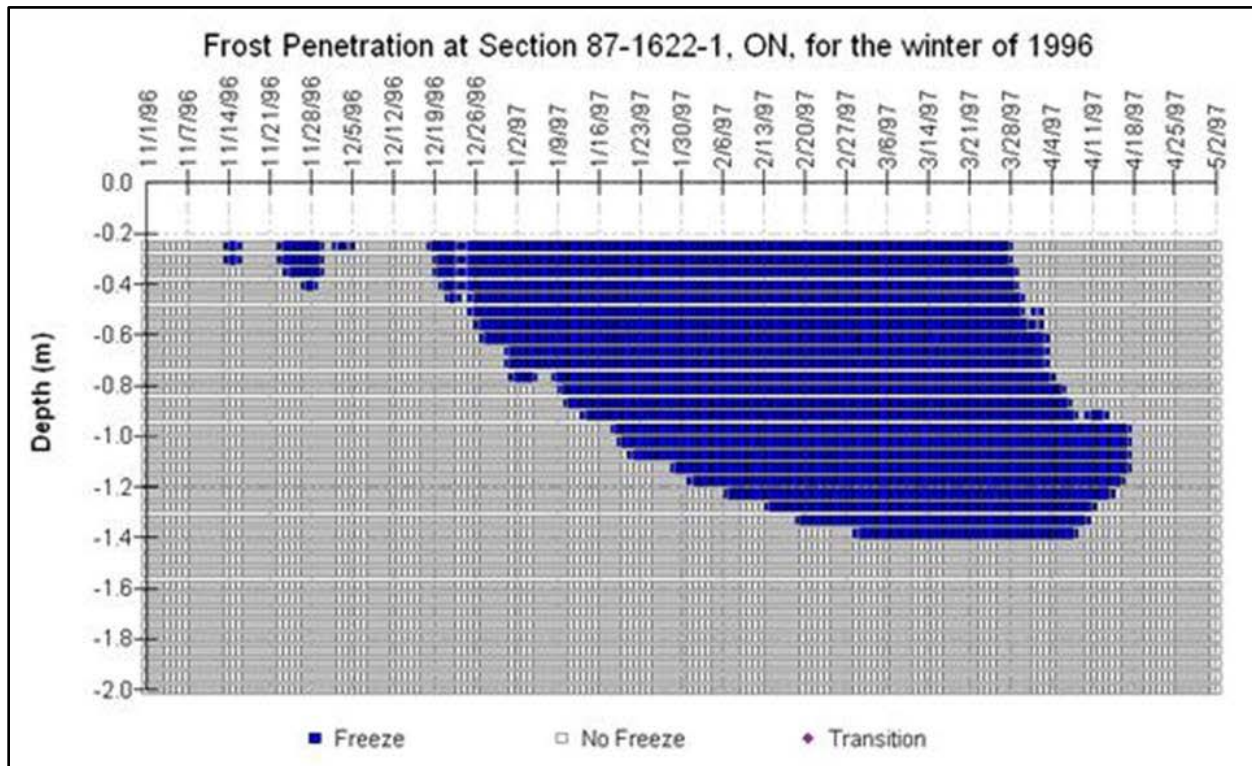


Figure D-1. A measured frost penetration profile for a bare roadway site near Parry Sound, ON (winter of 1996/97). The area denoted in blue represents frozen soil. (after Federal Highway Administration, 2008).

The three main methods of tracking the depth/thickness of frozen soil in the field include i) direct physical probing (including the use of cone penetrometers), ii) field installation of visual frost gauges (or 'frost tubes'), and iii) field measurement of soil temperature profiles using nests of resistance thermometers or thermocouples/thermistors. The use of empirical or analytical/numerical models represents a fourth method, by allowing the position of the freezing front to be estimated through the winter season (Schellekens & Williams, 1993). Examples of widely used models that are 'time-tested and proven' are:

- i) empirical ('freezing index' [°C·day] method)
- ii) analytical/numerical (SHAW model)

These two models will be discussed in some detail in the following sections.

1.2 Concepts of freezing and thawing degree-days (and 'freezing index')

The term 'degree-day' is simply defined as a measure of the departure of the mean daily air temperature from a reference air temperature. These departures can be accumulated over defined periods of time, and used as an 'index' of the effect of air temperature on a variable of interest (Boyd, 1976). Depending on the particular degree-day index, temperature departures can be treated in one of two different ways, as follows:

- i) countervailing departures are treated as zero, and do not contribute to the accumulated total
e.g., the 'growing degree-day' (GDD) variable is based on positive departures above the reference air temperature (i.e., 5°C in Canada). GDD is used by agronomists/farmers to gauge heat accumulation during the growing season (May - Sept. in Canada) in order to predict plant/crop phenological development rates, etc. Negative departures are treated as zero and have no effect on the accumulated total
- ii) countervailing departures do contribute to the accumulated total
e.g., the 'freezing degree-day' (FDD) variable is based on negative departures below the reference air temperature (i.e., 0°C). Any countervailing departures above the reference air temperature (referred to as the 'thawing degree-day' [TDD] variable) decrease the accumulated FDD total

It is important to clarify the units and dimensions of FDD (and TDD). In the literature, the units for FDD are typically reported as '°C-days', which can be misinterpreted. The dimensions of FDD are [T · t], where 'T' is temperature' and 't' is time. Therefore, the correct units of FDD are '°C·day'.

Calculation of the FDD and TDD variables are as follows (Boyd, 1976):

$$\text{FDD or TDD} = \sum(\bar{T} - 0^{\circ}\text{C}) \quad \text{Eqn. D-1}$$

where: FDD = freezing degree-days (°C·day)

TDD = thawing degree-days (°C·day)

\bar{T} = mean daily air temperature (°C) = $0.5(T_1 + T_2)$

T_1 = maximum daily air temperature (°C)

T_2 = minimum daily air temperature (°C)

The effect of TDDs on the accumulated FDD total can be seen in Fig. D-2. By tracking the FDD total from Nov. 2007 to April 2008 for a site south of Buffalo, NY, it is clear that there were several brief thaw periods through the winter of 2007/08, including a week-long 'January thaw' from Jan. 4 to 11, 2008 (Vermette & Christopher, 2008).

Figure D-3 shows a more generalized schematic of seasonal data similar to that in Fig. D-2 in order to illustrate the method used to determine the 'freezing index' (FI). In general terms, FI is the product of i) the number of degrees (°C) that the air temperature is below the freezing point of water (0°C), and ii) the time (in days), integrated over a time period of interest. More specifically, FI is defined as the number of degree-days (above and below 0°C) between the highest point in the autumn and the lowest point in the spring on the cumulative degree-day vs. time curve for a winter season (Chisholm & Phang, 1981), as shown in Fig. D-3. Any autumn or spring month that encompasses a seasonal maximum or minimum in FDDs is referred to as a 'change-over' month (i.e., Nov. and April in Fig. D-3, respectively). The method of tallying FDDs

and TDDs in 'change-over' months is more complex than the simple algorithm shown in Eqn. D-1, and that method is described in Boyd (1976).

1.3 Relationship between freezing index and freezing front depth

Much of the research on frost penetration depth has been carried out by highway engineers working with asphalt/concrete surfaces (e.g., roads or airport runways/aprons) or aggregate surfaces that are free of snow and ice. Hence, the knowledge/technology acquired in the engineering field can be transferred to other fields of study interested in freezing of bare soils (i.e., no snow or vegetation cover). Bare soils represent the 'worst case scenario' in terms of the maximum depth of the freezing front, because there is no insulating cover of snow or vegetation (Boyd, 1976).

Figure D-2 shows a strong correlation between accumulated FDDs through a winter season and the depth to the freezing front, until the spring 'change-over' month (March, in this case) is encountered. The 'lack of fit' during the spring 'change-over' month has prompted researchers to recently propose adjustments to the established procedures for FDD accumulation, as follows:

- i) a better predictive tool is to relate frost penetration depth to the 'rate' at which FDDs are accumulated, expressed as FDD day⁻¹ (Vermette & Christopher, 2008)
- ii) an addendum to the 'rate' adjustment noted in (i) above, is the addition of adjustments for daylength and sun angle (Vermette & Kanack, 2012)

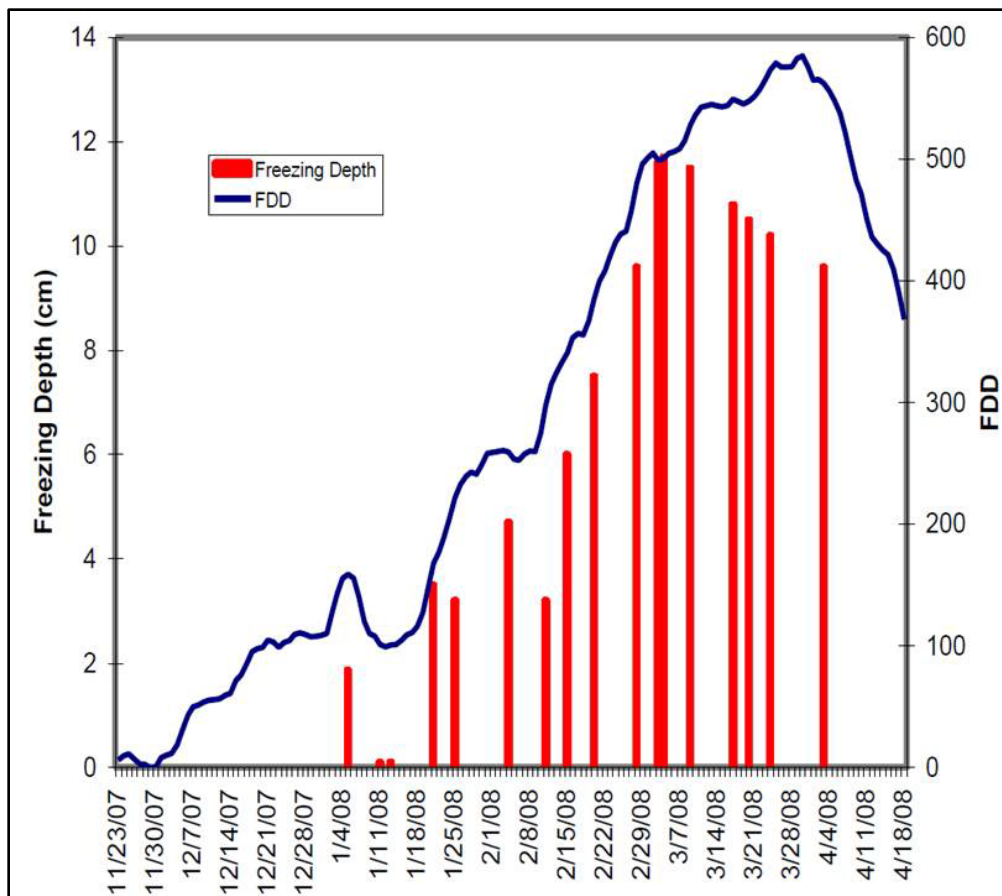


Figure D-2. Plot of accumulated FDDs vs. depth of frost penetration. (after Vermette & Christopher, 2008).

These proposed refinements have not been adopted in the PARSC - 003 study because of the following:

- i) the reported predictive capability of the simple FI method is sufficiently precise for the Tier 1 model in this study (see [i] above)
- ii) the daylength and sun angle refinements have their largest beneficial effect on the predictive capability during the spring 'change-over' month when frost heave is no longer a significant risk (see [ii] above)

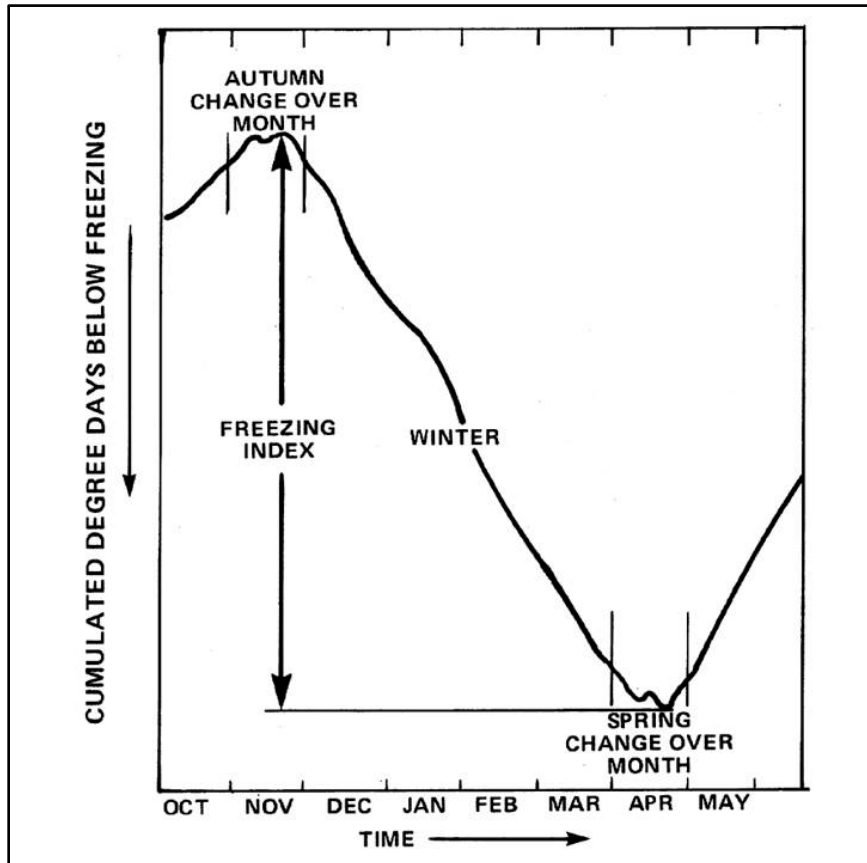


Figure D-3. Calculation of the freezing index.
(after Chisholm & Phang, 1981).

When the maximum depth of frost penetration is plotted against FI, many researchers have noted a strong curvilinear relationship (Brown, 1964). The root function shown in Fig. D-4 is a Canadian example based on 5 years of data (1970-75) collected on highway sites by the Ontario Ministry of Transportation and Communications (Chisholm & Phang, 1981). Equation D-2 is widely used in Ontario and elsewhere to estimate the dependent variable (maximum depth of frost penetration) from a single independent variable (freezing index).

$$P = -0.328 + 0.0578 \sqrt{FI} \quad \text{Eqn. D-2}$$

where: P = maximum depth of frost penetration (m)

FI = freezing index (°C·day)

Equation D-2 is shown as the solid line in Fig. D-4. A second regression equation was created independently from Eqn. D-2 (shown as the broken line in Fig. D-4), but it was virtually identical. Both equations were formulated by the Ontario Ministry of Transportation and Communications (Chisholm & Phang, 1981). It should also be noted that both equations do not pass directly through the origin of the plot, which causes both functions to estimate slightly negative frost penetration depths if FI is very low. Equation D-2 suggests that FI must reach a low threshold level (FI = 34 °C·day) before any measurable frost penetration (1 cm) would be apparent (Chisholm & Phang, 1981).

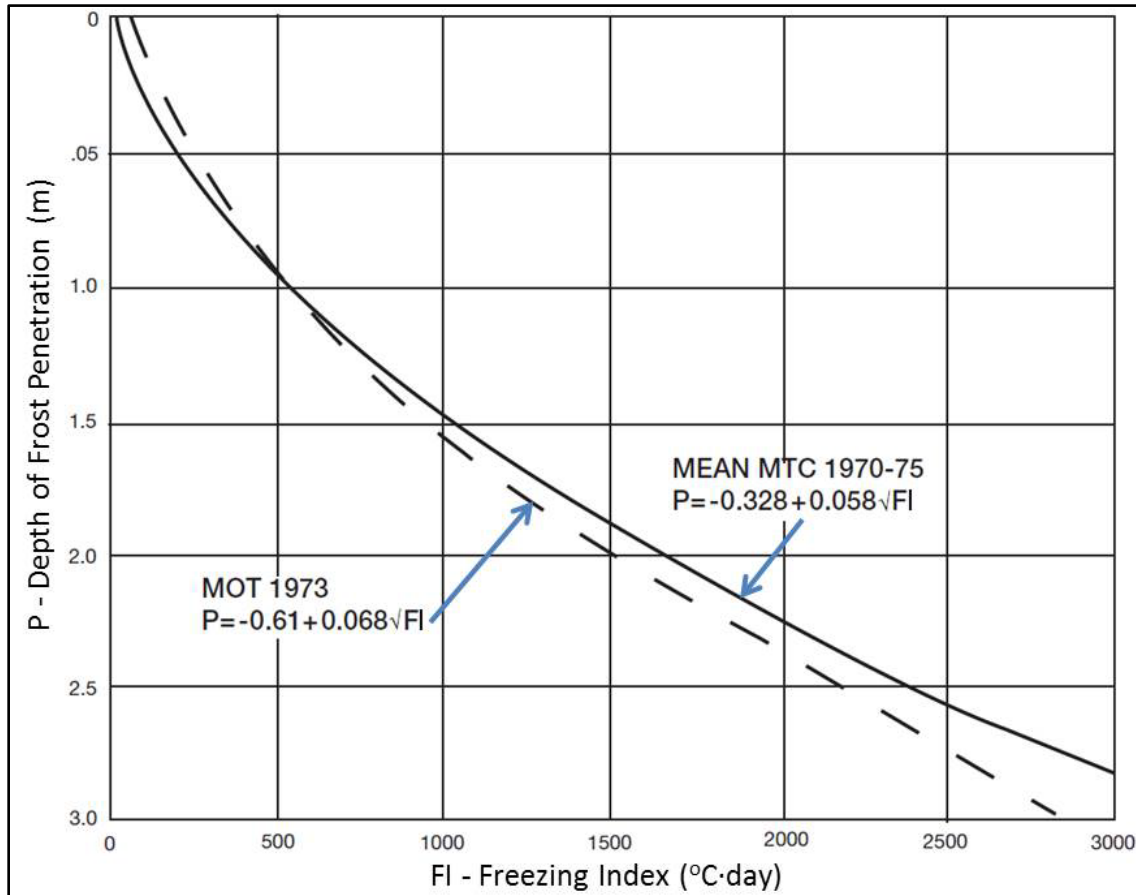


Figure D-4. Simple regression equations that can be used to estimate the maximum depth of frost penetration in Ontario from the freezing index. (after Chisholm & Phang, 1981).

Table D-1 has been assembled by applying Eqn. D-2 to calculated FI data from meteorological stations across Canada (Dow Chemical Company, 2008).

Table D-1. Freezing index (°C·day) and estimated freezing front depth for 177 locations across Canada (after Dow Chemical Company, 2008).

Station	Freezing Degree-Days (°C·day)	Max. Frost Penetration Depth (cm)
British Columbia		
Abbotsford A	25	0
Beaton River A	2,164	237
Comox A	331	73
Cranbrook A	730	124
Dog Creek A	809	132
Fort Nelson A	2,513	258
Fort St. John A	1,582	198
Kamloops A	335	73
Kimberley A	797	131
New Westminster	19	0
Penticton A	174	44
Port Hardy A	18	0
Prince George A	928	144
Prince Rupert A	36	2
Princeton A	617	111
Quesnel A	809	132
Sandspit A	19	0
Smithers A	832	134
Smith River A	2,703	269
Terrace A	354	76
Tofino A	11	0
Vancouver A	17	0
Victoria A	16	0
Williams Lake A	489	95
Yukon Territory		
Aishihik A	2,799	274
Dawson	3,430	307
Haines Junction	2,499	257
Mayo	3,030	286
Snag A	3,598	315
Teslin A	2,086	232
Watson Lake A	1,823	215
Whitehorse	1,986	226
Northwest Territories		
Cape Dyer A	3,921	330
Coral Harbour A	4,751	367
Fort McPherson	4,304	348
Frobisher Bay A	3,903	330
Hay River A	3,062	288
Inuvik A	4,680	364
Norman Wells A	3,903	330
Resolute Bay A	6,203	424
Tuktoyaktuk	4,919	374
Yellowknife A	3,614	316
Alberta		
Banff	1,091	159
Calgary A	995	150
Cold Lake A	1,763	211
Cowley A	785	130
Edmonton A	1,441	187
Embarras A	2,466	255
Fort McMurray A	2,236	241
Grande Prairie A	1,648	203
Jasper	1,047	155
Lake Louise	1,561	196
Lethbridge A	737	125
Medicine Hat A	1,005	151
Peace River A	2,114	234
Penhold A	1,437	187
Red Deer	1,323	178
Suffield A	1,255	173
Vermilion A	1,790	213
Saskatchewan		
Broadview A	1,802	213

Table D-1 (cont'd.)

Dafoe A	2,068	231
Estevan A	1,470	190
Moose Jaw A	1,419	186
North Battleford A	1,877	218
Prince Albert A	2,077	232
Regina A	1,764	211
Saskatoon A	1,824	215
Swift Current A	1,846	216
Uranium City A	3,084	289
Yorkton A	1,799	213
Manitoba		
Brandon A	1,882	219
Churchill A	3,721	321
Flin Flon	2,377	250
Gimli A	1,898	220
MacDonald A	1,688	205
Neepawa A	1,823	215
Portage La Prairie A	1,586	198
Rivers A	1,842	216
Winnipeg A	1,806	214
Ontario		
Algonquin Park	1,193	168
Belleville	635	113
Brampton	570	106
Brantford	439	89
Chalk River	1,164	165
Chatham	295	67
Cochrane	1,838	216
Collingwood	542	102
Dryden	1,886	219
Georgetown	602	110
Guelph	586	108
Hamilton	368	78
Huntsville	920	143
Iroquois Falls	1,882	219
Kapuskasing A	1,911	221
Kenora A	1,762	211
Kingston	678	118
Kirkland Lake	1,802	213
Kitchener	546	103
Lindsay	803	132
London A	479	94
Moosonee	2,267	243
Niagara Falls	380	80
North Bay	1,228	170
Orangeville	791	130
Orillia	831	134
Ottawa A	1,016	152
Owen Sound	553	104
Parry Sound	843	136
Peterborough	758	127
Port Arthur (Thunder Bay)	1,412	185
St. Catharines	281	64
St. Thomas	394	82
Samia	372	79
Sault Ste. Marie A	924	144
Simcoe	417	86
Sioux Lookout A	1,917	221
Stratford	596	109
Sudbury A	1,334	179
Timmins A	1,756	210
Toronto	349	76
Toronto A	498	97
White River	1,858	217
Windsor A	314	70
Woodstock	516	99

Table D-1 (cont'd.)

Québec		
Bagotville A	1,593	199
Baie Comeau A	1,399	184
Chicoutimi	1,409	185
Drummondville	1,015	152
Gagnon A	2,342	248
Gaspé	1,118	161
La Malbaie	1,135	163
Mont Laurier	1,292	176
Montréal A	879	139
Québec	1,012	152
Québec A	1,144	163
Sept-Îles A	1,526	194
Sherbrooke	878	139
Sorel	1,109	160
Tadoussac	1,132	162
Three Rivers	1,188	167
New Brunswick		
Edmundston	1,233	171
Fredericton A	867	138
Moncton A	776	129
Pennfield Ridge A	654	116
Sackville	652	115
St. George	619	112
Saint John	557	104
Saint John A	632	113
Sussex	743	125
Woodstock	945	145
Nova Scotia		
Annapolis Royal	329	72
Cheticamp	531	101
Debert A	631	113
Greenwood A	453	91
Halifax	309	69
Halifax A	476	94
Ingonish Beach	460	92
Liverpool	252	59
Shearwater A	388	81
Springfield	518	99
Sydney A	451	90
Truro	569	106
Yarmouth A	231	55
Prince Edward Island		
Alliston	556	104
Charlottetown A	667	117
Summerside A	690	120
Newfoundland		
Argentia A	264	61
Bonavista	474	93
Buchans A	958	147
Churchill Falls A	2,677	267
Comer Brook	622	112
Gander International A	671	117
Goose A	1,816	214
Grand Falls	774	129
St. John's	360	77
Stephenville A	514	99
Wabush Lake A	2,604	263

NOTE: place names followed by 'A' indicates that meteorological data originated from an airport weather station

It is noteworthy that the estimated maximum depth of frost penetration for Parry Sound, ON based on 30-year climatic normals is 136 cm (Table D-1), while an example (measured) frost penetration profile for a bare (snow-free) roadway site in the same area of Ontario was about 140 cm (Fig. D-1).

Table D-2 summarizes much of the large amount of data contained in Table D-1 (i.e., 159 estimated depths of maximum frost penetration in southern Canada). The region of the country north of 60°N latitude (NT, NU, YT) was excluded in the Table D-2 analysis since the study area for this project (PARSC - 003) includes only southern Canada. Use of the 90 and 120 cm depth thresholds in Table D-2 reflects the recommendation by PARSC that a pipeline depth range of 90 to 120 cm (to the top of the pipeline) be used in any frost heave simulations in this study (see Appendix E).

In southern Canada as a whole, only about 18% and 38% of the meteorological stations showed estimated frost depths of < 90cm and < 120 cm, respectively. At the provincial level, some large regional disparities emerge. For example, the three prairie provinces (AB, SK, MB) and QC show no meteorological stations where the freezing front would not encounter even the deepest pipeline placement (i.e., at 120 cm) during a normal winter season. It must be re-emphasized, however, that the FI method represents a 'worst case scenario' for freezing front depth since it presumes a bare soil condition throughout the winter season (i.e., no snow or vegetation cover to insulate the soil from frigid air temperatures), akin to a roadway surface (Boyd, 1976).

Table D-2. Summary of data in Table D-1 by province and nationwide.

Meteorological Station Location	Total	Maximum estimated frost penetration depth (cm)	
		< 90 cm	< 120 cm
----- # of meteorological stations -----			
BC	24	12	14
AB	17	0	0
SK	11	0	0
MB	9	0	0
ON	45	10	21
QC	16	0	0
NB	10	0	5
NS	13	5	13
PE	3	0	2
NL	11	2	6
Canada (excluding NT, NU, YT)	159	29	61

Figure D-5 shows the most recent rendition available (based on 30-year climatic normals [1951-80]) of the mapped spatial distribution of isotherms across Canada, where the isotherms represent the annual total FDDs (below 0°C) (Env. Canada, 1988). The map has been generated using the same sort of locational point data from meteorological stations (30-year climatic normals) that are contained in Table D-1.



Figure D-5. Map of annual total freezing degree-days below 0°C across Canada. (after Environment Canada, 1988).

1.4 Relationship between freezing index and frost heave

Gandahl (1977) assembled data from a number of multi-year roadway test sites in Sweden in order to directly relate the measured degree of frost heave to FI. While it is known that the function relating maximum frost penetration depth to FI is quite curvilinear (Brown, 1964), as seen in Fig. D-4, Gandahl (1977) showed that the function relating frost heave to FI was strongly linear for most of the test sites (i.e., strong positive correlation). Figure D-6 shows an example plot from one of the test sites, where FI explained 96% of the variation in frost heave ($r^2 = 0.960$). As with Fig. D-4, the function shown in Fig. D-6 does not pass through the origin of the plot, which will cause the function to estimate slightly negative frost heave values if FI is very low. The equation shown in Fig. D-6 suggests that FI must reach a low threshold level (FI = 111 °C·day) before any measurable frost heave (1 cm) would be apparent (Gandahl, 1977). Gandahl (1977) also noted

that the depth to the groundwater table was the dominant site variable influencing the magnitude of the quotient 'FI/frost heave'. This finding is consistent with the view of Groenevelt & Grant (2013) that it is the hydraulic conductivity (saturated or unsaturated) of the unfrozen soil (beneath the frozen fringe) that primarily determines soil susceptibility to frost heave.

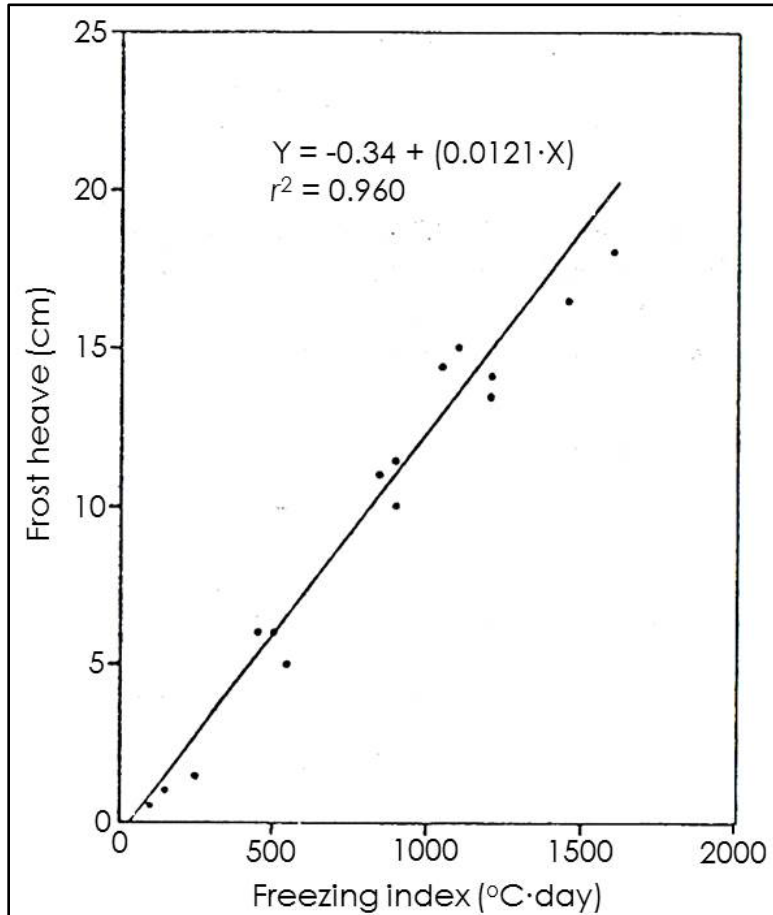


Figure D-6. Linear regression of frost heaving (cm) against freezing index (°C·day) for an example road test section in Sweden. (after Gandahl, 1977).

2. Climate and soil models

2.1 Preface

Section 1 (above) dealt with empirical 'climate-only' models with respect to estimation of the maximum depth of frost penetration in winter. Climate-only models generally assume a 'bare soil' surface condition (i.e., no snow or vegetation cover). In instances where it is important to simulate the downward migration of the 0°C isotherm in the soil with different types of insulating covers, much more sophisticated analytical/numerical models are required.

Most researchers with an interest in estimating the depth of frost penetration in cold climate regions regard the SHAW (Simultaneous Heat and Water) model of Flerchinger & Saxton (1989) as i) 'time-tested and proven', and ii) the 'state-of-the-art' model of choice for most freezing soil applications.

The following illustrates the prominence of the SHAW model in the soil research community. DeGaetano *et al.* (1996) developed a physically-based soil freezing model that was applied across the continental U.S. (DeGaetano *et al.*, 1997; 2001). The model estimated the maximum depth of frost penetration primarily by simulating the process of thermal diffusion, and as such had very modest data input requirements (i.e., daily air temperature, snow depth, precipitation). DeGaetano *et al.* (2001) pointed out, however, that numerous refinements have been made to this model since its inception by incorporating new sub-routines based on those contained in the 'state-of-the-art' SHAW model of Flerchinger & Saxton (1989).

2.2 Some examples of past studies involving the SHAW model

In the U.S., Kennedy & Sharratt (1998) evaluated the comparative ability of the SHAW (Flerchinger & Saxton, 1989) and SOIL (Jansson, 1991) models in estimating the depth and timing of freezing fronts in Alaska and Minnesota. Both models estimated the depth of the freezing front reasonably well when the simulated snow depth agreed with recorded snow depth. Lin & McCool (2006) also concluded that their energy budget approach to simulating the magnitude and variations in the depth of snow cover and depth of frost penetration was inferior to the '1D finite difference' SHAW (Flerchinger & Saxton, 1989) and SOIL (Jansson, 1991) models.

In Canada, Hayhoe (1994) reported that the SHAW model estimated snow depth, maximum depth of frost penetration, and the date of last day of snow cover very well. Fallow *et al.* (2004; 2007) successfully used the SHAW model to conduct risk assessments of unsuitable winter soil conditions for field-based farm operations. Kahimba *et al.* (2009) successfully used the SHAW model to estimate soil temperature and water content profiles, as well as the depth of frost penetration in agricultural soils in Manitoba. Wang *et al.* (2010) used the SHAW model to estimate soil water content profiles for continuous wheat rotations in Alberta.

Overseas, Li *et al.* (2012) and Zhang *et al.* (2012) successfully used the SHAW model to investigate overwinter soil hydrological and temperature dynamics in alpine cold regions of northern China. Khalili *et al.* (2012) also successfully applied the SHAW model in estimating the maximum depth of frost penetration in cold climate (arid and semi-arid) regions of Iran.

2.3 SHAW (Simultaneous Heat and Water) model

2.3.1 Overview of the SHAW model

The following is an abridged version of the SHAW model overview publication released by USDA-ARS (2004). Full technical documentation for the SHAW model can be found in Flerchinger (2000).

2.3.1.1 Technical background

The Simultaneous Heat and Water (SHAW) model is a one-dimensional (1D) finite difference model originally developed to simulate soil freezing and thawing (Fig. D-7). The model's ability to simulate heat and water movement through plant cover, snow, residue and soil for predicting climate and management effects on soil freezing, snowmelt, runoff, soil temperature, water, evaporation, and transpiration has been well demonstrated.

The SHAW 1D model simulates a one-dimensional vertical profile extending from the top of a plant canopy or the snow, residue or soil surface to a specified depth within the soil. The system is represented by integrating detailed physics of vegetative cover, snow, residue and soil into one simultaneous solution. The model is sufficiently flexible to represent a broad range of conditions and the system may or may not include a vegetative canopy, snow, or a residue layer. Interrelated heat, water and solute fluxes are computed throughout the system and include the effects of soil freezing and thawing. Daily or hourly predictions include evaporation, transpiration, soil frost depth, snow depth, runoff and soil profiles of temperature, water, ice and

solutes.

Weather conditions above the upper boundary and soil conditions at the lower boundary define heat and water fluxes into the system. Water and heat flux at the surface boundary include absorbed solar radiation, long-wave radiation exchange, and turbulent transfer of heat and vapor. A layered system is established through the vegetation canopy, snow, residue and soil, with each layer represented by a 'node'.

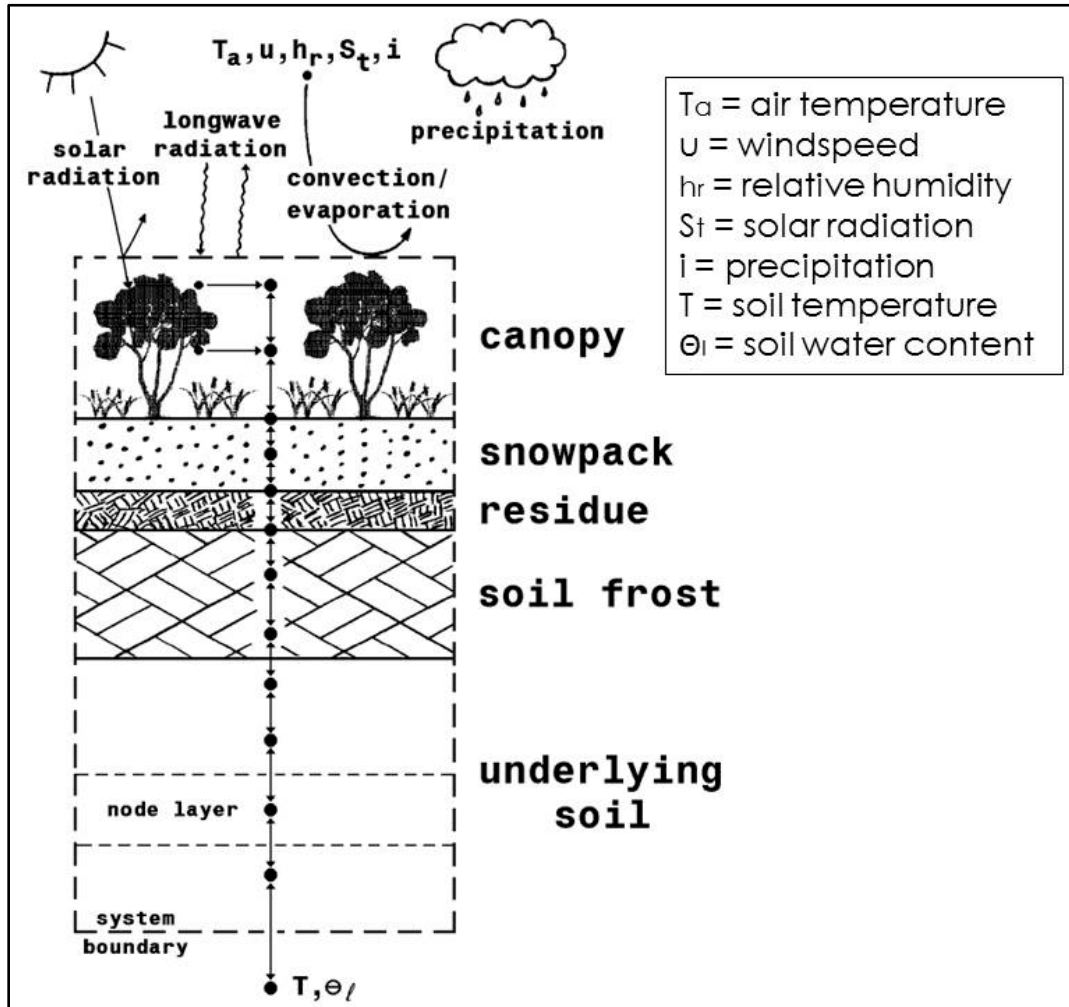


Figure D-7. The biogeoclimatic system as described by the 1D SHAW model. (after Flerchinger, 2000).

2.3.1.2 Soil freezing and thawing

The SHAW 1D model represents one of the more detailed models of snowmelt and soil freezing and thawing. The SHAW model was originally developed by Flerchinger & Saxton (1989), and later updated by Flerchinger & Pierson (1991) and Flerchinger *et al.* (1996). The model is capable of simulating the complex wintertime phenomena of snow accumulation and melt, detailed soil freezing and thawing (including freezing-induced moisture migration), solute effects, frost formation, solute translocation, and frozen soil related runoff. Heat, water and solute equations are solved iteratively until a simultaneous solution is found.

2.3.1.3 Snow accumulation and melting

Energy and mass transfer calculations for snow within the SHAW 1D model are patterned after the point energy and mass balance model developed by Anderson (1976). The energy balance of the snow includes solar and long-wave radiation exchange, sensible and latent heat transfer at the surface, and vapor transfer within the snowpack. Absorbed solar radiation, corrected for local slope, is based on measured incoming short-wave radiation, with albedo estimated from grain size, which in turn is estimated from snow density. Liquid water is routed through the snowpack using attenuation and lag coefficients, and the influence of metamorphic changes of compaction, settling and grain size on density and albedo are considered.

2.3.1.4 Input data requirements

Input data requirements for the SHAW 1D model include: initial snow depth and density; initial soil temperature and water content profiles; daily or hourly weather conditions (air temperature, wind speed, humidity, precipitation and solar radiation); general site information; and parameters describing the vegetative cover, snow, residue and soil. General site information includes slope, aspect, latitude, and surface roughness parameters. Residue or litter properties include residue loading, thickness of the residue layer, percent cover and albedo. Input soil parameters are dry bulk density, saturated hydraulic conductivity, as well as coefficients for the matric potential-water content relation, and the albedo-water content relation.

3. Summary (Appendix D)

A simple 'climate-only' model (i.e., requiring only air temperature data) was required to estimate the maximum depth of frost penetration for the reconnaissance 'Tier 1' frost heave modeling effort. It was concluded from this literature review that the 'freezing index' ($^{\circ}\text{C}\cdot\text{day}$) scheme is the recommended method of choice for the PARSC - 003 study (see Table D-1).

A more complex 'climate and soil' model was required to estimate the depth of frost penetration for the 'Tiers 2 and 3' frost heave modeling effort. It was concluded from this literature review that the SHAW 1D model is the recommended method of choice for the PARSC - 003 study.

References (Appendix D)

Anderson, E.A. 1976. A point energy and mass balance model of a snow cover. NOAA Tech. Rep. NWS 19, U.S. Department of Commerce, National Oceanic and Atmosphere Administration, National Weather Service, Silver Spring, MD. 150 pp.

Boyd, D.W. 1976. Normal freezing and thawing degree-days from normal monthly temperatures. Can. Geotech. J. 13:176-180.

Brown, W.G. 1964. Difficulties associated with predicting depth of freeze or thaw. Can. Geotech. J. 1(4):215-226.

Chisholm, R.A. and W.A. Phang. 1981. Aspects of prolonged exposure of pavements to sub-zero temperatures. Part 1 - Measurement and prediction of frost penetration in highways. Policy Planning and Research Division, Ontario Ministry of Transportation and Communications, Downsview, ON. 75 pp.

DeGaetano, A.T., M.D. Cameron and D.S. Wilks. 2001. Physical simulation of maximum seasonal soil freezing depth in the United States using routine weather observations. *J. Applied Meteorology* 40:546-555.

DeGaetano, A.T., D.S. Wilks and M. McKay. 1996. A physically-based model of soil freezing in humid climates using air temperature and snow cover data. *J. Applied Meteorology* 35(6):1009-1027.

DeGaetano, A.T., D.S. Wilks and M. McKay. 1997. Extreme-value statistics for frost penetration depths in northeastern United States. *J. Geotech. Geoenviron. Eng.* 123(9):828-835.

Dow Chemical Company. 2008. Calculating insulation needs to fight frost heave by comparing freezing index and frost depth. 5 pp. Available at: http://msdssearch.dow.com/PublishedLiteratureDOWCOM/dh_01f6/0901b803801f6296.pdf?filep ath=styrofoam/pdfs/noreg/178-00754.pdf&fromPage=GetDoc (verified Oct. 6, 2014)

Environment Canada. 1988. Annual total freezing degree-days below 0°C. Climatic Atlas (Canada). Available at: http://climate.weather.gc.ca/prods_servs/historical_publications_e.html (verified Oct. 6, 2014)

Fallow, D.J., D.M. Brown, J.D. Lauzon and G.W. Parkin. 2007. Risk assessment of unsuitable winter conditions for manure and nutrient application across Ontario. *J. Environ. Quality* 36:31-43.

Fallow, D.J., J.D. Lauzon, D.M. Brown, and G.W. Parkin. 2004. Identification of the variation in risk of winter conditions across Ontario. Report prepared for the Ontario Ministry of Agriculture, Food and Rural Affairs, Guelph, ON. March, 2004. 23 pp.

Federal Highway Administration. 2008. Long-term pavement performance computed parameter: frost penetration. Chapter 7. Frost penetration analysis results. U.S. Dep't. of Transportation. Available at: <http://www.fhwa.dot.gov/publications/research/infrastructure/pavements/ltpp/08057/07.cfm> (verified Oct. 6, 2014)

Flerchinger, G.N. 2000. The Simultaneous Heat and Water (SHAW) model. Technical Report NWRC 2000-09, Northwest Watershed Research Centre, USDA, Agricultural Research Service, Boise, ID. 37 pp. Available at: <http://www.usmarc.usda.gov/SP2UserFiles/Place/53620000/ShawDocumentation.pdf> (verified Oct. 6, 2014)

Flerchinger, G.N. and F.B. Pierson. 1991. Modeling plant canopy effects on variability of soil temperature and water. *Agr. and Forest Meteorol.*, 56:227-246.

Flerchinger, G.N. and K.E. Saxton. 1989. Simultaneous heat and water model of a freezing snow-residue-soil system I. Theory and development. *Transactions ASAE* 32:565-571.

Flerchinger, G.N., J.M. Baker and E.J.A. Spaans. 1996. A test of the radiative energy balance of the SHAW model for snowcover. *Hydrol. Proc.*, 10:1359-1367.

Gandahl, R. 1977. Frost heaving on roads in relation to freezing index. p. 206-215. *In* D. Anderson, A. Jacobsson and R. Pusch (eds.). *Proc. Int'l. Symp. Frost Action in Soils*, Vol. 1, Lulea, Sweden.

- Groenevelt, P.H. and C.D. Grant. 2013. Heave and heaving pressure in freezing soils: A unifying theory. *Vadose Zone J.* 12(1). 11 pp.
- Hayhoe, H.N. 1994. Field testing of simulated soil freezing and thawing by the SHAW model. *Can. Agric. Eng.* 36(4):279-285.
- Jansson, P-E. 1991. Soil water and heat model. Technical description. Report no. 165, Dep't. of Soil Science, Swedish Univ. Agric. Sci., Uppsala, Sweden.
- Kahimba, F.C., R. Sri Ranjan and D.D. Mann. 2009. Modeling soil temperature, frost depth, and soil moisture redistribution in seasonally frozen ground. *Applied Engineering in Agriculture* 25:871-882.
- Kennedy, I. and B. Sharratt. 1998. Model comparisons to simulate soil frost depth. *Soil Sci.* 163(8):636-645.
- Khalili, A., H. Rahimi and Z. Aghashariatmadary. 2012. Validation of SHAW model in determination of maximum soil frost depth in typical arid and semi-arid zones of Iran. *J. Agr. Sci. Tech.* 14:1185-1192.
- Li, Z., L. Ma, G.N. Flerchinger, L. Ahuja, H. Wang and Z. Li. 2012. Simulation of overwinter soil water and soil temperature with SHAW and RZ-SHAW. *Soil Sci. Soc. Am. J.* 76:1548-1563.
- Lin, C. and D.K. McCool. 2006. Simulating snowmelt and soil frost depth by an energy budget approach. *Transactions ASABE* 49(5):1383-1394.
- Schellekens, F.J. and P.J. Williams. 1993. Depth of frost penetration. p. 807-814 *In* M.R. Carter (ed.) *Soil Sampling and Methods of Analysis*. Canadian Society of Soil Science. CRC Press, Lewis Publishers, Boca Raton, FL.
- USDA-ARS. 2004. Overview of the SHAW model. United States Department of Agriculture, Agricultural Research Service. 6 pp. Available at: <http://www.ars.usda.gov/SP2UserFiles/Place/53620000/SHAWSummary.pdf> (verified Oct. 6, 2014)
- Vermette, S.J. and S. Christopher. 2008. Using the rate of accumulated freezing and thawing degree days as a surrogate for determining freezing depth in a temperate forest soil. *Middle States Geographer* 41:68-73.
- Vermette, S.J. and J. Kanack. 2012. Modeling frost line soil penetration using freezing degree-day rates, day length, and sun angle. p. 143-156. *In* M. Pelto and R. Kelly (eds.), 69th Eastern Snow Conference, Claryville, NY.
- Wang, H., G.N. Flerchinger, R. Lemke, K. Brandt, T. Goddard and C. Sprout. 2010. Improving SHAW long-term soil moisture prediction for continuous wheat rotations, Alberta, Canada. *Can. J. Soil Sci.* 90:37-53.
- Zhang, Y., G. Cheng, X. Li, X. Han, L. Wang, H. Li, X. Chang and G.N. Flerchinger. 2012. Coupling of a simultaneous heat and water model with a distributed hydrological model and evaluation of the combined model in a cold region watershed. *Hydrological Processes* <http://dx.doi.org/10.1002/hyp.9514>.

APPENDIX E
Pipeline Depth

Pipeline Depth (LitRev3)

1. Background

Activities within pipeline ROWs are governed by the *National Energy Board Act*, the *Pipeline Crossing Regulations*, and agreements negotiated between landowners and pipeline companies (NEB, 2010, p. 31). For example, landowners require written approval to install sub-surface drainage systems, or to till to depths greater than 30 cm within a pipeline ROW (see Fig. 2.10 [Volume 1]). Nevertheless, it is in the best interest of pipeline companies to ensure that pipelines installed in cropland areas are sufficiently deep to protect them from incidental contact from normal farm operations (i.e., 'factor of safety').

Sub-surface tile drainage is a common practice in all Canadian provinces, outside of the semi-arid croplands of southern Alberta and Saskatchewan (Madramootoo *et al.*, 2007). For example, about 43% (1.5M ha) of Ontario's total cropland has been tile drained to date (Fraser & Fleming, 2001), and the tiled area is increasing rapidly given that over 30,000 km of perforated pipe are installed annually across the province (Pearce, 2011). Recommended tile drain depths range from 60 cm in fine-textured soils, to 120 cm in coarse-textured soils (OMAFRA, 2007). In cropland areas in Ontario, pipeline companies generally try to ensure that pipelines are placed deeper than existing or proposed sub-surface file drain systems or municipal drains (E. Mozuraitis, per. comm., 2013).

The significance of the above is revealed if minimum 'depth of cover' (DOC) criteria are contrasted for Alberta (regulated provincially) and Ontario (not regulated provincially). Pipelines traversing cropland areas in Alberta must have at least 80 cm of soil cover in accordance with the 'Pipeline Rules' (Province of Alberta, 2005), which suggests that normal farm operations in that province rarely (if ever) reach this depth. The concentration of transmission (hydrocarbon) pipelines in Alberta, in comparison to much of the remainder of the country (Fig. E-1), underscores the need for comprehensive, dedicated legislation (i.e., 'Pipeline Act') in that province.

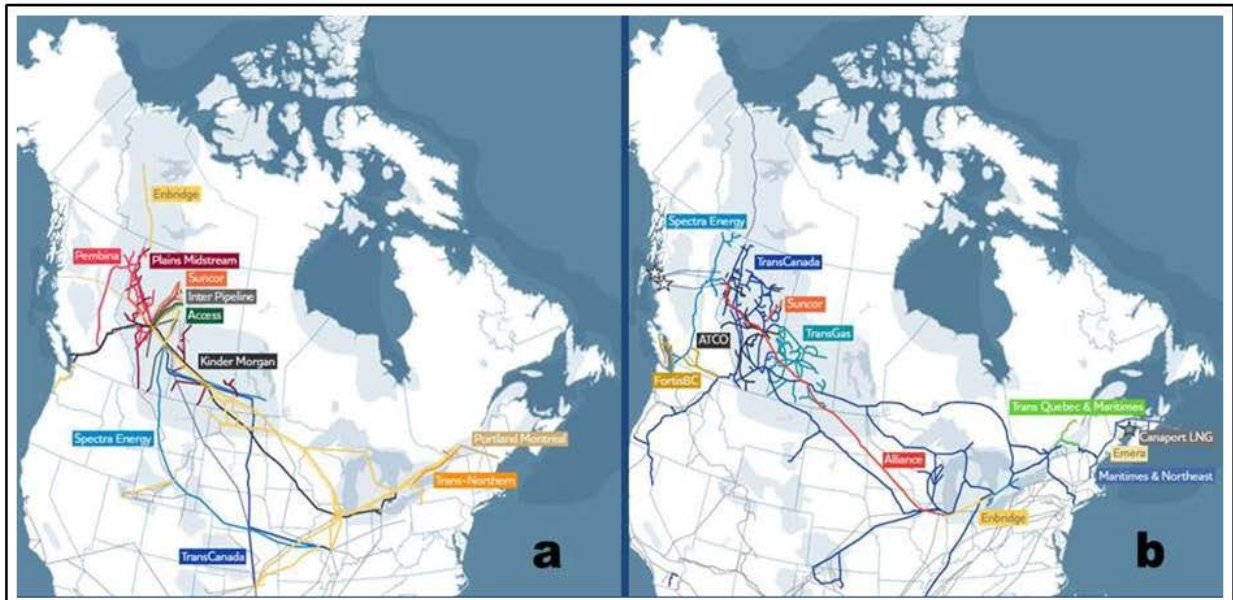





Figure E-1. Map of current pipeline transmission network for a) liquid hydrocarbon products, and b) natural gas. (source: CEPA, 2014).

In contrast, Ontario does not specifically regulate minimum soil cover (OEB, 2011), but pipeline contractors generally try to ensure that pipelines are installed below the level of local sub-surface tile drain systems, as noted above. Hence, they typically aim to have 120 cm (or 4') of soil cover in cropland areas, but it is often closer to 150 cm (or 5') in current practice (E. Mozuraitis, per. comm., 2013). In parts of the province where there is little intensive agriculture (e.g., much of northern Ontario), pipeline contractors aim to have 90 cm (or 3') of soil cover. However, older existing pipelines (dating back to the 1950's to 1970's) may be much shallower than the depths noted above, due to less stringent (or absent) guidelines at that time and/or several decades of soil erosion and compaction. For these reasons, it should be noted that PARSC has recommended that a pipeline depth range of 90 to 120 cm (to the top of the pipeline) be used in any frost heave simulations in this study.

2. Regulations on pipeline DOC surveys (Canada & USA)

For the most part, the 'depth of soil cover' issue is self-regulated within the Canadian pipeline industry by way of the EDP Toolbox, which is 'a collection of damage prevention shared learnings and practices for onshore, hazardous liquid transmission pipeline operation' (EDP Toolbox, 2014). Table E-1 shows that there is some variation in DOC criteria between the USA and Canada, and between Alberta and the remainder of Canada. For agricultural areas, operating pipelines must have a minimum DOC of 80 cm in Alberta (as set out in the 'Pipeline Rules' [Province of Alberta, 2005]), but only 60 cm in the remainder of Canada. The required periodicity of DOC surveys for a given stretch of pipeline is 10 years in all of Canada.

Table E-1: Minimum depth of cover guidelines. (source: EDP Toolbox, 2014).

Location		Type of Pipeline	Class Location	Minimum cover for buried operating pipelines		
						
General (other than as indicated below)		Any	Any	30"	0.60m	0.80m
Below travelled surface	Highway	Any	Any	48"	1.20m	1.40m
	Highway ditch	Any	Any	36"	0.75m	1.40m
Below travelled surface	Road	Any	Any	48"	1.20m	1.20m
	Road ditch	Any	Any	36"	0.75m	1.10m
Below base of rail	Cased	Any	Any	62"	1.60m	1.60m
	Uncased	Any	Any	10'	3.05m	3.05m
Rail ditch	Cased	Any	Any	36"	1.00m	1.00m
	Uncased	Any	Any	36"	2.00m	2.00m
Water crossing		Any	Any	48"	1.20m	1.20m
Water crossing (in rock)		Any	Any	*18"	0.60m	0.60m
Drainage or irrigation ditch invert		Any	Any	30"	0.75m	0.80m

In contrast, operating pipelines in the USA must have a minimum DOC of 76.2 cm (30") in agricultural areas (Table E-1), but some states have enacted their own regulations. For example, Washington State's regulations on DOC are consistent with the national guidelines (i.e., 76.2 cm [30"]), but Washington State has shortened the periodicity required for DOC surveys to 5 years (or 3 years, if the area in question is subject to erosion and sub-soiling) (Washington State Legislature, 2008).

3. Methods used for pipeline DOC surveys

There are numerous private-sector companies in western Canada and internationally (DoC Mapping, 2014) that carry out a wide range of 'pipeline integrity' field investigations, including DOC surveys. Pipeline companies require this information to allow monitoring of the effect of surface soil erosion and/or pipeline upheaval on altering the position of the pipe relative to the soil surface, potentially leading to exposure.

Pipeline DOC surveys are routinely carried out on pipelines that have been installed under shallow bodies of water due to the enhanced risk of pipeline upheaval or sediment shifting in submerged environments. Seeger (2011) identified four methods that are commonly used in tandem to measure DOC over an existing pipeline: a) physical probing from the water surface or by a diver, b) gradiometer array, c) pulse induction system, and d) chirp sub-bottom profiler.

The pipeline industry also routinely carries out DOC surveys within onshore ROWs (Figs. E-2 and E-3) using a wide array of non-contacting geophysical instruments (from the surface), 'smart pigs' (from within the pipeline itself), and other methods. The purpose of these surveys is to ensure that there is sufficient soil cover so that i) soil-engaging equipment does not come in contact with the pipe, and ii) the overburden pressure is adequate to continue to secure/anchor the pipe in place. DOC and coating integrity surveys are often conducted in tandem from the surface using the same equipment, and the data are tabulated with the corresponding GPS coordinates. The geophysical locating equipment measures the depth to the center of the pipeline, so DOC profiles are determined by correcting the measured values by one pipe radius (E-MAC Corrosion Inc., 2014). Many of the geophysical instruments used in onshore DOC surveys have typical error variances of $\pm 5\%$ (Midwest Surveys Inc., 2014).

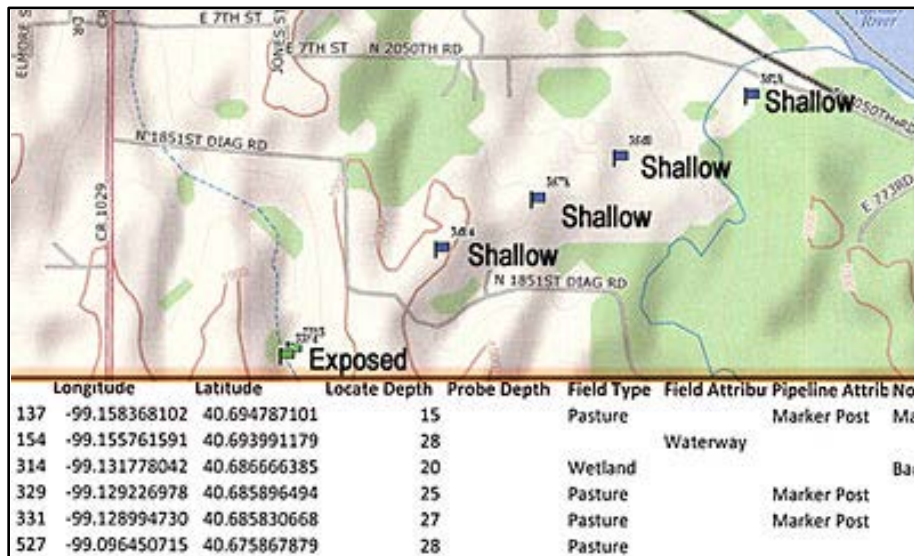


Figure E-2. An example of an aerial pipeline DOC survey map showing locations where a pipeline is too shallow or exposed. (source: Subsurface Solutions, 2014).

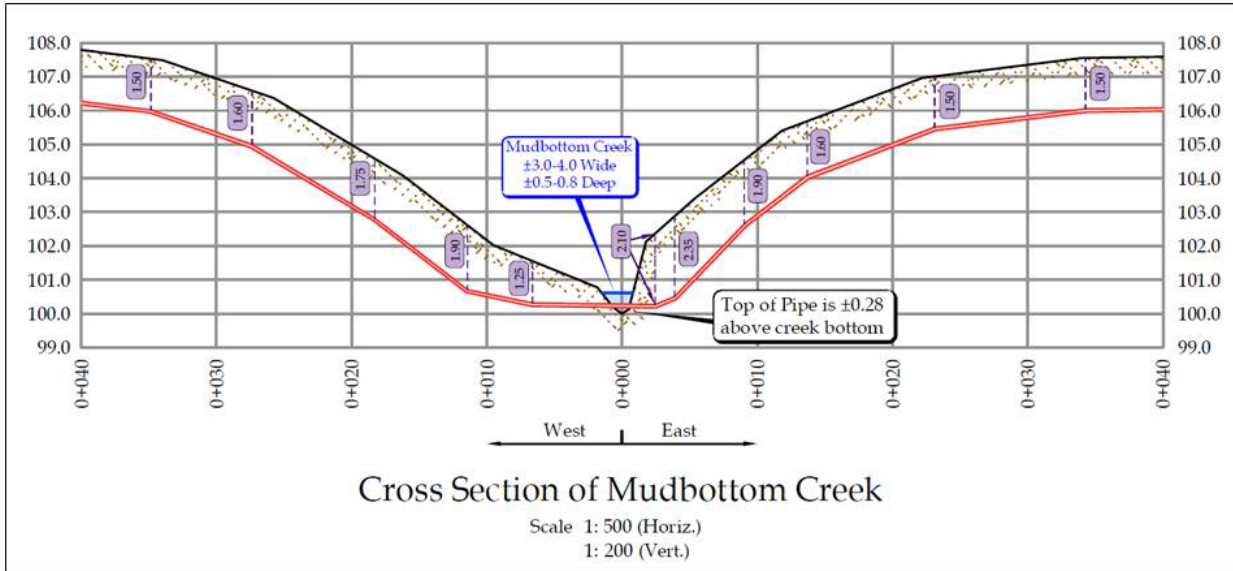


Figure E-3. An example of a cross-sectional pipeline DOC survey in the vicinity of the Mudbottom Creek, AB. All DOC measurements shown are in meters. (source: Compass Geomatics Ltd., 2014).

4. Soil compaction

Soil compaction is a form of land degradation that is operative in many agricultural regions of southern Canada (Fig. E-4) (Miller, 1985; Rennie, 1985). Despite the introduction of flotation tire systems for high axle load agricultural equipment used in common field crop production in recent years (Fig. E-5), incidental compaction of the soil remains problematic on the Canadian agricultural landscape.



Figure E-4. A potato field after harvest near Orangeville, ON, showing the intensity of wheel traffic often required for commercial vegetable crop production. (photo: R.A. McBride).

While soil densification is not a direct potential geotechnical cause of pipeline exposure (see Section 2 [Volume 1]), it can lead to a reduction in the depth of soil cover over pipelines (NEB, 2010, p. 31). It should be noted, however, that soil densification could affect pipeline exposure indirectly because soil compaction can increase the rate of soil loss from water erosion (Voorhees *et al.*, 1979) (see Section 5.3.4 [Volume 1]).

Incidental compaction of the soil can occur within pipeline ROWs from normal farm operations (Blunden *et al.*, 1994; McBride *et al.*, 2000), apart from soil-engaging farm operations which are regulated during the operating lifespan of a pipeline (NEB, 2010, p. 32). Comprehensive computer models are available that can estimate the stress distribution beneath moving farm vehicles (Fig. E-6), and estimate the wheel rut depth and the degree of sub-surface soil densification (Jakobsen & Dexter, 1989; O'Sullivan *et al.*, 1999).



Figure E-5. The level of ground pressure exerted on the soil by modern, often over-sized agricultural equipment, such as a) liquid manure tankers, and b) grain carts, can be diminished with flotation tire systems. (photos: R.A. McBride).



Figure E-6. An illustration of a) high axle-load wheel traffic on an agricultural field near Embro, ON (photo: R.A. McBride), inducing b) deep soil rutting as the soil reacts to forces exerted by the tires of a tractor and a liquid manure tanker.

Table E-2 shows that there are several forms of soil degradation that are operative on the Canadian agricultural landscape. Attempts to estimate the cost of each process show wide regional disparities (Table E-2). For example, soil compaction is not believed to be a significant problem within the Prairie Ecozone (southern AB, SK, MB) due to deep groundwater tables and the significant evapotranspirational deficit during the growing season. The geoclimatic conditions in the remainder of the country, however, cause soil compaction to be a significant risk (particularly in southern QC).

Table E-2. Estimated costs of soil degradation in Canada. (after Miller, 1985; Rennie, 1985).

Province or region	Erosion	Organic matter loss	Acidification	Salinity	Compaction
----- \$ Millions/yr -----					
BC	10	11	5	-	12
AB	200	144	5	80	-
SK	220	170	50	120	-
MB	10	-	-	12	-
ON	68	-	1	-	21
QC	10	-	4	-	100
Atlantic	11	-	6	-	6

- insignificant, or no data available

5. Summary (Appendix E)

The 'depth of soil cover' (DOC) issue is largely self-regulated within the Canadian pipeline industry, including the periodicity of geophysical DOC surveys. In cropland areas in Ontario, pipeline companies generally try to ensure that pipelines are placed deeper than existing or proposed sub-surface tile drain systems (up to 120 cm deep) or municipal drains. Incidental soil compaction (densification) from normal farm operations occurring within pipeline ROWs can lead to a reduction in DOC over pipelines.

References (Appendix E)

Blunden, B.G., R.A. McBride, H. Daniel and P.S. Blackwell. 1994. Compaction of a sand by rubber tracked and tyred vehicles. *Australian Journal of Soil Research* 32:1095-1108.

Canadian Energy Pipeline Association (CEPA). 2014. Library (maps). Available at:
<http://www.cepa.com/wp-content/uploads/2013/06/cepa-natural-gas-may-30.pdf>
<http://www.cepa.com/wp-content/uploads/2014/06/cepa-liquids-sept18.pdf>
 (verified Oct. 6, 2014).

Compass Geomatics Ltd. 2014. Red Deer, AB. Available at:
<http://compassgeomatics.ca/Profile%20Sample.pdf>
 (verified Oct. 6, 2014).

DoC Mapping, LLC. 2014. New Orleans, LA and San Diego, CA. Available at:
<http://www.docmapping.com/data.html>
 (verified Oct. 6, 2014).

EDP Toolbox. 2014. Excavation damage prevention toolbox.
<http://www.edptoolbox.org/documents/Pipeline-Depth-of-Cover.pdf>
(verified Oct. 6, 2014).

E-MAC Corrosion Inc. 2014. Edmonton, AB. Available at:
<http://www.e-mac.ca/Engineering/IndirectAssessmentSurveys.aspx>
(verified Oct. 6, 2014).

Fraser, H. and R. Fleming. 2001. Environmental benefits of tile drainage - Literature review. Report prepared by the University of Guelph (Ridgetown College) for the Land Improvement Contractors of Ontario (LICO). October, 2001. 25 pp.

Jakobsen, B.F. and A.R. Dexter. 1989. Prediction of soil compaction under pneumatic tyres. *J. Terramechanics* 26(2):107-119.

Madramootoo, C.A., W.R. Johnston, J.E. Ayars, R.O. Evans and N.R. Fausey. 2007. Agricultural drainage management, quality and disposal issues in North America. *Irrigation and Drainage* 56:S35-S45.

McBride, R.A., N.B. McLaughlin and D.W. Veenhof. 2000. Performance of wheel and track running gear on liquid manure spreaders. *Canadian Agricultural Engineering* 42:19-25.

Midwest Surveys Inc. 2014. Calgary, AB. Available at:
<http://midwestsurveys.com/services/integrity/>
(verified Oct. 6, 2014).

Miller, M.H. 1985. Soil degradation in eastern Canada: its extent and impact. *Can. J. Agr. Economics* 33:17-18.

Mozuraitis, Edward. 2013. Soil Specialist and Environmental Inspector (Pipelines), Stantec Consulting Inc., Guelph, ON. (personal communication).

National Energy Board (NEB). 2010. Pipeline Regulation in Canada: A Guide for Landowners and the Public. Revised September 2010. NEB Publications Office, Calgary, AB. 56 pp. Available at:
http://www.neb-one.gc.ca/clf-nsi/rthnb/pblcprtcpn/pplnrgltncnd/pplnrgltncnd_ndx-eng.html
(verified Oct. 6, 2014).

Ontario Energy Board (OEB). 2011. Environmental Guidelines for the Location, Construction and Operation of Hydrocarbon Pipelines and Facilities in Ontario. 6th Edition. 73 pp. Available at:
http://www.ontarioenergyboard.ca/OEB/_Documents/Regulatory/Enviro_Guidelines_Hydrocarb onPipelines_2011.pdf (verified Oct. 6, 2014).

Ontario Ministry of Agriculture, Food and Rural Affairs (OMAFRA). 2007. Drainage Guide for Ontario. OMAFRA Publ. 29. Agdex 700. Queen's Printer for Ontario, Toronto, ON. 87 pp.

O'Sullivan, M.F., J.K. Henshall and J.W. Dickson. 1999. A simplified method for estimating soil compaction. *Soil and Tillage Research* 49:325-335.

Pearce, R. 2011. Drainage statistics reveal some interesting facts about Ontario. *Drainage Contractor*, November 2011.

Province of Alberta. 2005. Pipeline Act. Pipeline Rules. Alberta Regulation 91/2005. Alberta Queen's Printer. 50 pp. Available at:
http://www.qp.alberta.ca/documents/Regs/2005_091.pdf (verified Oct. 6, 2014).

Rennie, D.A. 1985. Soil degradation: a western perspective. *Can. J. Agr. Economics* 33:19-29.

Seeger, R. 2011. Pipeline route and depth-of-cover survey considerations. *Pipeline and Gas Journal* 238(9).

Subsurface Solutions, LLC. 2014. Gretna, NE. Available at:
<http://www.subsurfacesolutions.com/DOC.asp>
(verified Oct. 6, 2014).

Voorhees, W.B., R.A. Young and L. Lyles. 1979. Wheel traffic considerations in erosion research. *Trans. ASAE* 22:786-790.

Washington State Legislature. 2008. Depth-of-cover survey. Washington Administrative Code regulation WAC 480-75-640. Hazardous Liquid Pipelines - Safety. Utilities and Transportation Commission. Available at: <http://apps.leg.wa.gov/wac/default.aspx?cite=480-75-640>
(verified Oct. 6, 2014).

APPENDIX F

Soil Structure and Strength of Frozen Soils

Soil Structure and Strength of Frozen Soils (LitRev 4)

1. Preface

The changes in soil structural form and stability attributable to the freeze-thaw process, and thus to the annual resiliency of soil structure, remain topics of considerable debate in the soil science field. This Appendix document provides a comprehensive review of the published research literature with respect to these changes by way of the main processes operative in the soil during winter conditions.

2. The effect of the freeze-thaw process on soil structure

2.1 The freezing process

Soil freezing is initiated as the 0°C isotherm ('freezing front') penetrates the ground surface and moves downwards. The passage of the 0°C isotherm does not guarantee ice nucleation as there may exist a depression of the freezing point resulting from factors including pore water impurities, capillarity and adsorption effects (Brown & Payne, 1990; Williams & Smith, 1989). The slow freezing of pore water may lead to the exclusion of dissolved constituents ahead of the freezing front (Radke & Berry, 1995). As freezing continues, the solute concentration of the remaining pore water increases, thus decreasing the ice nucleation temperature (Williams & Smith, 1989).

Williams & Smith (1989) state that the migration of ice into soil pore space is governed by the following equation:

$$T - T_o = \frac{v_l 2\sigma_{iw} T_o}{r_{iw} H_f} \quad \text{Eqn. F-1}$$

where:	T	=	temperature (°K)
	T_o	=	normal freezing temperature (°K)
	v_l	=	specific volume of water
	H_f	=	heat of fusion
	σ_{iw}	=	ice-water interfacial tension
	r_{iw}	=	radius of the ice-water interface

Equation F-1 shows that there is an inverse relationship between the ice nucleation temperature and the pore size. That is, the temperature of the soil system must drop below 0°C to initiate freezing in smaller pores. This equation is likely only valid for temperatures within a degree of 0°C (Williams & Smith, 1989), as with increasingly smaller pore spaces, the adsorbed water within them assumes a structural form that gives it very low freezing temperatures (Aoyama *et al.*, 1985; Low, 1961; Martin, 1960). The use of this equation is quite limited in practice for several reasons. First, no commonly accepted value exists for the ice-water interfacial tension, with commonly used values ranging from 10 mJ m⁻² to 45 mJ m⁻² (Penner, 1963), although Brown & Payne (1990) calculated that it could be as high as 58 mJ m⁻². Second, a hemispherical radius of the ice-water interface is assumed for a single-sized pore, neither of which exists in the soil system.

The freezing of pore water can result in the formation of different types of ice, as characterized by Trimble *et al.* (1958). Freezing may occur *in situ*, resulting in the formation of granular, honeycomb or stalactite frost. Granular frost typically consists of small ice crystals within the soil matrix, while honeycomb frost assumes a loose porous structure. Stalactite frost exists as loosely fused columnar ice crystals. These three types are often grouped under the common term of 'pore ice'. Alternatively, through the phenomenon of coupled heat and water flow, a suction force acts to draw pore water upwards to the point of ice nucleation, resulting in the growth of

segregational ice lenses. This type of freezing is referred to as concrete frost (Trimble *et al.*, 1958). As a result of these processes, segregation ice (i.e., ice lenses) actually forms at some distance behind the freezing front, with the zone between these two points being termed the 'frozen fringe' (Miller, 1972).

In an agricultural context, the freezing of the tilled soil layer or Ap horizon (i.e., the upper 15 cm) is of the most interest. The freezing rate is of particular interest as it can strongly affect the type of ice that forms, and therefore, the effect of the freezing process on soil strength development.

Under the strong temperature gradients that commonly exist close to the soil surface, upward water flow is minimized as the rapid advancement of the freezing front does not allow sufficient time for appreciable pore water movement to occur (Sharratt, 1995). Either pore ice may form as water freezes *in situ*, or many thin, closely-spaced lenses may result (Jung, 1931; Othman & Benson, 1993).

The formation of pore ice is viewed primarily as a destructive force in terms of soil structure (Bryan, 1971; Bullock *et al.*, 1988; Dombay & Kohnke, 1955), although a few studies note potential increases in aggregation (Hamilton, 1966; Leroueil *et al.*, 1991; Yong *et al.*, 1985). The approximate 9% volumetric expansion resulting from ice formation has been noted to rupture existing aggregates and increase the proportion of fine material (Chuvilin & Yazynin, 1988; Knocke & Trahern, 1989; Lebedenko & Shevchenko, 1988). However, Leo (1963) noted that the many small crystals associated with pore ice destroyed the micro-structure of the soil by destroying the micro-pores, rather than the aggregates, and increased aggregation through compression.

The water content at the time of freezing is an important factor in determining the effects of pore ice formation. At low water contents, the pore system may be sufficiently empty to largely accommodate the volumetric expansion associated with freezing. Data from Hamilton (1966) suggests that at water contents below approximately 65% saturation, freezing-induced desiccation of the soil surrounding the growing pore ice can lead to volumetric shrinkage in the soil. However, as water contents rise, the pore system is less able to accommodate this expansion, and structural deterioration may result. Kohnke & Werkhoven (1963), Hamilton (1966) and Bryan (1971) found a strong relationship between freezing and decreased aggregation at higher water contents. Conversely, Sillanpaa & Webber (1961) found that pore ice expansion during rapid freezing at saturation enhanced contact between soil particles and improved aggregation.

The specific location of the freezing pore water within the soil matrix becomes an important consideration. Soil aggregates are defined by a three-dimensional network of failure zones (Kay & Dexter, 1992). If it is assumed that the weakest failure zones are represented by the largest, most continuous pores, individual soil aggregates containing smaller and less continuous intra-aggregate micro-pores are separated by inter-aggregate macro-pores. Freezing is likely initiated in the inter-aggregate macro-pores as the 0°C isotherm penetrates the soil surface (Brown & Payne, 1990). At temperatures marginally below freezing, ice crystal growth would have the effect of compressing the soil aggregates and increasing the size of inter-aggregate pores. With a further drop in temperature, ice would eventually invade the successively smaller intra-aggregate micro-pores. As ice crystal growth would now be exerting a tensile stress on the aggregates, they would tend to shatter into smaller particles. This mechanism would be consistent with experiments showing increased structural deterioration at lower temperatures (Benoit, 1973; Bourbonnais & Ladanyi, 1985; Kivisaari, 1979; Van Dijk & Boekel, 1965). This may also explain the reduction in over-winter structural deterioration noted by Slater & Hopp (1951), Anderson & Bisal (1969), and Jones (1986) where insulation of the ground surface allowed only

constructive macro-pore freezing at temperatures only slightly below freezing, while preventing destructive micro-pore freezing at colder temperatures.

Larney *et al.* (1994) suggested that increases in the length of time a soil experiences near freezing temperatures is more destructive. They noted greater structural deterioration when the surface temperature cycled within a few degrees of freezing rather than when the soil was frozen to lower temperatures. This agrees with the findings of Alderfer (1946) who noted that cyclic freeze-thaw reduced aggregation while continuously frozen conditions had the opposite effect. Similarly, Edwards & Burney (1991) reported greater sediment concentrations in runoff from higher clay content soils under freeze-thaw conditions than under continuously frozen conditions. This suggests that, in terms of structural deterioration, cyclic freeze-thaw may be more important than longer duration cycles.

Some studies have attributed a decrease in the dispersion of aggregates with depth to the constraining effect of the surrounding soil mass (Blackmore, 1956; Blake *et al.*, 1976; Chepil, 1954). This factor, together with the destructive effects of shallow pore ice, could explain the greater structural stability of aggregates at greater depth, where the ultimate freezing temperatures are not as cold. More recent research, however, suggests that the growth of ice crystals in confined conditions is responsible for the crushing of aggregates, thus reducing their stability (Bullock *et al.*, 1988; Lehrsch *et al.*, 1990, 1991).

Other studies have suggested that, in addition to pore ice, segregation ice may also have an overall destructive influence on soil. Booth (1981) reported an unstable, disaggregated structure in a silty soil following slow, unidirectional freezing. Such deterioration usually occurs on a macro-scale and close to the soil surface. Closely-spaced multiple ice lenses resulting from strong near surface temperature gradients have the effect of loosening the overall fabric (Czurda, 1983; Federova & Yarilova, 1972; Kay *et al.*, 1985; Sage & D'Andrea, 1982), particularly if it was compacted prior to freezing (Konrad, 1989a). The cleaving of the existing soil by multiple closely-spaced ice lenses introduces planes of weakness, and the effects of segregational freezing more closely resemble those of pore ice formation.

A weaker temperature gradient usually exists at greater depths in the soil. The advancement of the freezing front is consequently much slower. If the permeability of the soil is sufficient to allow water migration to the zone of freezing, segregational ice lenses will form, with typically wider spacings than usually found in lenses nearer the surface. Many studies have found an increase in both aggregation (Alkire & Morrison, 1983; Jung, 1931; Krumbach & White, 1964; Williams, 1988) and stability (Gardner, 1945; Kemper *et al.*, 1989; Sillanpaa & Webber, 1961; Van Vliet-Lanoe & Dupas, 1991) as a result of segregational freezing and widely-spaced lenses. However, the desiccation experienced by the inter-lens soil may also play an important role in defining the structural form and stability resulting from the formation of segregational ice lenses.

2.2 Freeze-thaw frequency

Aggregate stability is generally inversely related to the number of freeze-thaw cycles (Benoit, 1973; Edwards, 1990, 1991; Mbagwu & Bazzoffi, 1989; Sillanpaa & Webber, 1961; Willis, 1955). In some studies, the most significant changes in soil structure have been noted to occur within the first five freeze-thaw cycles (Benoit & Voorhees, 1990; Edwards & Burney, 1987; Efimov *et al.*, 1981; Fippin, 1910; Johnson *et al.*, 1989; Konrad, 1989a, 1989b; McConkey *et al.*, 1990), although others suggest that it is not until between five and ten cycles that the maximum effect is exhibited (Slater & Hopp, 1949). Burney & Edwards (1987) depict this decrease in the effectiveness of freeze-thaw with an increasing number of cycles as an exponential relationship. This type of relationship is substantiated by Formanek *et al.* (1984) who found a 50% reduction in soil shear strength after the first freeze-thaw cycle, but little change with additional cycles.

Similarly, Orlov & Fursov (1988) noted maximum consolidation after the first cycle, and that after the second cycle, settlement was only 30-60% of previous values.

Some suggest that the effects of freeze-thaw are constructive and structural form and stability reach maximum values, whereas additional cycles are destructive (Bryan, 1971; Edwards, 1991; Lehrsch *et al.*, 1990, 1991; Molohe, 1988). However, part of this effect may be due to the method of sample preparation. Molohe (1988) discovered that soil aggregates experienced an increase in stability within the first three to six freeze-thaw cycles, followed by a gradual decline with additional cycles. Remoulded samples, on the other hand, showed the same initial increase in stability that was maintained over subsequent cycles. A fundamental difference may exist between samples freshly made in the laboratory and those that have been aged or seasoned in the field through previous exposure to a variety of natural processes including age hardening, freeze-thaw cycles and wetting-drying cycles (Konrad & Seto, 1994).

The substantial changes in the soil matrix following the first few freeze-thaw cycles influence the behaviour of the soil in subsequent freeze events. In the late fall, the initial freezing would likely be diurnal in nature under weakly negative radiational cooling. Freezing effects would therefore be minor, and likely constructive in nature as freezing is restricted to only macro-pore water, and restricted to the uppermost layers of the soil. As the aggregates are compacted, the macro-porosity of the surface layers increases, thus increasing permeability (Akram & Kemper, 1979; Aoyama *et al.*, 1985; Florkemeier *et al.*, 1989). Upon daytime thawing, the soil would experience wetting-drying cycles. Water would be able to percolate deeper into the soil than before freezing as a result of the increased macro-porosity. Subsequent freezing would extend marginally deeper into the soil as the latent heat of freezing would be less in this drier, previously-frozen layer.

The formation of ice lenses (with the associated soil desiccation) and the reduction in thickness of adsorbed water layers (with the associated soil consolidation) similarly cause an alteration of the soil's freezing characteristics. Not all researchers agree, however, on the factors dictating ice lens location. Konrad (1989b) suggested that on subsequent freezing, ice lenses would become more widely-spaced. Kivisaari (1979) maintained that ice lenses reform in the same position during each subsequent freeze event. Ice lens growth may be initiated in cracks formed through desiccation below the level of previous freezing (Van Vliet-Lanoe *et al.*, 1984), as these cracks would have the effect of disrupting the upward migration of pore water. Othman & Benson (1993) found a positive relationship between the number of lenses with a given depth of soil and the number of freeze-thaw cycles, suggesting that subsequent ice lens growth may act to fill in the areas between pre-existing lenses. As each ice lens location defines a failure zone upon thawing, the soil would become progressively more fractured.

In areas that experience prolonged periods of sub-zero temperatures, the number of freeze-thaw cycles experienced at the soil surface may be relatively small (Fraser, 1959). The effects of continuous freezing are not necessarily the same as those of freeze-thaw. Hinman & Bisal (1973) did not find increased percolation rates during continuous freezing as were noted during freeze-thaw, suggesting the pore system is not affected to the same degree, or in the same manner. Edwards & Burney (1989, 1991) found no inherent difference in the erodibility between surfaces exposed to continuous freeze and freeze-thaw, although significant interactions existed between the type of freezing, soil cover and ground cover. There is some evidence that soil water redistribution continues within the frozen soil (Burt & Williams, 1976; Engelmark, 1988; Hoekstra, 1966, 1969). Konrad (1989c) noted that with falling temperatures behind the least cold ice lens during penetration of the freezing front, the freezing of unfrozen adsorbed water can lead to structural changes. As continuously frozen conditions allow greater development of ice lenses, the consolidation and desiccation of the soil may be much more extensive (Nixon &

Morgenstern, 1973), resulting in an increase in stability over that resulting from cyclic freeze-thaw (Birecki & Gastol, 1968). The effects of continuous freezing may be entirely applicable, however, as the depth at which the effects are experienced the most may be beyond the normal depth of tillage.

Climate change is likely to alter the frequency of freeze-thaw cycles in northern temperate regions. Henry (2008) used climate models to predict a general pattern by the year 2050 of i) a decreased number of days of frozen soil, and ii) a decreased number of days with snow on the ground, although these projections were very regional in nature across Canada. The reduced snow cover with climate change is likely to increase the number of winter freeze-thaw cycles.

3. The role of inherent soil properties

3.1 Clay content

Clay content has been cited as a factor in controlling soil behaviour during freeze-thaw. Dobby & Kohnke (1955) and Czeratzki (1971) reported increased aggregation with freeze-thaw in soils with higher clay contents. Edwards & Burney (1987) and Edwards (1990, 1991) found greater aggregate stability with freeze-thaw in clay-rich soils. Similarly, deJong & Kachanoski (1988) noted less disaggregation under freeze-drying conditions in soils with higher clay contents. Van Vliet-Lanoë & Dupas (1991) suggested that a stable fabric results from a silt/clay ratio <3, and a metastable structure at ratios from 3 to 7. It is thought that the presence of clay aids in the formation of bridges between soil particles, thus increasing aggregation (Lehrsch, 1997).

The clay mineralogy may also have an influence on structural stability. Greene *et al.* (1974) found the well-aligned contiguous arrangement of a Ca-montmorillonite was more stable than a Ca-illite. The presence of polyvalent cations is generally assumed to contribute to greater structural stability through stronger interlayer bonding (Gardner, 1945; Rowell & Dillon, 1972). Yong *et al.* (1985), however, found that clay mineralogy was of minor significance in explaining soil aggregation.

Clay-water interactions have also been cited as a controlling factor. Several studies have noted a greater degree of freezing-induced fabric changes in soils rich in swelling clays (Czurda & Wagner, 1984, 1985; Mbagwu & Bazzoffi, 1989), and in soils with high plasticity indices (Brown & Payne, 1990; Chamberlain & Blouin, 1978; Chamberlain & Gow, 1979; Leroueil *et al.*, 1991). These changes have been attributed to the thixotropic behaviour of the clay, where under a freezing-induced stress, the clay plates undergo re-orientation. Upon removal of the stress, the subsequent clay re-orientation results in greater rigidity (Molope, 1988; Yong *et al.*, 1982).

Swelling clays (e.g., smectite, montmorillonite) generally contain greater quantities of water than non-swelling clays (e.g., kaolinite), but this water is tightly adsorbed onto clay surfaces, and is not as susceptible to temperature-induced migration under normal winter conditions, a few degrees below zero (Czurda & Schababerle, 1988). Lower sub-zero temperatures reduce the thickness of the adsorbed water layers resulting in desiccation and consolidation of the clay (Kivisaari, 1979). Aoyama *et al.* (1985) found that the resulting decreased 'liquid limit' was irreversible, suggesting increased stability as well.

The dehydration of clay interlayers may explain the conflicting results of these studies and those that claim decreased stabilities with increased clay content (Bisal & Nielsen, 1964; Bryan, 1971; Kerston & Cox, 1951). The former studies generally utilized samples prepared from a slurry, which would impart an initially high interlayer water content to the clays. Large changes in the structural state of the samples would be expected within the first few freeze-thaw cycles (Johnson *et al.*, 1979; Mostaghimi *et al.*, 1988), as the remoulded clays de-watered. Conversely, the latter studies used natural aggregates that were in more of an equilibrium state with respect

to the thickness of adsorbed water layers. Therefore, the experimental procedure may have had more of an influence on the outcome of the experiments than the amount and type of clay minerals.

3.2 Soil organic matter

Organic matter is often viewed as a soil constituent responsible for good structural form and stability (Tisdale & Oades, 1982). While a general increase in aggregation and stability has been associated with higher organic matter contents in several studies (Alderfer, 1946; Bullock *et al.*, 1988; Richardson, 1976; Unger, 1991), others have found little or no benefit under freeze-thaw conditions (Bryan, 1971; Slater & Hopp, 1951). Some studies have found that it is the interaction of organic matter with other soil properties, such as soil water or clay contents, which contributes to increased aggregation (deJong & Kachanoski, 1988; Domy & Kohnke, 1955; Lehrsch *et al.*, 1991). Mbagwu & Bazzoffi (1989) suggested that it is 'clay-polyvalent metal-humus' complexes that cause organic matter to contribute to aggregate stability, and that lower application rates are most effective.

Any beneficial effects due to elevated soil organic matter levels may not be sustained throughout the winter if numerous freeze-thaw cycles are experienced. There is evidence to suggest that the freeze-thaw process is also active on a very small scale, affecting processes including nutrient mobility (Cheng *et al.*, 1971; Honeycutt, 1995), and the denitrification process (Dorland & Beauchamp, 1991). Birecki & Gastol (1964) noted increased humic and fulvic acid mobility following freeze-thaw, although continuous freezing led to humic acid stabilization. Christensen & Christensen (1991) reported a 50% loss in bioavailable clay- and silt-associated organic matter after the first freeze-thaw cycle. Lehrsch *et al.* (1991) found higher aggregate stabilities associated with higher soil organic matter contents but only at lower water contents. Wang & Bettany (1993) suggested that variable long-term leaching rates may be the result of the breakdown of soil organic matter with freeze-thaw. Therefore, freeze-thaw cycles, and the resulting wet period prior to re-freezing, may at least partially nullify any structural gains afforded by the soil organic matter content.

4. The role of soil surface characteristics

There may be a substantial spatial variation in the effects of freezing temperatures as a result of the influence of the soil surface characteristics (Gorkov, 1983). As the freezing process is initiated by the radiative cooling of the surface, any surface conditions that influence this energy transfer may affect the freezing process. Investigations of these influences have focused primarily on surface roughness and the insulative effects of various soil, crop and snow management practices.

Several studies have investigated the role of surface plant residues or mulches in modifying the nature of soil freezing. Generally speaking, a bare soil surface will both freeze and thaw more rapidly than one with an insulative cover of mulch or crop residue (Gusev *et al.*, 1992; Kohnke & Werkhoven, 1963; Pikul *et al.*, 1986). As previously discussed, the rate of soil freezing can greatly affect the mode of freezing (Konrad & Nixon, 1994), and thus the extent of soil aggregation or disaggregation, although the water content at the time of freezing and the effects of the increased organic matter associated with the mulch or residue may also be important (Benoit *et al.*, 1962). Soils with higher initial water contents have generally been found to experience a greater degree of water re-distribution (Sharratt, 1995) and greater structural modification upon freezing (Kohnke & Werkhoven, 1963).

The presence of surface residues or mulches also influences the nature of the freeze-thaw process by allowing for the maintenance of snow cover. The presence of an insulative snow cover may be beneficial in terms of reducing the magnitude and frequency of freeze-thaw

events (Harris, 1974; Larney *et al.*, 1994), or destructive freeze-drying events (Anderson & Bisal, 1969; Armbrust *et al.*, 1982; Bisal & Nielsen, 1964; Bisal & Pelton, 1971; deJong & Kachanoski, 1988; Hinman & Bisal, 1968; Staricka & Benoit, 1995). Conversely, this effect may be overshadowed by slower heating and increased soil water content following spring snowmelt (Layton *et al.*, 1993).

An irregular surface resulting from tillage may intensify over-winter processes (Czeratzki, 1971) by increasing the surface area of soil (Blackmore, 1956), and the depth to which frost has a direct effect (Groenevelt & Kay, 1979; Kivisaari, 1979). For example, Mackie-Dawson *et al.* (1989) noted that freeze-thaw generated aggregates that were present to a greater depth in plowed versus unplowed soil. Gorkov (1983) noted that the permeability of the soil immediately following thawing was greater when the surface was left in a lumpy state prior to freezing. This greater permeability prevented soil saturation and destructive aggregate slaking during thawing. Conversely, the action of tillage itself may concentrate the effects of freezing within this zone by providing a loose, comparatively insulative soil cover (Jones, 1986). Therefore, soil management practices, particularly the adoption of minimal tillage systems, may have an important influence on the nature and effects of soil freezing.

Natural processes, however, tend to lead to a smoother soil surface over time. A decrease in the roughness of a plowed surface over the winter, suggesting a reduction in cloddiness, is commonly observed. This effect is likely dependent, at least to some extent, on soil texture. Voorhees *et al.* (1978) suggested that a coarse soil structure is more resistant to weathering and re-consolidation in a silty clay loam. This may be the result of some clods not freezing completely (Kivisaari, 1979). In such a case, while fall tillage may have beneficial effects in terms of late fall or early winter freeze-thaw, this advantage may be nullified by spring.

Frost tillage (van Es & Schindelbeck, 1995), whereby primary tillage is performed when a frozen surface layer exists but the subsurface is at a favourable water content, may be an alternative. Van Es & Schindelbeck (1995) noted the advantages of a rough surface as per Gorkov (1983), but argued that by allowing the surface layer to freeze prior to tillage, any beneficial structural effects may be longer preserved in the spring. Conversely, negative structural effects resulting from initial freezing may aggravate spring erosion under high water content conditions.

The nature of freezing, and the resulting form of ice, may also be affected by the roughness of the soil surface. On flat surfaces, the freezing front penetrates uniformly into the soil *ceteris paribus*, and one-dimensional freezing results. An irregular, cloddy surface resulting from fall tillage causes a variable advancement of the freezing front (Jones, 1986), with freezing being more three-dimensional in nature (Sapozhnikov *et al.*, 1987). Breakdown of the clods may be in a manner similar to aggregate breakdown during rapid wetting (i.e., slaking). Freezing effects, such as desiccation, on the surface layers of the clod are magnified by progressing in three dimensions towards the interior of the clod. Freezing would occur in more of a closed system (Wong & Haug, 1991), which may result in less stable particle aggregation. Therefore, while gravity, confinement and one-dimensional freezing on a flat surface may preclude aggregate breakdown, such actions operating in three dimensions may be sufficient to split the clod. This mechanism may explain the differential effects of freezing on aggregate size and depth in the case of an over-winter reduction in cloddiness (Bisal & Pelton, 1971; Chepil, 1954; Vallejo, 1982). The mechanisms responsible for more intensive frost action in the case of multi-directional freezing are not entirely clear, however, as several studies have found similar results regardless of whether freezing occurred in one or three dimensions (Chamberlain, 1981; McConkey *et al.*, 1990; Othman & Benson, 1993).

5. The effects of soil freezing

5.1 Soil strength

A measure of the effect of freeze-thaw alteration on structure is implied through the stress-strain behaviour of the soil (Bourbonnais & Ladanyi, 1985; Graham & Au, 1985; Leroueil *et al.*, 1991). While frozen soil can exhibit strengths over an order of magnitude higher than in their pre-frozen state, post-thaw strengths can be over an order of magnitude lower, depending largely on the water content at the time of freezing. Zebarth *et al.* (1984) found that strength increased with increasing water contents at the time of freezing only to a point. Higher water contents resulted in subsequent decreases in strength. It may be postulated that the critical water content represented that value where the volumetric expansion due to freezing resulted in an ice volume that exceeded the pore volume of the sample (Johnson *et al.*, 1979; Lee *et al.*, 1995), or where expansion effects due to growing pore ice began to overcome shrinkage effects due to the desiccation of the surrounding soil (Hamilton, 1966). Immediately following thaw, large decreases in shear strength are typically observed as the locations of former ice lenses become failure planes within the soil (Booth, 1981; Formanek *et al.*, 1984; Ogata *et al.*, 1985; Yong *et al.*, 1982). Pore ice can also alter the post-thaw strength of soil through an alteration of the original soil fabric. However, an increase in strength to near pre-freeze levels is often noted following 'thaw consolidation' (Formanek *et al.*, 1984; Johnson *et al.*, 1979; Sage & D'Andrea, 1982). Thaw consolidation is a loss in soil volume and a decrease in pore size resulting from the de-watering of a thawing soil.

Soil conditions prior to freezing are important in dictating whether the net effect of freeze-thaw is an increase or decrease in strength. Initially loose samples typically show greater increases in strength than do initially consolidated samples (Alkire & Morrison, 1982, 1983; Nagasawa & Umeda, 1985), likely due to the consolidation resulting from the freezing process. Consolidation during freezing can occur either within the frozen or unfrozen zones of the soil. Brown & Payne (1990) and Radke & Berry (1995) noted shrinkage of the soil between ice lenses, while Konrad & Nixon (1994) observed consolidation under the deepest ice lens. Conversely, Kay *et al.* (1985) found that the dry bulk density of the inter-lens soil remained unchanged from pre-freeze values. In both cases, the effect was the result of the desiccation of the soil as the pore water migrated towards growing ice lenses. In either case, an increase in soil strength may result.

5.2 Pore characteristics

The effects of freeze-thaw are detectable in the pore characteristics of the soil. The changes in the pore system can be just as significant as changes in structural form and stability. Most researchers have noted an increase in macro-porosity, particularly in fine-textured soils, as a result of freeze-thaw (Dyke & Egginton, 1988; Florkemeier *et al.*, 1989; Leo, 1963). Some studies report this as an increase in the permeability or hydraulic conductivity (Aoyama *et al.*, 1985; Hubbell & Staten, 1951). In many cases, this increase was found to be at the expense of micro-porosity, as the void ratio and final water retention characteristics decreased while hydraulic conductivities increased (Benoit & Voorhees, 1990; Chamberlain, 1981). However, some claimed that total porosity remained essentially constant in spite of increased permeabilities (Florkemeier *et al.*, 1989). A few studies, however, noted increases in micro-porosity (Bunting, 1983). In any case, these changes reflect an alteration of the arrangement of mineral particles within the soil. In the case of an aggregated soil, the macro-porosity and the micro-porosity are analogous to inter- and intra-aggregate pores, respectively.

Some have found that the change in permeability is isotropic (Chamberlain, 1981; Chamberlain & Blouin, 1978), resulting from the formation of both vertical and horizontal fissures as a result of freezing. Others, however, maintain that only the horizontal permeability is dramatically increased as a result of the discontinuities remaining in sites of former ice lenses. Dyke & Egginton (1990) measured permeability increases of as much as four orders of magnitude. Yet others suggest that only vertical permeabilities are increased, as thaw consolidation effectively closes the horizontal discontinuities. Chamberlain & Blouin (1978) noted a post-freezing vertical

permeability two orders of magnitude higher than the pre-freeze value.

This contradiction on the effect of freezing may be explained by the nature of the freeze-thaw process. Shipitalo & Protz (1987) and Mackie-Dawson *et al.* (1989) found that macro-porosity decreased in the surface layers of the soil over the winter. Similarly, Wittsell & Hobbs (1965) and Harris (1990) report the existence of a low permeability layer at the surface. The most rapid freezing occurs at the soil surface, resulting in the likely formation of more structurally-damaging pore ice. The highly variable water contents experienced in the surface layers of the soil will also affect the nature of the freezing process, and therefore, the effect on the pore system (Chamberlain *et al.*, 1990). Similarly, as thawing progresses from the surface downwards, this situation would likely be compounded by the inhibition of downward drainage by frozen layers at depth, resulting in saturation of the soil surface.

5.3 Post freeze-thaw consolidation

While often referred to as 'thaw consolidation' (Nixon & Morgenstern, 1973), Chamberlain (1981) suggests that observed soil consolidation is more likely the result of the freezing process. The time of measurement is an important consideration in determining whether frost action results in net increase or decreases in water permeabilities. As noted above, thaw consolidation is a loss in soil volume and a decrease in pore size resulting from the de-watering of a thawing soil. If soil aggregates experience consolidation during the freezing process, they would not be capable of re-absorbing all of the melt water, regardless of whether water re-distribution and segregational freezing occurred (Williams & Smith, 1989). Higher post-freeze water permeabilities resulting from the existence of inter-aggregate macro-pores may minimize the destructive effects of excess water by allowing rapid drainage of pore water immediately after thawing. However, Kivisaari (1979) and Alkire & Morrison (1982) suggest that this open structure is only metastable (and prone to collapse as soil drying and consolidation proceeds). Chamberlain & Blouin (1978) found that after 40 days, the pre-frozen water permeability was re-established as a result of thaw consolidation. Similarly, Egginton & Dyke (1990) measured water permeabilities up to three orders of magnitude greater in thawing soil than after consolidation was complete.

As thawing proceeds from the surface downwards, the existence of underlying soil that is still frozen may inhibit drainage. Similarly, the existence of a melting snowpack at this point in time, or high spring precipitation amounts, would exacerbate the situation by supplying even more water to the pore system (Layton *et al.*, 1993). This wetting could lead to rapid aggregate breakdown through slaking or differential swelling (Kay & Dexter, 1992; Utomo & Dexter, 1981a, 1981b). Therefore, while the action of freezing may be directly responsible for increased macro-porosity, this action may be quickly reversed by thaw consolidation.

A certain amount of thaw consolidation may actually be required to effect an improvement in structural form and stability over the winter. While consolidation of soil aggregates occurs during the freezing process, the resulting aggregates approach an 'ideal' size in the order of <1mm in diameter (Chepil, 1954; Sillanpaa, 1961). Since good soil 'tilth' requires a range of aggregate sizes, the amalgamation of smaller aggregates through thaw consolidation and subsequent cementation would be beneficial in creating larger aggregates. There is evidence that, without thaw consolidation, the soil would possess a poor structural state in the spring. When frozen soil is freeze-dried, ice sublimates from the pore system in the vapour phase, without melting. Such conditions are particularly likely in the late winter over bare soil surfaces during periods of low atmospheric humidity and high wind speeds (deJong & Kachanoski, 1988; van Dyk & Law, 1995). The three-dimensional structure of the soil that is otherwise modified through drying is preserved as water is drawn out of the pores (Rawlins *et al.*, 1963). However, without consolidation or wetting to re-distribute and re-activate cementing materials, destructive disaggregation of the soil mass results (Anderson & Bisal, 1969; Bisal & Nielsen, 1964; Hinman & Bisal, 1968; Smith *et al.*,

1991). The presence of a standing crop residue to maintain a snow cover (Armbrust *et al.*, 1982), or an insulating straw mulch layer (Gusev *et al.*, 1992), could help reduce evaporative losses, thus reducing freeze-drying effects. However, this may negatively affect the soil upon thawing by maintaining higher water contents and inhibiting soil warming (Anderson, 1971; Kohnke & Werkhoven, 1963; Merrill *et al.*, 1995; Pikul *et al.*, 1986).

5.4 Desiccation effects

Most of the work regarding freezing-induced desiccation and the concomitant volumetric shrinkage comes from the voluminous body of literature on frost heave. Ice lens growth is a result of the migration of pore water from below (Taber, 1929, 1930), thus desiccating the underlying soil (Skarzynska, 1985; Van Vliet-Lanoe & Dupas, 1991). As water is drawn out of progressively smaller inter- and intra-aggregate pores, strong negative pore water pressures draw the soil particles together (Alkire & Morrison, 1983; Broms & Yao, 1964; Hamilton, 1966; Heininen, 1977; Lehrs *et al.*, 1991; Konrad & Nixon, 1994; Konrad & Seto, 1994), and may result in the re-orientation of some fine particles (Benoit, 1973; Chamberlain, 1981; Chaney & Swift, 1986; Czurda & Schababerle, 1988; Leroueil *et al.*, 1991; Molope, 1988; Richardson, 1976). Pressures due to segregational frost heaving have been estimated to be in excess of 100 kPa (Chamberlain, 1989; Fukuda, 1982; Henry, 2000; Ingersoll & Berg, 1981; Seto & Konrad, 1994; Williams & Wood, 1985), and some authors have attributed this pressure to consolidation of the inter-lens soil, thus enhancing aggregation (Gardner, 1945; Heininen, 1977; Nixon & Morgenstern, 1973; Yamamoto *et al.*, 1988). This desiccation-induced shrinkage (Hamilton, 1966) may alone be responsible for the increased aggregation (Chamberlain & Gow, 1979; Williams, 1963) and stability (Perfect *et al.*, 1990) noted immediately after freezing. While the greatest changes occur within a few degrees below zero (Hamilton, 1966; Williams, 1988), progressively lower temperatures decrease the thickness of adsorbed water layers through drying, and intensify the consolidation of the soil (Aoyama *et al.*, 1985; Konrad, 1989b; Van Dijk & Boekel, 1965). Additionally, cementing materials such as clay, organic matter or salts may become concentrated or immobilized as a result of dehydration and consolidation (Kay & Dexter, 1992; Kemper *et al.*, 1989; Van Vliet-Lanoe & Dupas, 1991; Yong *et al.*, 1985). If new inter-particle bonds are able to form, improved structural form and increased aggregate stability often result.

5.5 Characteristic soil structures

Analyses of previously-frozen soils have noted a number of characteristic structural forms. One of the most common observations is that of a platy or banded structure (Coutard & Mucher, 1985; Egginton & Dyke, 1990; Federova & Yarilova, 1972; Gardner, 1945; Mermut & St. Arnaud, 1981; Pawluk, 1988; Van Vliet-Lanoe & Dupas, 1991). Evidence of particle sorting within this structure includes fine matrix material accumulations below skeletal grains (Fox & Protz, 1981), or above lens-shaped aggregates (Crompton, 1977; Van Vliet-Lanoe *et al.*, 1984). While translocations of fine material (Kivisaari, 1979), polyvalent cations and organic matter (Jakobsen, 1989) to lower horizons have been noted, Federova & Yarilova (1972) observed the effects of poorly expressed downward migration of substances in previously-frozen soil.

Fabric orientation within the surface horizons has also been described. Fox & Protz (1981) and Harris (1990) described the vertical alignment of the coarser particles, parallel to the direction of water migration during freezing (Chuvilin & Yazynin, 1988). Post & Dreibelbis (1942) proposed the terms 'concrete' and 'honeycomb' to describe soil fabrics resulting from freezing at low and high water contents, respectively. Smith *et al.* (1991) cautioned, however, that micro-morphological fabrics may be polygenetic, and therefore, not reliable indicators of freezing processes.

Vesicles have also been noted as being common in previously-frozen soils (Bunting, 1977, 1983; Coutard & Mucher, 1985; Dumanski, 1964). Van Vliet-Lanoe *et al.* (1984) and Harris (1990)

suggested that vesicles may be the result of a 'cryo-slaking' process where air expulsion during thaw induces structural collapse.

Such structures are strongly depth dependent, being restricted to the uppermost layers of the profile. Aggregate size is generally found to increase with depth, with smaller aggregates predominating near the surface where frost action, dominated by pore ice formation, is most intense (Federova & Yarilova, 1972; Koniscev *et al.*, 1973; Niewiadomski, 1968; Pawluk, 1988; Smith *et al.*, 1991). The aggregating effects of the freeze-thaw process have been found to be most pronounced near the surface on material that was previously dispersed (Hubbell & Staten, 1951). This observation is consistent with the findings of engineering studies on clay soils, which predominately make use of remoulded samples consolidated from a slurry. Under these conditions, freeze-thaw commonly results in nugget-like structures consisting of small aggregates separated by failure zones (Chamberlain & Gow, 1978; Graham & Au, 1985; Hamilton, 1966; Leroueil *et al.*, 1991).

While these structural forms have been found to be characteristic of previously frozen soils, it must be emphasized that, in an agricultural setting, they must be considered very temporary in nature. Their importance lies more as indicators of the freeze-thaw process than as potential long-term benefits, as tillage will likely destroy the aggregates, at least to some extent. This may not, however, be the case in soils that have received no-till management for extended periods. It is not known to what extent the cumulative effects of successive freeze-thaw events are responsible for the structural benefits of no-till management.

6. Summary (Appendix F)

The role of the freeze-thaw process in controlling structural form and stability remains unclear. Some research points to positive structural effects, such as increased aggregation and stability, and de-compaction in the surface layers of the soil. Other research, however, points to negative effects, including decreased aggregation and stability resulting from frost-induced crushing or dispersion. The annual seasonality of structural form and stability suggests that the over-winter period may play a key role in defining the structural resiliency of soil in regions where freezing temperatures are experienced for at least part of the year. At the same time, it must be recognized that annual weather variations may alter these effects, even from primarily constructive to primarily destructive, over time frames of only a few years.

Whether freezing results in the formation of pore ice or segregational ice is a key consideration, as the resulting effects of the two forms are thought to be quite different. The more destructive pore ice is the result of rapid freezing rates at high water contents, close to the soil surface. The growth of intra-aggregate ice crystals may shatter aggregates, or expanding inter-aggregate ice may either crush aggregates or compress them into a more stable configuration. Conversely, segregational ice involves the formation of ice lenses under slower rates of freezing at greater depths in the soil profile. The upward water migration towards the growing ice lens leads to desiccation and consolidation of both the underlying soil and the inter-lens layers. At the same time, structural discontinuities are formed in the soil at the ice lens locations. In either case, the efficacy of structural disruption is greater with multiple freeze-thaw cycles than continuous freezing conditions.

While the action of cementing materials has received attention in studies of age hardening and the effects of wetting-drying cycles, their role during the over-winter period is less well understood. Similarly, the effects of soil organic matter are not as well established. Conversely, clay content has been acknowledged as an important factor in determining the magnitude and efficacy over-winter processes.

The environmental conditions under which the soil freezes are thought to play a role in determining the effect on soil structure and stability. Surface cover, in the form of mulches and residues, and the subsequent snow cover they can trap and maintain, affect the rate of freezing by inhibiting radiational cooling of the soil. Similarly, the roughness of the soil surface affects both the surface area of soil exposed to freezing and the direction of penetration of the freezing front into the soil.

The interaction of soil properties, particularly the clay content, and the nature of the freezing process itself manifests itself in several ways, including affecting the degree and extent of desiccation during freezing and the soil strength, pore characteristics and the behaviour of the soil during thaw consolidation. The role of both freezing-induced desiccation and thaw consolidation in controlling the final structural form and stability of soil aggregates has not been fully explored.

The overall effects of these processes are of considerable importance as they can have strong influences on the fabric of the soil, and therefore, the water retention properties and nutrient availability as controlled by the pore system. Any structural stability imparted to the soil through these processes will, to a great extent, define the seasonal structural resiliency. The understanding of the spatial and temporal processes operating in the soil during the over-winter period will aid in the long-term management of the soil resource (Radke *et al.*, 1995; Sharratt, 1995).

References (Appendix F)

- Akram, M. and W.D. Kemper. 1979. Infiltration of soils as affected by the pressure and water content at the time of compaction. *Soil Sci. Soc. Am. J.* 43:1080-1086.
- Alderfer, R.B. 1946. Seasonal variability in the aggregation of Hagerstown silt loam. *Soil Sci.* 62:151-168.
- Alkire, B.D. and J.A. Morrison. 1983. Change in soil structure due to freeze-thaw and repeated loading. *Trans. Res. Rec.* 918:15-22.
- Anderson, C.H. 1971. Comparison of tillage and chemical summerfallow in a semiarid region. *Can. J. Soil Sci.* 51:397-403.
- Anderson, C.H. and F. Bisal. 1969. Snow cover effect on the erodible soil fraction. *Can. J. Soil Sci.* 49:287-296.
- Aoyama, K., S. Ogawa and M. Fukuda. 1985. Temperature dependencies of mechanical properties of soils subjected to freezing and thawing. p. 217-222. *In 4th Intl. Symp. Ground Freezing*, Sapporo, Japan.
- Armbrust, D.V., J.D. Dickerson, E.L. Skidmore and O.G. Russ. 1982. Dry soil aggregation as influenced by crop and tillage. *Soil Sci. Soc. Am. J.* 46:390-393.
- Benoit, G.R. 1973. Effect of freeze-thaw cycles on aggregate stability and hydraulic conductivity of three soil aggregate sizes. *Soil Sci. Soc. Am. Proc.* 37:3-5.
- Benoit, G.R. and W.B. Voorhees. 1990. Effect of freeze-thaw activity on water retention, hydraulic conductivity, density, and surface strength of two soils frozen at high water content. p. 45-53. *In Proc. Intl. Symp. Frozen Soil Impacts on Agric., Range, and Forest Lands*, Spokane, WA, Mar. 21-

22, 1990. CRREL Spec. Rep. 90-1.

Benoit, R.E., N.A. Willits and W.J. Hanna. 1962. Effect of rye winter cover crop on soil structure. *Agron. J.* 54:419-420.

Birecki, M. and J. Gastol. 1964. Influence of plants and soil freezing on the fractional humus composition in soil and soil aggregates. p. 955-965. *In* 8th Intl. Cong. Soil Sci., Bucharest, Romania.

Birecki, M. and J. Gastol. 1968. To the problem of influence of soil freezing and thawing upon soil physical and chemical properties and plant yield. *Roczniki Nauk Rolniczych* 94:363-379.

Bisal, F. and K.F. Nielsen. 1964. Soil aggregates do not necessarily break down over winter. *Soil Sci.* 98:345-346.

Bisal, F. and W.L. Pelton. 1971. Effect of freeze-drying on the surface properties of soils as measured by the heat of immersion. *Can. J. Soil Sci.* 51:229-233.

Blackmore, A.V. 1956. Time and temperature as factors in the dispersion of soil crumbs in water. *Australian J. Agric. Res.* 7:554-565.

Blake, G.R., W.W. Nelson and R.R. Allmaras. 1976. Persistence of subsoil compaction in a mollisol. *Soil Sci. Soc. Am. J.* 40:943-948.

Booth, D.B. 1981. Macroscopic behaviour of freezing saturated silty soils. *Cold Reg. Sci. Tech.* 4:163-174.

Bourbonnais, J. and B. Ladanyi. 1985. The mechanical behaviour of frozen sand down to cryogenic temperatures. p. 235-244. *In* 4th Int. Symp. Ground Freezing, Sapporo, Japan.

Broms, B.B. and L.Y.C. Yao. 1964. Shear strength of a soil after freezing and thawing. *J. Soil Mech. Found. Div., A.S.C.E.* 90:1-25.

Brown, S.C. and D. Payne. 1990. Frost action in clay soils. II. Ice and water location and suction of unfrozen water in clays below 0°C. *J. Soil Sci.* 41:547-561.

Bryan, R. 1971. The influence of frost action on soil-aggregate stability. *Trans. Inst. Brit. Geog.* 54:71-88.

Bullock, M.S., W.D. Kemper and S.D. Nelson. 1988. Soil cohesion as affected by freezing, water content, time and tillage. *Soil Sci. Soc. Am. J.* 52:770-776.

Bunting, R.T. 1977. The occurrence of vesicular structures in Arctic and sub-arctic soils. *Zeitschrift fur Geomorphologie* 21:187-195.

Bunting, R.T. 1983. High Arctic soils through the microscope: Prospect and retrospect. *Annals of the Assoc. American Geographers* 73:609-616.

Burney, J.R. and L.M. Edwards. 1987. Soil erosion under freeze/thaw conditions. Intl. Winter Meeting of the American Society of Agricultural Engineers, Chicago, IL. Paper No. 87-2601.

Burt, T.P. and P.J. Williams. 1976. Hydraulic conductivity of frozen soils. *Earth Surface Processes and Landforms* 1:349-360.

- Chamberlain, E.J. 1981. Overconsolidation effects of ground freezing. *Eng. Geol.* 18:97-110.
- Chamberlain, E.J. and S.E. Blouin. 1978. Densification by freezing and thawing of fine material dredged from waterways. p. 623-628. *In Proc. 3rd Intl. Conf. Permafrost.*
- Chamberlain, E.J. and A. Gow. 1979. Effect of freezing and thawing on the permeability and structure of soils. *Eng. Geol.* 13:73-92.
- Chamberlain, E., I. Iskandar and S.E. Hunsicker. 1990. Effect of freeze-thaw cycles on the permeability and macrostructure of soils. p. 145-155. *In Proc. Intl. Symp. Frozen Soil Impacts on Agric., Range, and Forestry Lands.* Spokane, WA.
- Chaney, K. and R.S. Swift. 1986. Studies on aggregate stability. I. Re-formation of soil aggregates. *J. Soil Sci.* 37:329-335.
- Cheng, B.T., S.J. Bourget and G.J. Ouellette. 1971. Influence of alternate freezing and thawing on the availability of some minerals. *Can. J. Soil Sci.* 51:323-328.
- Chepil, W.S. 1954. Seasonal fluctuations in soil structure and erodibility of soil by wind. *Soil Sci. Soc. Am. Proc.* 18:13-16.
- Christensen, S. and R.T. Christensen. 1991. Organic matter available for denitrification in different soil fractions: effect of freeze/thaw cycles and straw disposal. *J. Soil Sci.* 42:637-647.
- Chuvilin, Ye.M. and O.M. Yazynin. 1988. Frozen soil macro- and micro-texture formation. p. 320-323. *In Proc. 5th Intl. Conf. Permafrost, Trondheim, Norway.*
- Coutard, J.P. and H.J. Mucher. 1985. Deformation of laminated silt loam due to repeated freezing and thawing cycles. *Earth Surface Processes and Landforms* 10:309-319.
- Crampton, C.B. 1977. A study of the dynamics of hummocky microrelief in the Canadian north. *Can. J. Earth Sci.* 14:639-649.
- Czeratzki, W. 1971. The importance of ground frost in agriculture, especially in relation to soil cultivation. *Landbauforschung Volkenrode* 21:1-12.
- Czurda, K.A. 1983. Freezing effects on soils: Comprehensive Summary of the ISGF 82. *Cold Reg. Sci. Tech.* 8:93-107.
- Czurda, K.A. and R. Schababerle. 1988. Influence of freezing and thawing on the physical and chemical properties of swelling clays. p. 51-58. *In 5th Intl. Symp. Ground Freezing.*
- Czurda, K.A. and I.F. Wagner. 1984. Processes of frost-action in swelling clays. p. 111-117. *In Proc. 3rd Intl. Offshore Mech. and Arctic Eng. Symp.*
- Czurda, K.A. and J.F. Wagner. 1985. Frost heave and clay expansion in freshwater clays. p. 129-136. *In 4th Intl. Symp. Ground Freezing, Sapporo, Japan.*
- de Jong, E. and R.G. Kachanoski. 1988. Drying of frozen soils. *Can. J. Soil Sci.* 68:807-811.
- Domby, C.W. and H. Kohnke. 1955. The effect of freezing and thawing on structure of the soil

surface. *Agron. J.* 47:175-177.

Dorland, S. and E.G. Beauchamp. 1991. Denitrification and ammonification at low soil temperatures. *Can. J. Soil Sci.* 71:293-303.

Dumanski, J. 1964. Micropedological study of eluviated horizons. Unpubl. M.Sc. Thesis, Univ. of Saskatchewan, Saskatoon, SK.

Dyke, L. and P. Egginton. 1990. Influence of ice lens fabric on the hydraulic conductivity of thawing soil. p. 137-141. *In* Permafrost-Canada: Proc. 5th Can. Permafrost Conf. Nat. Res. Coun./Centre D'Etudes Nordiques, Univ. Laval, Coll. Nordicana No. 54.

Edwards, L.M. 1990. Effect of freeze/thaw on soil aggregate breakdown. p. 97-102. *In* J.A Stone, B.D. Kay and D.A. Angers (eds.) Soil Structure Research in Eastern Canada, Proc. Eastern Canada Soil Structure Workshop. Sept. 10-11, 1990, Guelph, ON.

Edwards, L.M. 1991. The effect of alternate freezing and thawing on aggregate stability and aggregate size distribution of some Prince Edward Island soils. *J. Soil Sci.* 42:193-204.

Edwards, L.M. and J.R. Burney. 1987. Soil erosion losses under freeze/thaw and winter ground cover using a laboratory rainfall simulator. *Can. Agric. Eng.* 29:109-115.

Edwards, L.M. and J.R. Burney. 1989. The effect of antecedent freeze-thaw frequency on runoff and soil loss from frozen soil with and without subsoil compaction and ground cover. *Can. J. Soil Sci.* 69:799-811.

Edwards, L.M. and J.R. Burney. 1991. Sediment concentration of inter-rill runoff under varying soil, ground cover, soil compaction, and freezing regimes. *J. Environ. Qual.* 20:403-407.

Efimov, S.S., N.N. Kozhevnikov, A.S. Kurilko, M. Nikitina and A.V. Stepanov. 1981. Influence of cyclic freezing-thawing on heat and mass transfer characteristics of clay soil. *Eng. Geol.* 18:147-152.

Egginton, P.A. and L.D. Dyke. 1988. The effect of thawing segregation ice on soil permeability and its implications for active layer hydrology. *Can. Geotech. Conf.*, pp. 124-131.

Engelmark, H. 1988. Rates of infiltration into frozen and unfrozen fine sand. *Can. J. Earth Sci.* 25:343-347.

Fedorova, N.N. and E.A. Yarilova. 1972. Morphology and genesis of prolonged seasonally frozen soils of Western Siberia. *Geoderma* 7:1-13.

Fippin, E.O. 1910. Some causes of soil granulation. *Proc. Amer. Soc. Agron.* 2:106-121.

Florkemeier, H., H.G. Frede and B. Meyer. 1989. The break-up of dense aggregates of less derived soils by frost. *Mitteilungen der Deutsche Bodenkundlichen Gesellschaft* 59:145-150.

Formanek, G.E., D.K. McCool and R.I. Papendick. 1984. Freeze-thaw and consolidation effects on strength of a wet silt loam. *Trans. Amer. Soc. Agric. Eng.* 27:1749-1752.

Fox, C.A. and R. Protz. 1981. Definition of fabric distributions to characterize the rearrangement of soil particles in the Turbic Cryosols. *Can. J. Soil Sci.* 61:29-34.

- Fraser, J.K. 1959. Freeze-thaw frequencies and mechanical weathering in Canada. *Arctic* 12:40-53.
- Fukuda, M. 1982. Experimental studies of coupled heat and moisture transfer in soils during freezing. *Contrib. Instit. Low Temp. Sci.* 31:35-91.
- Gardner, R. 1945. Some effects of freezing and thawing on the aggregation and permeability of dispersed soils. *Soil Sci.* 60:437-443.
- Gorkov, V.P. 1983. Effect of primary cultivation on the permeability of frozen soils. *Sov. Soil Sci.* 15:99-103.
- Graham, J. and V.C.S. Au. 1985. Effects of freeze-thaw and softening on a natural clay at low stresses. *Can. Geotech. J.* 22:69-78.
- Greene, R.S.B., A.M. Posner and J.P. Quirk. 1974. A study of the coagulation of montmorillonite and illite suspensions by calcium chloride using the electron microscope. p. 35-40. *In* W.W. Emerson, R.D. Bond and A.R Dexter (eds.) *Modification of Soil Structure*. John Wiley and Sons, Toronto, ON.
- Groenevelt, P.H. and B.D. Kay. 1979. Freezing of field soil in Ontario. p. 27-31. *In* 1979 Progress Report, Dept. Land Resource Science, Univ. of Guelph, Guelph, ON.
- Gusev, Ye.M., O.Ye. Busarova, A.A. Shurkhno and S.V. Yasinskiy. 1992. Effects of a straw mulch on the thermal conditions in soil after snow-cover loss: *Eurasian Soil Sci.* 24:12-23.
- Hamilton, A.B. 1966. Freezing shrinkage in compacted clays. *Can. Geotech. J.* 3:1-17.
- Harris, C. 1974. Autumn, winter and spring soil temperatures in Okstindan, Norway. *J. Glaciol.* 13:521-533.
- Harris, C. 1990. Micromorphology and microfabrics of sorted circles, Front Range, Colorado, U.S.A. p. 89-94. *In* *Permafrost-Canada: Proc. 5th Can. Permafrost Conf. Nat. Res. Coun./Centre D'Etudes Nordiques, Univ. Laval, Coll. Nordicana No. 54.*
- Heinonen, R. 1977. Towards "normal" soil bulk density. *Soil Sci. Soc. Am. J.* 41:1214-1215.
- Henry, H.A.L. 2008. Climate change and soil freezing dynamics: historical trends and projected changes. *Climatic Change* 87:421-434.
- Henry, K.S. 2000. A Review of the Thermodynamics of Frost Heave. CRREL Tech. Rep. TR00-16. 25 pp.
- Hinman, W.C. and F. Bisal. 1968. Alterations of soil structure upon freezing and thawing and subsequent drying. *Can. J. Soil Sci.* 48:193-197.
- Hinman, W.C. and F. Bisal. 1973. Percolation rate as affected by the infiltration of freezing and drying processes of soils. *Soil Sci.* 115:102-106.
- Hoekstra, P. 1966. Moisture movement in soils under temperature gradients with the cold side temperature below freezing. *Water Resources Res.* 2:241-250.

- Hoekstra, P. 1969. Water movement and freezing pressures. *Soil Sci. Soc. Am. Proc.* 33:512-518.
- Honeycutt, C.W. 1995. Soil freeze-thaw processes: Implications for nutrient cycling. *J. Minn. Acad. Sci.* 59:9-14.
- Hubbell, D.S. and G. Staten. 1951. Studies on soil structure: What it is, how cultural practices affect it, how it affects cotton yields. Agricultural Experimental Station, New Mexico College of Agriculture and Mechanic Arts and Soil Conservation Service, USDA, Tech. Bull. 363.
- Jakobsen, B.H. 1989. Evidence for translocations into the B horizon of a Subarctic Podzol in Greenland. *Geoderma* 45:3-17.
- Johnson, R.L., P. Bork and P. Layte. 1989. The effect of freezing and thawing on the dewatering of oil sands sludges. 14th Ann. Can. Land Reclamation Assoc. Conv., Calgary, AB, Aug. 27-31, 1989.
- Johnson, T.C., D.M. Cole and E.J. Chamberlain. 1979. Effect of freeze-thaw cycles on resilient properties of fine-grained soils. *Eng. Geol.* 13:247-276.
- Jones, C.W. 1986. Closed-system freezing of soil in earth dams and canals. *Can. Geotech. J.* 23: 1-8.
- Jung, E. 1931. Untersuchungen über die einwirkung des frostes auf den Erdboden. *Kolloidchem. Beihefte* 32:320-373.
- Kay, B.D. and A.R. Dexter. 1992. The influence of dispersible clay and wetting/drying cycles on the tensile strength of a red-brown earth. *Australian J. Soil Res.* 30:297-310.
- Kay, B.D., C.D. Grant and P.H. Groenevelt. 1985. Significance of ground freezing on soil bulk density under zero tillage. *Soil Sci. Soc. Am. J.* 49:973-978.
- Kemper, W.D., M.S. Bullock and A.R. Dexter. 1989. Soil cohesion changes. p.172:81-95. In W.E. Larson, G.R. Blake, R.R. Allmaras, W.R. Voorhees and S.C. Gupta (eds.) *Mechanics and Related Processes in Structured Agricultural Soils*. NATO ASI Series E: Applied Sciences. Kluwer Academic Publishers.
- Kerston, M.S. and A.E. Cox. 1951. The effect of temperature on the bearing value of frozen soils. *Highway Res. Board Bull.* 40:32-38.
- Kivisaari, S. 1979. Effect of moisture and freezing on some physical properties of clay soils from plough layer. *J. Sci. Agric. Society of Finland* 51:239-326.
- Knocke, W.R. and P. Trahern. 1989. Freeze-thaw conditioning of chemical and biological sludges. *Water Res.* 23:35-42.
- Kohnke, H. and C.H. Werkhoven. 1963. Soil temperature and soil freezing as affected by organic mulch. *Soil Sci. Soc. Amer. Proc.* 27:13-17.
- Koniscev, V.N., M.A. Faustova and V.V. Rogov. 1973. Cryogenic processes as reflected in ground microstructure. *Biul. Peryglacjalny* 22:213-219.

- Konrad, J.-M. 1989a. Influence of over consolidation on the freezing characteristics of a clayey silt. *Can. Geotech. J.* 26:9-21.
- Konrad, J.-M. 1989b. Effect of freeze-thaw cycles on the freezing characteristics of a clayey silt at various overconsolidation ratios. *Can. Geotech. J.* 26:217-226.
- Konrad, J.-M. 1989c. Influence of cooling rate on the temperature of ice lens formation in clayey silts. *Cold Reg. Sci. Tech.* 16:25-36.
- Konrad, J.-M. and J.F. Nixon. 1994. Frost heave characteristics of a clayey silt subjected to small temperature gradients. *Cold Reg. Sci. Tech.* 22:299-310.
- Konrad, J.-M. and J.T.C. Seto. 1994. Frost heave characteristics of undisturbed sensitive Champlain Sea clay. *Can. Geotech. J.* 31:285-298.
- Krumbach, A.W. and D.P. White. 1964. Moisture, pore space, and bulk density changes in frozen soil. *Soil Sci. Soc. Am. Proc.* 28:422-425.
- Larney, F.J., C.W. Lindwall and M.S. Bullock. 1994. Fallow management and overwinter effects on wind erodibility in Southern Alberta. *Soil Sci. Soc. Am. J.* 58:1788-1794.
- Layton, J.B., E.L. Skidmore and C.A. Thompson. 1993. Winter-associated changes in dry-soil aggregation as influenced by management. *Soil Sci. Soc. Am. J.* 57:1568-1572.
- Lebedenko, Yu.P. and L.V. Shevchenko. 1988. Cryogenic deformations in fine-grained soils. p. 396-400. *In Proc. 5th Intl. Conf. Permafrost, Trondheim, Norway.*
- Lee, W., N.C. Bohra, A.G. Altschaeffl and T.D. White. 1995. Resilient modulus of cohesive soils and the effect of freeze-thaw. *Can. Geotech. J.* 32:559-568.
- Lehrsch, G.A. 1997. Aggregate stability response to freeze-thaw cycles. p. 165-171. *In Intl. Symp. on Physics, Chemistry, and Ecology of Seasonally Frozen Soils, Fairbanks, AK. June 10-12, 1997.*
- Lehrsch, G.A., R.E. Sojka, D.L. Carter and P.M. Jolley. 1990. Effects of freezing on aggregate stability of soils differing in texture, mineralogy, and organic matter content. p. 61-69. *In Proc. Intl. Symp. Frozen Soil Impacts on Agric., Range, and Forestry Lands. Spokane, WA.*
- Lehrsch, G.A., R.E. Sojka, D.L. Carter and P.M. Jolley. 1991. Freezing effects on aggregate stability affected by texture, mineralogy, and organic matter. *Soil Sci. Soc. Am. J.* 55:1401-1406.
- Leo, M.W.M. 1963. Effect of freezing and thawing on some physical properties of soils as related to tomato and barley plants. *Soil Sci.* 96:267-274.
- Leroueil, S., J. Tardiff, M. Roy, P. La Rochelle and J.-M. Konrad. 1991. Effects of frost on the mechanical behaviour of Champlain Sea clays. *Can. Geotech. J.* 28:690-697.
- Low, P.F. 1961. Physical chemistry of clay-water interaction. *Advances in Agronomy* 13:269-327.
- Mackie-Dawson, L.A., C.E. Mullins, M.J. Goss, M.N. Court and E.A. Fitzpatrick. 1989. Seasonal changes in the structure of clay soils in relation to soil management and crop type. II. Effects of cultivation and cropping at Compton Beauchamp. *J. Soil Sci.* 40:283-292.

- Martin, R.T. 1960. Water vapour sorption on kaolinite: entropy of adsorption. *Clays and Clay Minerals* 8:102-114.
- Mbagwu, J.S.C. and P. Bazzoffi. 1989. Effect of freezing and thawing on the stability of soil aggregates treated with organic wastes. *Cold Reg. Sci. Tech.* 16:191-199.
- McConkey, B.G., C.D. Reimer and W. Nicholaichuk. 1990. Sealing earthen hydraulic structures with enhanced gleization and sodium carbonate. I. Laboratory study of the effect of a freeze-thaw cycle and a drying interval. *Can. Agric. Eng.* 32:163-170.
- Mermut, A.R. and R.J. St. Arnaud. 1981. Microband fabric in seasonally frozen soils. *Soil Sci. Soc. Am. J.* 45:578-586.
- Merrill, S.D., A.L. Black and T.M. Zobeck. 1995. Overwinter changes in dry aggregate size distribution influencing wind erodibility in a spring wheat-summerfallow cropping system. *J. Minnesota Acad. Sci.* 59:27-36.
- Miller, R.D. 1972. Freezing and heaving of saturated and unsaturated soils. *Highway Res. Rec.* 393:1-11.
- Molope, M.B. 1988. Changes in soil aggregate stability during simulated weather cycles. *S.-Afr. Tydskr. Plant Grond* 5:182-188.
- Mostaghimi, S., R.A. Young, A.R. Wilts and A.L. Kenimer. 1988. Effects of frost action on soil aggregate stability. *Trans. Am. Soc. Agric. Eng.* 31:435-439.
- Nagasawa, T. and Y. Umeda. 1985. Effects of the freeze-thaw process on soil structure. p. 219-224. *In* 4th Intl. Symp. Ground Freezing, Sapporo, Japan.
- Niewiadomski, W. 1968. Textural and structural changes in arable soil after autumn plowing, due to the effects of frost and liming. *Zesc. Probl. Postep. Nauk. Roln* 79:73-88.
- Nixon, J.F. and N.R. Morgenstern. 1973. The residual stress in thawing soils. *Can. Geotech. J.* 10:571-580.
- Ogata, N., T. Kataoka and A. Komiya. 1985. Effect of freezing-thawing on the mechanical properties of soil. p. 201-207. *In* 4th Intl. Symp. Ground Freezing, Sapporo, Japan.
- Orlov, O. and V.V. Fursov. 1988. Settlements of the foundations on seasonally freezing soils. p. 1441-1445. *In* Proc. 5th Intl. Conf. Permafrost.
- Othman, M.A. and C.H. Benson. 1993. Effect of freeze-thaw on the hydraulic conductivity and morphology of compacted clays. *Can. Geotech. J.* 30:236-246.
- Pawluk, S. 1988. Freeze-thaw effects on granular structure reorganization for soil materials of varying texture and moisture content. *Can. J. Soil Sci.* 68:485-494.
- Penner, E. 1963. Frost-heaving in soils. p. 97-202. *In* Proc. Permafrost Intl. Conf. National Academy of Science - National Research Council. Publication 1287.
- Perfect, E., W.K.P. van Loon, B.D. Kay and P.H. Groenevelt. 1990. Influence of ice segregation and solutes on soil structural stability. *Can. J. Soil Sci.* 70:571-581.

- Pikul, J.L., J.F. Zuzel and R.N. Greenwalt. 1986. Formation of soil frost as influenced by tillage and residue management. *J. Soil Water Conservation*. 41:196-199.
- Post, F.A. and F.R. Dreibelbis. 1942. Some influences of frost penetration and microclimate on the water relationships of woodland, pasture, and cultivated soils. *Soil Sci. Soc. Am. Proc.* 7:95-104.
- Radke, J.L. and E.C. Berry. 1995. Soil water and solute movement and bulk density changes in repacked soil columns as a result of freezing and thawing under field conditions. *Soil Sci.* 163:611-624.
- Rawlins, S.L., J.A. Kittrick and W.H. Gardner. 1963. Electron microscope observations of freeze-dried soil conditioners. *Soil Sci. Soc. Am. Proc.* 27:354-356.
- Richardson, S.J. 1976. Effect of artificial weathering cycles on the structural stability of a dispersed silt soil. *J. Soil Sci.* 27:287-294.
- Rowell, D.L. and P.J. Dillon. 1972. Migration and aggregation of Na and Ca clays by the freezing of dispersed and flocculated suspensions. *J. Soil Sci.* 23:442-447.
- Sage, J.D. and R.A. D' Andrea. 1982. Measurement of soil thaw weakening, p. 105-112. *In Proc. 3rd Intl. Symp. Ground Freezing*. Hanover, NH.
- Sapozhnikov, T.M., E.B. Skvortsova and V.N. Bgantsov. 1987. Role of freezing and thawing in thinning of soils. *Sov. Agric. Sci.* 9:17-21.
- Seto, J.T.C. and J.-M. Konrad. 1994. Pore pressure measurements during freezing of an overconsolidated clayey silt. *Cold Reg. Sci. Tech.* 22:319-338.
- Sharratt, B.S. 1995. Migration of water during winter in West Central Minnesota soils. *J. Minnesota Acad. Sci.* 59:15-18.
- Shipitalo, M.J. and R. Protz. 1987. Comparison of morphology and porosity of a soil under conventional and zero tillage. *Can. J. Soil Sci.* 67:445-456.
- Sillanpaa, M. 1961. The dynamic nature of soil aggregation as affected by cycles of freezing and thawing. *Acta Agron. Scand.* 11:87-94.
- Sillanpaa, M. and L.R. Webber. 1961. The effect of freezing-thawing and wetting-drying cycles on soil aggregation. *Can. J. Soil Sci.* 41:182-187.
- Skarzynska, K.M. 1985. Formation of soil structure under repeated freezing-thawing conditions, p. 213-218. *In 4th Intl. Symp. Ground Freezing*, Sapporo, Japan.
- Slater, C.S. and H. Hopp. 1949. The action of frost on the water-stability of soils. *J. Agric. Res.* 78:341-346.
- Slater, C.S. and H. Hopp. 1951. Winter decline of soil structure in clean-tilled soils. *Agron. J.* 43:1-4.
- Smith, C.A.S., C.A. Fox and A.E. Hargrave. 1991. Development of soil structure in some turbic cryosols in the Canadian low Arctic. *Can. J. Soil Sci.* 71:11-29.

- Staricka, J.A. and G.R. Benoit. 1995. Freeze-drying effects on wet and dry soil aggregate stability. *Soil Sci. Soc. Am. J.* 59:218-223.
- Taber, S. 1929. Frost heaving. *J. Geol.* 37:428-461.
- Taber, S. 1930. The mechanics of frost heaving. *J. Geol.* 38:303-317.
- Tisdale, J.M. and J.M. Oades. 1982. Organic matter and water-stable aggregation in soils. *J. Soil Sci.* 33:141-163.
- Trimble, G.R., R.S. Sartz and R.S. Pierce. 1958. How type of soil frost affects infiltration. *J. Soil Water Conservation* 13:18-82.
- Unger, P.W. 1991. Overwinter changes in physical properties of no-tillage soil. *Soil Sci. Soc. Am. J.* 55:778-782.
- Utomo, W.H. and A.R. Dexter. 1981a. Age hardening of agricultural top soils. *J. Soil Sci.* 32:335-350.
- Utomo, W.H. and A.R. Dexter. 1981b. Tillth mellowing. *Soil Sci.* 32:185-201.
- Vallejo, L.E. 1982. The effect of freeze-thaw cycles on the structure and the stability of soil slopes. p. 455-461. *In Proc. 3rd Intl. Symp. Ground Freezing, Hanover, NH.*
- van Dijk, H. and P. Boekel. 1965. Effect of drying and freezing on certain physical properties of peat. *Neth. J. Agric. Sci.* 13:248-260.
- van Dyk, D. and J. Law. 1995. Sublimation and aeolian sand movement from a frozen surface: experimental results from Presqu'île Beach, Ontario. *Geomorphology* 11:177-187.
- van Es, H.M. and R.R. Schindelbeck. 1995. Frost tillage for soil management in the Northeastern USA. *J. Minn. Acad. Sci.* 59:37-39.
- van Vliet-Lanoë, B., J.-P. Coutard, and A. Pissart. 1984. Structures caused by repeated freezing and thawing in various loamy sediments: A comparison of active, fossil and experimental data. *Earth Surface Processes and Landforms* 9:553-565.
- van Vliet-Lanoë, B. and A. Dupas. 1991. Development of soil fabric by freeze/thaw cycles - Its effect on frost heave. p. 189-195. *In Proc. 6th Intl. Symp. Ground Freezing.*
- Voorhees, W.B., C.G. Senst and W.W. Nelson. 1978. Compaction and soil structure modification by wheel traffic in the northern corn belt. *Soil Sci. Soc. Am. J.* 42:344-349.
- Wang, F.L. and J.R. Bettany. 1993. Influence of freeze-thaw and flooding on the loss of soluble organic carbon and carbon dioxide from soil. *J. Environ. Qual.* 22:709-714.
- Williams, P.J. 1963. Suction and its effects in unfrozen water of frozen soils. p. 225-229. *In Proc. Permafrost Intl. Conf. National Academy of Science - National Research Council Publication* 1287.
- Williams, P.J. 1988. Thermodynamic and mechanical conditions within frozen soils and their effects. p. 493-498. *In Proc. 5th Intl. Conf. Permafrost, Trondheim, Norway.*

Williams, P.J. and M.W. Smith. 1989. *The frozen earth: Fundamentals of geocryology*. Cambridge Univ. Press. 306 pp.

Williams, P.J. and J.A. Wood. 1985. Internal stresses in frozen ground. *Can. Geotech. J.* 22:413-416.

Willis, W.O. 1955. Freezing and thawing, and wetting and drying in soils treated with organic chemicals. *Soil Sci. Soc. Am. Proc.* 19:263-267.

Wittsell, L.E. and J.A. Hobbs. 1965. Soil compaction effects on field plant growth. *Agron. J.* 57:534-537.

Wong, L.C. and M.D. Haug. 1991. Cyclic closed-system freeze-thaw permeability testing of soil liner and cover materials. *Can. Geotech. J.* 28:784-793.

Yamamoto, H., T. Ohrai and H. Izuta. 1988. Effect of overconsolidation ratio of saturated soil on frost heave and thaw subsidence. p. 522-527. *In Proc. 5th Intl. Conf. Permafrost*, Trondheim, Norway.

Yong, R.N., P. Boonsinsuk and D. Murphy. 1982. Short-term cyclic freeze-thaw effect on strength properties of a sensitive clay. p. 97-104. *In Proc. 3rd Intl. Symp. Ground Freezing*, Hanover, NH.

Yong, R.N., P. Boonsinsuk and C.W.P. Yin. 1985. Alteration of soil behaviour after cyclic freezing and thawing. p. 187-195. *In Proc. 4th Intl. Symp. Ground Freezing*, Sapporo, Japan.

Zebarth, B.J., D. Lee and B.D. Kay. 1984. Impact resistance of three soils under varying moisture and subzero temperature conditions. *Can. Geotech. J.* 21:449-455.

APPENDIX G

Water and Wind Erosion within Transmission Pipeline ROWs



Water and Wind Erosion within Transmission Pipeline ROWs (LitRev5)

1. Preface

The six literature reviews undertaken in the PARSC - 003 study are focused primarily on the frost heave geohazard within pipeline ROWs, but it was also important to investigate soil erosion by wind and water as potential causes of pipeline exposure (DNV, 2010; PASC, 1996). It should be noted that soil erosion and frozen soils are inextricably linked in cold climate regions. While the rate of infiltration of snow meltwater through frozen soil is impeded by the presence of pore ice and ice segregation features, it is still sufficiently rapid to influence surface runoff and soil erosion (Watanabe *et al.*, 2013; Zhao *et al.*, 2013).

Soil erosion by water can be categorized as i) a 'hydrotechnical hazard' (associated with channelized flow and scouring of watercourses), or ii) a 'geotechnical hazard' (soil- or slope-related, including mass movements of soil) (DNV, 2010; Rizkalla, 2012; Savigny *et al.*, 2005). Only literature dealing with the latter (i.e., soil erosion by wind and water as 'geotechnical hazards') was investigated in this study, and reported here in Appendix G. Wind and water erosion (including mass movement of soil) are geotechnical hazards that can potentially reduce the 'depth of soil cover' (DOC), cause pipeline exposure, or even pipeline failure (Hann & Morgan, 2003; Savigny *et al.*, 2005).

Table G-1 shows that there are several forms of soil degradation that are operative on the Canadian agricultural landscape. Attempts to estimate the cost of each process show wide regional disparities. Clearly, soil salinization (including both 'saline' and 'salt-affected' soils) is a form of soil degradation that is unique to the Prairie Ecozone (southern Alberta, Saskatchewan, Manitoba). Of greater concern are soil erosion (primarily by wind, but also by water) and loss of organic matter from topsoils, which are costing the agricultural industry a great deal, particularly in southern Alberta and Saskatchewan. The popular practice of summerfallowing has been implicated as a major factor contributing to the state of both wind and water erosion in the Prairie Ecozone (Rennie, 1985), but summerfallow acreage has been declining significantly in recent decades (Campbell *et al.*, 2002).

Table G-1. Estimated costs of soil degradation in Canada. (after Miller, 1985; Rennie, 1985).

Province or region	Erosion	Organic matter loss	Acidification	Salinity	Compaction
----- \$ Millions/yr -----					
BC	10	11	5	-	12
AB	200	144	5	80	-
SK	220	170	50	120	-
MB	10	-	-	12	-
ON	68	-	1	-	21
QC	10	-	4	-	100
Atlantic	11	-	6	-	6

- insignificant, or no data available

2. Water erosion of soil on pipeline ROWs

There was only a moderate amount of relevant literature available on the topic of water erosion of soil on pipeline ROWs. In Eastern Canada, water erosion is the most serious agricultural soil degradation problem in Ontario, and is also of major concern in the Atlantic provinces and Quebec (Miller, 1985). In Western Canada, the severity of water erosion has been increasing rapidly, especially in the Prairie Ecozone which is thought to be a result diminished stability of surface soils (Rennie, 1985). In central Alberta, deforestation related to oil field development has induced significant gully erosion (St-Onge, 1978).

Since the late 1970's, the 'Universal Soil Loss Equation' (USLE) has been the tool of choice internationally for soil conservation planning (Wischmeier & Smith, 1978). The 'Revised Universal Soil Loss Equation' (RUSLE) is a more recent computerized version of the original handbook-based USLE (Stone & Hilborn, 2012). RUSLE includes improvements to many of the 'factor' estimates (i.e., empirical equations, nomographs), and can handle more complex combinations of tillage and crop management practices and a greater range of slope configurations. The newer RUSLE2 software can perform event-based erosion scenarios in order to predict long-term mean annual soil loss, but requires a much more comprehensive set of input information (Stone & Hilborn, 2012). Most recently, the Ontario Ministry of Agriculture, Food and Rural Affairs (OMAFRA) has adapted the RUSLE2 model for use on Ontario cropland by adding provincial climate and soil databases, and by polling the farm community in order to assemble the dominant tillage and crop rotation practices currently being used to produce the main crop types grown in the province (K. McKague, per. comm., 2013)

Historically, the efforts of pipeline engineers to prevent i) water erosion of soil, and ii) pipeline failures caused by other geotechnical hazards, on pipeline ROWs have not been entirely successful (Hann & Morgan, 2003; Ramsay, 1982; Ramsey & Burgess, 1985; Schmick, 2006). Available data on pipeline failure incidents attributable to geohazards cover only a short time frame (i.e., typically 25 years or less), but statistical analysis of these incident data suggests a relatively low failure frequency. This finding, however, is tempered by the fact most pipelines in operation have not yet experienced 'design events' (e.g., 1:100 year rainfall event) (Savigny *et al.*, 2005). Internationally, there are numerous private-sector companies that are well equipped to proactively supply erosion control and site stabilization services, as well as rectify incidents of pipeline exposure (e.g., Jones Contractors, Inc., 2014; Submar, Inc., 2014).

Today, geotechnical engineers proactively design and build a number of water erosion control features within pipeline ROWs where the terrain conditions warrant it, including subdrains, 'ditch plugs' ('sack breaker' or 'sand-bentonite' types), and 'diversion berms' ('waterways') (Marshall & Ruban, 1983). Diversion berms are shallow earthen berms/dikes, constructed either in a herringbone or diagonal pattern, that are often required to intercept surface runoff and divert it away from the pipeline trench (Marshall & Ruban, 1983). The USLE and its updates are used extensively to determine the appropriate spacing of diversion berms on pipeline ROWs. Morgan *et al.* (2003) showed that the plethora of 'empirical formulae' available for determining appropriate diversion berm spacings (i.e., for terrain slopes ranging from 5 to 50%) provided widely variable results. Alternatively, the USLE generated berm spacings that were very large on gentle slopes (i.e., often longer than the slope length itself), but unfeasibly short on slopes >25% (Morgan *et al.*, 2003). The findings for extreme slopes (e.g., mountainous terrain) are to be expected since the USLE was originally a tool created for soil conservation planning on agricultural landscapes (Wischmeier & Smith, 1978). Most recently, the USLE has been used in the creation of a risk matrix for pipeline exposure by water erosion. The study used the soil loss rate (estimated by the USLE) and the 'depth of soil cover' (DOC) to categorize pipeline exposure risks due to water erosion of soil (Gavassoni & Garcia, 2010). It should be noted that the USLE and its updates estimate soil loss arising from rill and gully erosion only, and do not predict mass

movement of soil which can dramatically increase the pipeline exposure risk on steep terrain (Fig. G-1).



Figure G-1. Pipeline exposure caused by mass movement of soil on steep terrain. (source: Jones Contractors, Inc., 2014).

In terms of pipeline abandonment strategies, the PARSC - 003 study only considers pipelines abandoned-in-place, but not pipeline removal (i.e., ROW disturbance). Swanson *et al.* (2010) reported on a case study in Alberta where a very early pipeline (constructed in 1925) was recently decommissioned by removing problematic segments amounting to 1/3 of its length, and leaving the remainder abandoned-in-place. It is known that the soil disturbance caused by pipeline removal can introduce soil erosion problems (e.g., exposed surface soil, ground subsidence, surface water channelling) that are not likely to be as significant with abandonment-in-place (DNV, 2010; PASC, 1996). For pipelines abandoned-in-place, ground subsidence due to corrosion and structural failure of the pipelines is not believed to be an imminent near-term problem, particularly for smaller diameter pipelines (DNV, 2010; PASC, 1996).

3. Wind erosion of soil on pipeline ROWs

The amount of relevant literature available on the topic of wind erosion of soil on pipeline ROWs

was very limited. In Eastern Canada, wind erosion is only significant on the coarse-textured soils of Prince Edward Island, on exposed organic soils in Quebec, and on some organic and coarse-textured soils in Ontario (Miller, 1985). In Western Canada, the incidence of wind erosion in the agricultural regions of British Columbia is insignificant. In the Prairie Ecozone (Palliser Triangle Region) of Western Canada, however, wind erosion is the dominant process responsible for the decline in soil quality (Rennie, 1985).

The magnitude of the wind erosion problem in the Prairie Ecozone has caused agronomists to investigate the use of the 'Wind Erosion Prediction System' (WEPS) to spatially evaluate the inherent wind erosion risk in that region (Coen *et al.*, 2004). WEPS is a process-based, continuous daily time step model which has the ability to predict wind erosion events in response to environmental and soil/crop management variations (Hagen, 2004; Hagen *et al.*, 1996). Figure G-2 shows representative maps generated by the WEPS model for two townships in Alberta (Coen *et al.*, 2004). The township in southern Alberta (near Lethbridge) was chosen to represent an area where the wind erosion risk was thought to be high, due to the particular soil-management-weather combinations present. This was corroborated by the WEPS model, which predicted wind erosion losses of 134 tonnes/ha or more in some map polygons (Fig. G-2a). The township in central Alberta (near Edmonton) was chosen to represent an area where the wind erosion risk was thought to be low. This was also corroborated by the WEPS model, which predicted wind erosion losses of no more than 2.2 tonnes/ha in any map polygons (Fig. G-2b).

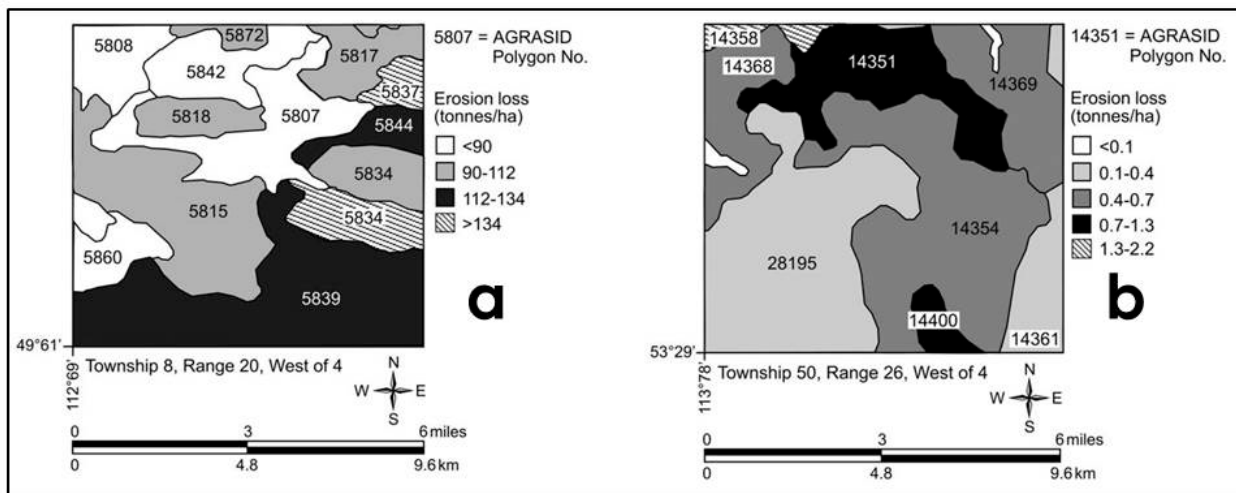


Figure G-2. Examples of WEPS wind erosion susceptibility maps for a) a township in southern Alberta near Lethbridge, and b) a township in central Alberta near Edmonton. (after Coen *et al.*, 2004).

Pipeline ROWs traversing dryland/rangeland areas in western North America can be prone to significant wind erosion, and even blowouts (Peterson, 2013; Zellmer and Taylor, 1991). Figure G-3 includes aerial and ground level views of such a blowout in southeastern New Mexico, where Peterson (2013) investigated the efficacy of three methods to remediate disturbed areas within a pipeline ROW (i.e., orchard tree brush, net structures and snow fencing).

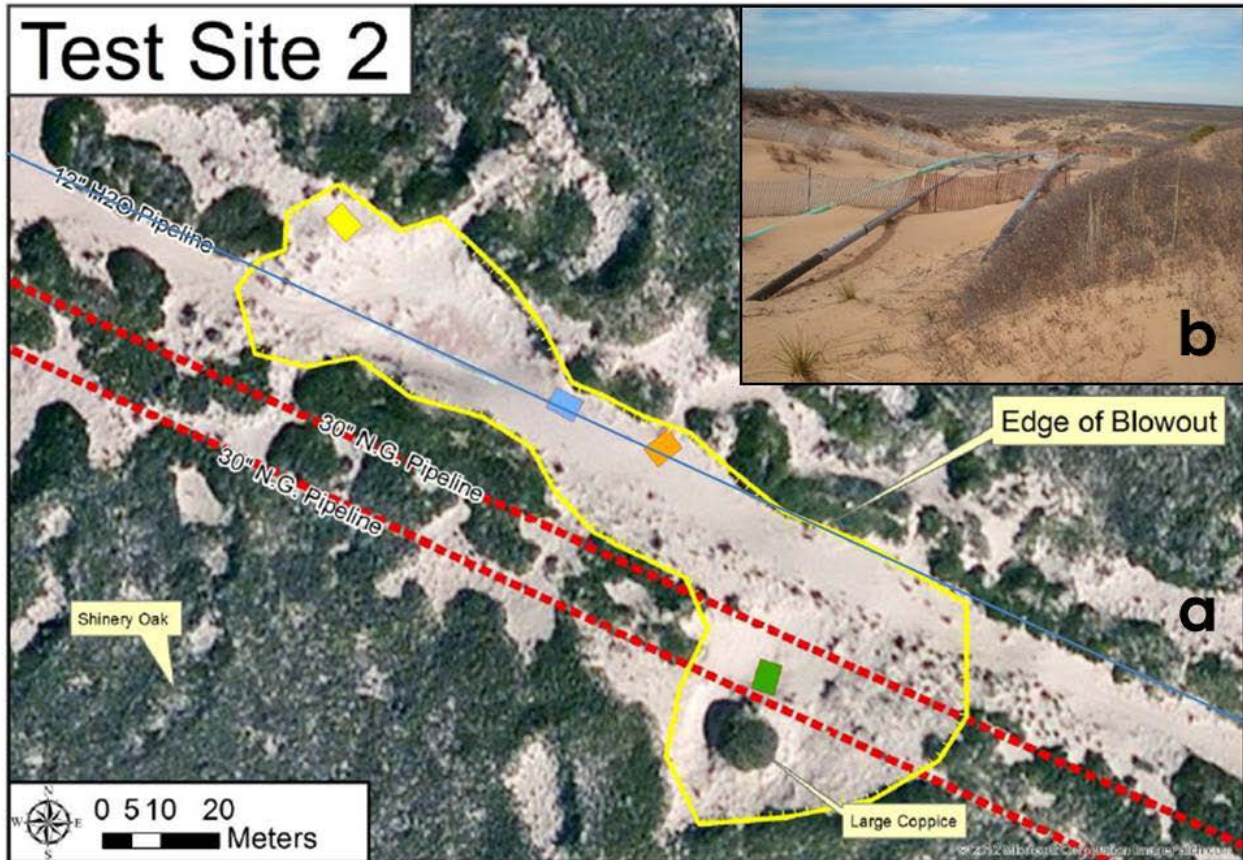


Figure G-3. A dryland blowout caused by wind erosion on a pipeline ROW in southeastern New Mexico, with imagery from two perspectives: a) an aerial view, and b) a ground level view. The blowout is outlined in yellow, the two natural gas pipelines are outlined in red, and the water pipeline is outlined in blue. (after Peterson, 2013).

Walker *et al.* (1996) successfully used wind barriers (i.e., agricultural straw bales, brush mulch) within pipeline ROWs to aid in the recovery of native prairie vegetation in the Great Sand Hills region of Saskatchewan. Zellmer & Taylor (1991) used different combinations of site treatments, including native hay mulch, to stabilize and revegetate blowout areas within pipeline ROWs in the Texas panhandle. The most successful individual revegetation method was 'sprigging', which involves the planting of sprigs at spaced intervals in furrows or holes. Sprigs are plant segments cut from rhizomes or stolons that include crowns and roots (Zellmer & Taylor, 1991).

Some conventional methods that are used successfully in more humid temperate climates to stabilize disturbed areas do not perform as well in dryland/rangeland areas. In Fig. G-4, a pipeline company had repaired a dryland blowout site in southeastern New Mexico by mounding locally-available sand material over the exposed pipeline and covering this with a geotextile erosion mat. The image shown in Fig. G-4 was taken only one year after the repair work, and the geotextile is shown to be badly fragmented, presumably by wind damage and sand abrasion (Peterson, 2013).

One of the newer commercial products intended for use on pipeline ROWs and other disturbed sites to control wind (or water) erosion is wood-strand erosion control mulch (Dooley & Perry, 2013). In contrast to agricultural straw (Fig. G-5), it is weed-free, long-lasting and wind-resistant.



Figure G-4. A dryland blowout caused by wind erosion on a pipeline ROW in southeastern New Mexico, with a damaged geotextile erosion mat emplaced only one year prior. (after Peterson, 2013).

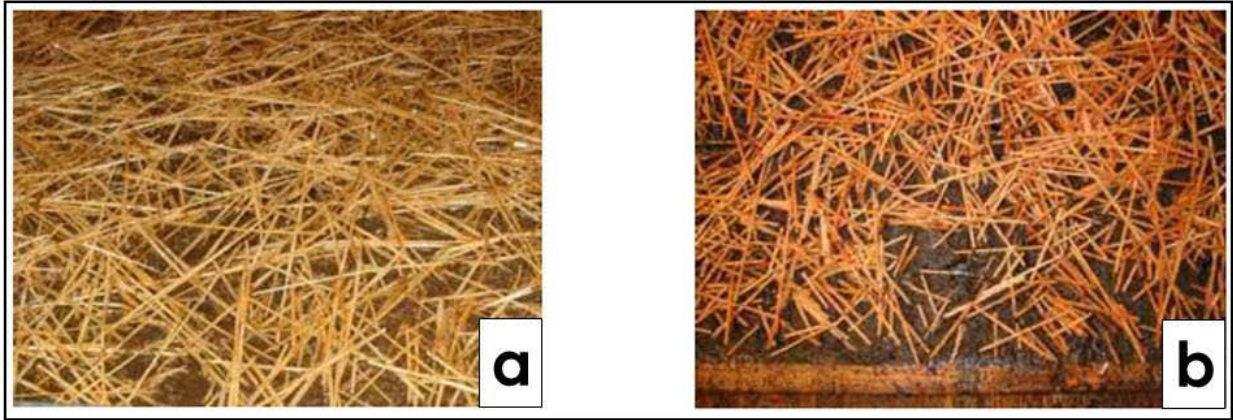


Figure G-5. Contrasting images of two alternative erosion control mulches, both at 70% soil cover, with a) showing agricultural wheat straw, and b) showing commercial wood-strand erosion control mulch. (after Dooley & Perry, 2013).

4. Summary (Appendix G)

Wind and/or water erosion (including mass movement of soil) are geotechnical hazards that can potentially reduce the 'depth of soil cover' (DOC), cause pipeline exposure, or even pipeline failure. The 'Universal Soil Loss Equation' (USLE) is used extensively by pipeline engineers

to determine i) the appropriate spacing of diversion berms on pipeline ROWs, and ii) pipeline exposure risk. In areas prone to wind erosion, the 'Wind Erosion Prediction System' (WEPS) is an effective soil conservation planning model, including within pipeline ROWs.

References (Appendix G)

Campbell, C.A., R.P. Zentner, S. Gameda, B. Blomert and D.D. Wall. 2002. Production of annual crops on the Canadian prairies: trends during 1976-1998. *Can. J. Soil Sci.* 82:45-57.

Coen, G.M., J. Tatarko, T.C. Martin, K.R. Cannon, T.W. Goddard and N.J. Sweetland. 2004. A method for using WEPS to map wind erosion risk of Alberta soils. *Environmental Modelling and Software* 19(2):185-189.

Det Norske Veritas (DNV). 2010. Pipeline abandonment scoping study. A report prepared for the National Energy Board (NEB). 85 pp. Available at: <http://www.neb-one.gc.ca/clf-nsi/rthnb/pblcprtcpn/pplnbndnmnt/pplnbndnmntscpngstd.pdf> (verified Oct. 6, 2014).

Dooley, J.H. and M.C. Perry. 2013. Field experience with wood-strand erosion control mulch on mine and pipeline projects. 18 pp. *In* 2013 National Meeting of the American Society of Mining and Reclamation ('Reclamation across Industries'), June 1-6, 2013, Laramie, WY.

Gavassoni, E. and C.B. Garcia. 2010. Prediction of exposure risk for buried pipelines due to surface erosion. p.192-201. *In* S.E. Burns, S.K. Bhatia, C.M.C. Avila and B.E. Hunt (eds.) *Proc. 5th Int'l. Conf. on Scour and Erosion (ICSE-5)*. ASCE, Geotechnical Special Publ. no. 210. Nov. 7-10, 2010, San Francisco, CA.

Hagen, L.J. 2004. Evaluation of the Wind Erosion Prediction System (WEPS) erosion submodel on cropland fields. *Environmental Modelling and Software* 19(2):171-176.

Hagen, L.J., L.E. Wagner and J. Tatarko. 1996. Wind Erosion Prediction System (WEPS) - Technical Documentation. 284 pp. Available at: <http://www.weru.ksu.edu/weps/wepshome.html> (verified Oct. 6, 2014).

Hann, M.J. and R.P.C. Morgan. 2003. Prevention of bio restoration failures along pipeline rights-of-way. p. 227-233. *In* H.M. Fox and H.R. Elliott (eds.) *Land reclamation: extending the boundaries*. *Proc. 7th Int'l. Conf. of the Int'l. Affiliation of Land Reclamationists*, Runcom, UK, May, 2003.

Jones Contractors, Inc. 2014. Henderson, TN. Available at: http://jonescontractors.com/?page_id=89 (verified Oct. 6, 2014).

Marshall, R.G. and T.F. Ruban. 1983. Geotechnical aspects of pipeline construction in Alberta. *Can. Geotech. J.* 20:1-10.

McKague, Kevin (CPESC, P.Eng.). 2013. Rural Water Quality Engineer. Environmental Management Branch, Food Safety and Environment Division, Ontario Ministry of Agriculture, Food and Rural Affairs, Woodstock, ON. (personal communication).

Miller, M.H. 1985. Soil degradation in eastern Canada: its extent and impact. *Can. J. Agr. Economics* 33:7-18.

Morgan, R.P.C., Ts.E. Mirtskhoulava, V. Nadirashvili, M.J. Hann and A.H. Gasca. 2003. Spacing of berms for erosion control along pipeline rights-of-way. *Biosystems Engineering* 85(2):249-259.

Peterson, K. 2013. Remediation of sand dune blowouts along pipeline rights of way. MSc thesis. Department of Geography, The University of New Mexico, Albuquerque, NM. Available at: http://repository.unm.edu/bitstream/handle/1928/23207/Knut%20Peterson%20Thesis%20Final%2012_12_2012.pdf?sequence=1 (verified Oct. 6, 2014)

Pipeline Abandonment Steering Committee (PASC). 1996. Pipeline abandonment: a discussion paper on technical and environmental issues. November, 1996. 37 pp. Available at: <http://www.neb-one.gc.ca/clf-nsi/rsftyndathnvrnmnt/sfty/rfrncmtrl/pplnbndnmnttchnclnvrnmntl-eng.html> (verified Oct. 6, 2014)

Ramsay, S.A. 1982. To what extent is topsoil conservation necessary in pipelining? *International Right of Way Association (IRWA). Right of Way Magazine*, Aug. 1982. p. 25-29.

Ramsey, J.F. and S.A. Burgess. 1985. Pipeline construction: prevention of impacts to agricultural lands. *International Right of Way Association (IRWA). Right of Way Magazine*, Aug. 1985. p. 7-10.

Rennie, D.A. 1985. Soil degradation: a western perspective. *Can. J. Agr. Economics* 33:19-29.

Rizkalla, M. 2012. A global perspective on pipeline geohazards. *Pipelines International* 14:42.

Savigny, K.W., M. Porter and M. Leir. 2005. Geohazard management trends in the onshore pipeline industry. 9 pp. *In Geoline 2005. Int'l. Symposium on Geology and Linear Development*. Lyon, France, May 23-25, 2005.

Schmick, J. 2006. Complexities of pipeline easement damages on Midwest farmland. *International Right of Way Association (IRWA). Right of Way Magazine*, Nov./Dec. 2006. p. 32-37.

St-Onge, D.A. 1978. Gully erosion in the Swan Hills, Alberta. *Geographie Physique et Quaternaire* 32(4):361-368.

Stone, R.P. and D. Hilborn. 2012. Universal soil loss equation (USLE). OMAFRA Factsheet (Agdex 572/751). Ontario Ministry of Agriculture, Food and Rural Affairs, Toronto, ON. October, 2012. 8 pp.

Submar, Inc. 2014. Houma, LA. Available at: <http://submar.com/industries/energy/onshore-pipeline/> (verified Oct. 6, 2014).

Swanson, J.M., T. Kunicky and P. Poohkay. 2010. Environmental considerations for pipeline abandonment: a case study from abandonment of a southern Alberta pipeline. 7 pp. *In Proceedings 8th Intl. Pipeline Conference (IPC2010 - ASME)*, Calgary, AB. Sept. 27-Oct. 1, 2010.

Walker, D., L. Kremer and W. Marshall. 1996. Recovery of native prairie after pipeline construction in the Sand Hills region of Saskatchewan. p. 123-124. *In C.B. Powter, M.A. Naeth and D.A. Lloyd (eds.) Conservation and Reclamation: an Ecosystem Perspective. Annual Meeting of the Canadian Land Reclamation Association*, Calgary, AB, Sept. 18-20, 1996.

Watanabe, K., K. Tetsuya, S. Dun, J.Q. Wu, R.C. Greer and M. Flury. 2013. Water infiltration into a frozen soil with simultaneous melting of the frozen layer. *Vadose Zone J.* 12(1). 7 pp.

Wischmeier, W.H. and D.D. Smith. 1978. Predicting rainfall erosion losses - a guide to conservation planning. U.S. Dep't. of Agriculture, Agriculture Handbook No. 537. 69 pp.

Zellmer, S.D. and J.D. Taylor. 1991. Blowout revegetation on pipeline rights-of-way in the Texas Panhandle. Gas Research Institute, Chicago, IL. Environment and Safety Research Dep't. 105 pp.

Zhao, Y., T. Nishimura, R. Hill and T. Miyazaki. 2013. Determining hydraulic conductivity for air-filled porosity in an unsaturated frozen soil by the multistep outflow method. *Vadose Zone J.* 12(1). 10 pp.

APPENDIX H

Update DNV (2010) Report Literature Review on Frost Heaving



Update DNV (2010) Report Literature Review on Frost Heaving (LitRev6)

1. Overview

Details on the methodology used for *LitRev6* can be found in Section 4.3.5. Searches using the five keyword clusters yielded very little relevant literature, and no articles directly pertaining to frost heave of abandoned pipelines.

It had been suggested in DNV (2010) that research on frost heave of culvert pipes might serve as a useful proxy. In fact, the keywords 'frost heave culvert' provided the most useful information. Most research on frost heave of culvert pipes involves examining the effect of various insulating materials, but the experimental design usually includes uninsulated culvert pipe as an 'experimental control'. For example, Pyskadlo (1977) examined heat flux in a culvert-soil system, and found that uninsulated culvert pipe can significantly influence both frost depth in soil near the culvert pipe in winter as well as the rate of thawing in the spring. This observation corroborates the role of pipe metal as a strong thermal conductor in a culvert-soil or pipeline-soil system.

The citations for eight of the more useful references encountered (as well as their abstracts) are provided below.

2. Literature review results (including abstracts)

1. Bunch, C., G. Cameron and R.G. Mora. 2010. Guidelines to conducting threat susceptibility and identification assessments of pipelines prior to reactivation. 8th International Pipeline Conference, Calgary, AB. Sept. 27 – Oct. 1, 2010. ASME Proceedings, Pipeline Integrity Management. pp. 901-911.

Abstract

This paper provides guidelines to identify all threats and assess a pipeline's susceptibility to those threats in order to select appropriate and effective mitigation, monitoring, and prevention measures prior to reactivating pipelines. The intent of this paper is to provide pipeline operators, consultants and regulatory agencies with a generic threat assessment approach that has to be customized to the pipeline-specific characteristics and conditions, and the regulatory requirements of its own jurisdiction. A literature review and authors' experiences across the pipeline industry have identified the need for a generic, yet complete approach that guides pipeline integrity engineers in the methodologies that adequately and effectively assess threats prior to reactivation and that can be validated in a timely manner during the operations. Pipeline operators may be called on to reactivate pipelines that are facing challenges such as aging, changes in operational conditions, lack of maintenance and inconsistent integrity practices while facing constraints from increasing population density, higher pressure and flow throughput requirements of a competitive marketplace, and regulatory requirements insisting on higher levels of safety and protection of the environment. This paper was structured with the following components to assist the reader in conducting threat assessments: • Current regulations and recognized industry standards with respect to reactivating pipelines; • Definition of and differentiation between hazard and threat; • Hazard identification analysis for the known and potential situations, events and conditions; and • Threat susceptibility and identification analysis process for the known categories derived from the hazard identification process. A case study is described as an example of applying the guidelines to conduct threat susceptibility and identification assessments of a pipeline prior to its reactivation. The results from the threat susceptibility and identification assessment process can help operators, consultants and regulators in determining effective inspection, mitigation, prevention and monitoring measures.

2. Dai, H.M. and X.L. Wang. 1995. On the minimum depth of bridge and culvert foundations in seasonal frost regions. *Cold Regions Science and Technology* 23(2):183-190.

Abstract

Based on extensive field experiments related to frost heave susceptibility of clayey soil and fine sand and frost heave of different depths of foundations, those factors influencing depths of bridge and culvert foundations in seasonal frost regions were analysed in detail. These factors include the correction coefficient to standard frost penetration, the allowable thickness of frozen soil under foundations, the influence coefficient of frost penetration due to the depth of foundations, and so forth. A method and its related parameters for determining the minimum depth of bridge and culvert foundations are presented.

3. Dow Chemical Company. 2008. Insulation for insulated culvert construction. Available at: http://msdssearch.dow.com/PublishedLiteratureDOWCOM/dh_01fb/0901b803801fb029.pdf?filepath=styrofoam/pdfs/noreg/179-04501.pdf&fromPage=GetDoc (verified Oct. 6, 2014)

Abstract

The culvert test area temperature and elevation were monitored for two years. This study concluded that the Dow insulation was effective in preventing frost heave. Freezing temperatures were eliminated below the insulation.

4. Duquenois, C. and R.L. Sterling. 1991. Frost heave patterns and optimal design of insulated culverts. Underground Space Center, Univ. of Minnesota, Minneapolis, MN. Report prepared for the Minnesota Local Road Research Board, Materials and Research Laboratory, Maplewood, MN. June, 1991. 29 pp.

Abstract

When a culvert is placed under a road, the presence of air at freezing temperatures in the culvert may induce differential frost conditions in pavements. Also, a differential frost heave pattern can appear when the culvert is placed in a frost-susceptible soil. In this project, computer simulations of temperature distributions and frost heave patterns around culverts were carried out, and the effects of various insulation techniques were analyzed under weather conditions representative of Minnesota winters. The pavement slope variance, which is a commonly used variable describing the roughness (or loss of serviceability) of a given pavement section profile, proved to be a valuable indicator under frost heave conditions. Results indicate that culvert insulation reduces the value of the pavement slope variance throughout the freezing period: the higher the insulation thickness, the lower the resulting slope variance (or loss of serviceability).

5. Ferris, G. 2009. Differential frost heave at pipeline-road crossings. p. 68-78. In H.D. Mooers and J. Hinzmann (eds.) *Cold Regions Engineering 2009, Cold Regions Impacts on Research, Design, and Construction*. 14th Conference on Cold Regions Engineering, Duluth, MN. Aug. 31 - Sept. 2, 2009.

Abstract

Essentially all areas of Canada are affected by significant seasonal frost penetration. The effect of the frost penetration on roads and highways, especially the amount of total frost heave and the effect of the subsequent thaw, varies with soil type. Road design and construction must consider the effects of frost heave and subsequent spring thaw. The location and amounts of differential frost heave are especially important to pavement performance. Frost heave

behaviour can be manifest at pipeline crossings as "reverse frost heave", where the ground above the pipeline does not heave as much as the adjacent ground. If the amount of differential heave within pipeline crossing is large, it can lead to rough, and potentially unsafe, driving conditions. In the case of pipeline crossings, if rough road surface conditions occur in the right of way, highway agencies typically request compensation for additional maintenance costs from the pipeline company. A case study that shows the effects of differential frost heave at a pipeline road crossing is presented.

6. Pyskadlo, R.M. 1977. Attenuation of frost action: selected problems. New York State, Department of Transportation, Engineering Research and Development Bureau, Albany, NY. Report No. NYS-DOT-ERD-77-RR-39. 52 pp.

Abstract

This study addressed selected problems associated with frost action, with the following specific objectives: 1) determination of objectionable differential heaving at culverts, 2) study of heat transfer in a culvert-soil system, 3) evaluation of four experimental thermally insulated culverts, and 4) investigation of several methods for transition from fully insulated to uninsulated pavement. First, a survey in northern New York revealed that most differential frost heaves were occurring at culverts, but that only one of every eight culverts was associated with such heaves. Second, in the case of one instrumented culvert, the pipe appeared to aid in thawing of frozen soil but did not greatly influence frost depth in the soil near it; however, a second instrumented but uninsulated culvert serving as a control significantly influenced both thawing and frost depth in soil near the pipe. Third, of the four insulated culverts, three completely covered with insulation were effective in minimizing the potential for differential frost heaving; a fourth, where a continuous layer of insulation was placed below the pipe, was ineffective because it allowed the frost line to be drawn down and restricted upward warming of the pipe. Fourth, based on an instrumented field test, the concept of a tapered insulation transition appears valid in that it permits a gradual increase in frost penetration, which (theoretically) should decrease any abrupt change in vertical profile at the extremities of insulated pavements; varying the spacing of small strips of insulations was less effective. Finally, the concluding chapter documents the performance of several other transition sections, but because they were constructed before this study began and were not instrumented, no conclusions were drawn.

7. St. Pierre, M.A. 2006. Performance of insulated shallow cross pipes in a cold region. MSc thesis. Department of Civil Engineering, University of Maine, Orono, ME. *Electronic Theses and Dissertations*. Paper 795.
Available at: <http://digitalcommons.library.umaine.edu/etd/795/>
(verified Oct. 6, 2014)

Abstract

Pavement performance resulting from current installation practices for shallow cross pipes (culverts) has been problematic for departments of transportation in northern climates, such as Maine. Shallow cross pipes are located within the seasonal frost zone, typically ranging from 1.2 to 2.4 m (4 to 8 ft) below ground surface in Maine (Floyd, 1978). Differential heave of shallow cross pipes beneath Maine's highways can result in premature pavement failure reducing serviceability and quality of ride. The type of heave developed at cross pipes can also become a safety issue for the traveling public. In some cases, the heave remains after thawing, resulting in permanent displacement of the road surface. The cause of differential heave is generally attributed to discontinuities within the subgrade although variable access to water and exposure to the sun also contribute. Discontinuities such as the installation of shallow cross pipes create differences in the soil properties and/or thermal regime between the cross pipe trench

and the adjacent soil. The objective of this study was to evaluate the performance of shallow cross pipes insulated with extruded polystyrene insulation as a method to distribute differential heave over larger distances. Research consisted of field testing, instrumentation, and numerical modeling of insulated and uninsulated cross pipes at five selected sites across Maine. The effectiveness of the installation methods with extruded polystyrene insulation placed above and below the cross pipe were evaluated. Cross pipe installations were evaluated based on: influence of insulation, effect on pattern of frost penetration, surface frost heave, influence of soil type, and regional climatic effect. Experimental cross pipes were installed between May and October 2004 along Routes 11 in Nashville Plantation, 27 in Eustis, 117 in Buckfield/South Paris, 150 in Cornville, and 166 in Castine/Penobscot. A total of 15 experimental cross pipes were selected, reconstructed, instrumented, and monitored. Four types of test methods were constructed: (1) underlying insulation, (2) overlying insulation, (3) overlying insulation for very shallow cross pipes, and (4) control. Experimental cross pipes were instrumented with thermocouples, to measure the temperature profile in the vicinity of the cross pipe and frost penetration, and frost-free elevation benchmarks, to assist with measuring vertical displacement of the wearing surface. The thermocouples indicated that sections with insulation above the cross pipe significantly reduced the frost penetration into the underlying soils. The reduction in freezing temperatures limited the amount of frost action and subsequent total heave directly over the cross pipe. However, from the heave surveys, most pipes that develop heave have greater total heave away from the cross pipe than over the pipe resulting in greater differential heave. Results showed for sites that experienced significant total heave, the placement of insulation over the cross pipe increased the both the magnitude and abruptness of the differential heave. This showed that the length of the transition insulation on each side of the cross pipe was inadequate. The maximum differential heave was observed to occur at the end of the freezing season and start of the spring thaw.

8. Zhang, Y. and R.L. Michalowski. 2012. Frost-induced heaving of soil around a culvert. GeoCongress 2012: State of the Art and Practice in Geotechnical Engineering. Oakland, CA, March 25-29, 2012. pp. 4456-4465.

Abstract

A good portion of silty soils and clays are characterized by susceptibility to frost heaving. This phenomenon needs to be considered in seasonally freezing environments. The issue, however, is also encountered in artificial freezing (for construction purposes) and in pipeline operations where the medium transported may have below-freezing temperature and the surrounding soil is above freezing, or viceversa. Accounting for frost heave is important in transportation infrastructure, and of particular concern are the regions in soils where thermal boundary conditions make it possible for the freezing front to propagate into the soil at different rates, leading to differential frost heave. A constitutive model for frost heaving will be implemented in the finite element analysis, and boundary value problems will be simulated to reveal the behavior of soil during freezing in the neighborhood of a culverts passing below a road. An interesting outcome was found: the road above the culvert may experience a "bump" in the first few weeks of freezing, but later the frost heave directly above the culvert may slow down, leading to a "depression" in the surface above the culvert. The occurrence of a bump due to frost heave is a known phenomenon, but the likelihood of a depression is, so far, hypothetical.

References (Appendix H)

- Det Norske Veritas (DNV). 2010. Pipeline abandonment scoping study. A report prepared for the National Energy Board (NEB). 85 pp. Available at: <http://www.neb-one.gc.ca/clf-nsi/rthnb/pblcprtcptn/pplnbndnmnt/pplnbndnmntscpngstd.pdf> (verified Oct. 6, 2014).

APPENDIX I

Programming Code for the *Konrad_SP1.0*
Frost Heave Model (Mathcad version)

Programming Code for the *Konrad_SP1.0* Frost Heave Model (Mathcad version)

1. General overview

This appendix contains a portion of the entire Python *Konrad_SP1.0* frost heave model code that was re-written into a Mathcad 'worksheet' format (Mathcad, 2014). Initially, this was done because Mathcad automatically verifies and validates scientific calculations, checks the internal consistency of units, etc. It was also done in order to combine a variety of different elements (e.g., mathematics, descriptive text, supporting graphs) into the worksheet, which is naturally much more readable than Python program code (Python Software, 2014).

In Appendix J, 'summary' output tables from the Python program (*Konrad_SP1.0*) are presented for a trial SLC3.2 polygon (polygon i.d. = 809014) located in Alberta. The last record (row 13) in each of Tables J-1 to J-5 are highlighted in yellow. It is this last, or deepest, soil layer in the third soil association (5% aerial extent) that is used here in Appendix I to illustrate the soil-related sub-routines in the *Konrad_SP1.0* model, but in a Mathcad worksheet format.

This clay loam subsoil layer (or soil 'horizon') extends from 50 to 100+ cm below the surface, and has a SOM content of 1.72%kg kg⁻¹ and a D_b of 1.45 Mg m⁻³ (see Table J-1). All input data from SLC3.2 enter the Python *Konrad_SP1.0* model as CSV files (i.e., 'comma-separated values', or more generally 'character-separated values'). The output files from *Konrad_SP1.0* are also CSV files, which can then be imported into MS Excel and readily displayed in the format shown in Tables J-1 to J-6 (see Appendix J).

The first 11 pages of the Mathcad worksheet shown in this appendix outline the algorithms that make up the core of the *Konrad_SP1.0* program as outlined in Konrad (1999; 2005). The last 9 pages outline a simple sensitivity analysis of the Konrad (1999) equations used to determine the segregation potential (SP). It is this sort of detailed scrutiny in Mathcad that led to the observation that it is the $d_{50}(FF)$ and SSA parameters that are by far the two most important in the Konrad (1999; 2005) model, in terms of their effect on the computed SP values.

2. Some specifics on the Python *Konrad_SP1.0* model

The Python *Konrad_SP1.0* model is set up such that the user can work on two possible sources of soil data in Canada: i) the SLC3.2 soil database (see Appendix R), or ii) user-supplied soil data originating from site-specific areas.

Data source 1 (SLC3.2): When first initiated, the model automatically loads all of the necessary soil data from SLC3.2 for all of Canada, which requires about 4 minutes to complete. There are about 60,000 records (or 'soil layers') in the SLC3.2 soil database (only about 40,000 are useable), distributed across about 12,000 polygons. There are only about 4000 'useable' polygons, however, and even fewer (about 3,600 polygons) that can be used by the *Konrad_SP1.0* model. The Python *Konrad_SP1.0* model accesses 4 levels of information from SLC3.2:

Polygon attribute tables (PAT)	Soil layer tables (SLT)
Component tables (CMP)	Soil name tables (SNT)

The model then 'loops' through the records, requiring about 1-2 seconds/polygon to carry out the PTF calculations that will be used in the Konrad (1999; 2005) algorithms, including the complex $d_{50}(FF)$ curve fitting. The SLC3.2 data for Canada have been set up as CSV files that the Python model can access by soil layer, soil name, and up to 3 soil names per polygon. As noted earlier, the soil data from SLC3.2 enters the Python program as CSV files, and the Python program delivers the model results in the same CSV file format, which can then be imported into MS Excel for viewing.

Data source 2 (user-supplied data): When the model user has site-specific soil data that is to be processed with the Python *Konrad_SP1.0* model, the user must set up the data as CSV files in accordance with a specified format that the Python model will accept. The way the model is currently set up (version 1.0), the user will have to wait until the SLC3.2 data loads (about 4 minutes) before entry of the site-specific soil data can begin.

References (Appendix I)

Konrad, J.-M. 1999. Frost susceptibility related to soil index properties. *Can. Geotech. J.* 36:403-417.

Konrad, J.-M. 2005. Estimation of the segregation potential of fine-grained soils using the frost heave response of two reference soils. *Can. Geotech. J.* 42:38-50.

Mathcad. 2014. Parametric Technology Corporation (PTC), Needham, MA. Available at: <http://www.ptc.com/product/mathcad> (verified Oct. 6, 2014)

Python Software. 2014. Python 3.4.1 programming language. Available at: <https://www.python.org/> (verified Oct. 6, 2014)

Polygon 809014 last soil layer

"The analysis of frost heave data from several fine-grained soils confirmed that the segregation potential of saturated soils with no applied surcharge, SP0, was best related to the average size of the fines fraction (<75 um), d50(FF), its specific surface area, S_s, and the ratio of the material's water content to its liquid limit, w/wL."

basic soil properties

$$\rho_s := 2.65$$

$$\rho_b := 1.45$$

measured properties

$$\text{clay} := 30$$

$$\text{om} := 1.72$$

$$\text{oc} := \frac{\text{om}}{1.72}$$

fraction less than 0.425 micrometers

$$f_{425} := 0.80$$

fraction less than 0.075 micrometers

$$f_{075} := \frac{32.17712228 \cdot 2}{100}$$

$$f_{075} = 0.644$$

the mean grain size of the fines fraction (< 0.075 mm) expressed in micrometers

$$d50ff := 0.002642779 \cdot 1000$$

$$d50ff = 2.643$$

PTF Calculations

liquid limit gravimetric water content (%) for micaceous clay mineralogy,
Appendix K

$$wL := \frac{15.95 + 0.57 \cdot (\text{clay}) + 3.05 \cdot (\text{oc})}{100}$$

$$wL = 0.361$$

liquid limit gravimetric water content (%) for smectitic clay mineralogy,
Appendix K

$$wL := \frac{13.75 + 0.637 \cdot (\text{clay}) + 2.937 \cdot (\text{oc})}{100}$$

$$wL = 0.358$$

determine the void ratio at 1 kPa, Appendix M

$$\varepsilon_{1\text{kPa}} := \varepsilon_{wP} - (2.623 \cdot C)$$

$$\varepsilon_{1\text{kPa}} = -0.304$$

determine the void ratio for a 50kPa, Appendix M

$$\varepsilon_{50\text{kPa}} := \varepsilon_{1\text{kPa}} - (C \cdot \log(50))$$

$$\varepsilon_{50\text{kPa}} = -0.86$$

plastic limit gravimetric water content (%), Appendix K

$$w_P := \frac{14.28 + 0.12 \cdot (\text{clay}) + 3.05 \cdot (\text{oc})}{100}$$

$$w_P = 0.209$$

determine the void ratio at the liquid limit, Appendix M

$$\varepsilon_{wL} := w_L \cdot \frac{\rho_s}{\rho_w}$$

$$\varepsilon_{wL} = 0.949$$

determine the void ratio at the plastic limit, Appendix M

$$\varepsilon_{wP} := w_P \cdot \frac{\rho_s}{\rho_w}$$

$$\varepsilon_{wP} = 0.555$$

determine the effective stress at the liquid limit, Appendix M

$$\sigma_{wL} := 26.6 - (32.1 \cdot \log(\text{oc}))$$

$$\sigma_{wL} = 26.6$$

the effective stress at the plastic limit is set to 425 kPa, Appendix M

$$\sigma_{wP} := 425$$

$$\sigma_{wP} = 425$$

determine the consolidation index, Appendix M

$$C := \frac{\varepsilon_{wL} - \varepsilon_{wP}}{\log\left(\frac{\sigma_{wP}}{\sigma_{wL}}\right)}$$

$$C = 0.327$$

specific surface area of fines

$$S_s := 206 \cdot \text{m}^2 \cdot \text{gm}^{-1}$$

gravimetric water content (%)

$$w := 0.254872954$$

liquid limit gravimetric water content (%)

$$w_L := 0.360984592$$

frost depth (m)

$$X := 1.4$$

temperature gradient as a function of time (constant)

$$\text{grad}_t(t) := 47 \cdot \frac{\text{K}}{\text{m}}$$

$$T := 1440 \cdot \text{min}$$

$$\text{grad}_t(T) = 47 \frac{\text{K}}{\text{m}}$$

Calculations

plastic limit gravimetric water content (%)

$$w_P := \frac{14.28 + 0.12 \cdot (\text{clay}) + 3.05 \cdot (\text{oc})}{100}$$

$$w_P = 0.209$$

in situ volume of solids and voids

$$\text{rel_vol}_{\text{sol}} := \frac{\rho_b}{\rho_s}$$

$$\text{rel_vol}_{\text{sol}} = 0.547$$

$$\text{rel_vol}_{\text{void}} := 1 - \frac{\rho_b}{\rho_s}$$

$$\text{rel_vol}_{\text{void}} = 0.453$$

in situ porosity

$$n := 1 - \frac{\rho_b}{\rho_s}$$

$$n = 0.453$$

in situ void ratio

$$\varepsilon(v_s, v_v) := \frac{v_v}{v_s}$$

$$\varepsilon(\text{rel_vol}_{\text{sol}}, \text{rel_vol}_{\text{void}}) = 0.828$$

water content corrected to fines

$$wf := \frac{w}{f_{425}}$$

$$wf = 0.319$$

$$wf := wf$$

atterberg limits in relation to other properties of fine-grained soils
dolinar and skaabl 2013

$A_{Se} = p \cdot A_{Sce}$ (m²/g) is the external specific surface area of the soil and
 p is the content (%) of clay minerals in the soil divided by 100 ($0 < p < 1$)

$$A_{Se} := \left(\frac{\text{clay}}{100} \right) \cdot S_s \cdot \frac{\text{gm}}{\text{m}^2}$$

$$A_{Se} = 61.8$$

gravimetric water content at 1 kPa

$$w_1 := 33.46 \cdot \left(\frac{\text{clay}}{100} \right) + 1.39 \cdot A_{Se}$$

$$w_1 = 95.94$$

$$j_e := 0.05 \cdot \left(\frac{S_s \cdot \frac{\text{gm}}{\text{m}^2}}{\frac{\text{clay}}{100}} \right)^{0.27}$$

$$j_e = 0.292$$

gravimetric water content at 50 kPa of pressure

$$w_{50} := w_1 \cdot 50^{-j_e}$$

$$w_{50} = 30.652$$

void ratio at 50 kPa of pressure

$$\varepsilon_{50} := \varepsilon \left(\text{rel_vol}_{\text{sol}}, \frac{w_{50}}{100} \right)$$

$$\varepsilon_{50} = 0.56$$

porosity of fines

$$n_f := \frac{\varepsilon_{50}}{1 + \varepsilon_{50}}$$

$$n_f = 0.359$$

porosity of coarse material

$$n_c := n$$

$$n_c = 0.453$$

ratio

$$\frac{w_f}{w_L} = 0.883$$

konrad equation 5

$$\text{Perc_F}_V := \frac{n_c \cdot (1 - n_f)}{1 - n_f \cdot n_c}$$

$$\text{Perc_F}_V = 0.347$$

ratio of fines to porosity of fines

$$r_f := \frac{f_{075}}{\text{Perc_F}_V}$$

$$r_f = 1.857$$

calculate the overburden pressure at the freezing front (MPa)

$$Pe := \left[\left(\rho_b \cdot 1000 \cdot \frac{\text{kg}}{\text{m}^3} \cdot g \cdot X \cdot m \right) + \left(1000 \cdot \frac{\text{kg}}{\text{m}^3} \cdot g \cdot \rho_b \cdot w \cdot X \cdot m \right) \right] \cdot \frac{1}{1000000 \cdot \text{Pa}}$$

$$Pe = 0.024981$$

the overburden correction factor (d50ff in micromteres and a is in MPa⁻¹)
(from Konrad 2004)

$$a := 5 \cdot (d50ff)^{0.45}$$

$$a = 7.743$$

konrad equation 7

$$SPoSS := (116 - 75 \cdot \log(d50ff)) \cdot 10^3 \cdot \text{mm}^4 \cdot (\text{K}^{-1} \cdot \text{s}^{-1} \cdot \text{gm}^{-1})$$

$$SPoSS = 84.345 \frac{1}{\text{s K}} \frac{10^3 \cdot \text{mm}^4}{\text{gm}}$$

$$SP_o := \frac{SPoSS}{S_s}$$

$$SP_o = 40.944 \frac{1}{\text{s K}} 10^{-5} \cdot \text{mm}^2$$

konrad equation 6

$$SP_o := \begin{cases} 0 & \text{if } (r_f < 0.12) \\ 1.14 \cdot (r_f - 0.12) \cdot (SP_o) & \text{if } (1 > r_f \geq 0.12) \\ SP_o & \text{if } (r_f \geq 1) \end{cases}$$

$$SP_o = 40.944 \frac{1}{\text{s K}} 10^{-5} \cdot \text{mm}^2$$

konrad equation 8

$$SP := SP_o + 900 \cdot 10^{-5} \cdot \log\left(\frac{wf}{0.7 \cdot wL}\right) \cdot \text{mm}^2 \cdot \text{s}^{-1} \cdot \text{K}^{-1}$$

$$SP = 131.527 \frac{1}{\text{s K}} 10^{-5} \cdot \text{mm}^2$$

correct the SP value for the overburden pressure (kPa)

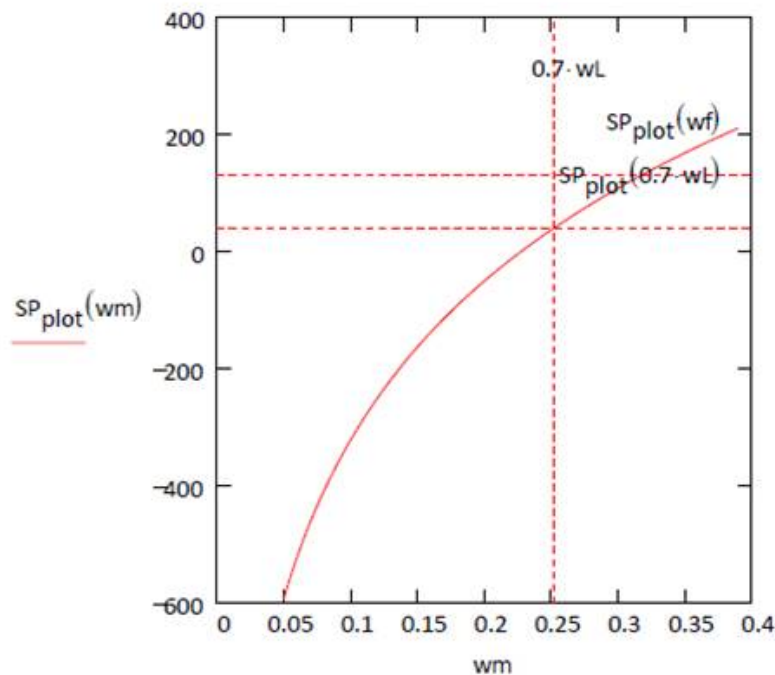
$$SP := SP \cdot e^{-a \cdot Pe}$$

$$SP = 108.395 \frac{1}{\text{s K}} 10^{-5} \cdot \text{mm}^2$$

plot of konrad equation 8, the water content correction

$$SP_{\text{plot}}(wm) := \left(SP_o + 900 \cdot 10^{-5} \cdot \log\left(\frac{wm}{0.7 \cdot wL}\right) \cdot \text{mm}^2 \cdot \text{s}^{-1} \cdot \text{K}^{-1} \right) \cdot (10^5 \cdot \text{mm}^{-2})$$

$$wm := 0.05, 0.051 \dots \frac{\text{rel_vol}_{\text{void}}}{\rho_b \cdot f_{425}}$$



from konrad 2005

changes start after the calculation of equation 7

konrad equation 7

$$SPoSS := (116 - 75 \cdot \log(d50ff)) \cdot 10^3 \cdot \text{mm}^4 \cdot (\text{K}^{-1} \cdot \text{s}^{-1} \cdot \text{gm}^{-1})$$

$$SPoSS = 84.345 \frac{1}{\text{s K}} \frac{10^3 \cdot \text{mm}^4}{\text{gm}}$$

define the reference values for the Specific Surface and the Frost heave response

$$S_{s_ref} := \begin{cases} 25.95 \cdot \frac{\text{m}^2}{\text{gm}} & \text{if } d50ff < 1 \\ (25.95 - 11.78 \cdot \log(d50ff)) \cdot \frac{\text{m}^2}{\text{gm}} & \text{if } d50ff \geq 1 \end{cases}$$

$$S_{s_ref} = 20.978 \text{m}^2 \frac{1}{\text{gm}}$$

$$SP_{o_ref} := \begin{cases} 489 \cdot (10^{-11} \cdot \text{m}^2 \cdot \text{K}^{-1} \cdot \text{s}^{-1}) & \text{if } d50ff < 1 \\ (489 - 232 \cdot \log(d50ff)) \cdot (10^{-11} \cdot \text{m}^2 \cdot \text{K}^{-1} \cdot \text{s}^{-1}) & \text{if } d50ff \geq 1 \end{cases}$$

$$SP_{o_ref} = 391.082 \frac{1}{\text{s K}} 10^{-5} \cdot \text{mm}^2$$

$$SP_{O_2} := \begin{cases} \text{if } \frac{S_s}{S_{s_ref}} < 1 \\ \left[\left(\frac{S_s}{S_{s_ref}} \cdot SP_{O_ref} \right) \right] \text{ if } \left(\frac{wf}{wL} \leq 0.8 \right) \\ \left[\left[\left(0.08 + 1.42 \cdot \frac{S_s}{S_{s_ref}} \right) \cdot SP_{O_ref} \right] \right] \text{ if } \left(\frac{wf}{wL} > 0.8 \right) \\ \text{if } \frac{S_s}{S_{s_ref}} \geq 1 \\ \left[\left(\frac{S_s}{S_{s_ref}} \right)^{-0.85} \cdot SP_{O_ref} \right] \text{ if } \left(\frac{wf}{wL} \leq 0.8 \right) \\ \left[\left[1.5 \cdot \left(\frac{S_s}{S_{s_ref}} \right) \right]^{-0.55} \cdot SP_{O_ref} \right] \text{ if } \left(\frac{wf}{wL} > 0.8 \right) \end{cases}$$

$$SP_{O_2} = 89.076 \frac{1}{sK} 10^{-5} \cdot \text{mm}^2$$

konrad equation 6

$$SP_{O_2} := \begin{cases} 0 \text{ if } (r_f < 0.12) \\ 1.14 \cdot (r_f - 0.12) \cdot (SP_{O_2}) \text{ if } (1 > r_f \geq 0.12) \\ SP_{O_2} \text{ if } (r_f \geq 1) \end{cases}$$

$$SP_{O_2} = 89.076 \frac{1}{sK} 10^{-5} \cdot \text{mm}^2$$

$$SP_O = 40.944 \frac{1}{sK} 10^{-5} \cdot \text{mm}^2$$

konrad equation 8

$$SP_2 := SP_{O_2} + 900 \cdot 10^{-5} \cdot \log\left(\frac{wf}{0.7 \cdot wL}\right) \cdot \text{mm}^2 \cdot \text{s}^{-1} \cdot \text{K}^{-1}$$

$$SP_2 = 179.659 \frac{1}{sK} 10^{-5} \cdot \text{mm}^2$$

correct the SP value for the overburden pressure (kPa)

$$SP2 := SP2 \cdot e^{-a \cdot Pe}$$

$$SP2 = 148.062 \frac{1}{s \cdot K} 10^{-5} \cdot mm^2$$

$$SP = 108.395 \frac{1}{s \cdot K} 10^{-5} \cdot mm^2$$

calculate v, the rate of frost heave per time

$$v(t) := SP \cdot grad_t(t)$$

$$v(T) = 5.095 \times 10^{-8} \frac{m}{s}$$

$$v2(t) := SP2 \cdot grad_t(t)$$

$$v2(T) = 6.959 \times 10^{-8} \frac{m}{s}$$

could calculate v over time then intergrate

$$h(t) := 1.09 \cdot \int_0^T v(t) dt$$

$$h(T) = 4.798 \text{ mm}$$

$$T = 24 \text{ hr}$$

$$h2(t) := 1.09 \cdot \int_0^T v2(t) dt$$

$$h2(T) = 6.554 \text{ mm}$$

$$T = 24 \text{ hr}$$

increase in water content at the frozen zone

$$wfz := \frac{h(T)}{1.09 \cdot X} \cdot \frac{1}{\rho_s \cdot m}$$

$$wfz = 1.186 \times 10^{-3}$$

$$wfz2 := \frac{h2(T)}{1.09 \cdot X} \cdot \frac{1}{\rho_s \cdot m}$$

$$wfz2 = 1.621 \times 10^{-3}$$

Sensitivity Test of the Konrad Segregation Potential Equations

Part 1: equation 7

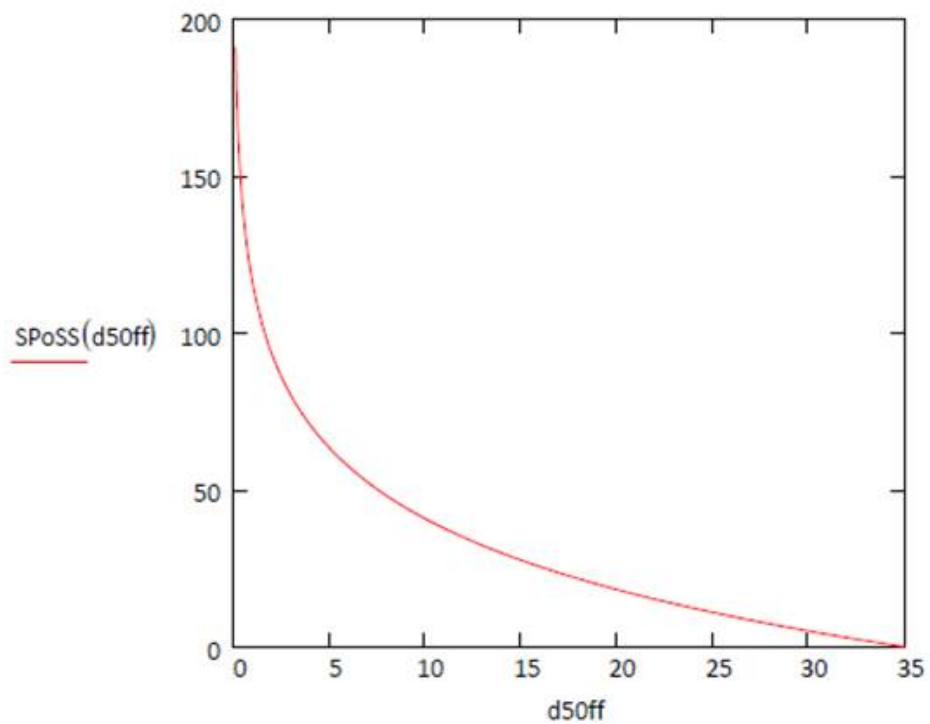
range of the mean particle size of the fines fraction

$$d50ff := 1 \cdot 10^{-1}, 2 \cdot 10^{-1} \dots 35$$

konrad equation 7

$$SPoSS(d50ff) := (116 - 75 \cdot \log(d50ff))$$

Plot of the SPoSS as a function of the mean particle size of the fines fraction



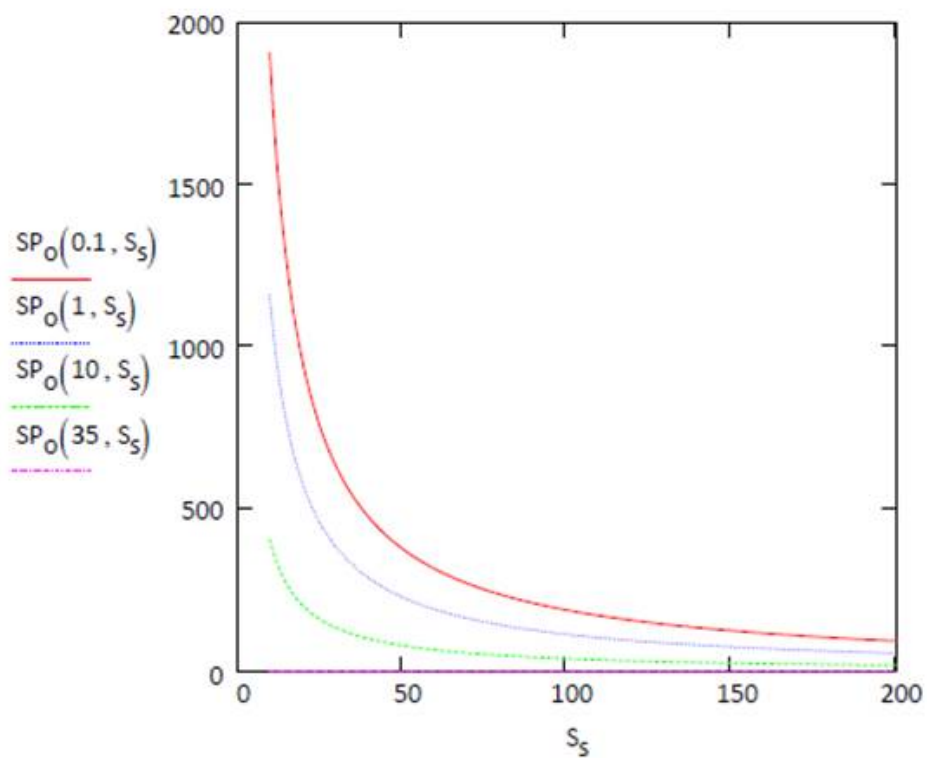
Part 2: the initial determination of SPo (the segregation potential at 0 stress)

range of the Specific Surface Area

$$S_s := 10, 11 \dots 200$$

$$SP_o(d_{50ff}, S_s) := \frac{SPoSS(d_{50ff})}{S_s} \cdot 100$$

Plot of the SPo (the Segregation potential under zero stress) as a function of four selected mean particle size of the fines fraction and the Specific Surface Area



Part 3: SPo (the segregation potential at 0 stress) corrected for the fine fraction ratio

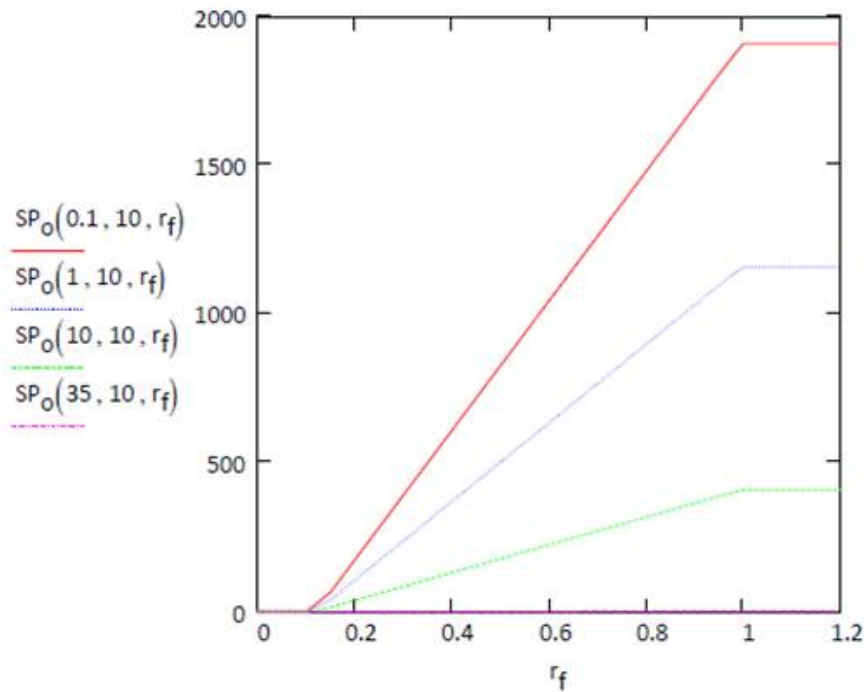
range of the fines fraction ratio

$$r_f := 0, 0.05 \dots 1.2$$

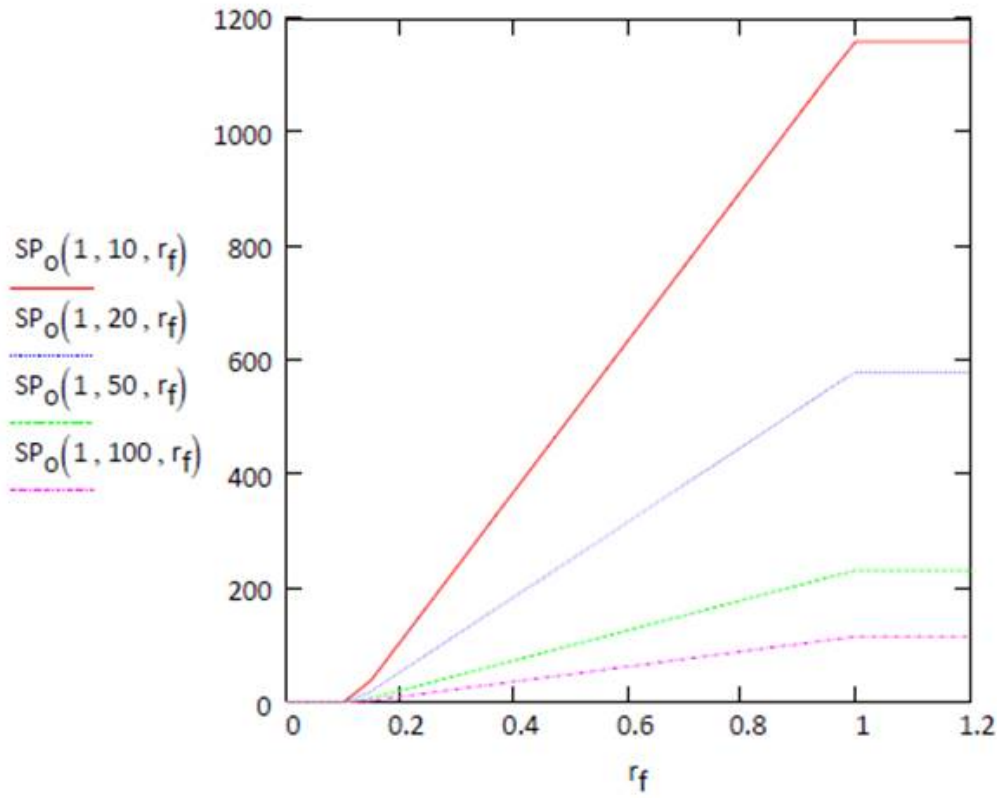
konrad equation 6

$$SP_o(d_{50ff}, S_s, r_f) := \begin{cases} 0 & \text{if } (r_f < 0.12) \\ 1.14 \cdot (r_f - 0.12) \cdot (SP_o(d_{50ff}, S_s)) & \text{if } (1 > r_f \geq 0.12) \\ SP_o(d_{50ff}, S_s) & \text{if } (r_f \geq 1) \end{cases}$$

Plot of the SPo (the Segregation potential under zero stress) as a function of four values of the selected mean particle size of the fines fraction, a constant Specific Surface Area and for a range of fine fraction ratios



Plot of the SPo (the Segregation potential under zero stress) as a function of a constant mean particle size of the fines fraction, four selected Specific Surface Area, and for a range of fine fraction ratios



Part 4: SP (the segregation potential) corrected for the ratio of gravimetric water content corrected for fine fraction to the liquid limit

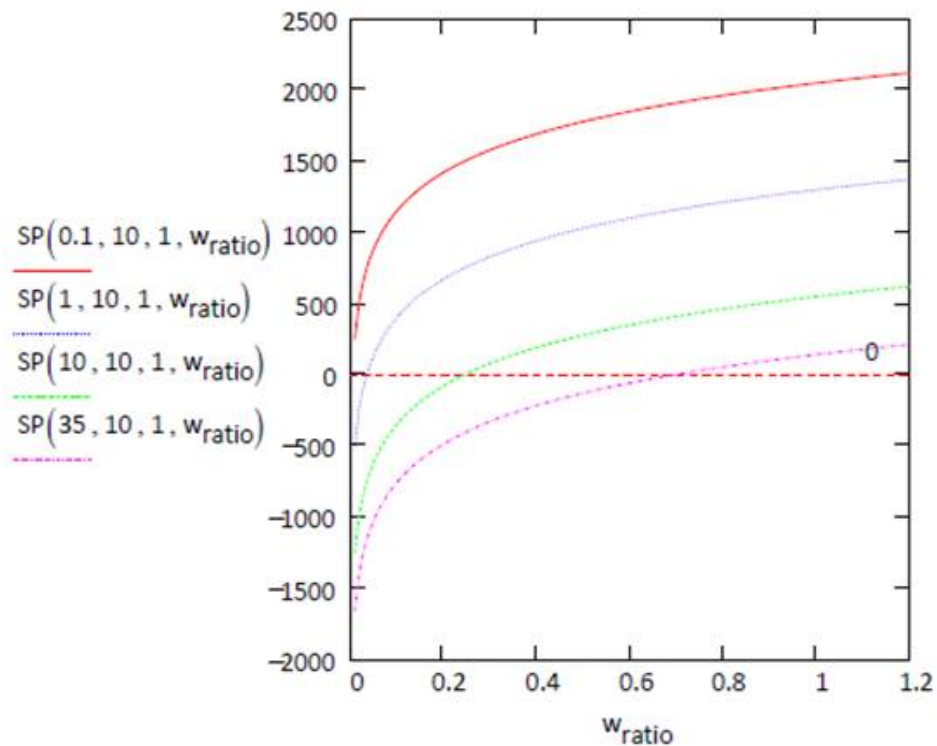
range of the ratio of gravimetric water content (corrected to fines) to the liquid limit

$$w_{\text{ratio}} := 0.01, 0.02 \dots 1.2$$

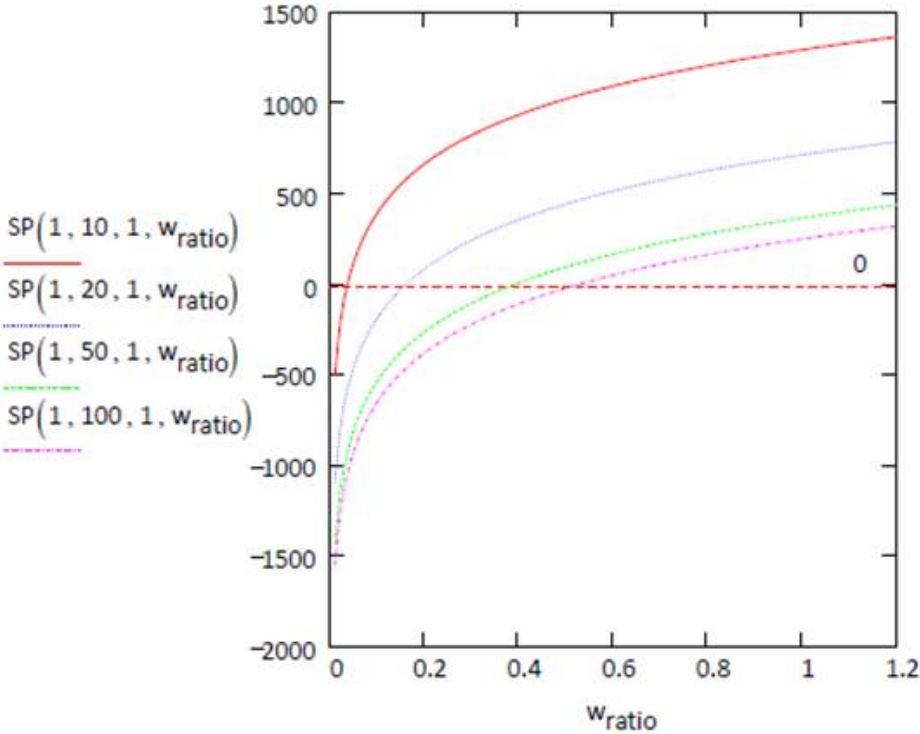
konrad equation 8

$$SP(d_{50f}, S_s, r_f, w_{\text{ratio}}) := SP_o(d_{50f}, S_s, r_f) + 900 \cdot \log\left(\frac{w_{\text{ratio}}}{0.7}\right)$$

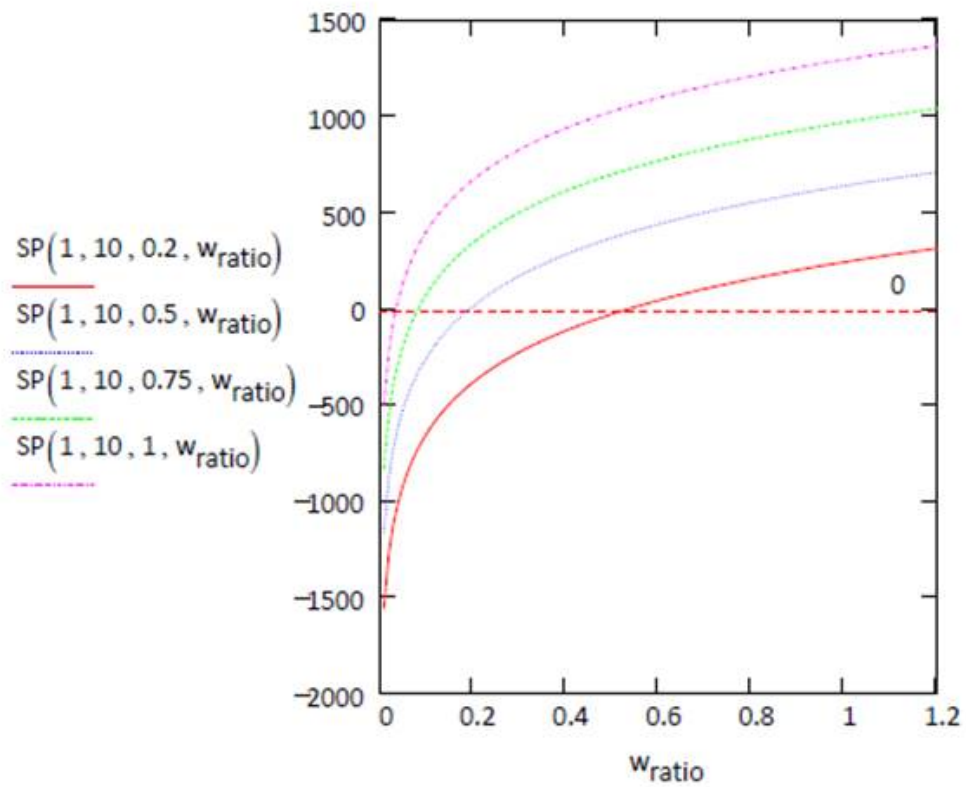
Plot of the SP (the Segregation potential) as a function of four values of mean particle size of the fines fraction, a constant Specific Surface Area, a constant ratio of fine fraction ratios, and a range of gravimetric water content ratios



Plot of the SP (the Segregation potential) as a function of a constant mean particle size of the fines fraction, four values of Specific Surface Area, a constant ratio of fine fraction ratios, and a range of gravimetric water content ratios



Plot of the SP (the Segregation potential) as a function of a constant mean particle size of the fines fraction, a constant value of Specific Surface Area, four values of the ratio of fine fraction ratios, and a range of gravimetric water content ratios



Part 5: SP (the segregation potential) corrected for the overburden pressure

correct the SP value for the overburden pressure (from 1 kPa to 50 kPa)

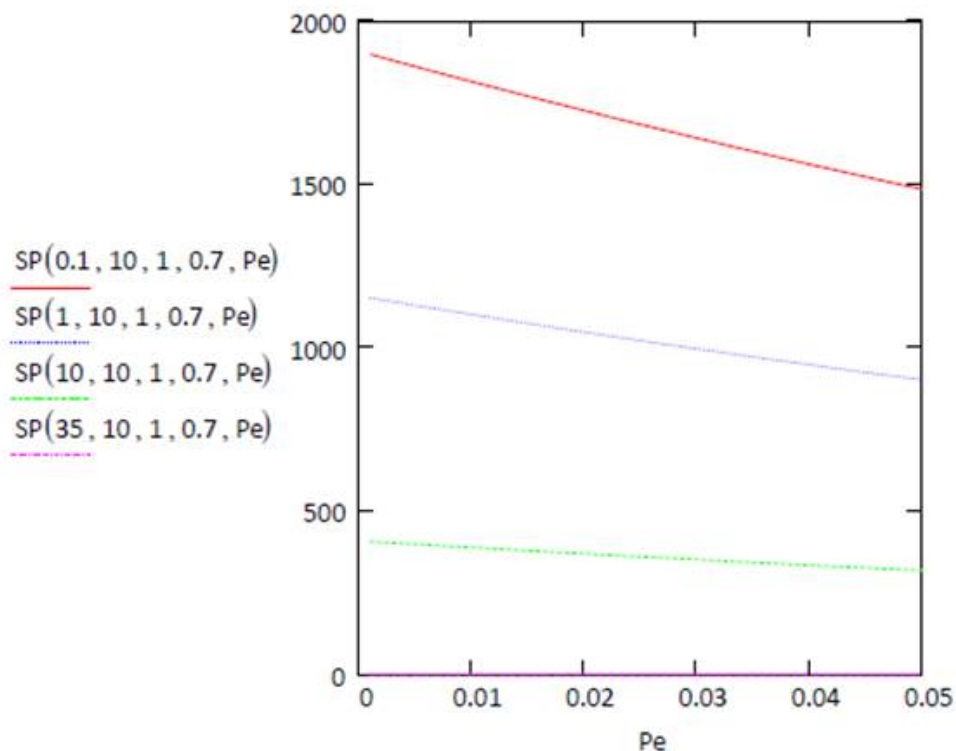
$$a := 5$$

a range of overburden pressures from 1 to 50 kPa

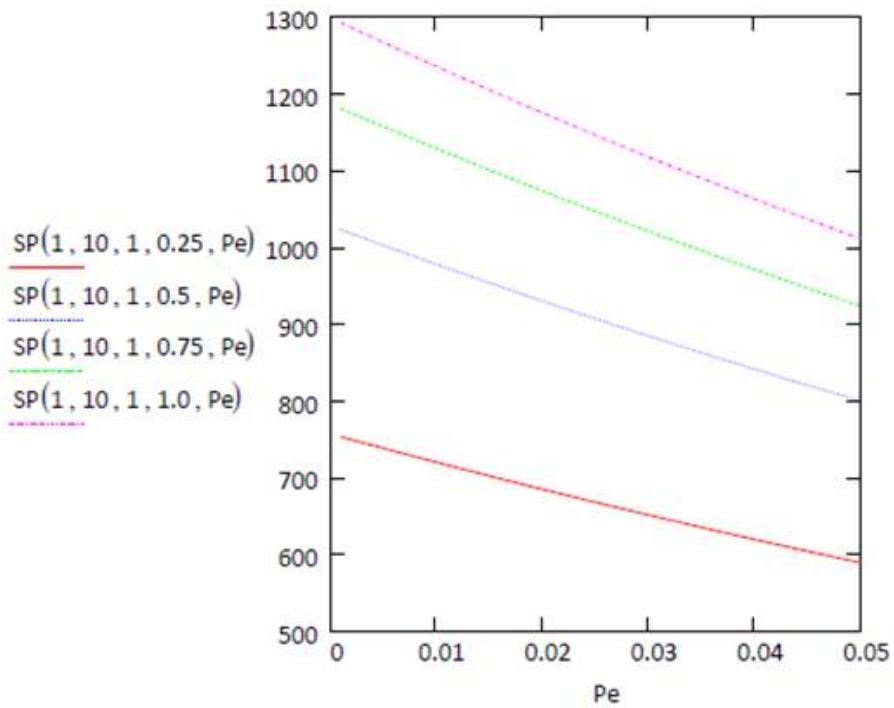
$$Pe := 0.001, 0.002 \dots 0.05$$

$$SP(d_{50ff}, S_s, r_f, w_{ratio}, Pe) := SP(d_{50ff}, S_s, r_f, w_{ratio}) \cdot e^{-a \cdot Pe}$$

Plot of the SP (the Segregation potential) as a function of four values of mean particle size of the fines fraction, a constant value of Specific Surface Area, a constant value of the ratio of fine fraction ratios, a constant value of gravimetric water content ratios, and a range of overburden pressures



Plot of the SP (the Segregation potential) as a function of a constant value of mean particle size of the fines fraction, a constant value of Specific Surface Area, a constant value of the ratio of fine fraction ratios, four specific values of gravimetric water content ratios, and a range of overburden pressures



APPENDIX J

Example Output from the *Konrad_SP1.0* Frost Heave Model

Example Output from the *Konrad_SP1.0* Frost Heave Model

1. General overview

Tables J-1 to J-6 are example 'summary' output tables generated by running the Python program (*Konrad_SP1.0*) for a trial SLC3.2 polygon (polygon i.d. = 809014) located in Alberta. The 'frost heave risk' scenario being considered here is one where the depth of frost penetration is 140 cm below the soil surface, and the temperature gradient between the soil surface and the freezing front is 20°C m⁻¹ (Table J-3).

Table J-1 shows that this polygon consists of three distinct 'soil associations' making up 15%, 80% and 5% of the total polygon area. The last record (row 13) in each of Tables J-1 to J-5 is highlighted in yellow. It is this last, or deepest, soil layer (50 - 100 cm below the surface) in the third soil association (5% aerial extent) that is used in Appendix I to illustrate the soil-related sub-routines in the *Konrad_SP1.0* model. Note that in these raw output tables (Tables J-1 to J-6), there has been no attempt to round off the calculated values.

Table J-2 shows the results of applying the McBride & Mackintosh (1984) water retention PTF to the loam- to clay loam-textured soils of polygon 809014. This step is necessary in order to estimate the gravimetric soil water content (*w*) at 'field capacity' that can be used to generate the '*w/w_L*' parameter required by the *Konrad_SP1.0* model (see Appendix A). Estimates of the 'field capacity' (unsaturated) '*w*' values are required in the Prairie Ecozone where polygon 809014 is located, but field-saturated '*w*' value estimates are required elsewhere in Canada (see Appendices Q and S).

Table J-3 shows the results of applying several PTFs to the basic soils data contained in Table J-1 in order to estimate the liquid limit (see Appendix K), the specific surface area (see Appendix L) and the d₅₀(FF) particle-size distribution parameter (see Appendix P). Along with the '*w/w_L*' parameter, these three soil properties are also required by the *Konrad_SP1.0* model (see Appendix A).

Tables J-4 and J-5 show the intermediate calculations in the *Konrad_SP1.0* model that ultimately lead to estimates of frost heave rates (i.e., 'heave' and 'heave2' estimates [mm day⁻¹]). The 'heave' values are derived from the model algorithms published in Konrad (1999). The 'heave2' values are derived from the model algorithms published in Konrad (2005) (see Appendix A). Table J-6 condenses the data in Tables J-4 and J-5 for the entire soil profile of each of the three soil associations in polygon 809014.

References (Appendix J)

Konrad, J.-M. 1999. Frost susceptibility related to soil index properties. *Can. Geotech. J.* 36:403-417.

Konrad, J.-M. 2005. Estimation of the segregation potential of fine-grained soils using the frost heave response of two reference soils. *Can. Geotech. J.* 42:38-50.

McBride, R.A. and E.E. Mackintosh. 1984. Soil survey interpretations from water retention data: I. Development and validation of a water retention model. *Soil Sci. Soc. Am. J.* 48:1338-1343.

Table J-1. Information extracted on Alberta polygon 809014 from the SLC3.2 database.

	poly_id	soil_name	province	centroid_x	centroid_y	percent	layer_no	upper	lower	sand	silt	clay	om	bd
0	809014	ABHDY~~~~~A	AB	1541013.9	1352483.01	15	1	0	12	25	50	25	2.58	1.15
1	809014	ABHDY~~~~~A	AB	1541013.9	1352483.01	15	2	12	22	32	56	12	2.752	1.4
2	809014	ABHDY~~~~~A	AB	1541013.9	1352483.01	15	3	22	36	17	47	36	1.72	1.5
3	809014	ABHDY~~~~~A	AB	1541013.9	1352483.01	15	4	36	52	12	56	32	0	1.35
4	809014	ABHDY~~~~~A	AB	1541013.9	1352483.01	15	5	52	75	17	54	29	0	1.35
5	809014	ABHDY~~~~~A	AB	1541013.9	1352483.01	15	6	75	100	32	41	27	0	1.5
6	809014	ABMAB~~~~~A	AB	1541013.9	1352483.01	80	1	0	15	32	40	28	3.096	1.25
7	809014	ABMAB~~~~~A	AB	1541013.9	1352483.01	80	2	15	29	39	33	28	2.236	1.4
8	809014	ABMAB~~~~~A	AB	1541013.9	1352483.01	80	3	29	62	36	37	27	0	1.5
9	809014	ABMAB~~~~~A	AB	1541013.9	1352483.01	80	4	62	106	38	34	28	0	1.45
10	809014	ABMAB~~~~~A	AB	1541013.9	1352483.01	80	5	106	140	38	34	28	0	1.45
11	809014	ABZGW~~~~~N	AB	1541013.9	1352483.01	5	1	0	20	40	40	20	8.6	1.15
12	809014	ABZGW~~~~~N	AB	1541013.9	1352483.01	5	2	20	50	40	30	30	3.44	1.4
13	809014	ABZGW~~~~~N	AB	1541013.9	1352483.01	5	3	50	100	40	30	30	1.72	1.45

Table J-2. Soil water release Information estimated by the McBride & Mackintosh (1984) water retention PTF.

	soil_class	theta_ms	theta_mi	theta_m15	psi_i	psi	theta_m	theta	air_poros	avail_wat
0	loam	0.492206727	0.442986054	0.127271616	2.600857926	100	0.341433095	0.392648059	0.173389677	0.002462857
1	silty loam	0.336927224	0.303234501	0.07730962	2.703721241	100	0.229479855	0.321271797	0.150426316	0.002130383
2	silt clay loam	0.289308176	0.274842767	0.162300556	2.483363178	100	0.245480764	0.368221146	0.065741118	0.001247703
3	silt clay loam	0.36338225	0.345213138	0.15137742	2.839955421	100	0.293301679	0.395957267	0.094608771	0.001915978
4	silt clay loam	0.36338225	0.345213138	0.141297576	2.868587866	100	0.289666129	0.391049274	0.099516764	0.002002975
5	clay loam	0.289308176	0.274842767	0.134403553	2.654924459	100	0.237149258	0.355723887	0.078238377	0.001541186
6	clay loam	0.422641509	0.401509434	0.139129312	2.849687486	100	0.325770823	0.407213529	0.121088358	0.002333019
7	clay loam	0.336927224	0.320080863	0.136909731	2.709454782	100	0.269245431	0.376943604	0.094754509	0.0018527
8	clay loam	0.289308176	0.274842767	0.134403553	2.635464005	100	0.236993143	0.355489714	0.07847255	0.001538844
9	clay loam	0.312296682	0.296681848	0.137869035	2.660514584	100	0.253366137	0.367380899	0.08544929	0.001674708
10	clay loam	0.312296682	0.296681848	0.137869035	2.660514584	100	0.253366137	0.367380899	0.08544929	0.001674708
11	loam	0.492206727	0.442986054	0.183395784	2.298423124	100	0.363620997	0.418164146	0.147873589	0.00207259
12	clay loam	0.336927224	0.320080863	0.147172942	2.651722097	100	0.272664426	0.381730197	0.089967916	0.001756881
13	clay loam	0.312296682	0.296681848	0.142898646	2.618627063	100	0.254872954	0.369565783	0.083264405	0.001623627

Table J-3. Results from the use of several PTFs to estimate the liquid limit (Appendix K), the specific surface area (Appendix L) and the particle-size distribution (Appendix P) soil parameters.

	wl	ssa	d50ff	d50ff_perc	d425_perc	X	grad_t
0	0.347726888	186	0.00554772	40.10487153	95.03943838	140	20
1	0.276675347	134	0.010800024	37.55002319	94.69253332	140	20
2	0.395184592	230	0.003230853	43.46883505	97.09058568	140	20
3	0.3419	214	0.004078866	45.8349573	98.92105404	140	20
4	0.3248	202	0.00466373	43.71047181	97.7488689	140	20
5	0.3134	194	0.004536743	36.50495685	90.56579194	140	20
6	0.373972266	198	0.004216493	36.45036625	90.31034252	140	20
7	0.35872997	198	0.00346058	32.81850719	84.96335151	140	20
8	0.3134	194	0.004164489	34.44505004	87.69003244	140	20
9	0.3191	198	0.003587547	33.34363123	85.79475198	140	20
10	0.3191	198	0.003587547	33.34363123	85.79475198	140	20
11		166	0.006619823	32.80526173	86.9452924	140	20
12	0.391469184	206	0.002642779	32.17712228	83.43773659	140	20
13	0.360984592	206	0.002642779	32.17712228	83.43773659	140	20

Table J-4. The intermediate frost heave and segregation potential calculations from Konrad (1999).

	wf	wf_wl	nf	rf	SPoSs	SPo	SPo_f	SP_w	SP_o	heave
0	0.359254116	1.033150236	0.43000043	1.880942742	60.19140808	32.36097209	32.36097209	184.5198675	146.7500484	2.764066511
1	0.24234208	0.875907747	0.193257418	1.793613732	38.493146	28.72622836	28.72622836	116.350523	82.41237699	1.552253603
2	0.252836835	0.639794263	0.489986261	3.092786627	77.80121365	33.82661463	33.82661463	-1.325313919	-1.066289657	-0.020083779
3	0.296500762	0.867214864	0.474733018	2.729028569	70.20954297	32.80819765	32.80819765	116.5340036	92.98860448	1.751458963
4	0.296337065	0.91236781	0.440671553	2.497285969	65.84499755	32.59653344	32.59653344	136.1612561	107.2088954	2.019300987
5	0.261853016	0.835523345	0.391172416	2.294258265	66.74418864	34.40422095	34.40422095	103.5787147	80.5333372	1.516861513
6	0.360723716	0.964573442	0.447691357	1.907513954	69.12864342	34.91345627	34.91345627	160.2269905	128.9125629	2.428093905
7	0.316895964	0.883383019	0.419864014	1.923546424	75.56383202	38.16355153	38.16355153	129.1094576	104.3058784	1.96462208
8	0.270262351	0.862355937	0.391172416	2.164797539	69.53287349	35.84168736	35.84168736	117.3713531	92.13216784	1.735327808
9	0.295316591	0.925467225	0.411341373	2.035755004	74.39017894	37.57079744	37.57079744	146.7075001	117.5291713	2.213685447
10	0.295316591	0.925467225	0.411341373	2.035755004	74.39017894	37.57079744	37.57079744	146.7075001	117.5291713	2.213685447
11	0.418218154		0.358752354	1.440535426	54.43652091	32.79308489	32.79308489			
12	0.326787899	0.834772984	0.443315434	1.938292801	84.34543677	40.94438678	40.94438678	109.7676977	90.82168482	1.710644598
13	0.305464847	0.846199127	0.434673435	2.019055001	84.34543677	40.94438678	40.94438678	115.0814663	94.83595864	1.786254248

Table J-5. The intermediate frost heave and segregation potential calculations from Konrad (2005).

	Ss_ref	SPo_ref	SPo_2	SPo_f2	SP_w2	SP_o2	heave2
0	17.1843305	316.3654223	128.0474958	128.0474958	280.2063912	222.8502655	4.197429321
1	13.7762568	249.245465	106.9875054	106.9875054	194.6118	137.845715	2.596351611
2	19.95024396	370.8384209	46.41646279	46.41646279	11.26453424	9.062951945	0.170702512
3	18.75784555	347.3548529	136.5801798	136.5801798	220.3059857	175.7937215	3.311109903
4	18.07232095	333.8538591	132.758418	132.758418	236.3231407	186.0730694	3.504723477
5	18.2135539	336.6353569	137.4602464	137.4602464	206.6347401	160.660279	3.026068488
6	18.58807226	344.0112703	140.4678609	140.4678609	265.7813951	213.8376358	4.027674637
7	19.59882588	363.9174537	152.9871026	152.9871026	243.9330086	197.0703557	3.711859563
8	18.65156333	345.2616886	142.8374471	142.8374471	224.3671128	176.1198789	3.317253143
9	19.4144841	360.2869535	150.6756801	150.6756801	259.8123828	208.1388751	3.92033734
10	19.4144841	360.2869535	150.6756801	150.6756801	259.8123828	208.1388751	3.92033734
11	16.28042955	298.563638	0	0			
12	20.97812327	391.0818844	166.9950642	166.9950642	235.8183751	195.1158911	3.675046831
13	20.97812327	391.0818844	166.9950642	166.9950642	241.1321437	198.711389	3.742768753

Table J-6. Calculation of the segregation potential and frost heave for Alberta polygon 809014.

	poly_id	soil_name	slope	percentage	watertable	drainage	province	centroid_x	centroid_y	poly_shape
809014__1	809014	ABMAB~~~~~A	C	80			AB	1541013.92	1352483.02	polygon
809014__2	809014	ABHDY~~~~~A	A	15			AB	1541013.92	1352483.02	polygon
809014__3	809014	ABZGW~~~~~N	A	5			AB	1541013.92	1352483.02	polygon

Pe	a	SP_o	heave	SP_o2	heave2
0.02479206	8.88441692	117.704571	2.21698913	208.4495	3.92618801
0.0245722	9.87426714	81.2637008	1.53061806	162.117321	3.05351216
0.02438532	7.74278827	95.2809541	1.79463583	199.643796	3.76033082

APPENDIX K

Estimation of the Consistency (Atterberg) Limits of Southern Ontario Soils

Estimation of the Consistency (Atterberg) Limits of Southern Ontario Soils

1. Preface

One of the soil parameters required for estimation of the 'segregation potential' (SP), in accordance with Konrad (1999), is the liquid limit (w_L) (see Appendix A). Further, the influence of overburden pressure on frost heave and the SP parameter can be accounted for by an empirical relationship involving the compression index (C_c) of the soil (Konrad, 1999). The PTF that is to be used in this study to estimate C_c requires both the liquid limit (w_L) and the plastic limit (w_P) as input data (see Appendix K). Testing for both soil consistency limits is typically performed in tandem in soil mechanical laboratories, so PTFs for w_L , w_P and the plasticity index (PI) will be presented in this section, in conjunction with a validation step.

2. Soil consistency (Atterberg) limits

The soil consistency (Atterberg) limits have clear physical meaning as 'mechanical transition points' in cohesive/plastic soils (Higashiyama, 1992), and as such have relevance to field soil conditions. These test indices are often used to derive mechanical properties and qualities of soil substrates, as well as to evaluate soil trafficability and efficacy of cultivation (Baumgartl, 2002). For example, the optimal soil water content for soil-engaging operations is at or somewhat below w_P (Baumgartl, 2002), where yielding in response to external mechanical stresses induces brittle failure/fracture (Higashiyama, 1992). The soil consistency limits are also strongly related to the two shear strength parameters of cohesion and angle of shearing resistance (Baumgartl, 2002), and Faure (1981) likened the w_P to a soil 'compaction sensitivity threshold' water content.

Clearly, w_P is a water content that is likely to occur frequently under field conditions because most soil profiles (topsoil and subsoil) will have sufficient porosity to accommodate this amount of soil water under unsaturated or field-saturated conditions. This is less likely to be the case for the w_L test index (i.e., the ratio $w/w_L < 1$), which is linked to both the susceptibility of soil to creep (i.e., onset of viscous flow properties) and to frost heaving susceptibility. Konrad (1999) suggested that the ratio w/w_L is one of three parameters that define the relative frost heaving susceptibility of soils. One of the other parameters is specific surface area (SSA), which is also closely correlated with w_L (Dolinar *et al.*, 2007; Hammel *et al.*, 1983). In order to easily relate field measurements of gravimetric soil water content (w) to the test index w_L (i.e., the ratio w/w_L) for soils in southern Ontario, algorithms will need to be developed allowing reliable estimation of w_L for soils in this part of Canada.

3. Objective (Appendix K)

The objective of this section (Appendix K) is to calibrate and validate linear regression equations for estimating the soil consistency (Atterberg) limits for soils in southern Ontario (i.e., micaceous clay mineralogy). This objective would be achieved by a) assembling available soil data of diverse texture from a number of the more recent soil inventories carried out in southern Ontario (PTF calibration data set [see Appendix O]), and b) accessing alternate published data from the same general region (independent validation data set). Detailed information on the two data sets and the methodology used are provided in Section 4.5.2.

4. Results and discussion

4.1 Estimation of soil consistency limits (Linear regression model calibration and validation)

The 203 soil horizons from the 5-municipality region in southern Ontario had a wide range of physical properties (see Appendix O). Clay content ranged from 11 to 77% kg kg^{-1} , and soil organic carbon (SOC) content ranged from 0 to 3.94% kg kg^{-1} . The ranges for the w_L , w_P and plasticity index (PI) were from 16.5 to 72.5%, 12.5 to 35.5% and 0.5 to 45.0% kg kg^{-1} , respectively. The Pearson's correlation matrix showed that the soil consistency test indices were strongly and significantly ($P < 0.05$) correlated to soil constituents (sand, silt, clay and SOC contents).

Past research has shown that the dominant influences on the soil consistency limits are the clay and SOC contents, with the amount and type of exchangeable cations or of certain minerals (e.g., carbonate, gypsum) having a lesser influence (Akpokodje, 1985; Dexter & Chan, 1991; Gill & Reaves, 1957; Smith *et al.*, 1985). Table K-1 shows the results from linear regressions carried out with this data set using clay content and/or SOC content as independent variables. There were 52 soil horizons with SOC contents below the detection limit, so these simple regressions (Eqns. K-2 and K-4) were carried out with a single independent variable (clay content). The predictive capability (r^2) of Eqns. K-1 and K-2 (w_L) was much higher than that of Eqns. K-3 and K-4 (w_P), which has been frequently observed with soil data sets from elsewhere (Culley *et al.*, 1981; de Jong *et al.*, 1990; Odell *et al.*, 1960; Smith *et al.*, 1985). The general observation that SOC content does not influence soil plasticity (i.e., PI) to any great degree (Baumgartl, 2002) was strongly corroborated, as the SOC regression coefficients in Eqns. K-1 and K-3 were identical. Clearly, the SOC variable was not significant when regressed upon PI, and so Eqn. K-5 has only clay content as an independent variable.

Table K-1. Regression equations for the estimation of the Atterberg limits from soil constituents ($n = 203$).

Atterberg test index	SOC content group	n	Regression coefficients			r^2	RMSE	Eqn. no.
			Clay	SOC [†]	Intercept			
			-----	%kg kg ⁻¹	-----		%kg kg ⁻¹	
Liquid limit	> 0	151	0.57	3.05	15.95	0.809 [†]	4.75	[K-1]
	= 0	52	0.59	-	16.07	0.790 [†]	4.65	[K-2]
Plastic limit	> 0	151	0.12	3.05	14.28	0.604 [†]	2.84	[K-3]
	= 0	52	0.16	-	13.29	0.471 [†]	2.57	[K-4]
Plasticity Index	all	203	0.45	-	1.89	0.714 [†]	4.61	[K-5]

[†] Significant at $P < 0.0001$

[†] SOC = soil organic carbon content (%kg kg⁻¹)

The predictive capability of Eqns. K-1 to K-5, as well as the regression coefficients and intercepts (Table K-1), were somewhat similar in magnitude to many of those reported for soils in other parts of the world (Culley *et al.*, 1981; de Jong *et al.*, 1990; de la Rosa, 1979; Gill & Reaves, 1957; Odell *et al.*, 1960; Smith *et al.*, 1985). By far the closest match, however, was inexplicably between Eqn. K-2 and soils from Israel ($w_L = 15.345 + 0.575 \text{ clay}$) reported by Smith *et al.* (1985).

Validation of Eqns. K-1, K-3 and K-5 was carried out with an independent data set also originating from southern Ontario (Joosse & McBride, 2003). Of the 36 soil horizons available, 32 of these had clay and SOC contents that fell within the range of those in the calibration data set. Figure K-1 shows very good correspondence between w_L estimated by Eqn. K-1 and the measured values ($r^2 = 0.871$, RMSE = 2.6%), with the regression line being statistically indistinguishable from the 1:1 line ($P < 0.05$). Figure K-2 shows reasonably good correspondence between w_P estimated by Eqn. K-3 and the measured values ($r^2 = 0.790$, RMSE = 1.9%), but the regression line is statistically distinguishable from the 1:1 line in both the slope and intercept ($P < 0.05$). Figure K-3 shows good correspondence between PI estimated by Eqn. K-5 and the measured values ($r^2 = 0.880$, RMSE = 1.8%), with the intercept of regression line being statistically indistinguishable from the 1:1 line ($P < 0.05$).

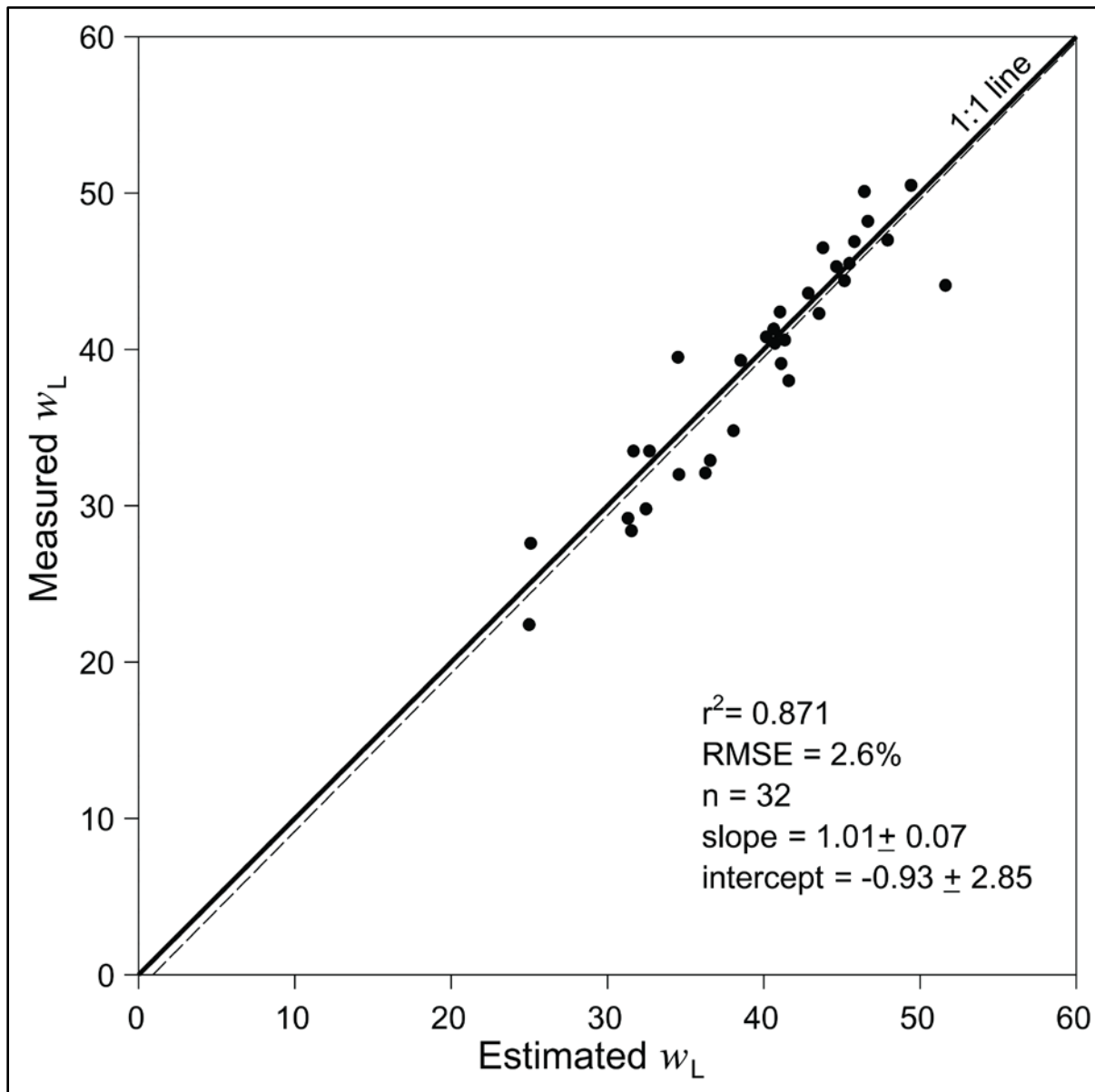


Figure K-1. Significant regression ($P < 0.0001$) of measured liquid limit (ASTM D423-72) upon estimated liquid limit (Eqn. K-1), shown as the broken line, with descriptive statistics including standard errors of the slope and intercept ($n = 32$).

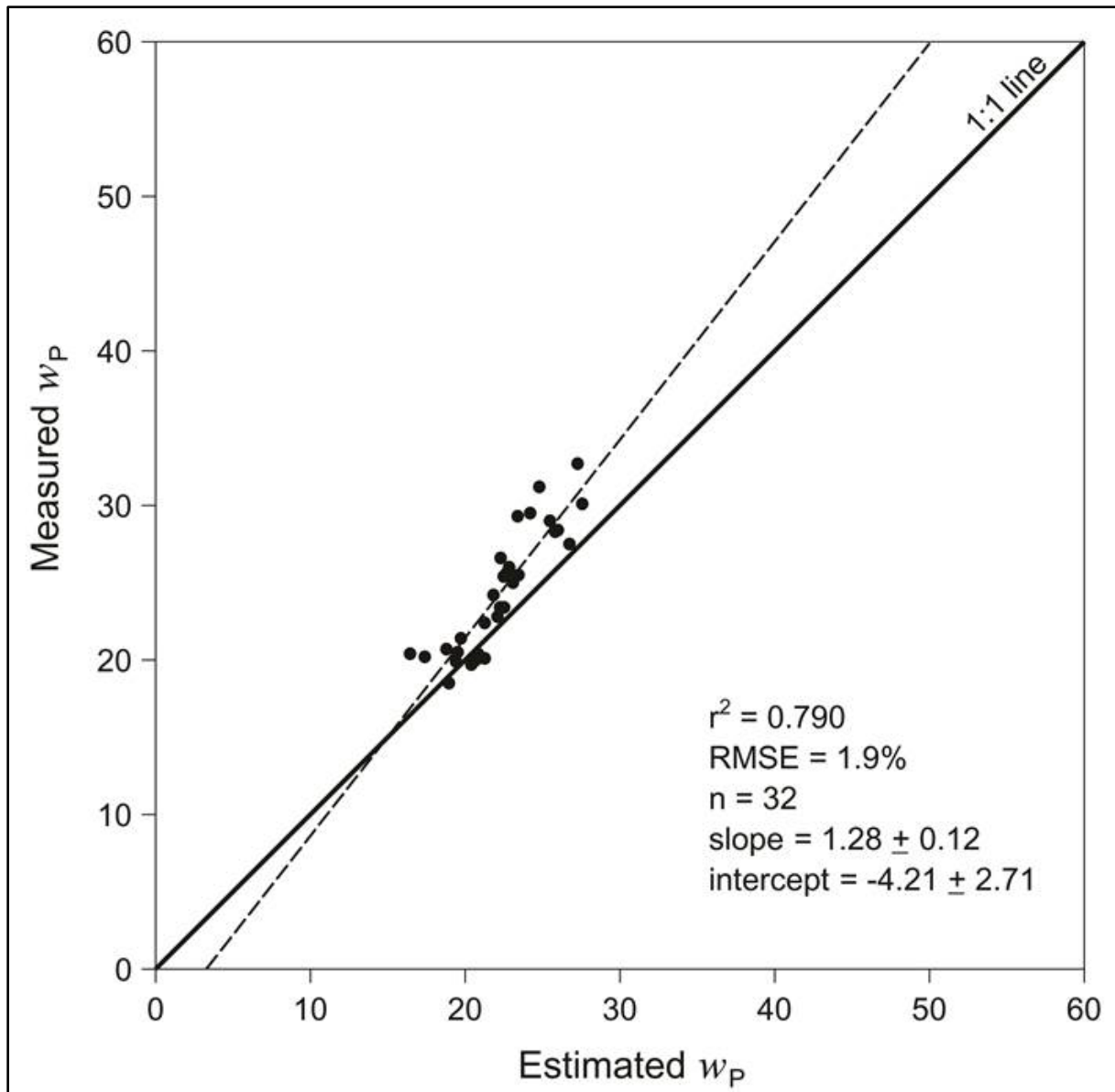


Figure K-2. Significant regression ($P < 0.0001$) of measured plastic limit (ASTM D424-71) upon estimated plastic limit (Eqn. K-3), shown as the broken line, with descriptive statistics including standard errors of the slope and intercept ($n = 32$).

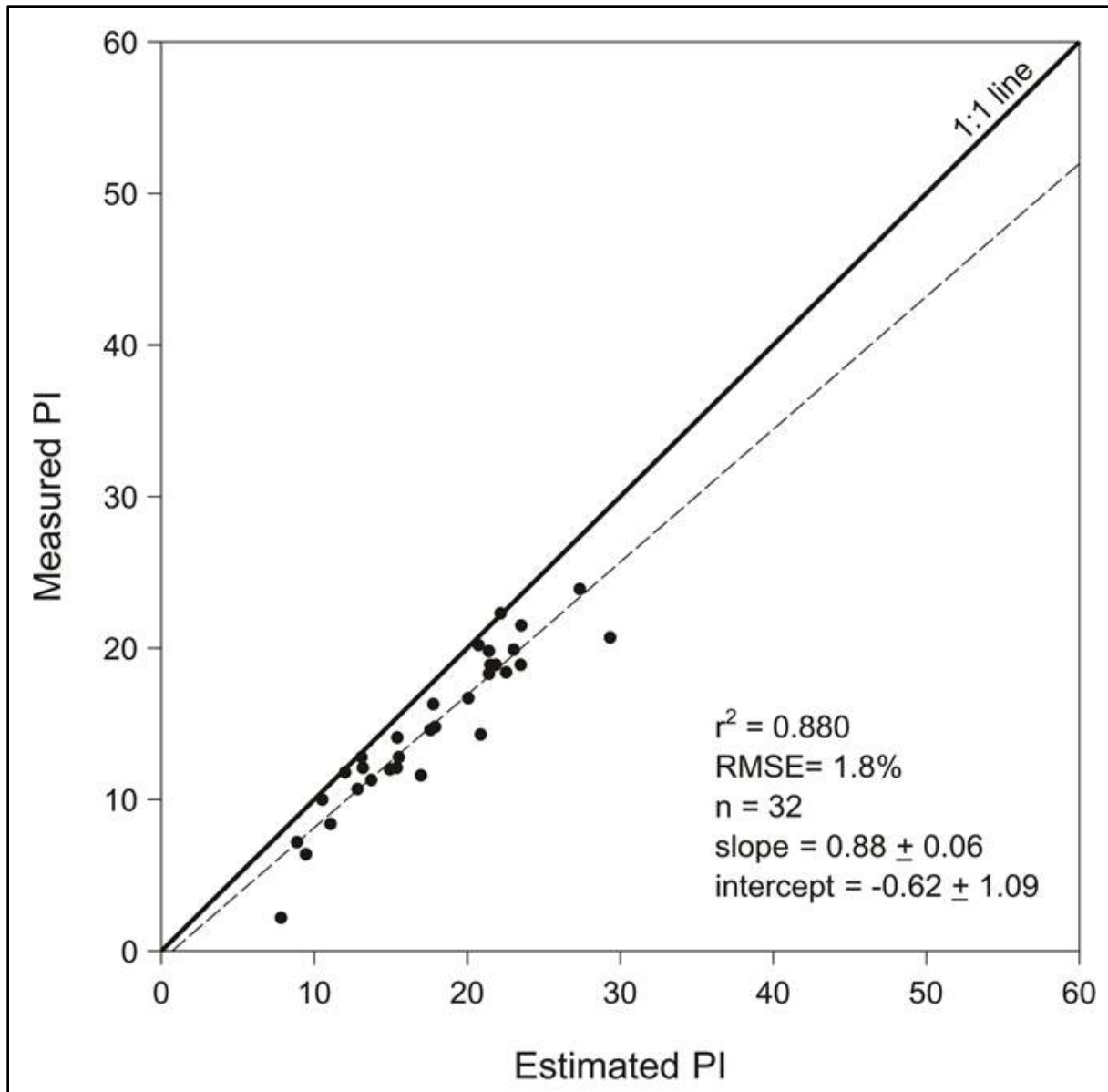


Figure K-3. Significant regression ($P < 0.0001$) of measured plasticity index upon estimated plasticity index (Eqn. K-5), shown as the broken line, with descriptive statistics including standard errors of the slope and intercept ($n = 32$).

5. Summary (Appendix K)

It can be concluded that a useful set of statistical regression equations have been developed that are capable of estimating the soil consistency (Atterberg) limits for soils in southern Ontario (i.e., micaceous clay mineralogy) with acceptably high predictive capability for most agronomic and engineering applications.

References (Appendix K)

Akpokodje, E.G. 1985. The engineering classification of some Australian arid zone soils. Bull. Int. Assoc. Eng. Geol. 31:5-8.

ASTM Int'l. 2010. Standard test methods for liquid limit, plastic limit, and plasticity index of soils (ASTM D4318-10). 2010 Annual Book of ASTM Standards. Vol. 04.08. American Society for Testing and Materials Int'l. West Conshohocken, PA.

Baumgartl, T. 2002. Atterberg limits. p. 89-93. *In* R. Lal (ed.). Encyclopedia of Soil Science. 1st edition. Marcel Dekker, Inc., New York, NY.

Culley, J.L.B., B.K. Dow, E.W. Presant and A.J. MacLean. 1981. Impacts of installation of an oil pipeline on the productivity of Ontario cropland. Research Branch, Agriculture Canada. Contribution No. 66. 88 pp.

de Jong, E., D.F. Acton and H.B. Stonehouse. 1990. Estimating the Atterberg limits of southern Saskatchewan soils from texture and carbon contents. *Can. J. Soil Sci.* 70:543-554.

de la Rosa, D. 1979. Relation of several pedological characteristics to engineering qualities of soil. *J. Soil Sci.* 30:793-799.

Dexter, A.R. and K.Y. Chan. 1991. Soil mechanical properties as influenced by exchangeable cations. *J. Soil Sci.* 42:219-226.

Dolinar, B, M. Misic and L. Trauner. 2007. Correlation between surface area and Atterberg limits of fine-grained soils. *Clays Clay Miner.* 55:519-523.

Faure, A. 1981. A new conception of the plastic and liquid limits of clay. *Soil Tillage Res.* 1:97-105.

Gill, W.R. and C.A. Reaves. 1957. Relationship of Atterberg limits and cation exchange capacity to some physical properties of soil. *Soil Sci. Soc. Am. Proc.* 21:491-497.

Hammel, J.E., M.E. Sumner and J. Burema. 1983. Atterberg limits as indices of external surface areas of soils. *Soil Sci. Soc. Am. J.* 47:1054-1056.

Higashiyama, I. 1992. Shedding light on the fundamental insight behind a primitive soil test – the Atterberg limits test as an example of a common test. *Irrigation Engineering and Rural Planning* 22:1-4.

Joose, P.J. and R.A. McBride. 2003. Assessing physical soil quality of plastic soils of differing mineralogy and pre-stress history using mechanical parameters: I. Saturated compression tests. *Can. J. Soil Sci.* 83:45-63.

Konrad, J.-M. 1999. Frost susceptibility related to soil index properties. *Can. Geotech. J.* 36:403-417.

Odell, R.T., T.H. Thornburn and L.J. McKenzie. 1960. Relationships of Atterberg limits to some other properties of Illinois soils. *Soil Sci. Soc. Am. Proc.* 24:297-300.

Smith, C.W., A. Hadas, J. Dan and H. Koyumdjisky. 1985. Shrinkage and Atterberg limits in relation to other properties of principal soil types in Israel. *Geoderma* 35:47-65.

APPENDIX L

Estimation of the Specific Surface Area of Soils

Estimation of the Specific Surface Area of Soils

1. Preface

One of the soil parameters required for estimation of the 'segregation potential' (SP), in accordance with Konrad (1999), is the specific surface area (SSA) (see Appendix A). There are numerous laboratory methods available to measure SSA (Aylmore, 2002; de Jong, 1999), but Konrad (1999) argued that methods that determine the area per unit mass of both the external and internal surfaces of mineral particles (e.g., ethylene glycol [EGME] or methylene blue techniques) are preferred for SP estimation and analysis over those that only measure the external surfaces (e.g., BET-N₂ method). de Jong (1999) found that the simple water sorption method provided results that were in much better agreement with the EGME method, in comparison to the BET-N₂ method, for Saskatchewan soils.

2. Methods to estimate SSA of soils

2.1 Estimation of SSA using the water sorption method

The SSA of a soil can be estimated if the thickness of the adsorbed water film is known for a particular water pressure potential greater than about pF 3.0. Considerable research effort has been directed at refining this method since the 1960s. Puri & Murari (1964) found that a soil in equilibrium with an atmosphere of 53% relative vapour pressure adsorbs one molecular monolayer of water regardless of the clay minerals present or the magnitude of the SSA of the soil. At the hygroscopic relative humidity of 93.9%, the effective water film thickness is 0.575 nm (2 molecular monolayers) comprised of one water monolayer and hydration layers on adsorbed cations (van der Marel, 1966).

Abrol & Khosla (1966) studied the relationship between the gravimetric soil water content at a pressure potential of -1.5 MPa (i.e., permanent wilting point) and the SSA of East Indian soils (Fig. L-1).

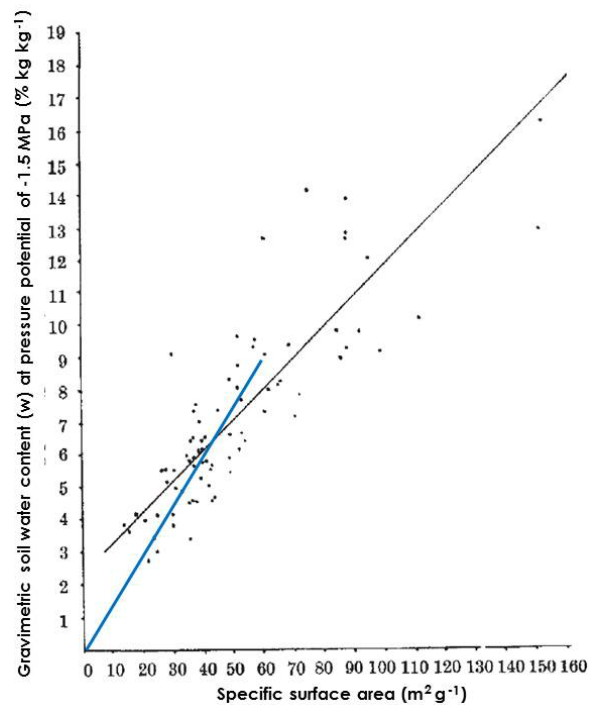


Figure L-1. Plot of the gravimetric soil water content at a pressure potential of -1.5MPa (w_{w_p}) vs. the specific surface area of East Indian soils. (after Abrol & Khosla, 1966).

Considerable scatter in the data for large SSA values forced the regression equation to intercept the y-axis at a gravimetric soil water content of 2.4% g g⁻¹ rather than at the origin (Fig. L-1). Consequently, a singular water film thickness cannot be inferred from this full data set. However, up to a SSA of about 60 m² g⁻¹, the scatter plot (fitted with a blue line) suggests that about 5 molecular monolayers of water are adsorbed on mineral surfaces at pF 4.18 (i.e., pressure potential of -1.5 MPa).

Gardner (1968) argued that closer to 10 monolayers may be adsorbed at this pressure potential, but no supporting experimental evidence was provided. McQueen & Miller (1974) suggested that 10 monolayers are present at pF 2.5 and only 3 or 4 at pF 5.0. Unfortunately, most soil water retention models (e.g., McBride & Mackintosh, 1984) cannot be used with any degree of confidence beyond pF 4.18 and it is thought that pore geometry still has a significant effect on the quantity of water retained at pF 2.5. Petersen *et al.* (1996) found that Danish soils consistently had between 4 and 8 molecular monolayers of water on mineral surfaces at pF 4.18.

2.2 Estimation of SSA using soil constituents

Attempts made by researchers to devise statistically-based PTFs for SSA estimation using soil constituents (e.g., particle-size distribution) as independent variables have not been as successful for SSA as they have been for many other soil properties (Wosten, 2002). For example, Whitfield & Reid (2013) attempted this for soils from northeastern Alberta with unsatisfactory results.

2.3 Estimation of SSA using soil engineering test indices

Attempts made by researchers to devise statistically-based PTFs for SSA estimation using soil engineering test indices (e.g., soil consistency limits) as independent variables have shown some promise (Dolinar *et al.*, 2007; Hammel *et al.*, 1983). The shortcoming of this potential PTF development approach is the lack of data on the liquid limit, plastic limit, or other soil mechanical properties for a sufficiently wide range of Canadian soils.

3. Objective (Appendix L)

The objective of this section (Appendix L) is to calibrate and validate a PTF for estimating the specific surface area of soils in southern Ontario (i.e., micaceous clay mineralogy). This objective would be achieved by formulating a PTF based on the water sorption method, and validating that PTF by accessing alternate published data from the same general region (independent validation data set). More details on the methodology used are provided in Section 4.5.3.

4. Estimation of SSA for this study

Given the above findings from the literature, it is proposed for the PARSC - 003 study that the SSA of soils be estimated using the water sorption method based on the water film thickness on mineral surfaces at pF 4.18, as per Eqn. L-1:

$$SSA = \chi (w_{wp}) \quad \text{Eqn. L-1}$$

where: SSA = specific surface area (m² g⁻¹)

w_{wp} = gravimetric soil water content at the permanent wilting point, or pF 4.18 (kg kg⁻¹)

χ = proportionality constant, dependent on the number of molecular H₂O monolayers assumed to adsorb on mineral surfaces at pF 4.18 as follows:

7 monolayers ($\chi = 497$)
8 monolayers ($\chi = 435$)
9 monolayers ($\chi = 386$)
10 monolayers ($\chi = 348$)

Since non-expansive clay minerals do not show any significant hysteresis in their water sorption isotherms (Grim, 1968), Eqn. L-1 should provide reasonable estimates of both adsorption and desorption SSA measurements.

Figure L-2 shows that w_{wp} can be reliably estimated for Ontario soils with knowledge of only the clay content (McBride & Mackintosh, 1984). Figure L-2 also supports the observation that the silt and sand fractions of soils contribute very little to the total surface area (Warkentin, 1972; de Kimpe *et al.*, 1979). The lack of scatter in the plot further indicates that the dominant types of clay minerals present in Ontario soils (clay mica, chlorite, interstratified phyllosilicates [Kodama, 1979]) possess similar water adsorption properties and the particle-size distribution within the <2 μm fraction is relatively uniform (de Kimpe *et al.*, 1979). Together, Fig. L-2 and Eqn. L-1 suggest that an Ontario soil comprised of 100% kg kg^{-1} clay would have an estimated SSA of about 168 $\text{m}^2 \text{g}^{-1}$ (assuming 7 molecular H_2O monolayers).

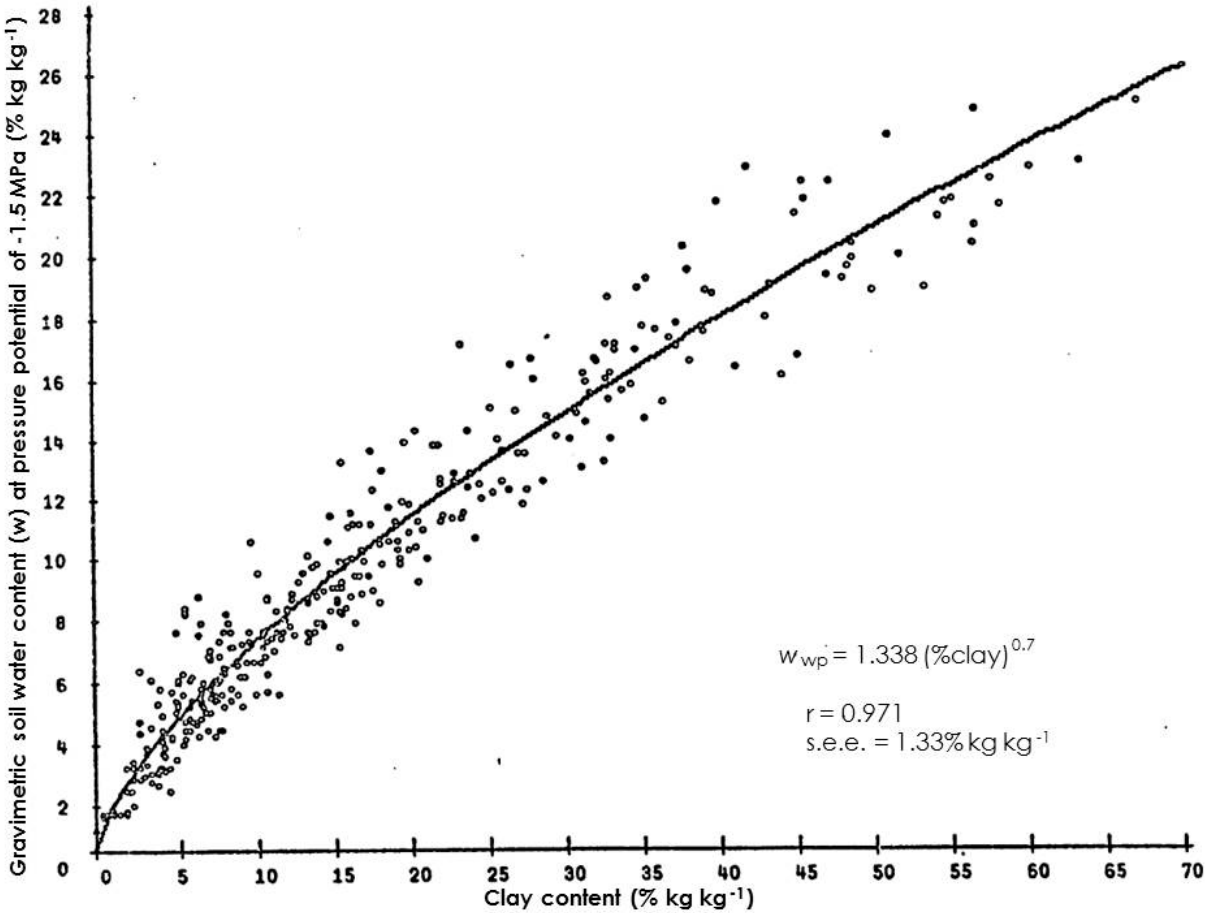


Figure L-2. Plot of the gravimetric soil water content at a pressure potential of -1.5MPa (w_{wp}) vs. clay content of Ontario soils. (after McBride & Mackintosh, 1984).

In contrast to the general configuration of the Fig. L-2 plot, Fig. L-3 shows the effect of a significant component of expanding clay minerals (e.g., smectites, montmorillonites) on the w_{wp} vs. clay content relationship for soils from the U.S. Midwest (Iowa). Here, a SSA of $168 \text{ m}^2 \text{ g}^{-1}$ would be predicted for a smectite-rich soil comprised of only about 60% kg kg^{-1} clay (assuming 7 molecular H_2O monolayers). About 8% of agricultural soils in the Prairie provinces of Canada have significant quantities of expanding clay minerals and exhibit 'vertic' properties (Anderson, 2010). In Quebec, de Kimpe *et al.* (1979) found that the total surface area (internal and external surfaces) of the clay fraction of several Gleysolic soils in the St. Lawrence Lowlands ranged from 130 to $285 \text{ m}^2 \text{ g}^{-1}$. Taking the mean mineralogical composition of the $<2 \mu\text{m}$ separate to be about 35% primary minerals ($<2 \text{ m}^2 \text{ g}^{-1}$), 16% smectites ($810 \text{ m}^2 \text{ g}^{-1}$), 9% vermiculites ($350 \text{ m}^2 \text{ g}^{-1}$), 33% chlorites and clay micas ($100 \text{ m}^2 \text{ g}^{-1}$), and 7% amorphous materials ($200 \text{ m}^2 \text{ g}^{-1}$), an overall SSA of about $208 \text{ m}^2 \text{ g}^{-1}$ might have been anticipated. Clearly, it will be important to characterize the mineralogical composition of the $<2 \mu\text{m}$ fraction of soils across Canada (Kodama, 1979) in order to reliably estimate SSA using the water sorption method.

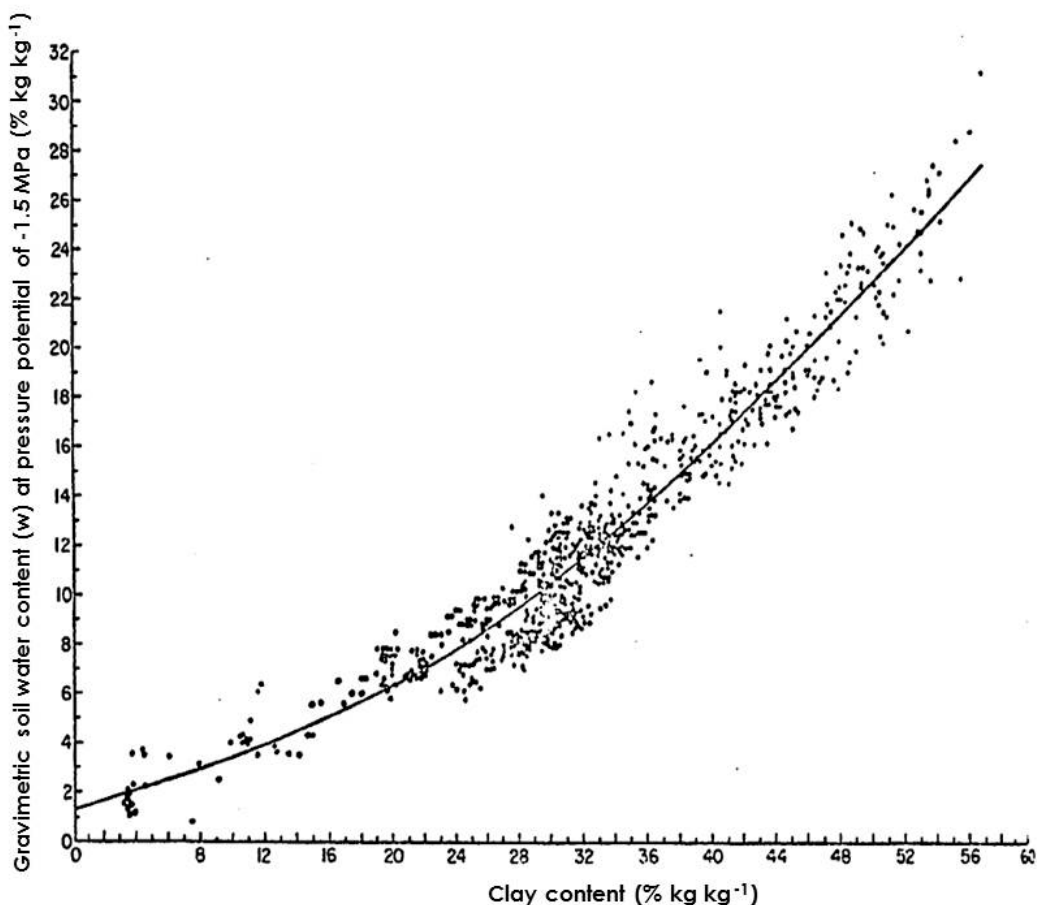


Figure L-3. Plot of the gravimetric soil water content at a pressure potential of -1.5 MPa (w_{wp}) vs. clay content as determined by the hydrometer method for 730 Iowa soils. (after Nielsen & Shaw, 1958).

An alternative method of estimating w_{wp} , apart from its relationship to soil clay content alone (Figs. L-2 and L-3), is to use multiple regression. de Jong & Loebel (1982) developed statistical equations for the various soil orders in Canada using both the silt and clay contents as independent variables and w_{wp} as the dependent variable, but the R^2 values ranged from 0.23 to 0.83 for subsoil (B and C) horizons. Another method of estimating w_{wp} is to use PTFs that

estimate the entire soil water retention curve. Givi *et al.* (2004) did this for 13 widely used PTFs (Table L-1). However, the highest reported correlation coefficient (*r*-value) was only 0.774, which is well below that of the functions shown in Fig. L-2 ($r = 0.971$) or in Fig. L-3 ($r = 0.808$).

Table L-1. Evaluation of thirteen PTFs for estimating the w_{wp} of Iranian soils. (after Givi *et al.*, 2004).

PTFs	<i>r</i>	SDs	SDm	SB	SDSD	LCS	MSD	Intercept	Slope
BSSS ^a	0.709	0.039	0.057	0.000012	0.000323	0.001291	0.00162	0.1422*	0.4862*
BSST ^b	0.774	0.032	0.057	0.000576	0.000627	0.000822	0.00202	0.1288*	0.4342*
Brakensiek	0.704	0.039	0.057	0.000398	0.000292	0.001344	0.00203	0.1168*	0.4937*
EPIC	0.661	0.023	0.057	0.000006	0.001153	0.00089	0.00205	0.1953*	0.2673*
Hutson	0.586	0.015	0.057	0.000004	0.001742	0.00072	0.00246	0.2295*	0.1571*
Rawls	0.685	0.043	0.057	0.001139	0.000174	0.001572	0.00288	0.0940*	0.5267*
Campbell	0.756	0.027	0.057	0.001378	0.000874	0.000764	0.00301	0.1346*	0.3640*
Ra-Brak ^c	0.753	0.045	0.057	0.001947	0.000143	0.001265	0.00335	0.0651	0.5956*
Baumer	0.539	0.055	0.057	0.00162	0.000003	0.002897	0.00452	0.0887	0.5223*
Vereecken	0.180	0.041	0.057	0.00637	0.000243	0.003872	0.01048	0.3144*	0.1312*
Manrique	0.748	0.033	0.057	0.009752	0.000543	0.000968	0.01126	0.0518	0.4423*
Rosetta	0.646	0.023	0.059	0.017068	0.001295	0.000974	0.01933	0.0704*	0.2538*
Mayr-Jarvis	0.769	0.008	0.057	0.044891	0.002328	0.00023	0.04744	0.0262*	0.1183*

SDs: standard deviation of simulated values (m^3/m^3), SDm: standard deviation of measured values (m^3/m^3), SB: squared bias (m^3/m^3), SDSD: squared difference between standard deviations (m^3/m^3), LCS: lack of positive correlation weighted by the standard deviations (m^3/m^3) and MSD: mean-squared deviation (m^3/m^3).

^a British Soil Survey Subsoil.

^b British Soil Survey Topsoil.

^c Rawls–Brakensiek.

* Intercept significantly different from 0, and slope significantly different from 1, $P < 0.05$.

5. Validation of the water sorption method for Ontario soils

A small independent data set (southern Ontario soils) published by Ross (1978) was used to validate the SSA estimation procedure involving Fig. L-2 and Eqn. L-1. In order to eliminate any possible confounding effects of soil organic matter on SSA estimation (Aylmore, 2002; Martel *et al.*, 1978), eight subsoil horizons were selected for this validation step (Table L-2). This is reasonable since transmission (hydrocarbon) pipelines are typically installed at depth below the solum horizons (see Section 4.3.2). The clay contents of the eight C horizons varied from 14 to 70% $kg\ kg^{-1}$. The preferred EGME method was used by Ross (1978) to measure SSA for these soils. Table L-1 clearly shows that reasonably good estimates of SSA are obtained using the water sorption method if it is assumed that between 8 and 10 molecular monolayers of water are adsorbed on the mineral surfaces at pF 4.18 (i.e., estimated SSA values that are closest to the measured values are highlighted in green).

6. Summary (Appendix L)

It can be concluded that a useful PTF has been developed that is capable of estimating the specific surface area of soils in southern Ontario (i.e., micaceous clay mineralogy) with acceptably high predictive capability for most agronomic and engineering applications.

Table L-2. Validation of SSA estimates for eight Ontario subsoils using the water sorption method.

Soil Horizon	Clay Content *	Estimated W _{wp} **	Estimated SSA				Measured SSA *
			Number of H ₂ O monolayers				
			7	8	9	10	
	%kg kg ⁻¹	kg kg ⁻¹	-----	m ² g ⁻¹	-----	m ² g ⁻¹	
IICk	42	0.1831	92	80	71	64	80
Ck	39	0.1739	87	76	67	61	67
Ck	14	0.0849	42	37	33	30	21
Ck	65	0.2486	124	108	96	87	89
Ck	43	0.1862	93	81	72	65	56
Ck	20	0.1089	54	47	42	38	35
Ckg	70	0.2618	131	114	101	91	98
Ckg	64	0.2459	123	107	95	86	92

* - measured data originating from Ross (1978)

** - estimated data using the soil water retention model of McBride & Mackintosh (1984)

References (Appendix L)

Abrol, I.P. and B.K. Khosla. 1966. Surface area: a rapid measure of wilting point of soils. *Nature* 212:1392-1393.

Anderson, D. 2010. Vertisolic soils of the prairie region. *Prairie Soils and Crops Journal* 3(5):29-36. Available at: <http://www.prairiesoilsandcrops.ca/articles/volume-3-5-screen.pdf> (verified on Oct. 6, 2014)

Aylmore, L.A.G. 2002. Specific surface area. p. 1289-1292. *In* R. Lal (ed.). *Encyclopedia of Soil Science*. 1st edition. Marcel Dekker, Inc., New York, NY.

de Jong, E. 1999. Comparison of three methods of measuring surface area of soils. *Can. J. Soil Sci.* 79:345-351.

de Jong, R. and K. Loebel. 1982. Empirical relations between soil components and water retention at 1/3 and 15 atmospheres. *Can. J. Soil Sci.* 62:343-350.

de Kimpe, C.R., M.R. Laverdiere and Y.A. Martel. 1979. Surface area and exchange capacity of clay in relation to the mineralogical composition of Gleysolic soils. *Can. J. Soil Sci.* 59:341-347.

Dolinar, B, M. Misic and L. Trauner. 2007. Correlation between surface area and Atterberg limits of fine-grained soils. *Clays Clay Miner.* 55:519-523.

- Gardner, W.R. 1968. Availability and measurement of soil water. p. 107-135. In T.T. Kozlowski (ed.) Water deficits and plant growth (vol. 1). Academic Press, New York, NY.
- Givi, J., S.O. Prasher and R.M. Patel. 2004. Evaluation of pedotransfer functions in predicting the soil water contents at field capacity and wilting point. *Agricultural Water Management* 70:83-96.
- Grim, R.E. 1968. *Clay Mineralogy*. 2nd ed., McGraw-Hill, New York, NY.
- Hammel, J.E., M.E. Sumner and J. Burema. 1983. Atterberg limits as indices of external surface areas of soils. *Soil Sci. Soc. Am. J.* 47:1054-1056.
- Kodama, H. 1979. Clay minerals in Canadian soils: their origin, distribution and alteration. *Can. J. Soil Sci.* 59:37-58.
- Konrad, J.-M. 1999. Frost susceptibility related to soil index properties. *Can. Geotech. J.* 36:403-417.
- Martel, Y.A., C.R. de Kimpe and M.R. Laverdiere. 1978. Cation-exchange capacity of clay-rich soils in relation to organic matter, mineral composition, and surface area. *Soil Sci. Soc. Am. J.* 42:764-767.
- McBride, R.A. and E.E. Mackintosh. 1984. Soil survey interpretations from water retention data: I. Development and validation of a water retention model. *Soil Sci. Soc. Am. J.* 48:1338-1343.
- McQueen, I.S. and R.F. Miller. 1974. Approximating soil moisture characteristics from limited data: empirical evidence and tentative model. *Water Resources Research* 10:521-527.
- Nielsen, D.R. and R.H. Shaw. 1958. Estimation of the 15-atmosphere moisture percentage from hydrometer data. *Soil Sci.* 86:103-106.
- Petersen, L.W., P. Moldrup, O.H. Jacobsen and D.E. Rolston. 1996. Relations between specific surface area and soil physical and chemical properties. *Soil Sci.* 161(1):9-21.
- Puri, B.R. and K. Murari. 1964. Studies in surface area measurements II. Surface area from a single point on the water isotherm. *Soil Sci.* 97:341-343.
- Ross, G.J. 1978. Relationships of specific surface area and clay content to shrink-swell potential of soils having different clay mineralogical compositions. *Can. J. Soil Sci.* 58:159-166.
- van der Marel, H.W. 1966. Cation exchange, specific surface and absorbed H₂O molecules. *Z. Pflanzenernaehr. Bodenk.* 114:161-175.
- Warkentin, B.P. 1972. Use of liquid limit in characterizing clay soils. *Can. J. Soil Sci.* 52:457-464.
- Whitfield, C.J. and C. Reid. 2013. Predicting surface area of coarse-textured soils: Implications for weathering rates. *Can. J. Soil Sci.* 93:621-630.
- Wosten, J.H.M. 2002. Pedotransfer functions. p. 967-971. In R. Lal (ed.). *Encyclopedia of Soil Science*. 1st edition. Marcel Dekker, Inc., New York, NY.

APPENDIX M

Estimation of the Compression Index of Southern Ontario Soils



Estimation of the Compression Index of Southern Ontario Soils

1. Preface

According to Konrad (1999), the influence of overburden pressure on frost heave and the 'segregation potential' (SP) can be accounted for by an empirical relationship involving the compression index (C_c) of the soil. Appendix M presents a series of algorithms that together constitute a PTF on soil compressibility, and allow the reliable estimation of C_c for cohesive soils in southern Ontario.

2. Background

A study carried out in southern Ontario investigated the usefulness of the 'preconsolidation stress' (σ_c') in characterizing the pre- and post-traffic structural state of agricultural soils as well as their vulnerability to further loss of total porosity with wheel traffic (McBride & Jooose, 1996; Veenhof & McBride, 1996). In soil mechanics, this empirically-measured variable is defined as the maximum vertical stress that has acted on an overconsolidated (saturated) soil in the past. In unsaturated soils, however, this variable is regarded more commonly as the stress above which soil deformation greatly increases, since many other factors contributing to structural strength come into play such as large effective stresses caused by freezing or drying, the presence of organic and inorganic stabilizing materials, and age-hardening or hard setting behaviour (Kay, 1990). The σ_c' variable has been found to be very useful in establishing the degree of agricultural soil overconsolidation as well as maximum allowable wheel loads to avoid further compression of soils in agricultural fields, including that caused by construction class equipment in pipeline ROWs.

Recent research has corroborated the hypothesis that the compressive behaviour (static, uniaxial) of structured subsoils in Ontario can be predicted reasonably well from the consolidation behaviour of those same soils when in a remoulded (slurried) condition, and hence from their Atterberg consistency limits (McBride & Baumgartner, 1992). As a result, a PTF has been developed that can assist in characterizing the degree of overconsolidation of soils without the need for an extensive and costly soil compression testing program. This simple set of functions estimates the preconsolidation stress from dry bulk densities (void ratios) measured *in situ* and from other soil properties needed to estimate the normal consolidation line (NCL).

Testing of this PTF has been carried out by assembling the necessary data on soil physical and engineering properties for all soil series characterized by O.C.S.R.E. (Ontario Centre for Soil Resource Evaluation) during the course of the five most recent county-level soil inventory upgrades in southern Ontario that meet the minimum data requirements (McBride & Jooose, 1996).

3. Objective (Appendix M)

The objective of this section (Appendix M) is to report on a PTF for estimating the compression index of cohesive soils in southern Ontario (i.e., micaceous clay mineralogy). This PTF has already been calibrated and validated elsewhere in the literature. More details on the methodology used are provided in Section 4.5.4.

4. PTF calculations

McBride & Jooose (1996) introduced a series of calculations which determine the *minimum possible* σ_c' from the estimated NCL of a soil (Fig. M-1). This sequence of equations is presented in Eqns. M-1 through M-7 and comprise the PTF.

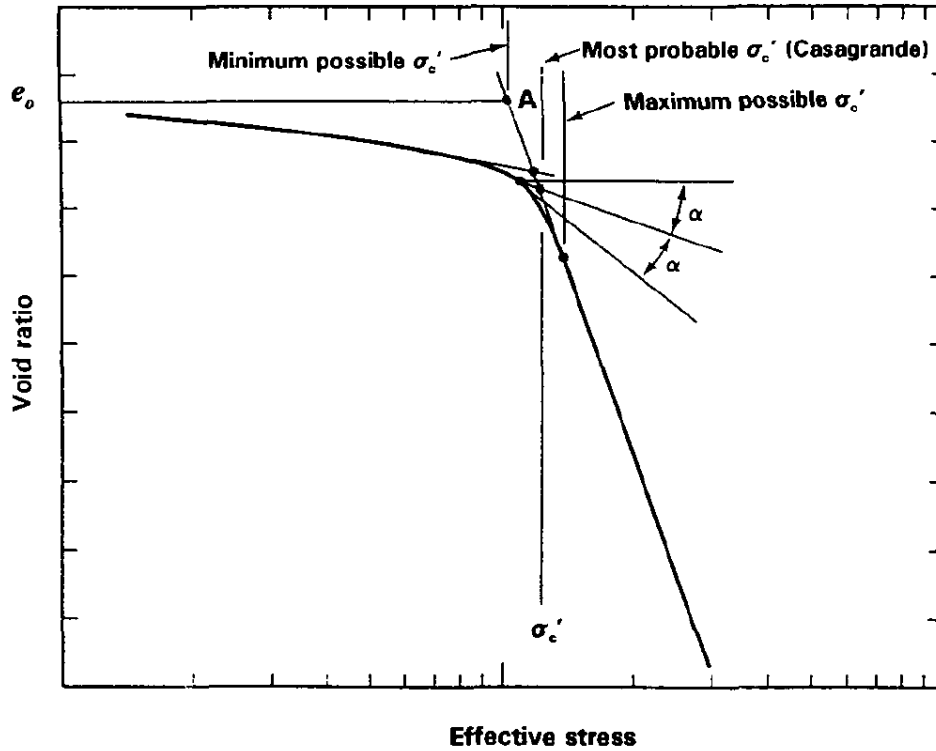


Figure M-1. Three methods for determining the preconsolidation stress from plotted compression data, including the traditional Casagrande method. (after McBride & Joosse, 1996).

To express the NCL in $e(\log \sigma'_c)$ co-ordinates, Eqns. M-1 to M-3 are used to convert the *in situ* dry bulk density of a soil (D_b), as well as its liquid and plastic limits, into void ratios. Field dry bulk densities are transformed with the equation:

$$e_o = \frac{D_p}{D_b} - 1 \quad \text{Eqn. M-1}$$

where e_o is the *in situ* void ratio, D_b is the *in situ* dry bulk density (Mg m^{-3}), and D_p is the soil particle density (Mg m^{-3}). Given that Atterberg limits can be measured by slurry consolidation (McBride & Baumgartner, 1992), these test indices can be taken to represent saturated gravimetric water contents as follows:

$$e_{wL} = \frac{w_L \cdot D_p}{D_w} \quad \text{Eqn. M-2}$$

where e_{wL} and w_L represent the liquid limit expressed as a void ratio and a gravimetric soil water content (kg kg^{-1}), respectively, and D_w is the density of water (Mg m^{-3}) and:

$$e_{wP} = \frac{w_P \cdot D_p}{D_w} \quad \text{Eqn. M-3}$$

where e_{wP} and w_P represent the plastic limit expressed as a void ratio and a gravimetric soil water content (kg kg^{-1}), respectively.

The effective stresses at the liquid limit (σ'_{wL}) and plastic limit (σ'_{wP}) can be estimated with Eqn. M-4 and a constant 420 kPa, respectively (McBride & Baumgartner, 1992):

$$\sigma'_{wL} = 26.6 - (32.1 \log SOC) \quad \text{Eqn. M-4}$$

where SOC is the soil organic carbon content ($\% \text{kg kg}^{-1}$). Equations M-5 and M-6 are used to compute the NCL slope (C_c^*) and the void ratio at unit stress ($e^*_{1\text{kPa}}$), respectively, for a given soil. This is done by using the two known points, (e_{wL}, σ'_{wL}) and (e_{wP}, σ'_{wP}), and assuming a linear function in $e(\log \sigma')$ co-ordinates as follows:

$$C_c^* = \frac{e_{wL} - e_{wP}}{\log \left(\frac{\sigma'_{wP}}{\sigma'_{wL}} \right)} \quad \text{Eqn. M-5}$$

$$e^*_{1\text{kPa}} = e^*_{wP} + (2.623 C_c^*) \quad \text{Eqn. M-6}$$

The equation for the NCL is then:

$$e = e^*_{1\text{kPa}} - (C_c^* \log \sigma') \quad \text{Eqn. M-7}$$

The strength of this PTF lies in its ability to assess the degree of soil compactness and of soil compaction risk, where the available soil physical or engineering data are very limited (e.g., only soil texture, organic carbon content and dry bulk density data are required). The PTF is capable of making the following general interpretations on the mechanical properties of cohesive (plastic) soils:

1. determining the present state of overconsolidation (due to natural and/or anthropogenic causes) in agricultural soils
2. estimating the maximum allowable wheel loadings on these soils before significant additional compaction will occur
3. evaluating the risk of further soil compaction damage

5. Soil property estimations

The soil physical data available in the more recent published soil inventory reports (county level) and in SLC3.2 (national level) include the minimum essential properties (i.e., soil particle-size distribution, dry bulk density, and organic carbon content) required to apply the PTF. From these properties, the remaining soil characteristics can be estimated including the Atterberg limits (required in Eqns. M-2 and M-3) and particle density (required in Eqns. M-1, M-2 and M-3).

Soil consistency (Atterberg) limits for soils in southern Ontario (micaceous clay mineralogy) can be estimated from the regression equations found in Table M-1. Details on the derivation of these functions can be found in Appendix K (i.e., Table K-1 and Table M-1 are identical). Atterberg limits for soils in southern Saskatchewan (smectitic clay mineralogy) can be estimated from the regression equations found in de Jong *et al.* (1990).

Table M-1. Regression equations for the estimation of the Atterberg limits from soil constituents ($n = 203$).

Atterberg test index	SOC content group	n	Regression coefficients			r^2	RMSE	Eqn. no.
			Clay	SOC [‡]	Intercept			
Liquid limit	> 0	151	0.57	3.05	15.95	0.809 [†]	4.75	[K-1]
	= 0	52	0.59	-	16.07	0.790 [†]	4.65	[K-2]
Plastic limit	> 0	151	0.12	3.05	14.28	0.604 [†]	2.84	[K-3]
	= 0	52	0.16	-	13.29	0.471 [†]	2.57	[K-4]
Plasticity Index	all	203	0.45	-	1.89	0.714 [†]	4.61	[K-5]

[†] Significant at $P < 0.0001$

[‡] SOC = soil organic carbon content (%kg kg⁻¹)

The particle density (D_p) can be estimated for soils in southern Ontario using the following equation from McBride *et al.* (2012):

$$\frac{1}{D_p} = \frac{m_1}{2.719} + \frac{m_2}{1.478}$$

Eqn. M-8

where D_p is the soil particle density (Mg m⁻³), m_1 is the mass proportion of the mineral soil component, and m_2 is the mass proportion of the humic soil component.

6. Degree of soil overconsolidation

Three categories have been proposed by McBride *et al.* (2000) in order to partition the range of preconsolidation stress levels typically observed in agricultural soils, as follows:

1. slightly overconsolidated ($\sigma_c' < 20$ kPa)
2. moderately overconsolidated ($\sigma_c' = 20 - 100$ kPa)
3. severely overconsolidated ($\sigma_c' > 100$ kPa)

7. Inclusion criteria

The PTF is based largely on regression equations, so it should only be applied to soils that meet certain inclusion criteria. These criteria are based on the characteristics of the data upon which the PTF was originally developed. The criteria are as follows:

1. The PTF has only been tested for soils in southern Ontario, and may not be applicable to soils dominated by clay mineralogy other than clay mica (illite). For soils with smectitic clay mineralogy, it may be acceptable to use Atterberg limit estimates from de Jong *et al.* (1990) in Eqns. M-2 and M-3, but this has not been tested.
2. The equations developed by McBride & Joosse (1996) were generated from a dataset with virtually no samples exceeding a SOC of 5%kg kg⁻¹. Therefore, PTF results for soils with SOC > 5% should be used with caution.

3. The PTF is only applicable to cohesive soils. In general, Ontario soils with a clay content of less than about 10% kg kg⁻¹ are non-cohesive (McBride & Baumgartner, 1992) and are therefore not appropriate for application of the PTF. Even soils with 10-15% clay are marginally plastic at best.

8. PTF testing and model validation

Results of testing of this PTF can be found in McBride & Joosse (1996). Briefly, this testing revealed that σ_c' estimates tend to increase as clay content increases. Further, the degree of soil overconsolidation is generally lower in surface soils than in subsoils (i.e., lower σ_c' estimates), and is generally higher in agricultural areas than in non-agricultural areas.

McBride *et al.* (2000) report on an application of this PTF using the 'Soil Landscapes of Canada' (SLC1.0) database as an 'agri-environmental indicator' of soil compaction risk. An extensive literature review of potential alternative approaches to indicator development strongly suggested that this PTF represented the best approach available, given the nature and scope of the data available in the SLC1.0 dataset. The strong points of the PTF were that i) it had only modest data requirements, ii) it was scientifically sound yet easy to understand and use, and iii) it lent itself well to geographic or spatial representation within geographic information systems (GIS).

Classes of compaction risk were developed in this study by linking them to the three established compaction susceptibility classes noted above (high [$\sigma_c' < 20$ kPa], moderate [$\sigma_c' = 20 - 100$ kPa], low [$\sigma_c' > 100$ kPa]). The PTF was shown to provide reliable information for a provincial-level analysis of an agri-environmental indicator (i.e., trends and spatial distribution of the degree of soil overconsolidation) in eastern Canada.

9. Summary (Appendix M)

It can be concluded that a useful PTF (as reported elsewhere in the literature) is capable of estimating the compression index of cohesive soils in southern Ontario (i.e., micaceous clay mineralogy) with acceptably high predictive capability for most agronomic and engineering applications.

References

- de Jong, E., D.F. Acton and H.B. Stonehouse. 1990. Estimating the Atterberg limits of southern Saskatchewan soils from texture and carbon contents. *Can. J. Soil Sci.* 70:543-554.
- Kay, B.D. 1990. Rates of change of soil structure under different cropping systems. p. 1-52. *In* Advances in soil science (vol. 12). Springer-Verlag New York, Inc., New York, NY.
- Konrad, J.-M. 1999. Frost susceptibility related to soil index properties. *Can. Geotech. J.* 36:403-417.
- McBride, R.A. and N. Baumgartner. 1992. A simple slurry consolidometer designed for the estimation of the consistency limits of soils. *J. of Terramechanics* 29:223-238.
- McBride, R.A. and P.J. Joosse. 1996. Overconsolidation in agricultural soils. II. Pedotransfer functions for estimating preconsolidation stress. *Soil Sci. Soc. Am. J.* 60:373-380.
- McBride, R.A., P.J. Joosse and G. Wall. 2000. Risk of soil compaction. p. 95-103 (Chapter 10) *In* T. McRae, C.A.S. Smith and L.J. Gregorich (eds.). Environmental sustainability of Canadian agriculture: Report of the Agri-Environmental Indicator Project. Agriculture and Agri-Food Canada, Ottawa, ON.

McBride, R.A., R.L. Slessor and P.J. Joosse. 2012. Estimating the particle density of clay-rich soils with diverse mineralogy. *Soil Sci. Soc. Am. J.* 76(2):569-74.

Veenhof, D.W. and R.A. McBride. 1996. Overconsolidation in agricultural soils. I. Compression and consolidation behavior of remolded and structured soils. *Soil Sci. Soc. Am. J.* 60:362-373.

APPENDIX N

Estimation of the Standard Proctor Density Test Indices of Southern Ontario Soils



Estimation of the Standard Proctor Density Test Indices of Southern Ontario Soils

1. Preface

The Standard Proctor Density test indices ('Maximum Dry Density' [MDD] and 'Optimum Water Content' [OWC]) are useful measures of soil strength or degree of soil overconsolidation in order to contrast soil strength within a pipeline trench area to that outside the ROW (Ivey and McBride, 1999) during different soil water and temperature regime conditions (Figs. N-1 and N-2). This information can help to assess the susceptibility of pipelines to exposure caused by frost heave (i.e., overburden pressure). PTFs were developed for the MDD and OWC parameters using the same soil data base (see Appendix O) and statistical procedures described in Section 4.5.2.

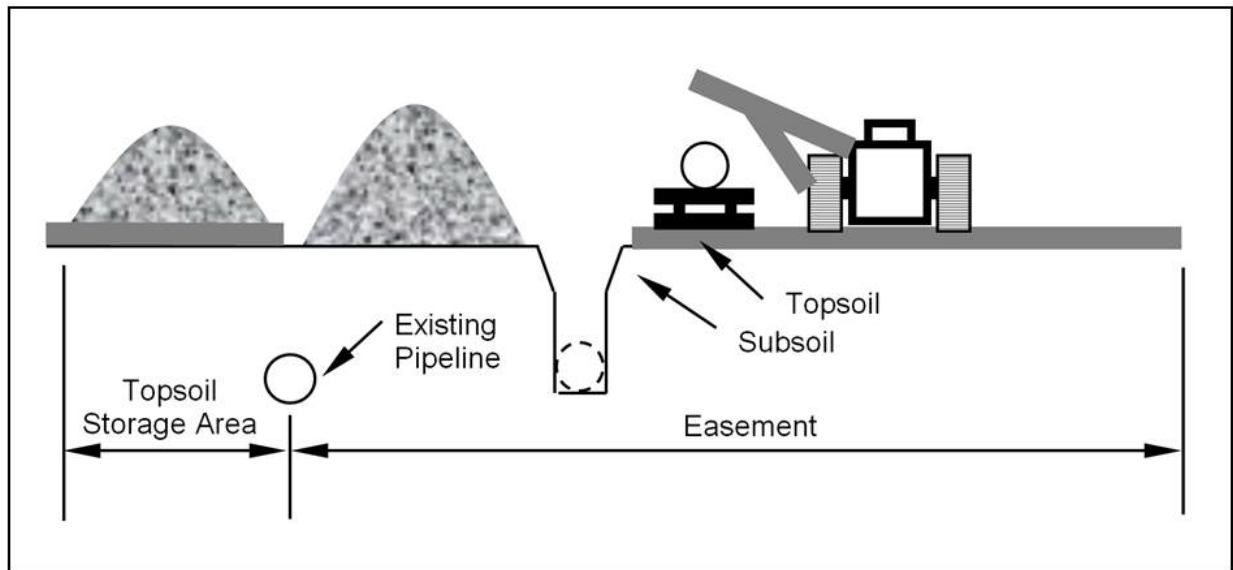


Figure N-1. Schematic of pipeline installation involving soil stripping, trenching and pipelaying operations.

2. Background

Engineers have been using the concept of soil 'reference densities' on construction sites for decades. However, there is increasing interest among agronomists in using soil reference densities for defining the optimal degree of soil compactness for crop growth and yield (or at least an upper dry bulk density limit for specific soil types). Test indices from the Standard Proctor Density test are often used (Carter, 1990) because the 'impact' compaction method is time-tested and proven (widely recognized and accepted in many disciplines), and existing data are occasionally available in soil survey data bases. The alternative is to carry out the more laborious and time consuming 'static' loading (oedometer) tests at some predefined total stress level (Hakansson, 1990).

These approaches are somewhat inflexible since the stress level of the test is usually fixed, is often somewhat arbitrarily chosen (Etana *et al.*, 1997; Hakansson, 1990), and may not always be the most appropriate stress to consider for the intended application. In some applications, the appropriate stress to use in oedometer testing may not always be obvious, which may require that uniaxial tests be performed at multiple stress levels.



Figure N-2. Back-filling of pipeline trench in variable terrain (*foreground* - shallow to bedrock; *background* - steep topography over drumlin) (photo: R.A. McBride).

Numerous studies have attempted to determine the 'apparent equivalent stress' (or 'equivalent static load') of the Standard Proctor Density test, but there is little agreement in the literature. Raghavan *et al.* (1977) reported an empirically-derived compactive effort value of 1.76 MPa, but others have used kinetic energy-based approaches to infer values as high as 1.875 MPa (Panayiotopoulos & Mullins, 1985). Elementary principles of mechanics suggest that the total compactive effort is much less at about 0.60 MPa (ASTM, 2007).

A review of the relevant literature shows that most earlier regression-based attempts at MDD and OWC estimation fall into one of three groups:

- i) PTFs that include soil constituent variables only (e.g., particle-size distribution, SOC)
- ii) PTFs that include soil consistency limit variables only (e.g., liquid limit, plastic limit)
- iii) PTFs that include both soil constituent and consistency limit variables

For example, de la Rosa (1979) and Culley *et al.* (1981) used only soil constituent variables, whereas Ring *et al.* (1962) and Howard *et al.* (1981) used a combination of particle-size distribution and soil consistency (Atterberg) limit variables. In this study, only category (i) was considered.

3. Objective (Appendix N)

The objective of this section (Appendix N) is to calibrate linear regression equations for estimating the Standard Proctor Density test indices (MDD and OWC) for soils in southern Ontario (i.e., micaceous clay mineralogy). This objective would be achieved by assembling available soil data of diverse texture from a number of the more recent soil inventories carried out in southern Ontario (PTF calibration data set [see Appendix O]). Detailed information on the PTF calibration data set and the methodology used are provided in Sections 4.5.2 and 4.5.5.

4. Results and discussion

4.1 Estimation of Standard Proctor density test indices (Linear regression model calibration)

The 203 soil horizons from the 5-municipality region in southern Ontario had a wide range of physical properties (see Appendix O). Clay content ranged from 11 to 77% kg kg⁻¹, and soil organic carbon (SOC) content ranged from 0 to 3.94% kg kg⁻¹. The ranges for the MDD and OWC parameters were from 1.427 to 1.963 Mg m⁻³ and from 11.6 to 28.6% kg kg⁻¹, respectively. The Pearson's correlation matrix showed that the Standard Proctor Density test indices were strongly and significantly ($P < 0.05$) correlated to soil constituents (sand, silt, clay and SOC contents).

4.2 Regression results for Maximum Dry Density (MDD)

Figure N-3 and Table N-1 show the MDD regression results for soil constituent independent variables. The model using linear components showed significant effects for SOC, clay and silt contents ($R^2 = 0.770$, RMSE = 0.056 Mg m⁻³). Use of the square root transformation of SOC did not improve the model, so this transformation was not used for MDD estimation. A significant quadratic effect for clay, and the interaction term (SOC x clay content) existed, giving slightly improved predictive capability ($R^2 = 0.791$, RMSE = 0.054 Mg m⁻³).

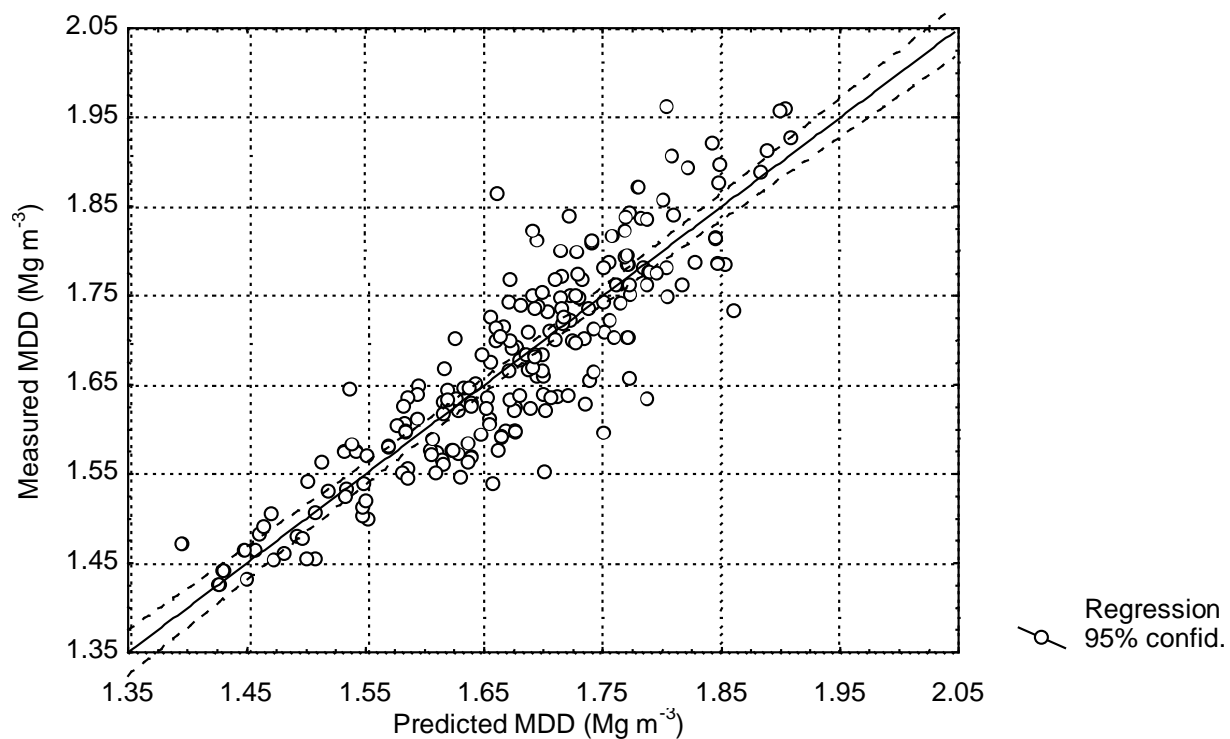


Figure N-3. Estimation of MDD based on linear effects for soil constituents (Eqn. N-1).

Table N-1. Regression equations for the estimation of the Standard Proctor test indices from soil constituents ($n = 203$).

Standard Proctor test index	Regression coefficients					R^2	RMSE	Eqn. no.
	Sand	Silt	Clay	SOC [†]	Intercept			
	----- %kg kg ⁻¹ -----							
Maximum Dry Density	ns	-0.00228	-0.00561	-0.0813	2.055	0.770 [†]	0.056 Mg m ⁻³	[N-1]
Optimum Water Content	-0.082	ns	0.125	1.992	15.070	0.795 [†]	1.65% kg kg ⁻¹	[N-2]

ns - not significant at $P < 0.05$

† - significant at $P < 0.0001$

‡ SOC = soil organic carbon content (%kg kg⁻¹)

Figure N-4 shows a clear distinction in the way that SOC influences the MDD parameter for the topsoil (Ap) horizons when compared to the subsoil (B and C) horizons. The reason for this is not clear, although it may be related to the type of organic carbon present in the topsoils in relation to the subsoil horizons, and the influence that this material has on soil elasticity and resiliency to compactive forces. In order to investigate this further, the regression analysis for MDD prediction was repeated for the 44 Ap horizons only. In general, there was an improvement in the predictive capability of the soil constituent model ($R^2 = 0.836$, RMSE = 0.041 Mg m⁻³).

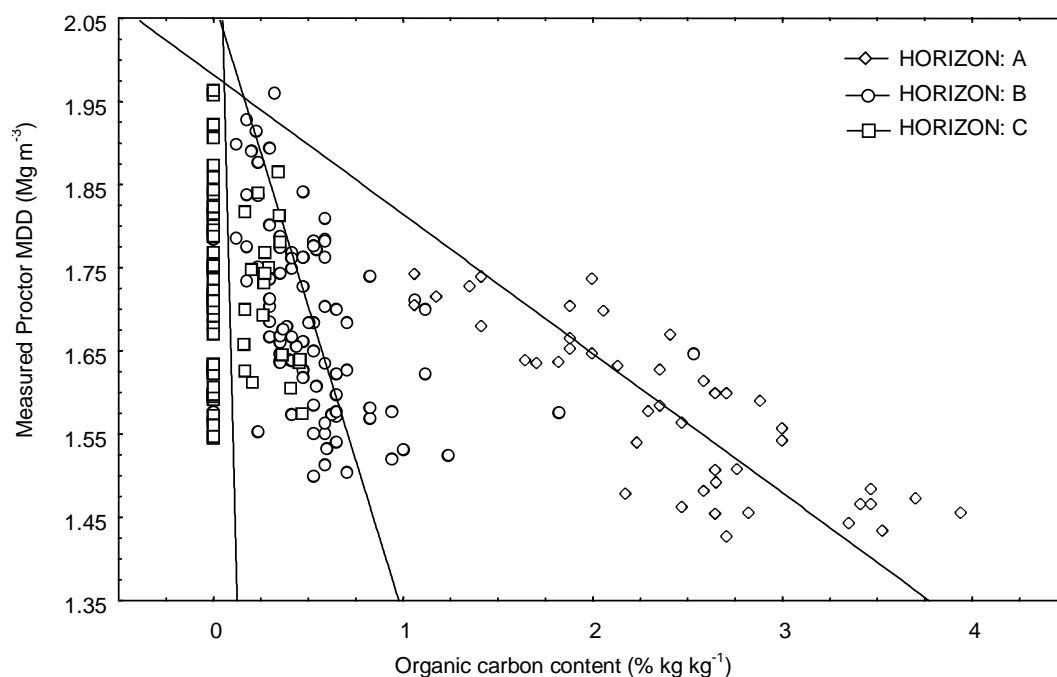


Figure N-4. Scatterplot of the influence of soil organic carbon content on the MDD parameter by horizon.

4.3 Regression results for Optimum Water Content (OWC)

Figure N-5 and Table N-1 show the OWC regression results for the soil constituent independent variables. Testing for significant effects produced a model that included the clay, sand, and SOC contents ($R^2 = 0.795$, $RMSE = 1.65\% \text{ kg kg}^{-1}$). No significant quadratic or interaction terms of the significant linear effects existed.

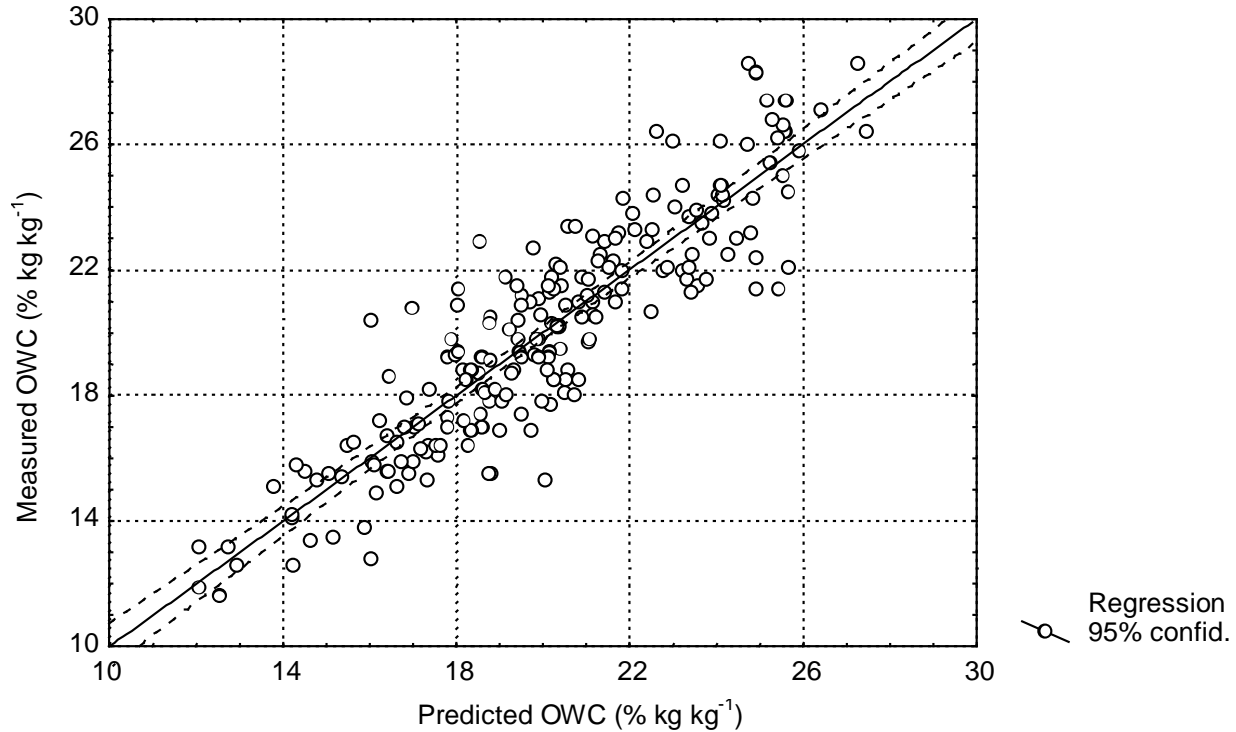


Figure N-5. Estimation of OWC based on linear effects for soil constituents (Eqn. N-2).

4.4 Reference densities

As noted earlier, engineers routinely use 'reference densities' when intentionally compacting soil materials on construction sites (e.g., earthen embankments, landfill liners, roadbeds). Typically, an engineer will strive for a degree of compaction in the range of 95 - 100% of the Standard Proctor MDD.

Agronomists have also recognized the utility of soil reference densities for defining the optimal degree of soil compactness for crop growth and yield. To illustrate, the soil data from Appendix O were used to determine the mean reference densities of the topsoil and subsoil horizons for agricultural soils in southern Ontario. Quotients were determined for each of the 203 horizons (Appendix O) from the *in situ* dry bulk density (D_b) in the field and the corresponding lab-measured Standard Proctor MDD value. The 44 topsoil (Ap) horizons had a mean reference density of 0.78, whereas the mean reference densities of the subsoil horizons (90 B horizons; 69 C horizons) were much higher at 0.86 and 0.89, respectively (Fig. N-6). These data may provide useful guidance for pipeline engineers when soil profiles are being re-constructed in pipeline trenches (Figs. N-1 and N-2), and for environmental inspectors during pipeline 'clean-up' operations (Fig. N-7).

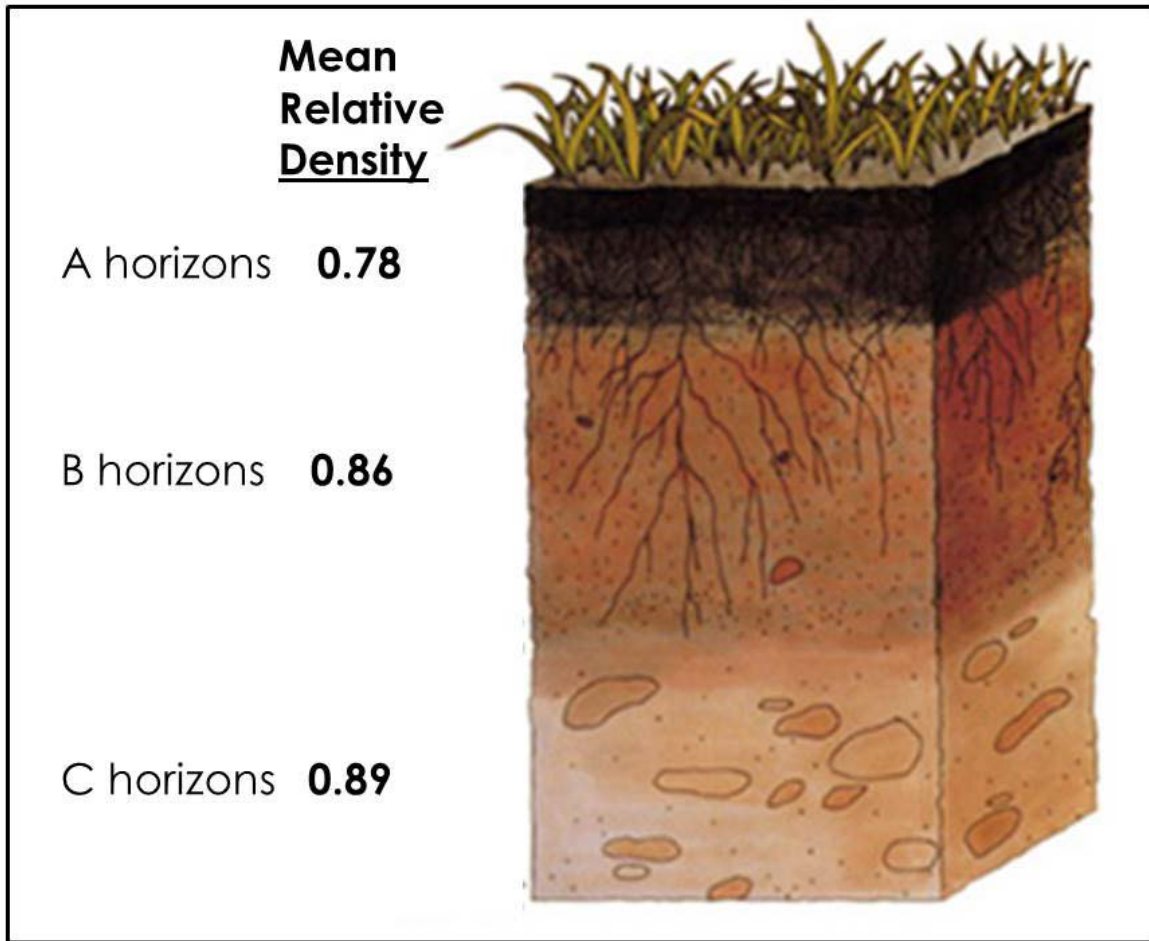


Figure N-6. Mean relative densities of the A, B and C horizons of the 5-municipality soil data set (Appendix O).

5. Summary (Appendix N)

It can be concluded that a useful pair of statistical regression equations have been developed that are capable of estimating the Standard Proctor Density test indices (MDD and OWC) of southern Ontario soils (i.e., micaceous clay mineralogy) with acceptably high predictive capability for most agronomic and engineering applications.



Figure N-7. Environmental inspector (pipelines) conducting soil cone penetrometer testing to verify the efficacy of deep-ripping (sub-soiling) operations in the trench and workspace areas of a pipeline ROW (photo: R.A. McBride).

References (Appendix N)

ASTM. 2007. Test methods for laboratory compaction characteristics of soil using standard effort ($600 \text{ kN}\cdot\text{m}/\text{m}^3$). (D 698-00a). *In* 2007 Annual Book of ASTM Standards, Vol. 04.08, American Society for Testing and Materials, West Conshohocken, PA.

Carter, M.R. 1990. Relative measures of soil bulk density to characterize compaction in tillage studies on fine sandy loams. *Can. J. Soil Sci.* 70:425-433.

Culley, J.L.B., B.K. Dow, E.W. Presant and A.J. MacLean. 1981. Impacts of installation of an oil pipeline on the productivity of Ontario cropland. Research Branch, Agriculture Canada. Contribution No. 66. 88 pp.

de la Rosa, D. 1979. Relation of several pedological characteristics to engineering qualities of soil. *J. Soil Sci.* 30:793-799.

Etana, A., R.A. Comia and I. Hakansson. 1997. Effects of uniaxial stress on the physical properties of four Swedish soils. *Soil and Tillage Research* 44:13-21.

Hakansson, I. 1990. A method for characterizing the state of compactness of the plough layer. *Soil and Tillage Research* 16:105-120.

Howard, R.F., M.J. Singer and G.A. Frantz. 1981. Effects of soil properties, water content, and compactive effort on the compaction of selected California forest and range soils. *Soil Sci. Soc. Am. Proc.* 45:231-236.

Ivey, J.L. and R.A. McBride. 1999. Delineating the zone of topsoil disturbance around buried utilities on agricultural land. *Land Degradation and Development* 10:531-544.

Panayiotopoulos, K.P. and C.E. Mullins. 1985. Packing of sands. *Journal of sands. J. Soil Sci.* 36:129-139.

Raghavan, G.S.V., E. McKyes and B. Beaulieu. 1977. Prediction of clay soil compaction. *Journal of Terramechanics* 14:31-38.

Ring, G.W., J.R. Sallberg and W.H. Collins. 1962. Correlation of compaction and classification test data. p. 55-75. *In* *Compaction and correlation between compaction and classification data.* Highway Research Board, Bulletin 325.

APPENDIX O

Five Municipality Soil Data Set for Southern Ontario



Cty	SS	SH	SD	Sa	Si	CI	Text	D _b	SOM	SOC	W _P	W _L	PI	MDD	OWC
H	Berrien	IIBtgj	44-60	28	37	35	CL	1.47	0.74	0.44	21.0	42.0	21.0	1.656	21.4
H	Berrien	IICk	85+	6	63	31	SICL	1.67	0.28	0.16	19.0	34.0	15.0	1.700	20.5
H	Beverly	Bt	27-50	1	54	45	SIC	1.41	1.06	0.62	21.0	52.5	31.5	1.573	24.3
H	Beverly	Ck	50+	4	52	44	SIC	1.58	0.28	0.16	21.0	41.5	20.5	1.626	23.4
H	Beverly	Ap	0-14	6	63	31	SICL	1.24	4.80	2.82	27.1	42.5	15.4	1.455	26.1
H	Beverly	Btgj	21-47	2	40	58	SIC	1.53	0.90	0.53	22.4	38.2	15.8	1.650	22.0
H	Beverly	Bt	27-37	7	56	37	SICL	1.47	0.66	0.39	24.0	45.0	21.0	1.679	21.1
H	Beverly	Ck	37+	7	64	29	SICL	1.53	0.34	0.20	18.0	33.0	15.0	1.748	18.7
H	Beverly	IICk2	63+	8	48	45	SIC	1.75	0.46	0.27	19.0	36.0	17.0	1.743	18.8
H	Bookton	IICk	50+	8	56	36	SICL	1.62	0.45	0.26	17.0	33.0	16.0	1.732	19.4
H	Brant	Bt	20-64	2	68	30	SICL	1.43	0.67	0.39	20.0	37.0	17.0	1.640	20.4
H	Brant	Ck	64+	2	84	14	SIL	1.47	0.27	0.16	18.0	31.0	13.0	1.658	20.8
H	Brantford	IICk	54+	2	43	55	SIC	1.6	0.61	0.36	19.0	39.0	20.0	1.645	20.7
H	Gobles.lp	IIBt	31-46	20	40	40	SICL	1.52	0.85	0.50	16.5	37.0	20.5	1.684	19.8
H	Gobles.lp	IICk	46+	18	53	29	SICL	1.76	0.28	0.16	16.0	31.0	15.0	1.817	16.1
H	Haldimand	Bmg	20-38	4	20	76	HC	1.41	1.02	0.60	31.0	60.0	29.0	1.533	21.4
H	Haldimand	Ck	38+	1	23	77	HC	1.54	0.79	0.46	27.0	46.0	19.0	1.575	25.0
H	Haldimand	Ck	63+	2	38	60	HC	1.57	0.78	0.46	25.0	46.0	21.0	1.640	21.7
H	Kelvin	Btg	32-50	27	43	30	CL	1.43	1.00	0.59	15.5	34.0	18.5	1.810	17.3
H	Kelvin	Ckg	50+	9	59	32	SICL	1.86	0.40	0.24	14.5	28.5	14.0	1.840	15.5
H	Lincoln	IICk	50+	7	50	44	SIC	1.62	0.46	0.27	19.0	35.0	16.0	1.768	18.5
H	Maplewood	Ckg	28-87	2	74	25	SIL	1.69	0.49	0.29	17.0	27.5	10.5	1.750	18.2
H	Ontario	Ap	0-15	20	55	25	SIL	1.38	3.63	2.14	22.5	36.3	13.8	1.632	21.0
H	Ontario	Bt	18-45	17	51	32	SICL	1.56	0.92	0.54	18.9	34.9	16.0	1.772	17.8
H	Ontario	Ck	45+	11	50	39	SICL	1.66	0.59	0.35	16.0	30.0	14.0	1.813	16.9
H	Silver Hill	IIBtg	70-110	51	36	13	L	1.61	0.34	0.20	14.0	19.5	5.5	1.890	12.6
H	Smithville	Ck	45+	2	37	62	HC	1.46	0.77	0.45	18.5	44.5	26.0	1.636	21.5
H	Smithville.lp	IIBt	16-29	3	35	62	HC	1.49	0.92	0.54	23.0	40.0	17.0	1.608	23.5
H	Smithville.lp	IICk	41+	1	33	66	HC	1.52	0.69	0.41	24.5	47.0	22.5	1.605	24.4
H	Toledo	Bmg	26-46	5	49	46	SIC	1.53	0.62	0.36	24.0	41.0	17.0	1.676	21.0
H	Toledo	Ckg2	64+	4	50	45	SIC	1.68	0.58	0.34	20.0	36.0	16.0	1.865	19.7
H	Toledo	Cg1	42-52	26	52	22	SIL	1.42	0.60	0.35	18.0	32.0	14.0	1.781	16.7
H	Toledo.cp	IICkg	44+	5	53	42	SIC	1.67	0.44	0.26	18.0	40.0	22.0	1.693	21.5

H	Vanessa	Bg	28-66	63	25	12	VFSL	1.65	0.55	0.32	15.9	20.4	4.5	1.960	13.2
H	Vittoria	Btj	34-60	54	33	13	FSL	1.74	0.38	0.22	14.0	25.0	11.0	1.914	13.2
H	Wauseon	2Ckg	60+	2	50	48	SIC	1.56	0.35	0.21	20.0	44.0	24.0	1.612	22.5
H	Welland	Bg	15-47	31	24	45	C	1.54	1.40	0.82	17.8	40.1	22.3	1.740	19.3
M	Tavistock.tp	Ap	0-18	30	55	15	SIL	1.34	2.80	1.65	22.1	29.9	7.8	1.638	19.2
M	Tavistock.tp	Btgj	28-44	30	51	19	SIL	1.35	0.90	0.53	18.3	30.3	12.0	1.777	15.9
M	Tavistock.tp	lICkgj	51-85	25	50	25	SIL	1.52	0.00	0.10	15.6	29.2	13.6	1.858	14.9
M	Tavistock	Ap	0-20	19	63	18	SIL	1.36	2.40	1.41	20.5	29.0	8.5	1.739	17.0
M	Tavistock	Btgj	29-41	20	48	32	SICL	1.35	0.70	0.41	17.0	34.0	17.0	1.768	16.4
M	Tavistock	Ckgj	41-72	13	64	23	SIL	1.41	0.00	0.10	14.5	25.0	10.5	1.873	15.5
M	Tavistock	lICkgj	72-100	2	50	49	SIC	1.51	0.00	0.10	17.5	36.0	18.5	1.716	21.2
M	Beverly	Bmgj	22-35	10	47	43	SIC	1.39	1.40	0.82	30.3	47.2	16.9	1.569	22.3
M	Beverly	Btgj	35-54	7	44	49	SIC	1.37	0.90	0.53	27.3	45.7	18.4	1.585	21.0
M	Beverly	Ckg	54-105	3	49	48	SIC	1.42	0.00	0.10	24.4	40.0	15.6	1.692	18.5
M	Thorndale	Ap	0-21	24	58	18	SIL	0.97	6.70	3.94	31.9	42.2	10.3	1.455	24.7
M	Thorndale	Bmgj	21-37	24	62	14	SIL	1.28	1.00	0.59	23.2	29.8	6.6	1.635	20.4
M	Thorndale	Bt	37-47	31	46	23	L	1.34	0.70	0.41	18.0	32.3	14.3	1.762	17.2
M	Thorndale	Ckgj	47-100	33	49	18	L	1.5	0.00	0.10	15.3	26.9	11.6	1.922	13.4
M	Embro	Ap	0-30	21	58	21	SIL	1.32	4.40	2.59	25.5	36.4	10.9	1.613	20.6
M	Embro	Bmgj	30-63	23	59	18	SIL	1.46	1.00	0.59	19.5	32.3	12.8	1.785	16.5
M	Embro	lIBmgj	63-78	29	55	15	SIL	1.42	0.50	0.29	18.0	28.8	10.8	1.894	13.5
M	Brookston	Ap	0-11	23	36	41	C	1.1	5.90	3.47	29.5	56.8	27.3	1.483	25.4
M	Brookston	Bg1	11-38	20	34	46	C	1.35	1.90	1.12	17.0	47.1	30.1	1.622	21.3
M	Brookston	Bg2	38-61	21	35	44	C	1.39	1.10	0.65	17.0	47.1	30.1	1.622	21.3
M	Brookston	Ckg	61-100	21	47	32	CL	1.44	0.00	0.10	14.9	38.2	23.3	1.793	18.2
M	Perth	Ap	0-19	14	52	34	SICL	1.22	5.10	3.00	26.5	43.0	16.5	1.542	24.2
M	Perth	Bmgj	19-31	16	48	37	SICL	1.16	1.60	0.94	24.0	46.0	22.0	1.577	21.4
M	Perth	Btgj	31-45	37	27	36	CL	1.23	1.80	1.06	23.5	45.0	21.5	1.711	18.1
M	Perth	Ckgj	45-85	8	49	45	SIC	1.47	0.00	0.10	19.0	41.5	22.5	1.823	15.3
M	Muriel	Ap	0-22	19	57	23	SIL	1.12	3.40	2.00	25.3	34.8	9.5	1.647	20.2
M	Muriel	Bt	28-38	10	52	38	SICL	1.35	0.60	0.35	30.2	40.9	10.7	1.660	21.0
M	Muriel	Bm	38-71	11	51	39	SICL	1.42	0.40	0.24	31.2	42.1	10.9	1.553	21.2
M	Muriel	Ckgj	71-102	9	62	29	SICL	1.4	0.00	0.10	29.5	38.4	8.9	1.710	19.3
M	Ekfried	Ap	0-20	10	46	44	SIC	1.1	4.40	2.59	27.5	49.5	22.0	1.481	22.4

M	Ekfried	Bmgj	20-33	6	47	47	SIC	1.31	1.00	0.59	24.5	52.5	28.0	1.563	22.3
M	Ekfried	Btgj	33-50	3	40	57	C	1.56	0.70	0.41	24.0	58.0	34.0	1.574	22.0
M	Ekfried	Ckgj	50-61	2	50	48	SIC	1.44	0.00	0.10	21.0	49.5	28.5	1.634	21.8
M	Ekfried	Ckg	61-90	2	45	53	SIC	1.45	0.00	0.10	21.5	48.0	26.5	1.607	22.1
E	Tuscola	Ap	0-17	23	65	12	SIL	1.21	3.80	2.24	25.0	30.5	5.5	1.539	21.8
E	Tuscola	Bmgj1	17-30	9	79	12	SIL	1.28	1.00	0.59	22.0	24.0	2.0	1.704	17.0
E	Tuscola	Bmgj2	30-51	12	72	17	SIL	1.45	0.50	0.29	22.0	24.0	2.0	1.704	17.0
E	Tuscola	II Ckgj	60-83	4	77	19	SIL	1.49	0.00	0.10	18.5	27.5	9.0	1.752	17.1
E	Muriel	Ap	0-21	24	41	35	CL	1.44	2.30	1.35	20.5	35.0	14.5	1.727	17.7
E	Muriel	Bmgj	21-29	22	40	38	CL	1.43	1.90	1.12	20.0	44.0	24.0	1.700	18.5
E	Muriel	Btgj	29-35	18	39	43	C	1.38	1.10	0.65	20.0	44.0	24.0	1.700	18.5
E	Muriel	Btgj	35-47	17	40	43	SIC	1.54	0.00	0.10	17.0	38.5	21.5	1.723	17.8
E	Muriel	Ckgj	47+	20	45	35	SICL	1.55	0.00	0.10	17.0	38.5	21.5	1.723	17.8
E	Gobles	Ap	0-20	19	52	29	SICL	1.22	4.00	2.35	24.5	37.5	13.0	1.627	21.4
E	Gobles	Bmgj	20-37	8	41	51	SIC	1.39	1.10	0.65	22.5	52.0	29.5	1.577	23.8
E	Gobles	Ckgj	37-60	10	53	37	SICL	1.46	0.00	0.10	19.0	38.5	19.5	1.750	18.2
E	Gobles	Ckg	60+	15	56	28	SICL	1.62	0.00	0.10	18.0	32.5	14.5	1.796	16.4
E	Tavistock.tp	Ap	0-26	20	62	18	SIL	1.17	4.10	2.41	21.0	34.5	13.5	1.669	18.1
E	Tavistock.tp	Btgj	26-35	23	56	21	SIL	1.35	1.00	0.59	18.0	31.0	13.0	1.763	15.9
E	Tavistock.tp	Btgj	35-50	22	58	20	SIL	1.44	0.80	0.47	18.0	31.0	13.0	1.763	15.9
E	Tavistock.tp	II Ckgj	58+	14	59	27	SIL	1.57	0.00	0.10	16.0	31.0	15.0	1.823	16.2
E	Strathburn	Ap	0-22	13	34	53	C	1.28	4.50	2.65	26.5	54.0	27.5	1.491	25.8
E	Strathburn	Bg1	22-37	6	32	62	HC	1.25	2.10	1.24	27.0	70.0	43.0	1.525	23.2
E	Strathburn	Bg2	37-52	2	27	71	HC	1.23	0.90	0.53	27.5	72.5	45.0	1.500	24.3
E	Strathburn	Bg3	52-62	2	30	68	HC	1.32	0.00	0.10	23.5	57.5	34.0	1.577	21.3
E	Strathburn	Ckg	62+	2	36	61	HC	1.41	0.00	0.10	23.0	56.5	33.5	1.547	24.4
E	Ekfried	Ap	0-28	10	41	49	SIC	1.16	4.50	2.65	27.5	50.5	23.0	1.506	24.5
E	Ekfried	Btg	28-41	4	36	60	C	1.41	1.40	0.82	25.0	53.5	28.5	1.582	23.8
E	Ekfried	Ckg2	46-88	1	42	57	SIC	1.42	0.00	0.10	21.5	48.5	27.0	1.630	23.3
E	Ekfried	Ckg3	88-100	4	60	36	SICL	1.48	0.00	0.10	18.5	33.5	15.0	1.719	20.1
E	Colwood	Ap1	0-15	32	47	21	L	1.2	5.10	3.00	27.5	34.0	6.5	1.556	21.7
E	Colwood	Ap2	15-32	34	47	19	L	1.27	4.90	2.88	25.5	34.5	9.0	1.590	19.5
E	Colwood	Bg	32-51	35	50	15	L	1.48	0.60	0.35	19.0	26.5	7.5	1.788	15.3
E	Colwood	IIIBg	56-71	35	49	16	L	1.47	0.00	0.10	19.0	25.5	6.5	1.785	14.1

E	Colwood	III Ckg	71-84	30	55	15	SIL	1.41	0.00	0.10	18.0	24.5	6.5	1.815	15.6
E	Wauseon	II Ckg	74-100	6	56	38	SICL	1.5	0.00	0.10	18.0	37.0	19.0	1.748	18.8
E	Toledo	Ap	0-18	3	54	42	SIC	1.08	6.30	3.71	29.5	53.0	23.5	1.472	26.4
E	Toledo	Bg1	18-33	3	54	43	SIC	1.26	3.10	1.82	24.5	54.5	30.0	1.576	23.0
E	Toledo	Ckg1	48-72	8	59	33	SICL	1.3	0.00	0.10	21.5	50.5	29.0	1.629	22.9
E	Toledo	Ckg2	72-100	2	63	35	SICL	1.39	0.00	0.10	17.5	34.5	17.0	1.736	18.7
E	Ekfried	Ap	0-22	7	34	59	C	1.16	4.60	2.71	33.5	58.0	24.5	1.427	28.6
E	Ekfried	Btgj	22-53	3	27	70	HC	1.31	1.70	1.00	27.5	68.0	40.5	1.531	26.4
E	Ekfried	Ckgj	53-73	2	33	65	HC	1.38	0.00	0.10	23.5	57.5	34.0	1.566	24.0
E	Ekfried	Ckg	73-100	1	32	67	HC	1.41	0.00	0.10	22.5	55.0	32.5	1.572	23.7
E	Gobles.lp	Ap	0-13	19	57	23	SIL	1.36	3.20	1.88	22.5	34.0	11.5	1.652	19.4
E	Gobles.lp	II Btgj	20-42	15	48	37	SICL	1.51	0.80	0.47	20.5	43.0	22.5	1.661	21.5
E	Gobles.lp	II Ckgj	42-100	9	59	32	SICL	1.58	0.00	0.10	17.5	33.5	16.0	1.813	16.9
E	Kelvin	Ap	0-19	27	36	37	CL	1.36	2.90	1.71	21.0	37.5	16.5	1.635	20.5
E	Kelvin	Bg1	19-33	16	34	50	C	1.55	1.20	0.71	20.5	51.0	30.5	1.627	22.9
E	Kelvin	Bg2	33-53	9	34	57	C	1.45	0.80	0.47	20.5	51.0	30.5	1.627	22.9
E	Kelvin	Ckg	53-100	8	45	47	SIC	1.44	0.00	0.10	20.5	50.0	29.5	1.625	22.2
E	Tuscola	Ap1	0-16	47	40	13	L	1.12	4.50	2.65	24.5	30.0	5.5	1.599	18.8
E	Tuscola	Ap2	16-32	46	41	13	L	1.27	4.60	2.71	24.5	30.0	5.5	1.599	18.8
E	Tuscola	Bmgj2	59-82	30	59	11	SIL	1.5	0.20	0.12	16.5	19.0	2.5	1.898	12.6
E	Tuscola	Btgj	82-90	16	64	20	SIL	1.49	0.30	0.18	18.0	27.5	9.5	1.838	15.1
E	Tuscola	Bmgj3	90-124	29	60	11	SIL	1.5	0.20	0.12	20.0	23.0	3.0	1.786	15.8
E	Beverly	Ap1	0-12	11	60	29	SICL	1.46	2.00	1.18	20.0	36.5	16.5	1.715	19.2
E	Beverly	Ap2	12-25	10	60	30	SICL	1.49	1.80	1.06	20.5	39.0	18.5	1.705	18.8
E	Beverly	Btgj	25-33	4	60	36	SICL	1.43	0.60	0.35	21.5	43.0	21.5	1.668	20.6
E	Beverly	Ckgj1	33-57	3	67	30	SICL	1.52	0.00	0.10	19.5	39.5	20.0	1.703	19.2
E	Beverly	Ckgj2	57-100	2	75	23	SIL	1.59	0.00	0.10	19.0	32.5	13.5	1.788	17.0
E	Tuscola	Ap	0-28	50	36	14	L	1.35	3.50	2.06	21.5	26.5	5.0	1.698	17.9
E	Tuscola	Btgj	40-52	37	44	19	L	1.46	0.80	0.47	15.5	27.0	11.5	1.841	15.4
E	Tuscola	Ckgj	52-116	5	75	20	SIL	1.42	0.00	0.10	17.5	28.5	11.0	1.844	16.3
E	Brant	Ap	0-28	34	50	16	SIL	1.41	1.80	1.06	19.0	26.0	7.0	1.742	15.6
E	Brant	Bm	28-37	34	50	16	SIL	1.41	1.00	0.59	17.5	29.5	12.0	1.782	16.4
E	Brant	Bt	37-42	15	63	21	SIL	1.34	0.90	0.53	17.5	29.5	12.0	1.782	16.4
K	Gobles	Ap	0-23	21	55	24	SIL	1.28	2.40	1.41	20.0	30.5	10.5	1.679	18.0

K	Gobles	Bt1	23-36	10	49	41	SIC	1.47	0.70	0.41	20.0	43.0	23.0	1.639	20.3
K	Gobles	Bt2	36-52	20	43	37	SICL	1.46	0.60	0.35	20.0	43.0	23.0	1.639	20.3
K	Gobles	IIBt	52-82	23	43	34	CL	1.54	0.50	0.29	18.5	41.0	22.5	1.713	19.4
K	Gobles	IIICk	82-105	7	53	40	SICL	1.44	0.00	0.10	19.0	41.0	22.0	1.701	19.2
K	Brookston	Ap		15	41	44	SIC	1.33	4.20	2.47	26.5	47.0	20.5	1.563	22.5
K	Brookston	Bg1		14	40	46	SIC	1.32	1.20	0.71	20.0	43.0	23.0	1.684	19.8
K	Brookston	Bg2		18	40	42	C	1.45	0.90	0.53	20.0	43.0	23.0	1.684	19.8
K	Brookston	Ckg		19	45	36	SICL	1.42	0.00	0.10	22.5	50.5	28.0	1.597	20.9
N	Berrien	Btgj	44-60	67	16	17	VFSL	1.52	0.30	0.18	16.0	21.5	5.5	1.928	11.9
N	Berrien	IIBtg	60-77	23	36	41	C	1.51	4.30	2.53	22.0	47.0	25.0	1.646	22.1
N	Berrien	IICkg	77+	4	41	56	SIC	1.59	0.00	0.10	22.0	47.0	25.0	1.595	23.2
N	Chinguacousy	Ap	0-27	21	50	29	CL	1.25	3.20	1.88	20.0	35.0	15.0	1.703	18.0
N	Chinguacousy	Btgj	27-40	21	43	36	CL	1.53	0.80	0.47	18.5	42.0	23.5	1.727	19.1
N	Chinguacousy	Ckgj	40+	20	49	31	CL	1.69	0.00	0.10	16.0	32.0	16.0	1.839	15.3
N	Chinguacousy.rp	Ap	0-14	40	41	19	L	1.07	3.40	2.00	21.0	33.0	12.0	1.736	17.2
N	Chinguacousy.rp	Btgj1	14-30	24	37	38	CL	1.73	0.60	0.35	15.0	32.0	17.0	1.774	17.4
N	Chinguacousy.rp	Btgj2	30-40	27	35	38	CL	1.63	0.50	0.29	16.0	38.5	22.5	1.736	18.5
N	Chinguacousy.rp	Bmgj	40-66	32	40	28	CL	1.69	0.40	0.24	15.5	32.5	17.0	1.837	15.6
N	Chinguacousy.rp	Ckgj	66+	22	56	22	SIL	1.87	0.00	0.10	14.5	24.5	10.0	1.963	12.8
N	Colwood	Bg	23-35	47	33	20	L	1.69	0.40	0.24	15.0	23.5	8.5	1.877	14.2
N	Colwood	Ckgj1	35-52	54	31	15	SL	1.64	0.00	0.10	12.5	16.5	4.0	1.958	11.6
N	Colwood	Ckgj2	52-80	24	54	22	SIL	1.55	0.00	0.10	15.0	23.0	8.0	1.907	13.8
N	Haldimand	Ap	0-15	6	44	50	SIC	1.05	3.70	2.18	29.5	50.0	20.5	1.478	27.4
N	Haldimand	Btgj1	15-25	3	30	68	HC	1.27	1.20	0.71	27.0	55.0	28.0	1.504	28.6
N	Haldimand	Btgj2	25-38	1	29	70	HC	1.3	1.00	0.59	26.0	62.0	36.0	1.513	28.3
N	Haldimand	Ckgj	38+	1	35	64	HC	1.35	0.00	0.10	24.0	51.5	27.5	1.561	26.1
N	Haldimand.lp	Ap	0-17	10	54	36	SICL	1.36	4.00	2.35	24.0	40.0	16.0	1.584	22.5
N	Haldimand.lp	IIBtgj1	17-28	3	35	62	HC	1.51	1.60	0.94	24.5	56.5	32.0	1.520	23.0
N	Haldimand.lp	IIBtgj2	28-42	1	29	69	HC	1.51	1.10	0.65	24.0	57.0	33.0	1.540	21.4
N	Haldimand.lp	IICkgj	42+	1	36	63	HC	1.51	0.00	0.10	23.5	44.5	21.0	1.634	22.1
N	Jeddo.wp	Ap	0-19	32	41	27	CL	1.29	3.90	2.29	23.5	39.0	15.5	1.577	22.1
N	Jeddo.wp	Bg	19-49	40	36	24	L	1.56	0.70	0.41	17.0	34.5	17.5	1.749	16.5
N	Lincoln	Ap	0-15	12	38	50	C	1.22	4.50	2.65	27.5	52.0	24.5	1.454	27.4
N	Lincoln	Btg1	15-34	6	39	55	C	1.49	1.00	0.59	25.0	61.5	36.5	1.551	26.4

N	Lincoln	Btg2	34-62	3	34	63	HC	1.49	0.90	0.53	24.0	51.5	27.5	1.551	21.7
N	Lincoln	Ckg	62+	2	48	50	SIC	1.51	0.00	0.10	22.0	48.5	26.5	1.592	23.1
N	Malton	Ap	0-26	7	60	33	SICL	1.24	4.70	2.76	24.0	41.0	17.0	1.507	24.4
N	Malton	Bg	26-50	2	53	45	SIC	1.43	0.60	0.35	20.5	46.5	26.0	1.636	20.5
N	Malton	Ckg	50-85	3	53	44	SIC	1.53	0.00	0.10	16.5	39.0	22.5	1.710	20.2
N	Malton	II Ckg	85+	13	43	44	SIC	1.52	0.00	0.10	19.0	39.0	20.0	1.768	17.4
N	Malton.rp	Ap	0-19	16	46	38	SICL	0.97	6.00	3.53	32.5	51.0	18.5	1.433	26.6
N	Malton.rp	Bg	19-43	13	45	42	SIC	1.44	0.50	0.29	18.0	42.0	24.0	1.685	19.8
N	Malton.rp	Ckg	43-87	13	50	38	SICL	1.62	0.00	0.10	16.5	34.0	17.5	1.800	15.5
N	Maplewood	IIBg	59-89	5	65	30	SICL	1.51	0.50	0.29	18.5	36.0	17.5	1.801	16.9
N	Maplewood	II Ckg	89+	2	59	39	SICL	1.42	0.00	0.10	19.5	43.5	24.0	1.622	22.7
N	Niagara.lp	Ap	0-17	10	57	33	SICL	0.95	5.90	3.47	31.6	47.2	15.6	1.465	26.8
N	Niagara.lp	IIBtgj	17-39	4	36	60	HC	1.28	1.10	0.65	24.8	41.6	16.8	1.598	23.9
N	Niagara.lp	IIBt	39-53	6	38	56	C	1.45	0.80	0.47	18.5	49.0	30.5	1.618	23.3
N	Niagara.lp	II Ck	53+	5	39	56	C	1.45	0.00	0.10	25.9	49.1	23.2	1.624	23.0
N	Tavistock	Ap	0-24	30	56	13	SIL	1.23	3.10	1.82	21.0	27.5	6.5	1.636	19.8
N	Tavistock	Bmgj	24-40	30	58	12	SIL	1.27	0.80	0.47	19.0	20.8	1.8	1.763	15.5
N	Tavistock	Btgj1	40-54	17	57	26	SIL	1.46	0.60	0.35	15.3	33.0	17.7	1.743	16.4
N	Tavistock	II Ckg	70+	4	48	48	SIC	1.47	0.00	0.10	22.5	46.0	23.5	1.598	23.4
N	Tavistock.tp	Ap	0-27	49	38	13	L	1.22	3.20	1.88	22.5	27.5	5.0	1.665	18.6
N	Tavistock.tp	IIBtgj	54-74	10	48	42	SIC	1.69	0.40	0.24	16.5	35.5	19.0	1.751	17.8
N	Tavistock.tp	II Ckgj	74+	5	53	42	SIC	1.74	0.00	0.10	19.0	36.0	17.0	1.754	19.2
N	Toledo	Ap	0-29	7	51	42	SIC	0.9	5.70	3.35	35.5	46.0	10.5	1.442	27.1
N	Toledo	Bg1	29-41	9	48	43	SIC	1.4	0.70	0.41	21.0	46.5	25.5	1.667	20.9
N	Toledo	Bg2	41-55	11	52	38	SICL	1.57	0.50	0.29	21.0	46.5	25.5	1.667	20.9
N	Toledo	Ckg	55+	3	54	43	SIC	1.52	0.00	0.10	20.5	45.5	25.0	1.670	21.8
N	Toledo.rp	Ap	0-18	4	63	33	SICL	1.18	5.80	3.41	25.5	44.0	18.5	1.465	22.1
N	Toledo.rp	Btg	31-46	4	45	51	SIC	1.59	0.60	0.35	21.0	49.5	28.5	1.647	22.0
N	Toledo.rp	Ckg	46+	4	53	43	SIC	1.58	0.00	0.10	21.5	43.5	22.0	1.682	21.5
N	Tuscola.rp	Btgj	41-57	10	78	12	SIL	1.45	0.30	0.18	22.0	23.5	1.5	1.775	15.8
N	Vineland	Btgj	47-57	40	47	13	L	1.4	0.30	0.18	23.0	23.5	0.5	1.734	15.1
N	Welland	Ap	0-15	7	45	48	SIC	1.16	4.20	2.47	27.5	45.5	18.0	1.462	26.2
N	Welland	Btg1	15-34	3	28	69	HC	1.4	1.10	0.65	26.0	62.0	36.0	1.571	26.0
N	Welland	Ckg	43+	1	26	73	HC	1.42	0.00	0.10	27.5	56.0	28.5	1.545	24.7

Table Heading Key

Cty - County (H = Haldimand-Norfolk ; N = Niagara; M = Middlesex; E = Elgin; K = Kent)

SS - Soil Series

SH - Soil Horizon

SD - Soil Depth (cm)

Sa - Sand Content (%kg kg⁻¹)

Si - Silt Content (%kg kg⁻¹)

Cl - Clay Content (%kg kg⁻¹)

Text - Soil Textural Class (CSSC)

D_b - Soil Dry Bulk Density (Mg m⁻³)

SOM - Soil Organic Matter Content (%kg kg⁻¹)

SOC - Soil Organic Carbon Content (%kg kg⁻¹)

w_p - Plastic Limit (%kg kg⁻¹)

w_L - Liquid Limit (%kg kg⁻¹)

PI - Plasticity Index

MDD - Standard Proctor Maximum Dry Density (Mg m⁻³)

OWC - Standard Proctor Optimum Water Content (%kg kg⁻¹)

APPENDIX P

d50(FF) Soil Particle-size Distribution Parameter

d50(FF) Soil Particle-size Distribution Parameter

1. Preface

Konrad (1999) suggested that the particle-size distribution of the 'fines fraction' ($d < 0.075$ mm) is one of several parameters that define the relative frost heaving susceptibility of soils. He introduced a parameter for use in estimating the SP variable, referred to as the d50(FF) parameter, which can be determined manually (graphically).

2. Manual procedure to determine the d50(FF) parameter

The value of the d50(FF) particle-size parameter is normally determined manually (graphically) using a semi-log particle-size distribution chart (Fig. P-1), as depicted in Konrad (1999).

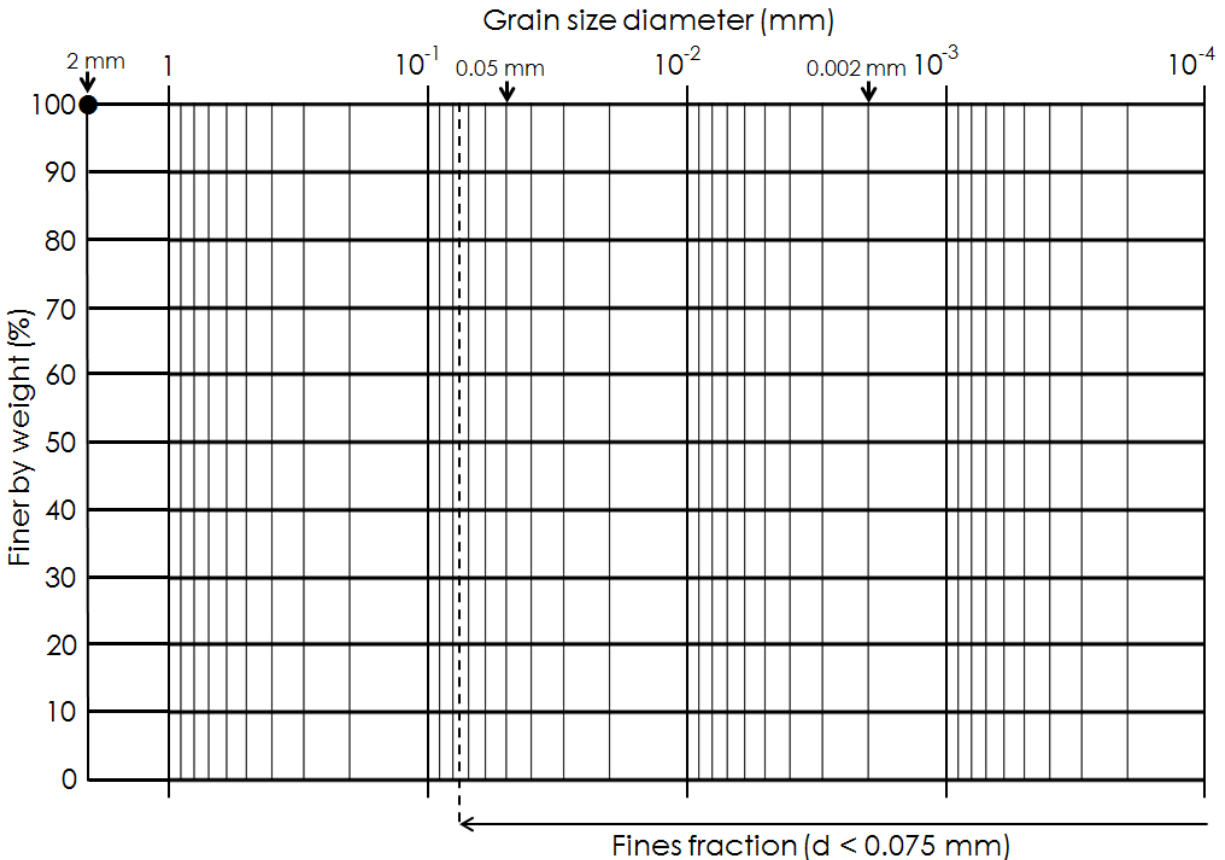


Figure P-1. Semi-log grain-size distribution chart that has been modified for the determination of the d50(FF) parameter. (after Konrad, 1999).

It should be noted that the maximum grain-size diameter on the chart (Fig. P-1) has been specifically set at 2 mm, since textural data reported for agricultural soil samples do not typically include the >2 mm fractions, unlike most engineering soil samples. For this reason, there is a pre-determined data point on the chart at the (x,y) co-ordinate of (2mm, 100%).

The steps required to determine the d50(FF) parameter will be illustrated here by working through an example (Fig. P-2). The test soil is the Ckg horizon of the Brookston clay soil series from southern Ontario. The textural soil data used (30% kg kg^{-1} sand; 27% kg kg^{-1} silt; 43% kg kg^{-1} clay) were extracted from the SLC3.2 system.

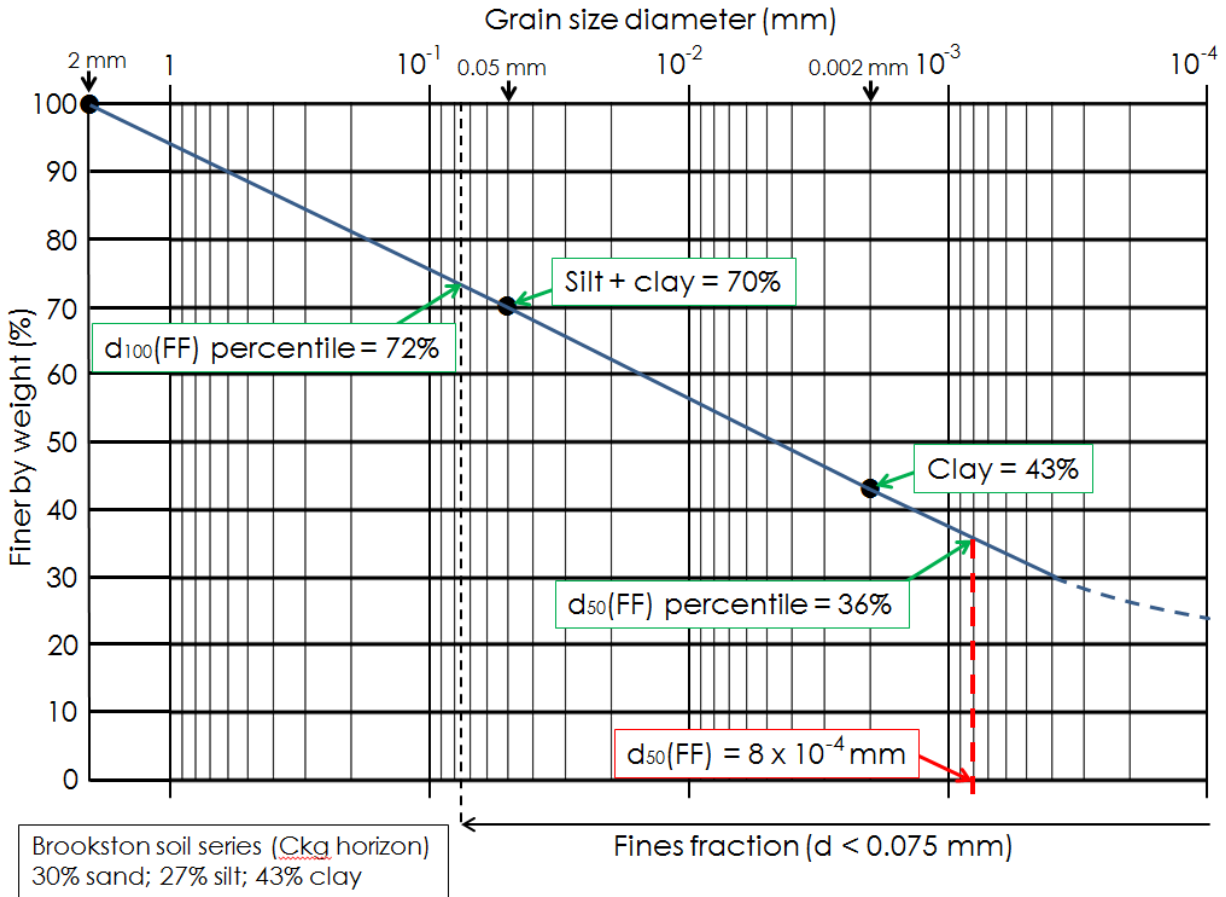


Figure P-2. Example to illustrate the use of the grain-size distribution chart to determine the d₅₀(FF) parameter (Ckg horizon of the Brookston soil series).

Steps

1. Plot the (silt + clay) 'finer by weight' percentile of the <2 mm material on the vertical line denoted by '0.05 mm'
2. Plot the clay 'finer by weight' percentile of the <2 mm material on the vertical line denoted by '0.002 mm'
3. Manually plot the 'best-fit' line through the three available data points
4. Determine the intersection point of the 'best-fit' line with the broken vertical line (---) that corresponds to the upper particle-size limit of the 'fines fraction' (0.075 mm). Read the corresponding value from the y-axis, or the d₁₀₀(FF) percentile, Divide this percentile by 2 to determine the d₅₀(FF) percentile
5. Determine the intersection point of the d₅₀(FF) percentile on the best-fit line. Read the corresponding value from the x-axis, or the d₅₀(FF) parameter (in millimeters)

3. Automated procedure to determine the d50(FF) parameter

It was necessary in this study to develop a 'pedotransfer function' (PTF) that would 'automate' the process of determining the d50(FF) particle-size parameter from the silt and clay contents. A 3-point curve-fitting sub-routine was written in the Python programming language that used either a 'cumulative probability density function' or an 'exponential function' to fit the particle-size data (rather than polynomials, splines, etc.). This sub-routine allowed interpolation of the d50(FF) particle-size parameter, and it was tested on all 47,000 soil layers (approx.) in the SLC3.2 soil data base.

Figure P-3 shows plots for 14 example soils from Alberta and Manitoba that were extracted from the SLC3.2 system. These prairie soils show a wide diversity of particle-size distribution (i.e., including some that were very coarse-textured or very fine-textured), which made the curve-fitting operation challenging. It should be noted that, for ease of computations, the x-axis has been reversed in this curve-fitting sub-routine (in relation to Fig. P-1). Figure P-3 shows that the degree of fit is excellent, and hence the reliability of the d50(FF) values is equally good.

References (Appendix P)

Konrad, J.-M. 1999. Frost susceptibility related to soil index properties. *Can. Geotech. J.* 36:403-417.

Figure P-3. Examples of automated PTF curve-fitting for estimating particle-size distribution parameters (Alberta and Manitoba soils).

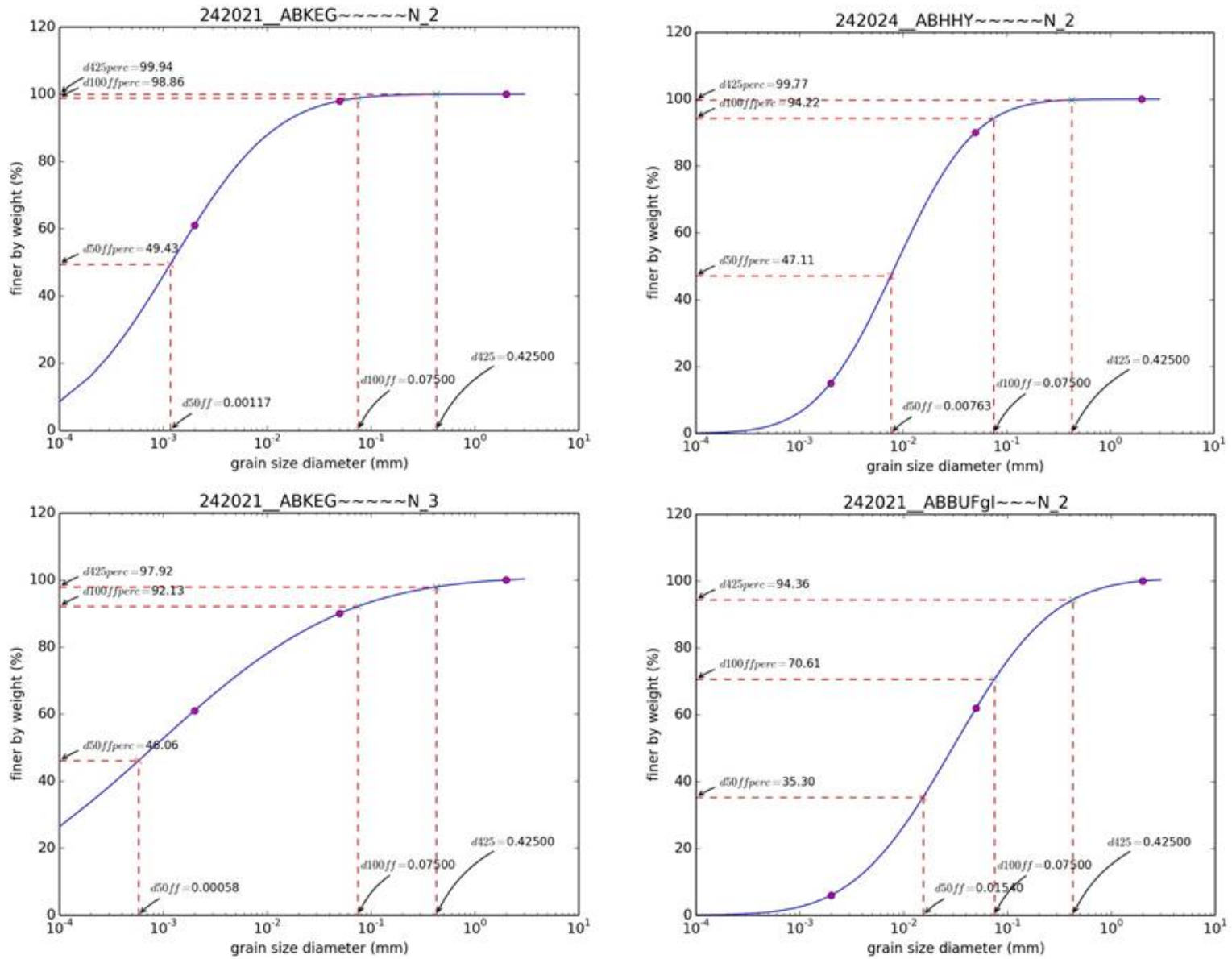


Figure P-3. Examples of automated PTF curve-fitting for estimating particle-size distribution parameters (Alberta and Manitoba soils).

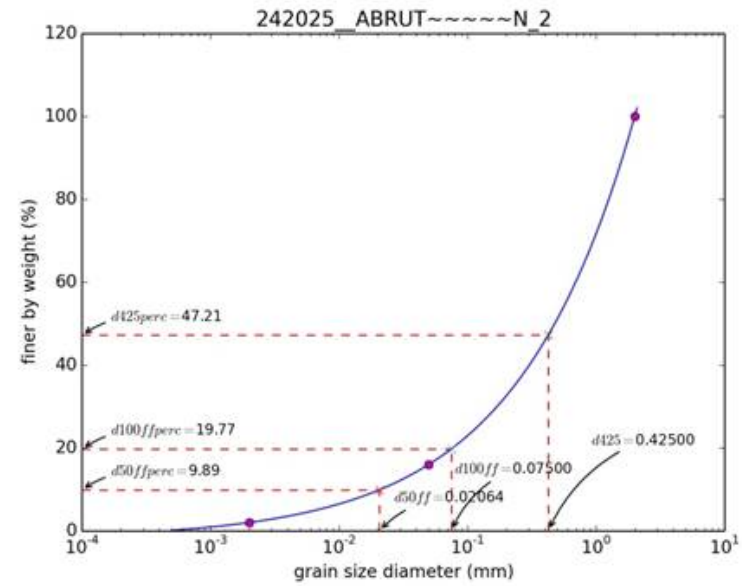
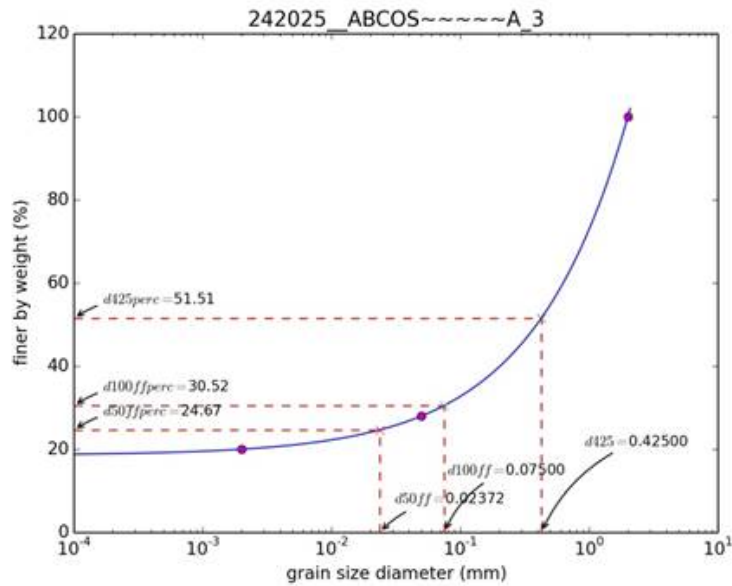
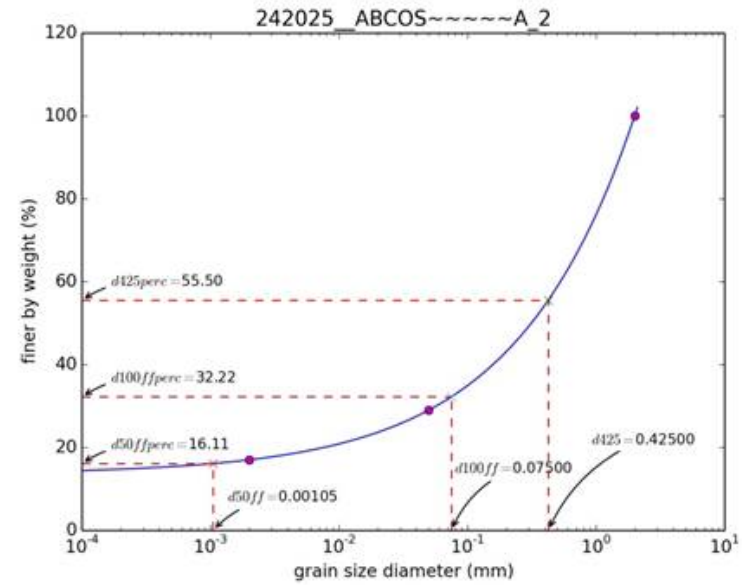
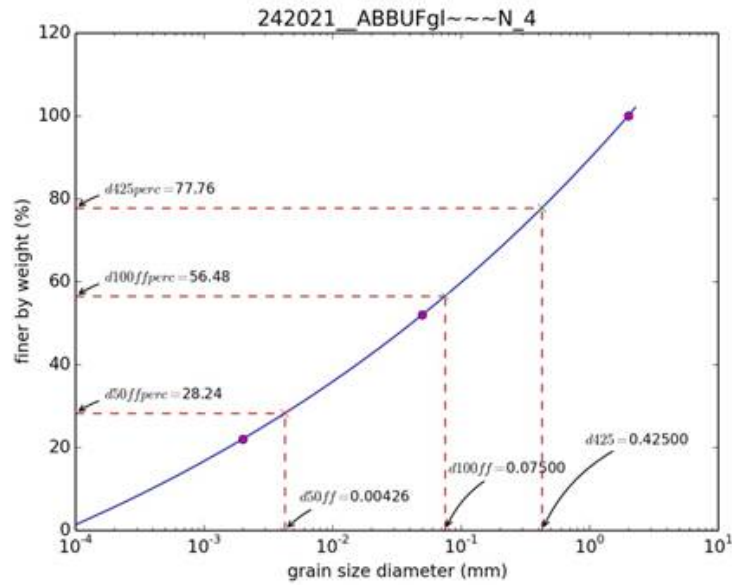


Figure P-3. Examples of automated PTF curve-fitting for estimating particle-size distribution parameters (Alberta and Manitoba soils).

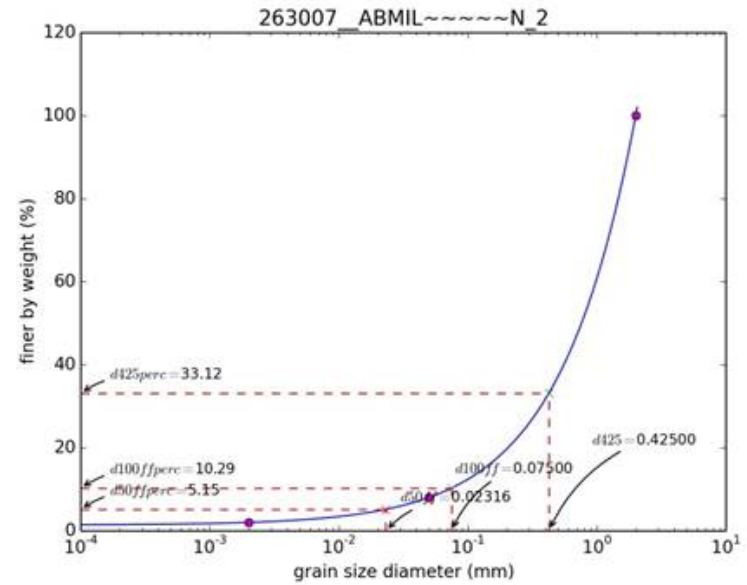
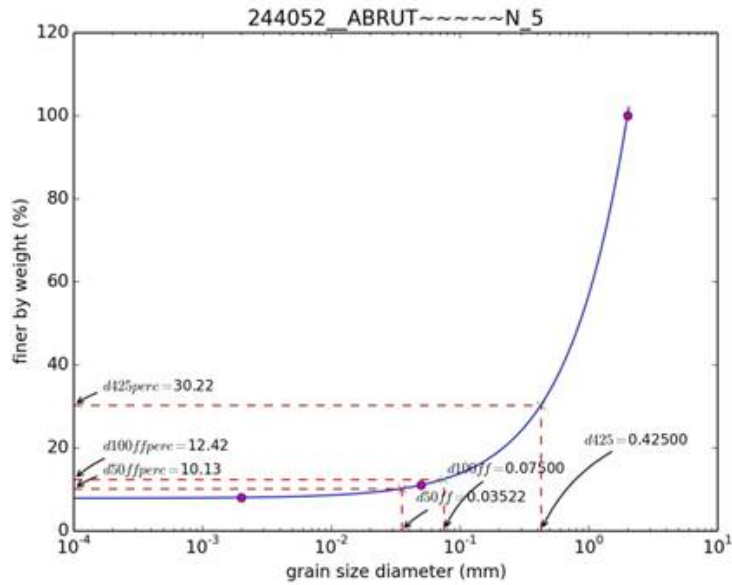
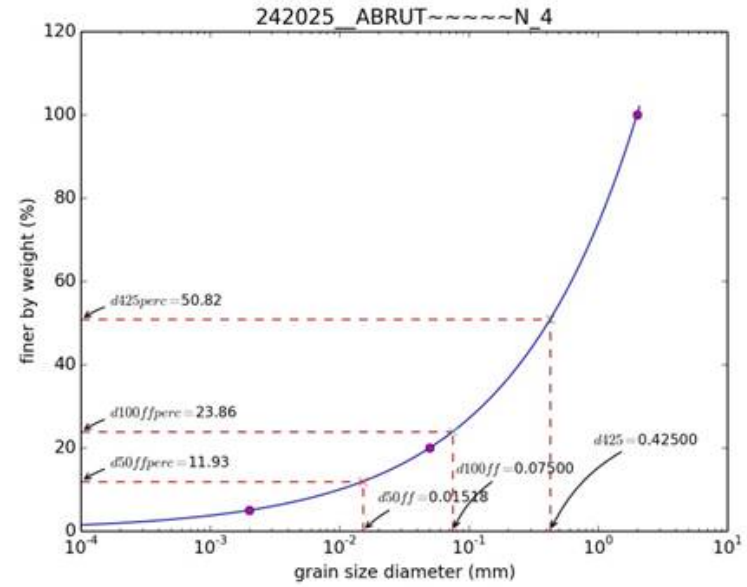
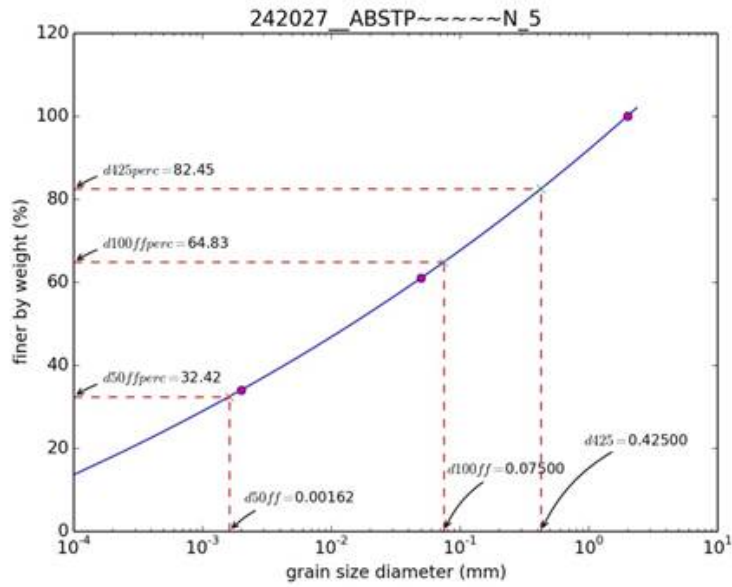
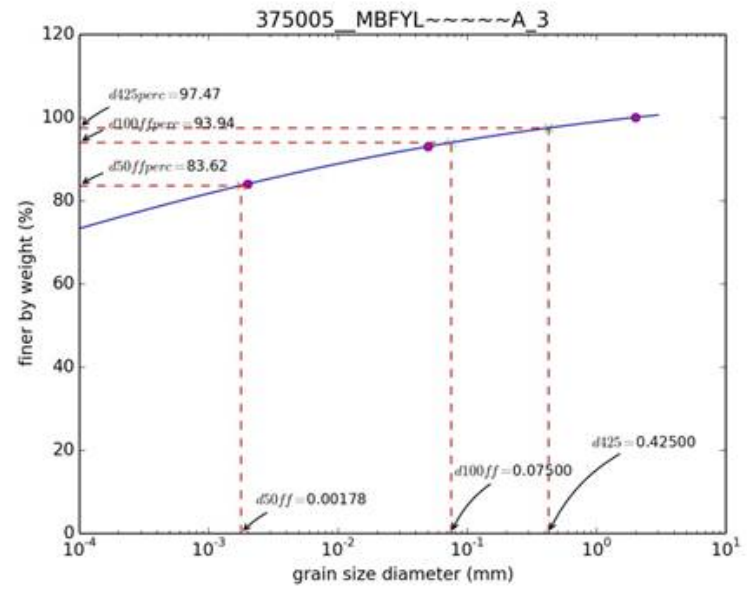
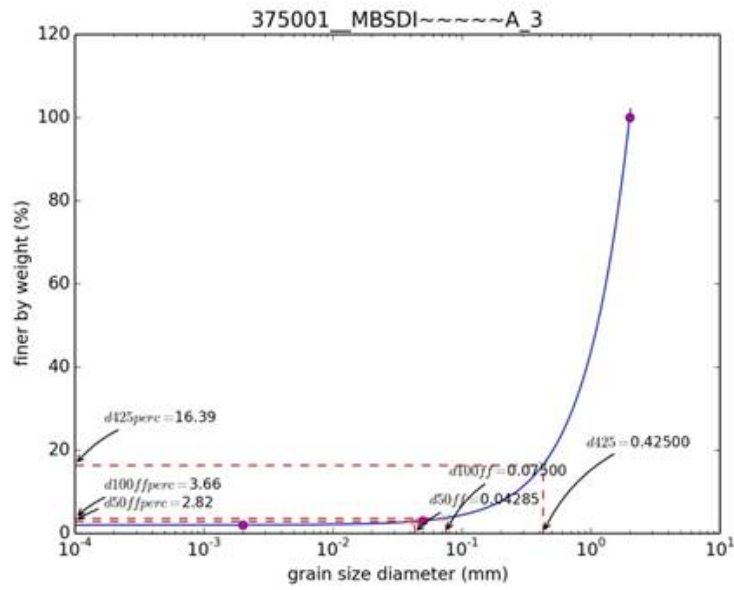


Figure P-3. Examples of automated PTF curve-fitting for estimating particle-size distribution parameters (Alberta and Manitoba soils).



APPENDIX Q

Relationships between Internal Soil Drainage Class and Seasonal Groundwater Table Depth

Relationships between internal soil drainage class and seasonal groundwater table depth

1. Preface

Because of the importance of both the soil temperature and soil water regimes in the frost heave process, it is vital to know the position of the groundwater table in the soil, particularly during the winter season. Groenevelt & Grant (2013) argue that it is the soil hydraulic conductivity ('unsaturated' in the vadose zone, or 'field-saturated' in the phreatic zone) that largely determines the risk of frost heave.

In cropland areas of southern Ontario, it is relatively rare for pipeline contractors to encounter groundwater tables in newly excavated trenches during the usual pipeline installation season of June to September (E. Mozuraitis, per. comm., 2013). Groundwater tables are typically at their deepest in the late summer-early autumn in regions with a humid, temperate climate (Fig. Q-1). Nevertheless, 'wet soil shutdown' conditions and open trenches with standing water in ROWs can result from extended periods of heavy, sustained rainfall during the pipeline installation season (Fig. Q-2).

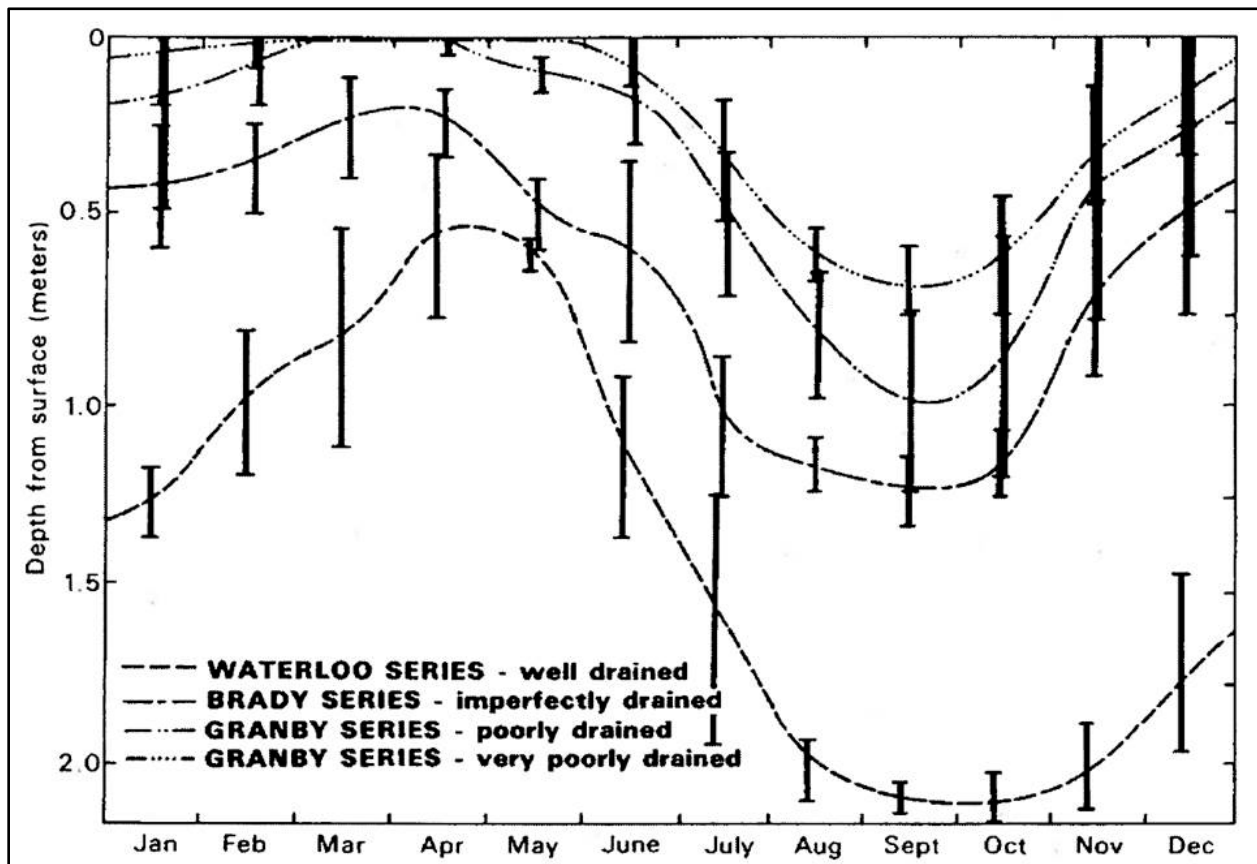


Figure Q-1. Average and seasonal variation in groundwater table levels in the Waterloo soil catena in southern Ontario during the period 1971-75 (after Mackintosh & van der Hulst, 1978).



Figure Q-2. Inundation of an open pipeline trench near Milton, ON after an extended period of heavy, sustained rainfall and surface runoff (photo: R.A. McBride).

2. Soil water regime

A soil catena (Fig. Q-3) is defined as 'a non-taxonomic grouping of a sequence of soils of about the same age, derived from similar parent materials and occurring under similar climatic conditions but having unlike characteristics because of variations in relief and drainage' (AAFC, 2013a). The 'unlike characteristics' in this definition are morphological differences reflected by varying 'internal soil drainage classes' distributed on different landscape positions in the soil catenary sequence (Fig. Q-3). These classes (e.g., well drained, poorly drained) approximate the degree, frequency and duration of soil wetness, and reflect average soil water regimes that are influenced by topographic and hydrological variables. Internal drainage of free water in a soil profile refers to the rapidity and extent of the removal of excess water from the soil in relation to additions from precipitation or groundwater (Day, 1983).

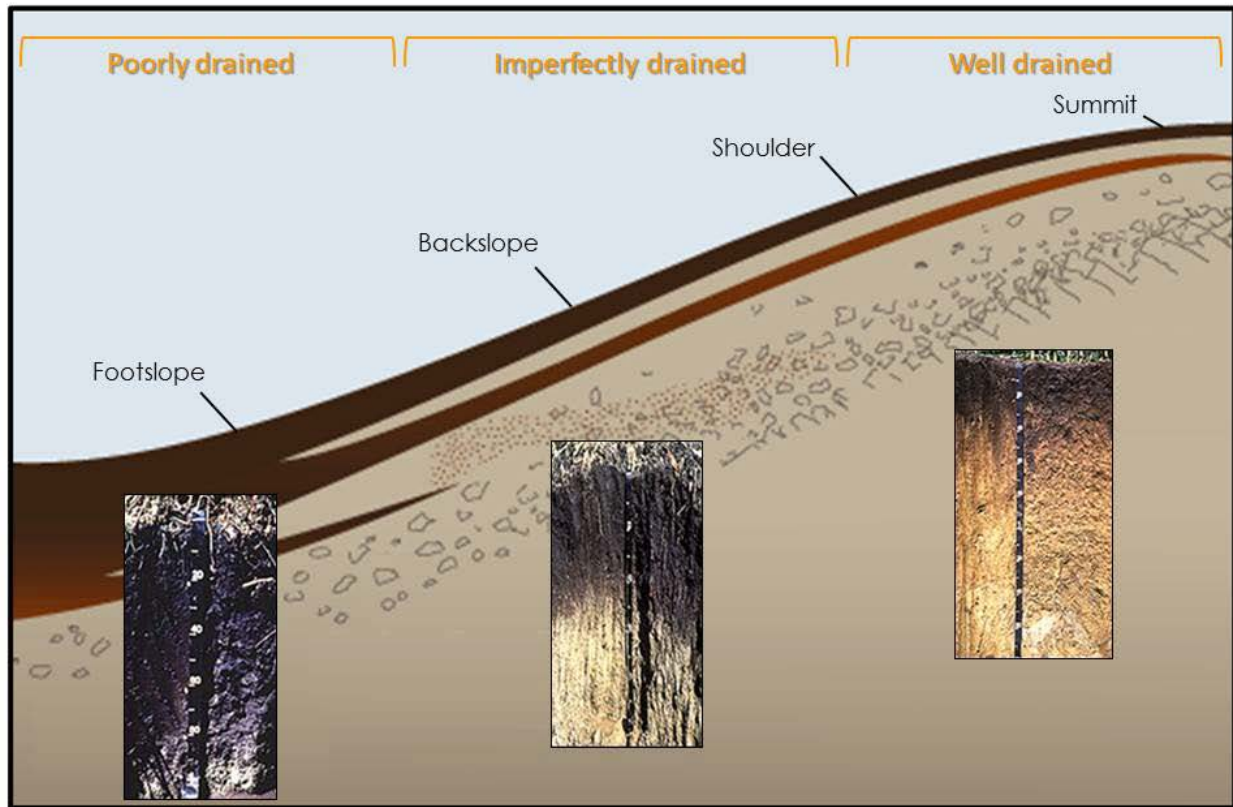


Figure Q-3. Cross-section of a landscape with moderate relief showing a soil catena sequence (i.e., different internal soil drainage classes on the same parent material). The example soil profile photographs illustrate the contrasting soil morphology attributable to natural differences in soil wetness.

3. Soil drainage classes and groundwater table relations

3.1 Humid, temperate climatic regions of Canada

Regions of Canada with humid, temperate climates have ample and well distributed precipitation, and modest evapotranspirational deficits during the growing season (May - September). Figure Q-1 shows field data measured and reported by Mackintosh & van der Hulst (1978) over a 5-year period from one medium-textured soil catena in southern Ontario. The researchers also reported results for several other coarse- and medium-textured soil catenas located in Wellington and Dufferin Counties, ON, where the test sites were i) free of restrictive soil layers that might impede water movement, and ii) naturally drained with no artificial sub-surface tile drains. Figure Q-4 shows the same field-measured trend lines as Fig. Q-1, but in a more simplified and idealized manner (i.e., without the standard error bars, etc.).

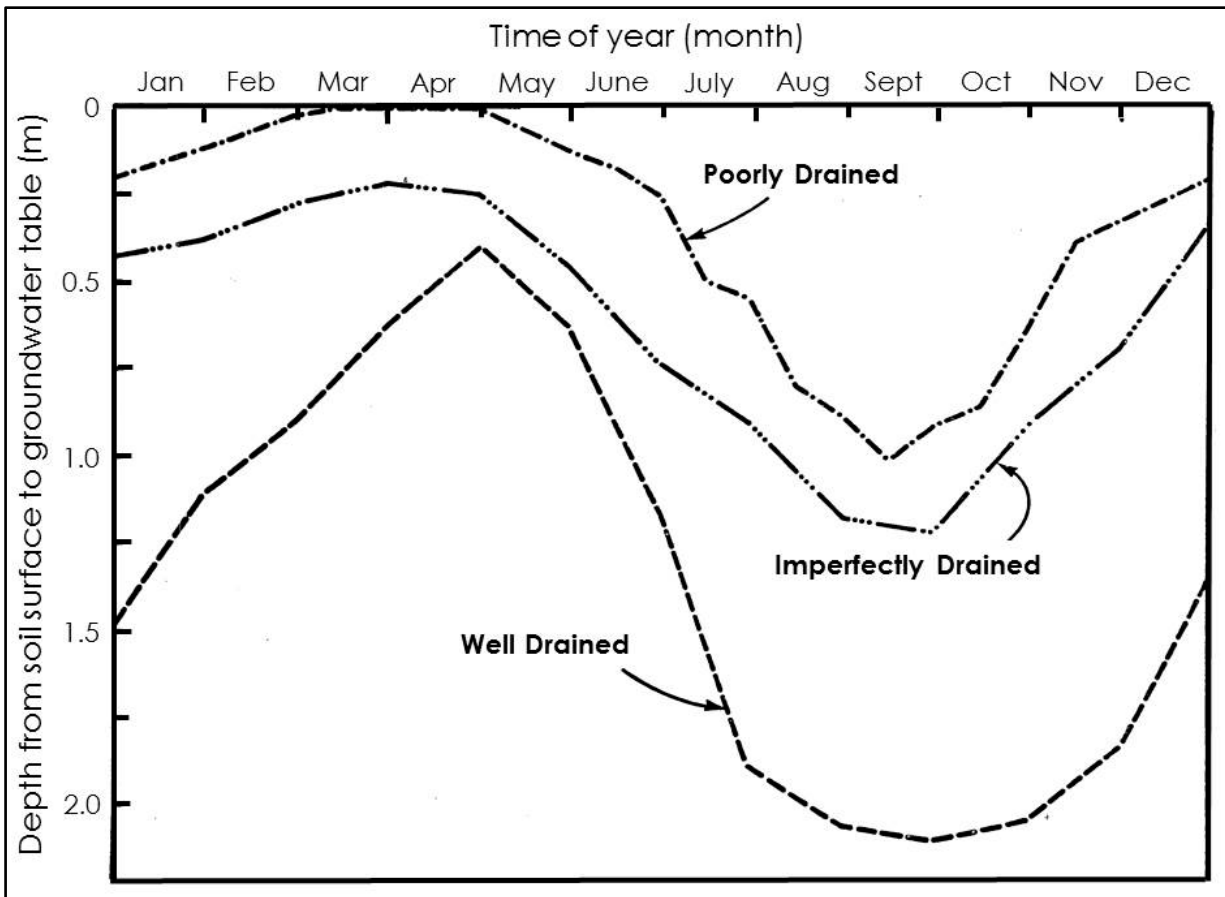


Figure Q-4. A simplified re-draft of Fig. Q-1 (after Mackintosh & van der Hulst, 1978).

McBride & Mackintosh (1976) verbally described these relationships based on general observations made during a soil inventory in New Brunswick, as follows:

Well drained - groundwater table is below 1.5 m of the surface for about 70% of the year

Imperfectly drained - groundwater table is within 1.0 m of the surface for about 50 to 60% of the year, and within 2.0 m of the surface throughout the year

Poorly drained - groundwater table is within 1.0 m of the surface for about 70 to 100% of the year

Very poorly drained - groundwater table is at the surface for about 70 to 80% of the year

Studies involving the measurement of the 'apparent groundwater table' over multiple years in eastern Canada and the northeastern U.S. generally corroborate Fig. Q-4 and the verbal descriptors listed above (Frittont & Olson, 1972; Hohner & Presant, 1985; Langille, 1993). These investigators carried out multi-year studies where they recorded the distance (cm) from the soil surface to the water surface in groundwater observation wells, comprised of perforated plastic pipes installed several meters deep into the soil.

3.2 Prairie Ecozone region of Canada

The Prairie Ecozone is characterized by a semi-arid climate (see Appendix S) with large evapotranspirational deficits during the growing season (May - September) and expansive irrigation districts to compensate for the precipitation shortfall. Alberta has about 563,000 ha of irrigated area in thirteen irrigation districts (Province of Alberta, 2014). Saskatchewan has about 138,000 ha of irrigated area, and another 202,000 ha of potential irrigation expansion from Lake Diefenbaker (Province of Saskatchewan, 2014). Manitoba has about 40,000 ha of irrigated area.

As noted in Section 2 (above), internal soil drainage refers to the rapidity and extent of the removal of excess water from the plant root zone in relation to additions from above (precipitation) or below (groundwater table). In humid, temperate climatic regions of Canada, both factors (i.e., soil hydraulic conductivity; groundwater table depth) are important in defining the internal soil drainage class. In the Prairie Ecozone, however, seasonal groundwater tables are comparatively deep (Fig. Q-5) and have limited influence on the soil water regime within the soil 'control section' (van der Kamp *et al.*, 2003). Hence, it is largely the amount of precipitation/irrigation and the unsaturated hydraulic conductivity of the soil that determines the soil water regime in semi-arid regions.

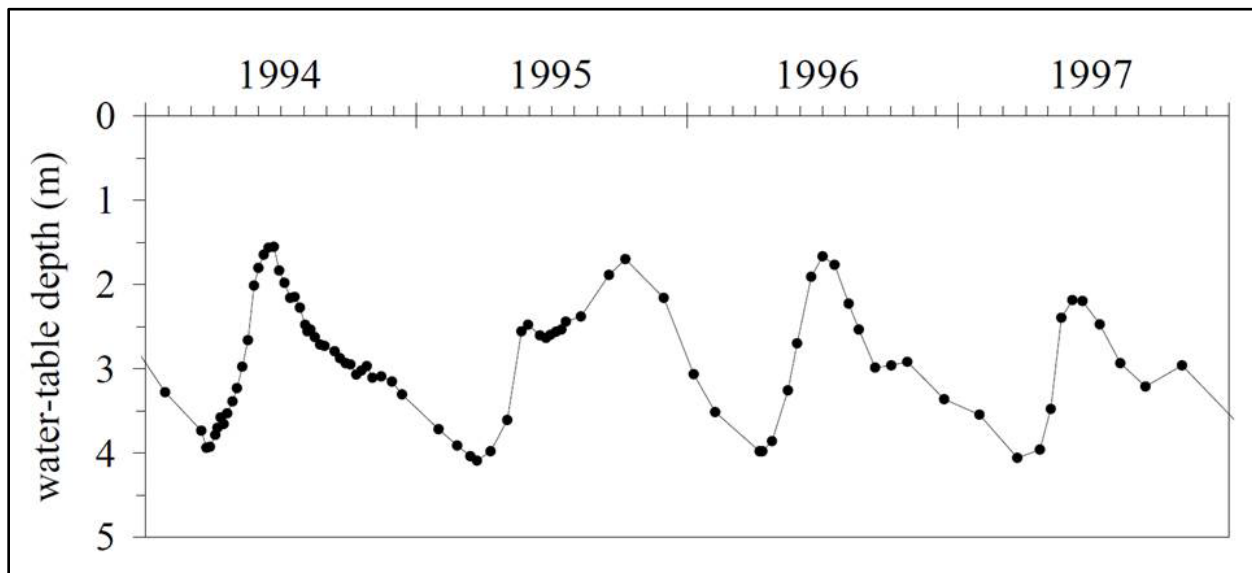


Figure Q-5. Seasonal groundwater table depth fluctuations over a 4-year period (St. Denis National Wildlife Area, SK). (after van der Kamp *et al.*, 2003).

4. Soil water regime and pipelines

Figure Q-6 shows a cross-section of a hill slope where the depth of a small-diameter pipeline characteristically conforms to the landscape configuration (i.e., installed at a relatively uniform depth of 90 - 120 cm). The depth of the groundwater table, however, varies considerably across the different landscape positions (i.e., summit, shoulder, backslope, footslope), and has given rise to the soil catenary sequence.

Figure Q-6 represents the soil water regime at a specific point in time. Figures Q-7 and Q-8, however, show an alternative way of viewing the relative positions of a pipeline and the groundwater table on a soil catenary landscape (spanning the winter season only).

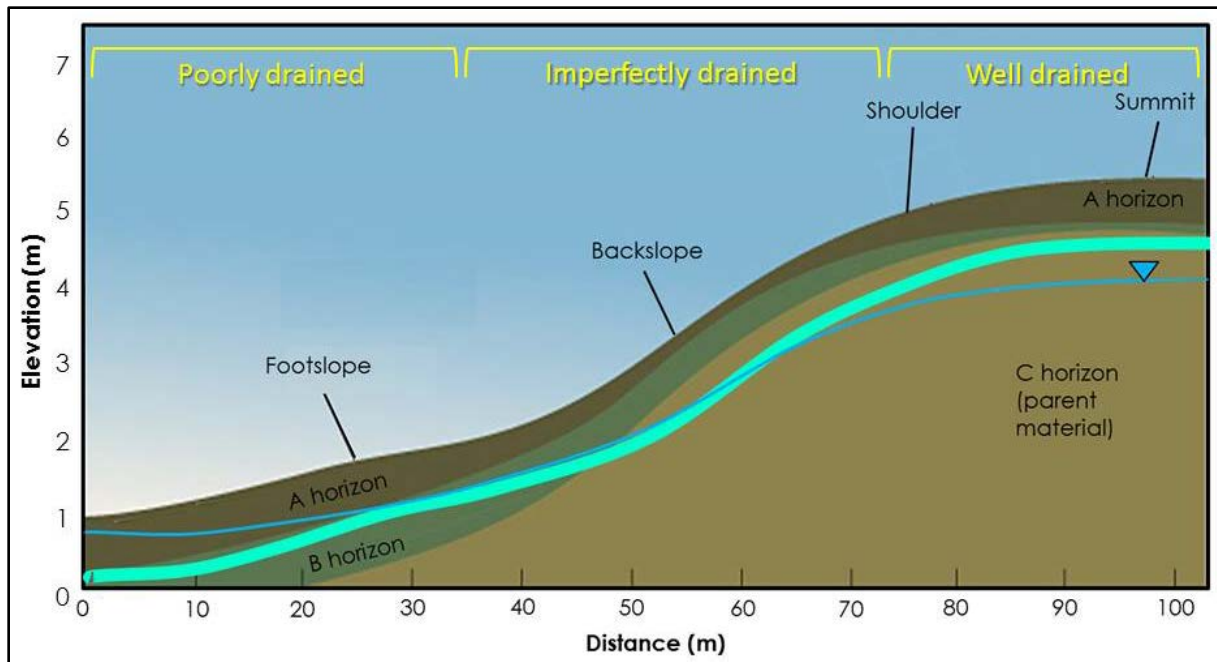

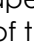


Figure Q-6. Cross-section of a landscape with moderate relief showing the soil catena sequence, and the relative positions of the groundwater table () and a small-diameter pipeline ().

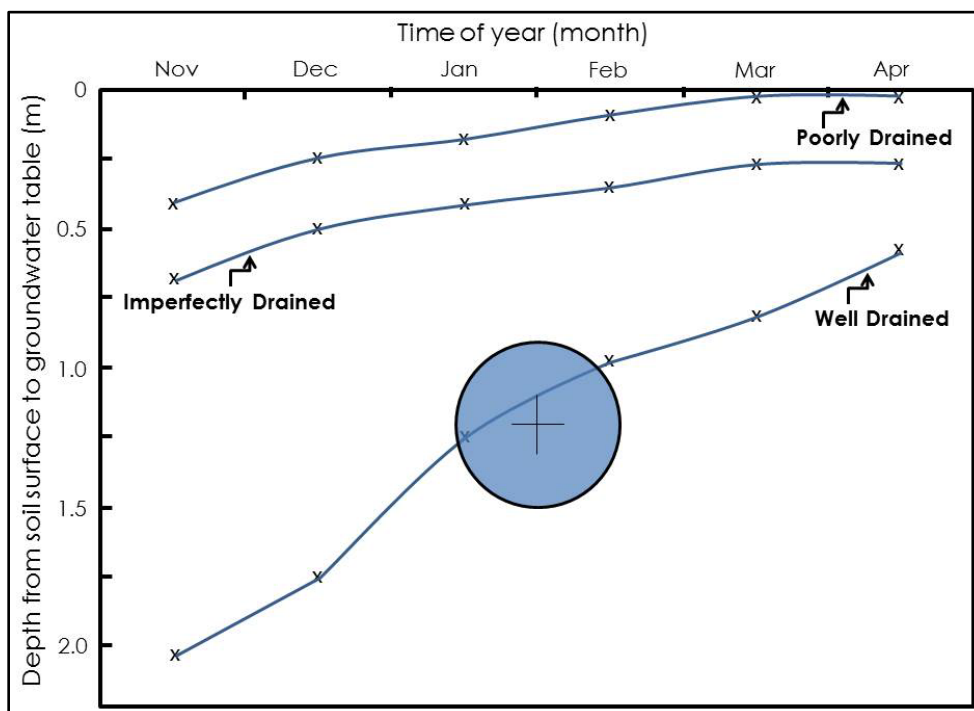


Figure Q-7. A re-draft of Fig. Q-4 showing the mean groundwater table depths by internal drainage class and by month (denoted by 'x'), and spanning the annual period of vulnerability to frost heave (after Mackintosh & van der Hulst, 1978). Also shown is a 60-cm diameter transmission pipeline installed at a depth of 90 cm below the soil surface.

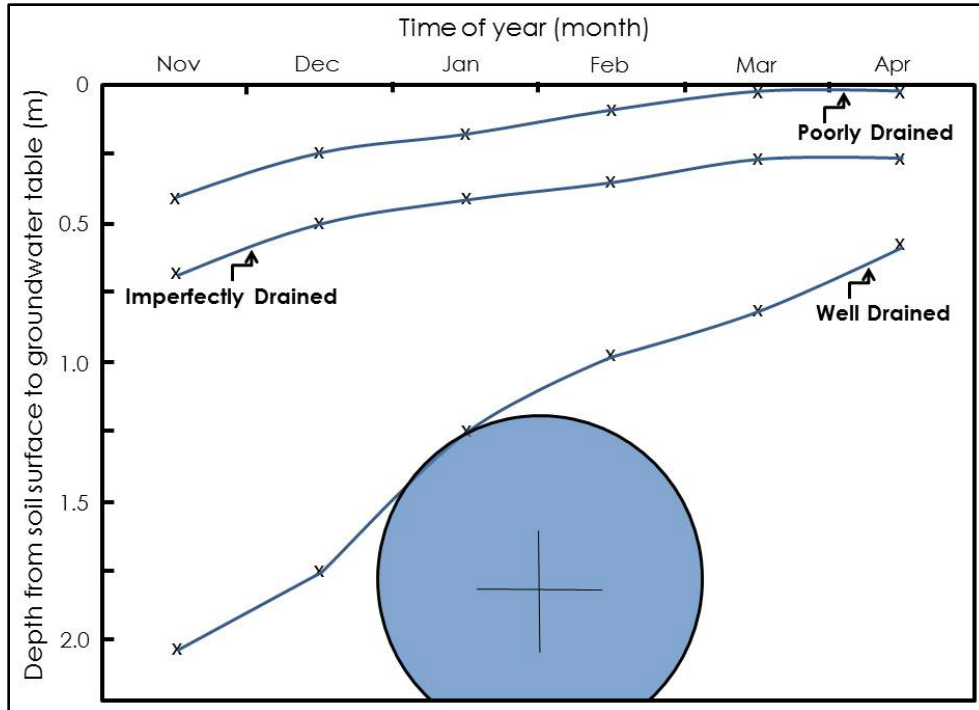


Figure Q-8. A re-draft of Fig. Q-4 showing the mean groundwater table depths by internal drainage class and by month (denoted by 'x'), and spanning the annual period of vulnerability to frost heave (after Mackintosh & van der Hulst, 1978). Also shown is a 122-cm diameter transmission pipeline installed at a depth of 120 cm below the soil surface.

Fig. Q-7: Pipeline (60-cm diam.), DOC 90 cm

Well drained site

Figure Q-7 shows that the seasonal groundwater table is positioned well below the bottom of the pipeline at the beginning of the winter season. By about January 1, the phreatic zone has risen to the base of the pipeline, and continues to rise steadily through the remainder of the winter season. The pipeline is completely enveloped by field-saturated soil by the end of February

Imperfectly or poorly drained site

Figure Q-7 shows that entire pipeline would be well below the seasonal groundwater table for the entire winter season

Fig. Q-8: Pipeline (122-cm diam.), DOC 120 cm

Well drained site

Figure Q-8 shows that the base of the pipeline has been encroached upon by the rising seasonal groundwater table by the beginning of the winter season. By mid- to late-January, the phreatic zone has risen to the top of the pipeline, and continues to rise steadily through the remainder of the winter season

Imperfectly or poorly drained site

Figure Q-8 shows that entire pipeline would be well below the seasonal groundwater table for the entire winter season

The core literature search on frost heave models in this study (Appendix C) revealed that most existing models assume that the soil is field-saturated during the winter season, including Konrad (1999). Figures Q-7 and Q-8 support this assumption in humid, temperate regions of Canada, but Fig. Q-5 suggests that unsaturated soil conditions will dominate in the Prairie Ecozone irrespective of the season.

5. Soil water regime and SLC3.2

The 'Soil Name Tables' (SNT) in SLC3.2 contain information on i) the internal soil drainage class (Table Q-1), and ii) the groundwater table characteristics, using a groundwater table that is 100 cm deep as a reference state (Table Q-2). The definitions for the internal soil drainage classes shown in Table Q-1 originated with the Canada Soil Information System (Day, 1983). Figures Q-9 and Q-10 provide a summary of the SNT information on these two soil water regime parameters (by province), and contrast the semi-arid Prairie Ecozone with the remainder of Canada (i.e., humid, temperate climatic regions).

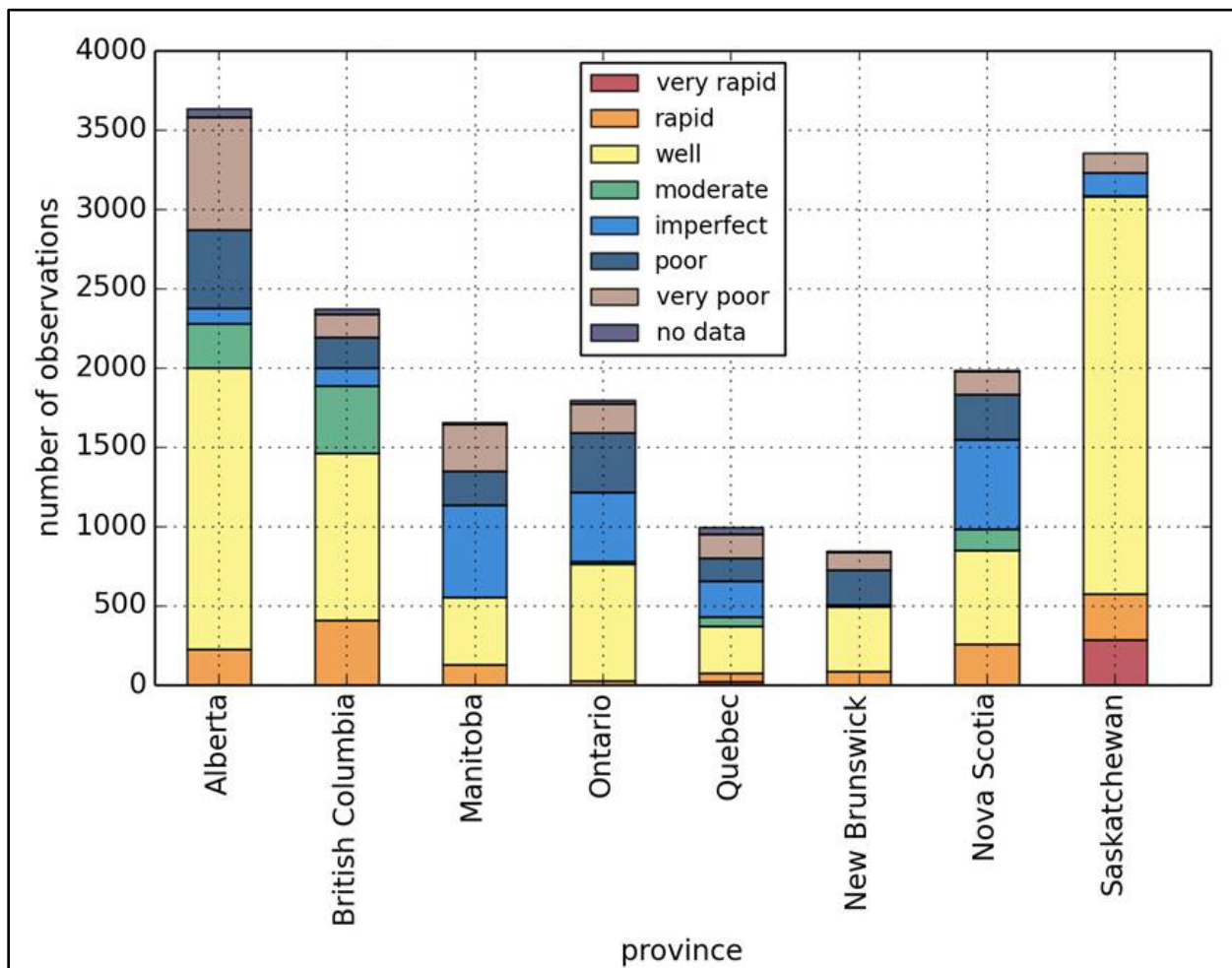


Figure Q-9. A histogram summarizing the internal soil drainage class information contained in SLC3.2 by province (see Table Q-1 for detailed legend).

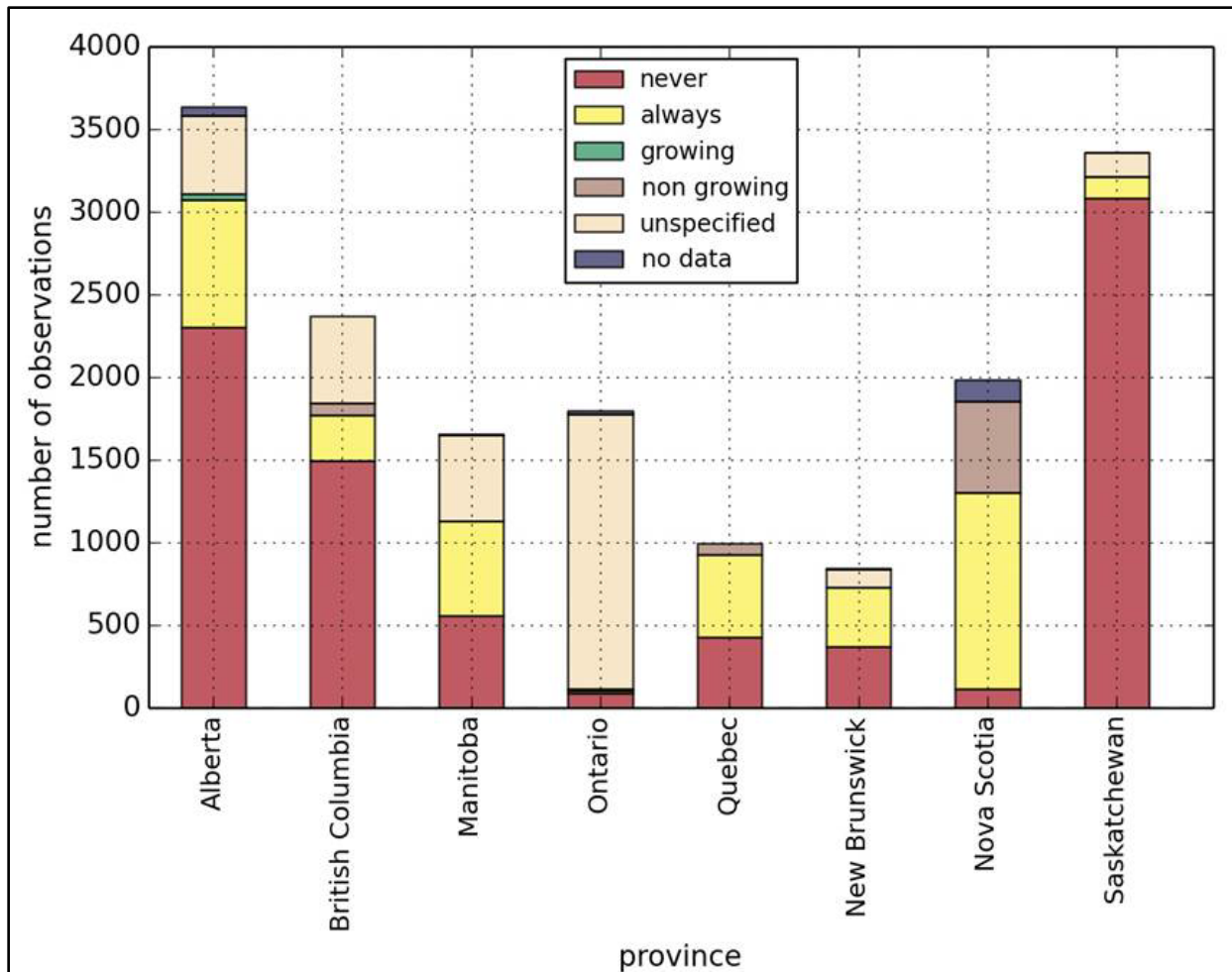


Figure Q-10. A histogram summarizing the groundwater table characteristics contained in SLC3.2 by province (see Table Q-2 for detailed legend).

The soil water regimes in semi-arid regions (e.g., AB & SK) are dominated by well drained soils with groundwater tables that are not present within 100 cm of the surface at any time during the year. Conversely, the soil water regimes in the remainder of Canada (e.g., QC & NB) show a widely distributed range of internal soil drainage classes (well, imperfect, poor) with groundwater tables that are evenly distributed between 'never' and 'always' present at a depth of 100 cm of the surface during the year. This corroborates the soil water regime information contained in Figs. Q-4 and Q-5.

Table Q-1. Internal soil drainage classes used in SLC3.2. (after AAFC, 2013b).

Code	Class	Description
VR	Very rapidly drained	Water is removed from the soil very rapidly in relation to supply. Excess water flows downward very rapidly if underlying material is pervious. There may be very rapid subsurface flow during heavy rainfall provided there is a steep gradient. Soils have very low available water storage capacity (usually less than 2.5 cm) within the control section and are usually coarse textured, or shallow, or both. Water source is precipitation.
R	Rapidly drained	Water is removed from the soil rapidly in relation to supply. Excess water flows downward if underlying material is pervious. Subsurface flow may occur on steep gradients during heavy rainfall. Soils have low available water storage capacity (2.5-4 cm) within the control section, and are usually coarse textured, or shallow, or both. Water source is precipitation.
W	Well drained	Water is removed from the soil readily but not rapidly. Excess water flows downward readily into underlying pervious material or laterally as subsurface flow. Soils have intermediate available water storage capacity (4-5 cm) within the control section, and are generally intermediate in texture and depth. Water source is precipitation. On slopes subsurface flow may occur for short durations, but additions are equaled by losses.
MW	Moderately well drained	Water is removed from the soil somewhat slowly in relation to supply. Excess water is removed somewhat slowly due to low perviousness, shallow water table, lack of gradient, or some combination of these. Soils have intermediate to high water storage capacity (5-6 cm) within the control section and are usually medium to fine textured. Precipitation is the dominant water source in medium to fine textured soils; precipitation and significant additions by subsurface flow are necessary in coarse textured soils.
I	Imperfectly drained	Water is removed from the soil sufficiently slowly in relation to supply, to keep the soil wet for a significant part of the growing season. Excess water moves slowly downward if precipitation is the major supply. If subsurface water or groundwater, or both, is the main source, the flow rate may vary but the soil remains wet for a significant part of the growing season. Precipitation is the main source if available water storage capacity is high; contribution by subsurface flow or groundwater flow, or both, increases as available water storage capacity decreases. Soils have a wide range in available water supply, texture, and depth, and are gleyed phases of well drained subgroups.
P	Poorly drained	Water is removed so slowly in relation to supply that the soil remains wet for a comparatively large part of the time the soil is not frozen. Excess water is evident in the soil for a large part of the time. Subsurface flow or groundwater flow, or both, in addition to precipitation are the main water sources; there may also be a perched water table, with precipitation exceeding evapotranspiration. Soils have a wide range in available water storage capacity, texture, and depth, and are gleyed subgroups, Gleysols, and Organic soils.
VP	Very poorly drained	Water is removed from the soil so slowly that the water table remains at or on the surface for the greater part of the time the soil is not frozen. Excess water is present in the soil for the greater part of the time. Groundwater flow and subsurface flow are the major water sources. Precipitation is less important except where there is a perched water table with precipitation exceeding evapotranspiration. Soils have a wide range in available water storage capacity, texture, and depth, and are either Gleysolic or Organic.
-	Not applicable	Drainage not applicable (rock, ice, etc)

Table Q-2. Groundwater table characteristics used in SLC3.2. (after AAFC, 2013b).

Code	Class	Description¹
YB	Always	The water table is always present in the soil.
YG	Growing season	The water table is present in the soil during the growing season.
YN	Non growing season	The water table is present in the soil during the non growing season.
YU	Unspecified period	The water table is present in the soil during an unspecified period.
NO	Never	The water table is not present in the soil at any time.
-	Not applicable	Not applicable.

¹ - indicates the presence of a groundwater table at a depth of 100 cm, and identifies its temporal characteristics.

References (Appendix Q)

Agriculture and Agri-Food Canada (AAFC). 2013a. Glossary of terms in soil science. Available at: <http://sis.agr.gc.ca/cansis/glossary/> (verified Oct. 6, 2014).

Agriculture and Agri-Food Canada (AAFC). 2013b. Soil Landscapes of Canada (version 3.2). Available at: <http://sis.agr.gc.ca/cansis/nsdb/slc/v3.2/index.html> (verified Oct. 6, 2014)

Day, J.H. (ed.). 1983. The Canada soil information system (CanSIS). Manual for describing soils in the field (1982 revised). Expert Committee on Soil Survey. Land Resource Research Institute, Contribution No. 85-52, Research Branch, Agriculture Canada, Ottawa, ON. 130 pp.

Frittont, D.D. and G.W. Olson. 1972. Depth to the apparent water table in 17 New York soils from 1963 to 1970. New York's Food and Life Sciences Bulletin, No. 13. March, 1972. 39 pp.

Hohner, B.K. and T. Present. 1985. Seasonal fluctuations of apparent water tables in selected soils in the Regional Municipalities of Niagara and Haldimand-Norfolk between 1978 and 1984. Ontario Institute of Pedology, Publication No. 85-6. July, 1985. 139 pp.

Langille, D.R. 1993. Seasonal fluctuations of water tables at selected sites in Nova Scotia. CLBRR Contribution No. 92-209 (Technical Bulletin 1993-11E). Centre for Land and Biological Resources Research, Research Branch, Agriculture Canada, Ottawa, ON. 93 pp.

Mackintosh, E.E. and J. van der Hulst. 1978. Soil drainage classes and soil water table relations in medium and coarse textured soils in southern Ontario. Can. J. Soil Sci. 58:287-301.

McBride, R.A. and E.E. Mackintosh. 1976. Soils and related environmental interpretations of the greater Saint John area, New Brunswick. Report prepared by E. Mackintosh Consultants Inc. for

the New Brunswick Department of Municipal Affairs and the Saint John Planning Commission. 197 pp.

Mozuraitis, Edward. 2013. Soil Specialist and Environmental Inspector (Pipelines), Stantec Consulting Inc., Guelph, ON. (personal communication).

Province of Alberta. 2014. Map of irrigation districts in Alberta. Available at: [http://www1.agric.gov.ab.ca/\\$department/deptdocs.nsf/all/irr12911](http://www1.agric.gov.ab.ca/$department/deptdocs.nsf/all/irr12911) (verified Oct. 6, 2014)

Province of Saskatchewan. 2014. Irrigation. Available at: <http://www.agriculture.gov.sk.ca/irrigation> (verified Oct. 6, 2014)

van der Kamp, G., M. Hayashi and D. Gallen. 2003. Comparing the hydrology of grassed and cultivated catchments in the semi-arid Canadian prairies. *Hydrological Processes* 17:559-575.

APPENDIX R
Soil Landscapes of Canada (SLC3.2)



Soil Landscapes of Canada (SLC3.2)

1. Preface

The Soil Landscapes of Canada (SLC) are a series of geographic information system (GIS) coverages that show the major characteristics of land and soil for all of Canada (Schut *et al.*, 2011). The SLC mapping was compiled at a uniform scale of 1:1M nationwide, and information is organized according to a uniform national set of soil and landscape criteria based on permanent natural attributes (AAFC, 2013a). The first SLC release was in 1991 (SLC1.0), and the most recent was in 2011 (SLC3.2). The PARSC - 003 study uses information from SLC3.2 (Fig. R-1).

The SLC mapping is based on existing (published) soil survey maps which have been recompiled at the smaller 1:1M scale. Each land area (or GIS polygon) on a SLC map is described by a standard set of attributes (Schut *et al.*, 2011). There are several thousand distinct polygons in SLC3.2, which can be seen in Fig. R-1. The full array of attributes that describe a distinct soil type and its associated landscape (e.g., surface form, slope, groundwater table depth) is called a 'soil landscape'. Individual SLC polygons may contain more than one distinct soil landscape component, and may also contain small but highly contrasting 'inclusion' components. The geographic location of these components within a specified SLC polygon is not defined (AAFC, 2013a). Example SLC3.2 map segments are shown in Fig. R-2 for southern Alberta, and in Fig. R-3 for southern Ontario.

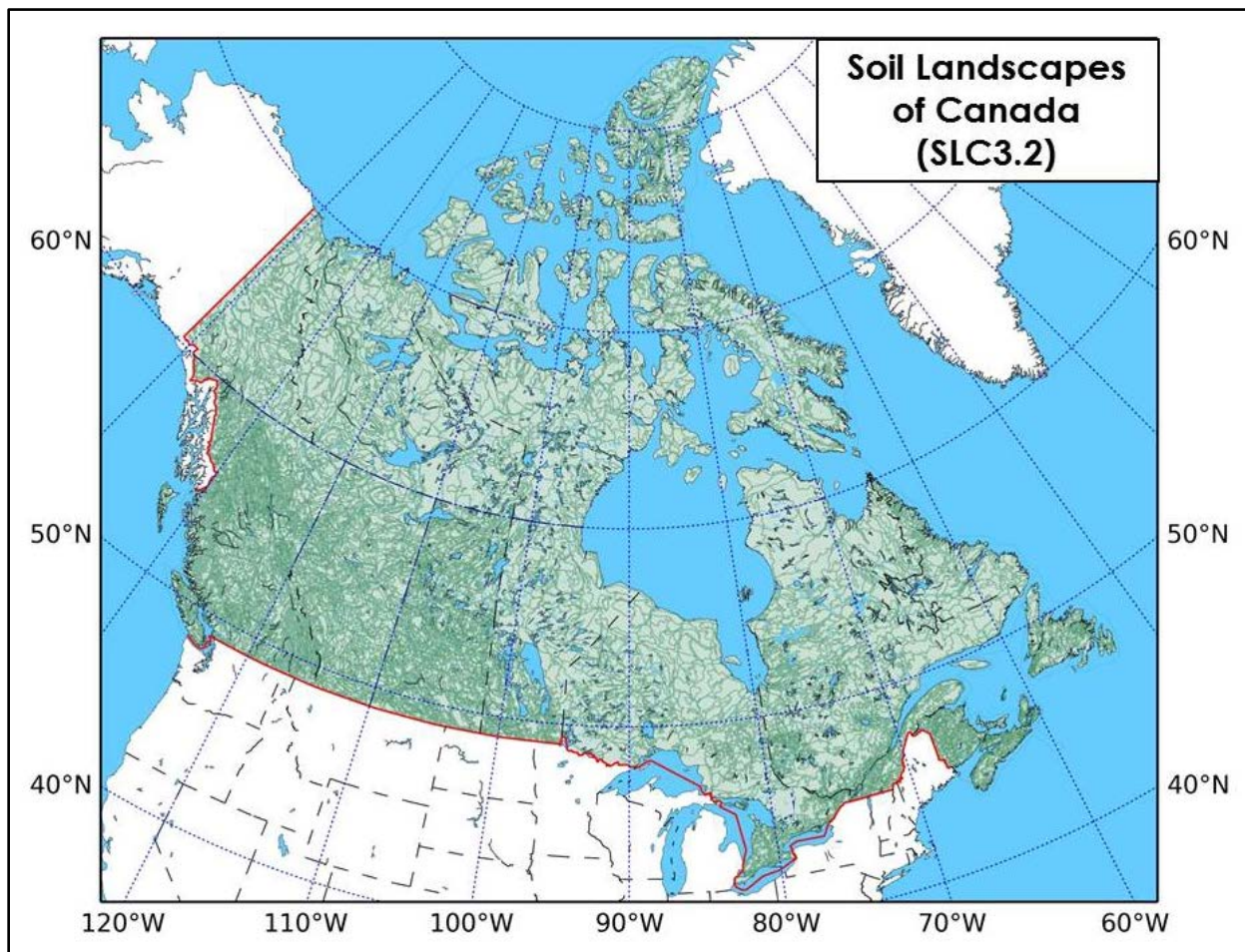


Figure R-1. The Soil Landscapes of Canada (SLC3.2) mapping, showing the network of polygons nationwide (outlined in green).

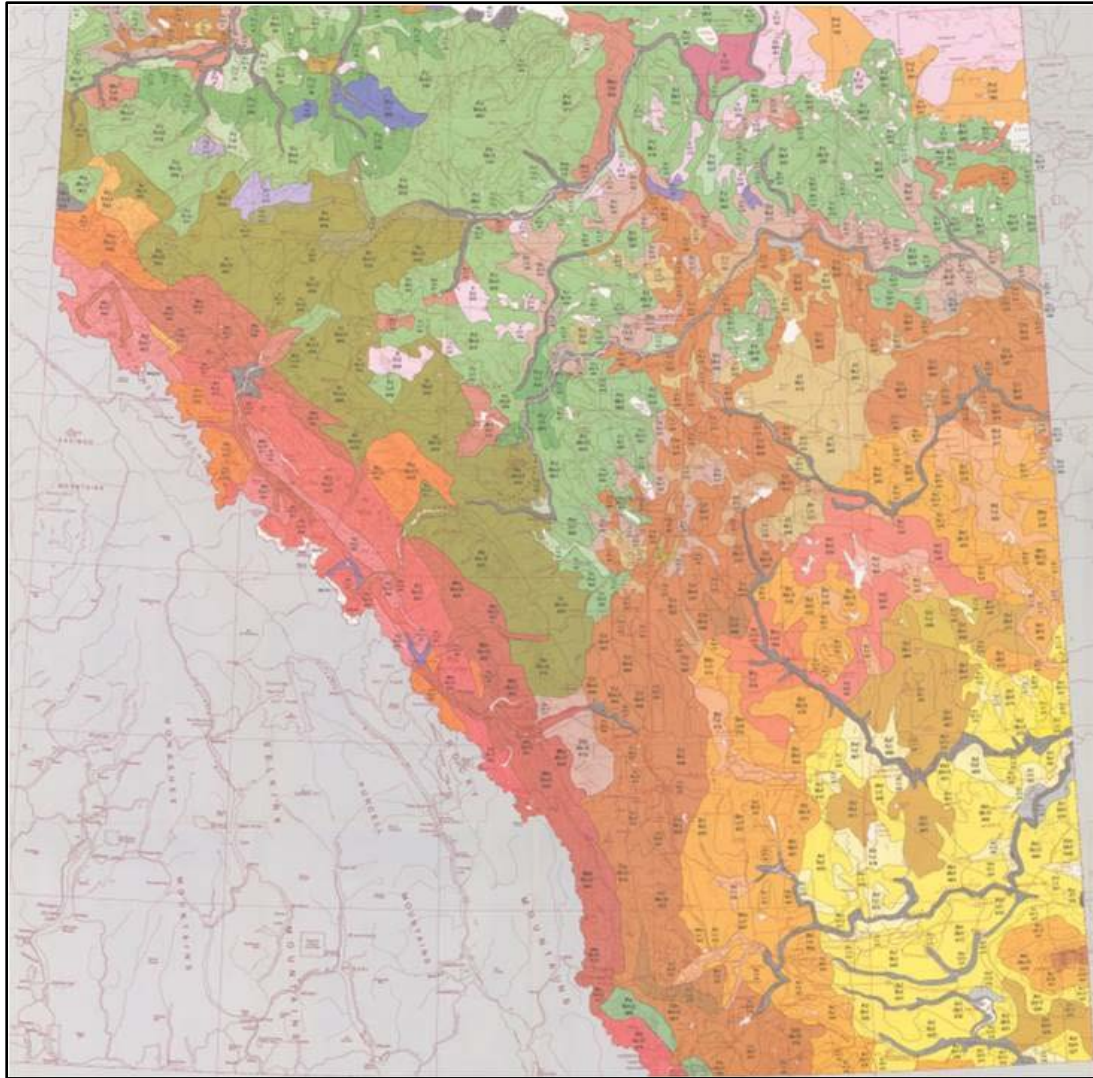


Figure R-2. SLC3.2 mapping for southern Alberta (original map scale 1:1M).
(source: AAFC, 2013a).

The SLC mapping was originally conceived as a standardized database consisting of major land/soil attributes important to plant growth, land management and soil degradation (AAFC, 2013a). It was later determined that this information represented a useful national framework to support other databases and programs (particularly within Environment Canada), such as the 'Ecological Land Classification' (ELC) framework and the 'State of the Environment' reporting program. A good example of the latter was the now-expired 'National Agri-Environmental Health Analysis and Reporting Program' (NAHARP), which reported on the environmental performance of the agricultural sector via a set of 'Agri-environmental Indicators' (AEIs) (AAFC, 2013b). The AEIs were intended to provide reliable, science-based information on the current state and changes in the conditions of the environment in agriculture at a regional or national scale in a manner that was both sensitive to regional variation in agriculture and consistent across Canada (Eilers *et al.*, 2010; Lefebvre *et al.*, 2006). The AEIs were generally calculated on the basis of SLC polygons using ancillary information from the Census of Agriculture (1981 - 2006). After the expiration of the NAHARP program, the 'Canadian Environmental Sustainability

Indicators' (CESI) program emerged to similarly track progress on key environmental sustainability issues in Canada (Env. Can., 2014).

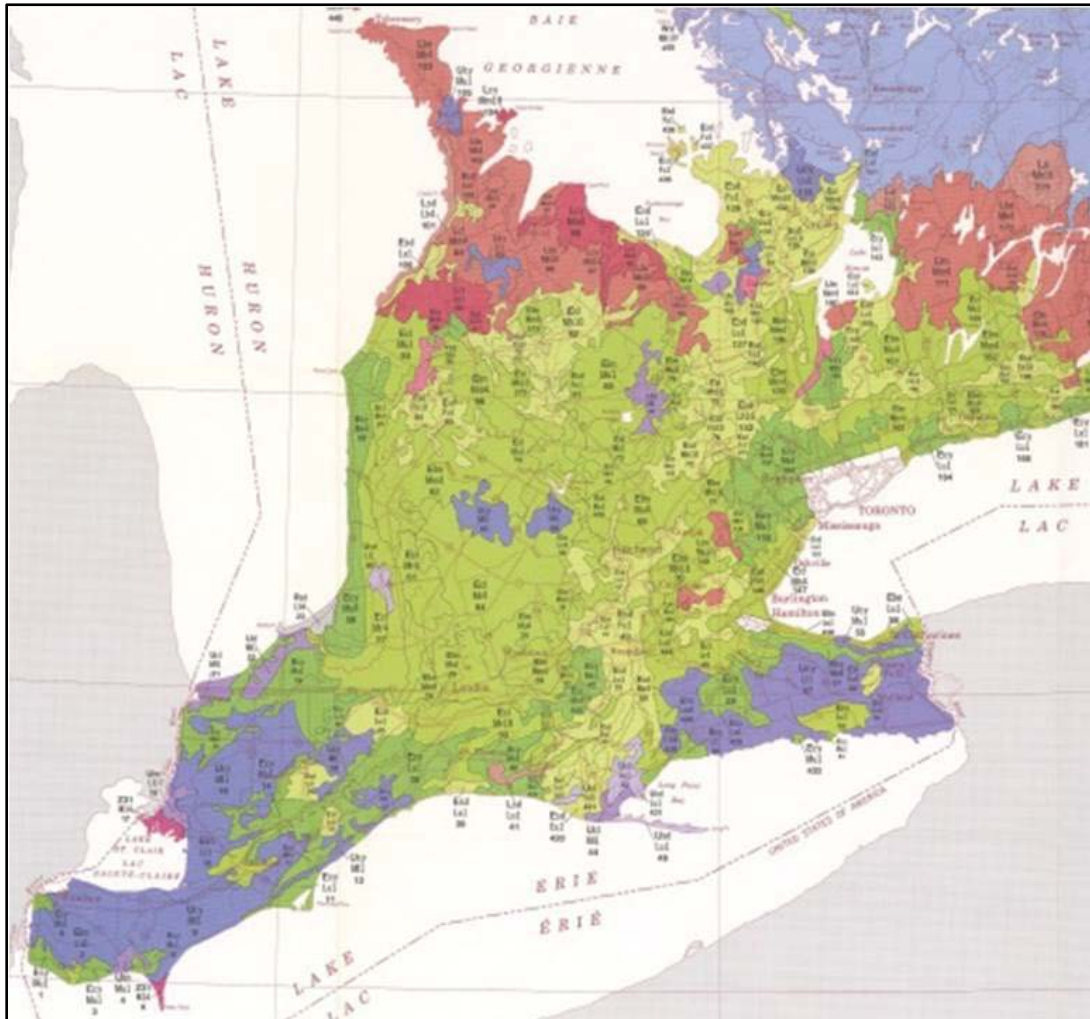


Figure R-3. SLC3.2 mapping for southern Ontario (original map scale 1:1M). (source: AAFC, 2013a).

2. Using SLC3.2 with PTFs

Pedotransfer functions (PTFs) are simple mathematical expressions (usually statistically-based) that 'translate the data that we have into the information that we need' (see Section 5.5). The land/soil 'data that we have' for the PARSC - 003 study originate directly from the SLC3.2 mapping. The land/soil 'information that we need' was generated by applying PTFs to the 'data that we have' in order to meet the input data requirements of the Konrad (1999) soil frost heave model (see Appendix A), which we have named *Konrad_SP1.0*. Figure R-4 shows the 'Entity Relationship Diagram' of SLC3.2. The two parts of this diagram that are of most direct use to the PARSC - 003 study and the operation of the Konrad (1999) model are the 'Soil Name Tables' (SNT) and the 'Soil Layer Tables' (SLT). The SNT contain soil characteristics that pertain to the entire soil profile, such as:

- groundwater table depth
- internal soil drainage class

The SLT contain soil properties that pertain to each of the soil layers (horizons) within the soil profile, such as:

- particle-size distribution
- soil organic carbon content
- dry bulk density
- saturated hydraulic conductivity

The 'Polygon Attribute Tables' (PAT) and the 'Component' (CMP) tables are also used by the Konrad (1999) frost heave model which was operationalized for the PARSC - 003 study.

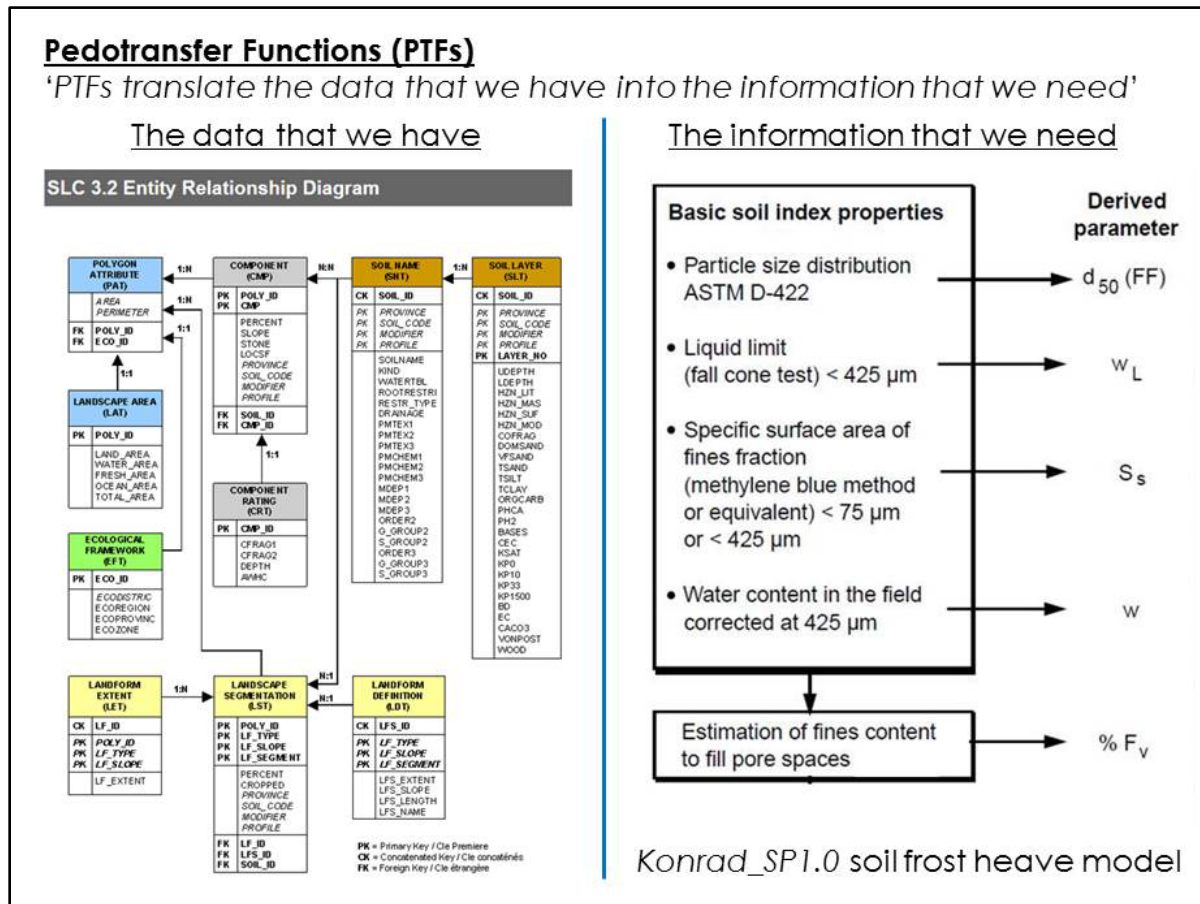


Figure R-4. The SLC3.2 'Entity Relationship Diagram' (left side), and the main input data requirements of the Konrad_SP1.0 soil frost heave model (right side). (after AAFC, 2013a; Konrad, 1999).

3. Using SLC3.2 in a GIS environment

The GIS 'shapefiles' contained in the SLC3.2 soil data base have been operationalized in the PARSC - 003 study by using the Python 3.4.1 programming language (Python Software, 2014), rather than by using proprietary GIS software (e.g., ArcGIS). This will enable the model user to identify the land/soil characteristics of an area of interest by i) specifying latitude/longitude co-ordinates, or ii) simply 'clicking' a pointing device at a geographic location on the GIS map of Canada. The Python program will identify the corresponding SLC soil map unit and provide access to the soil property database via the SNT, SLT, PAT and CMP files. This feature is illustrated in Fig. R-5, where the model user has identified a specific geographic location in Ontario by its latitude/longitude co-ordinates (45.5°N , 79.5°W), and the program denotes that location with a

black dot on the GIS map. The program also identifies the SLC3.2 polygon that encompasses these co-ordinates (shown in red), and this links the model user to the soil property data within that soil map unit. This capability is essential for the Tier 2 and Tier 3 frost heave models developed in the PARSC - 003 study.

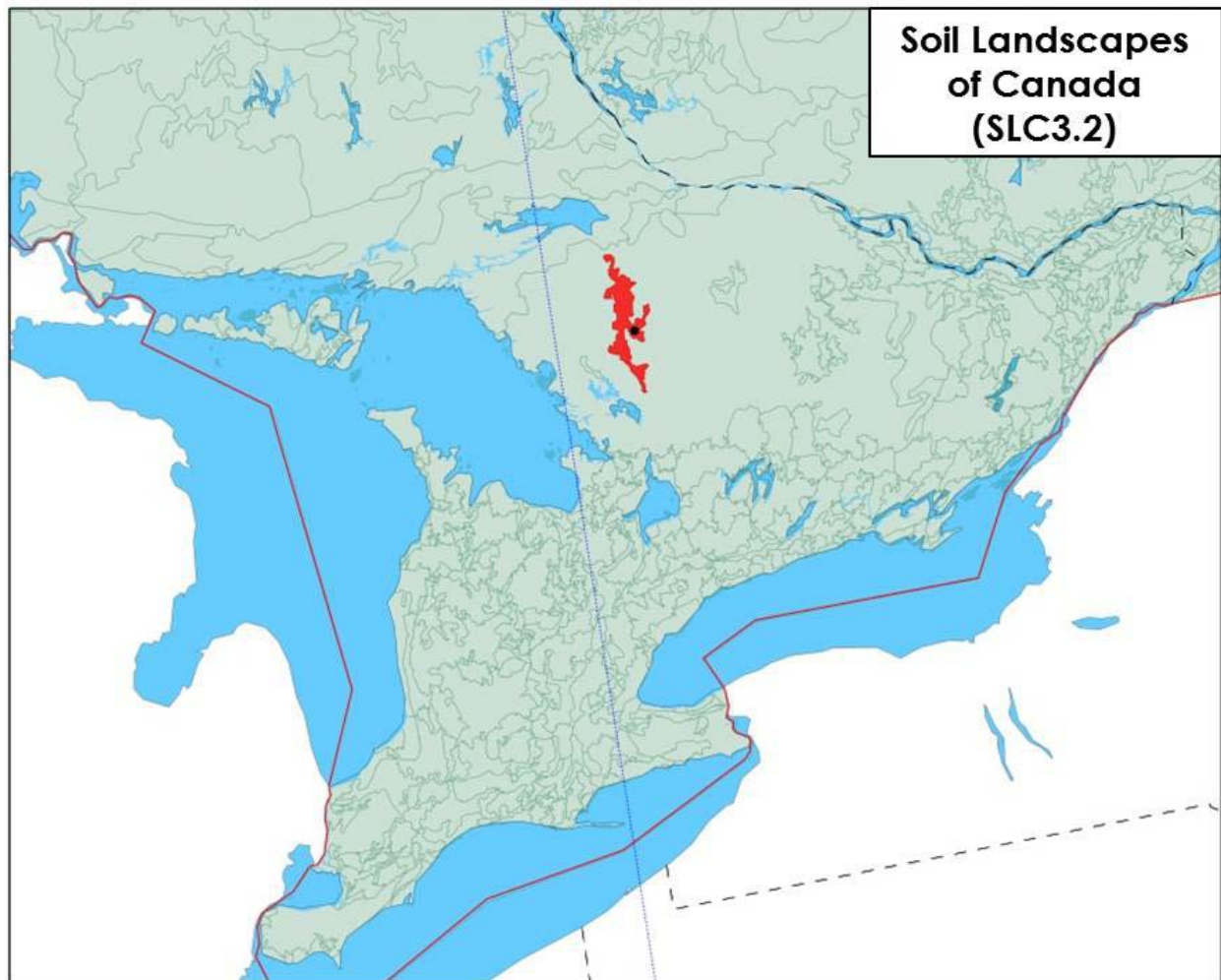


Figure R-5. A specific geographic location in Ontario (shown as a black dot) is identified by the program user by its latitude/longitude co-ordinates (45.5°N , 79.5°W). The program identifies the SLC3.2 polygon in question (shown in red), and this links the model user to the soil property data within that soil map unit.

It was necessary to partition the country into two regions where it may be necessary to apply different PTFs due to significant differences in the clay mineralogy of the soils (see Section 5.5). By identifying soil polygons where Chernozemic and Vertisolic soils are dominant (shown in red in Fig. R-6), the Prairie Ecozone was precisely delineated using SLC3.2 polygon boundaries. This step would ensure that the Konrad (1999) frost heave model would be applying the appropriate PTFs in estimating the SP parameter for any polygon in southern Canada.

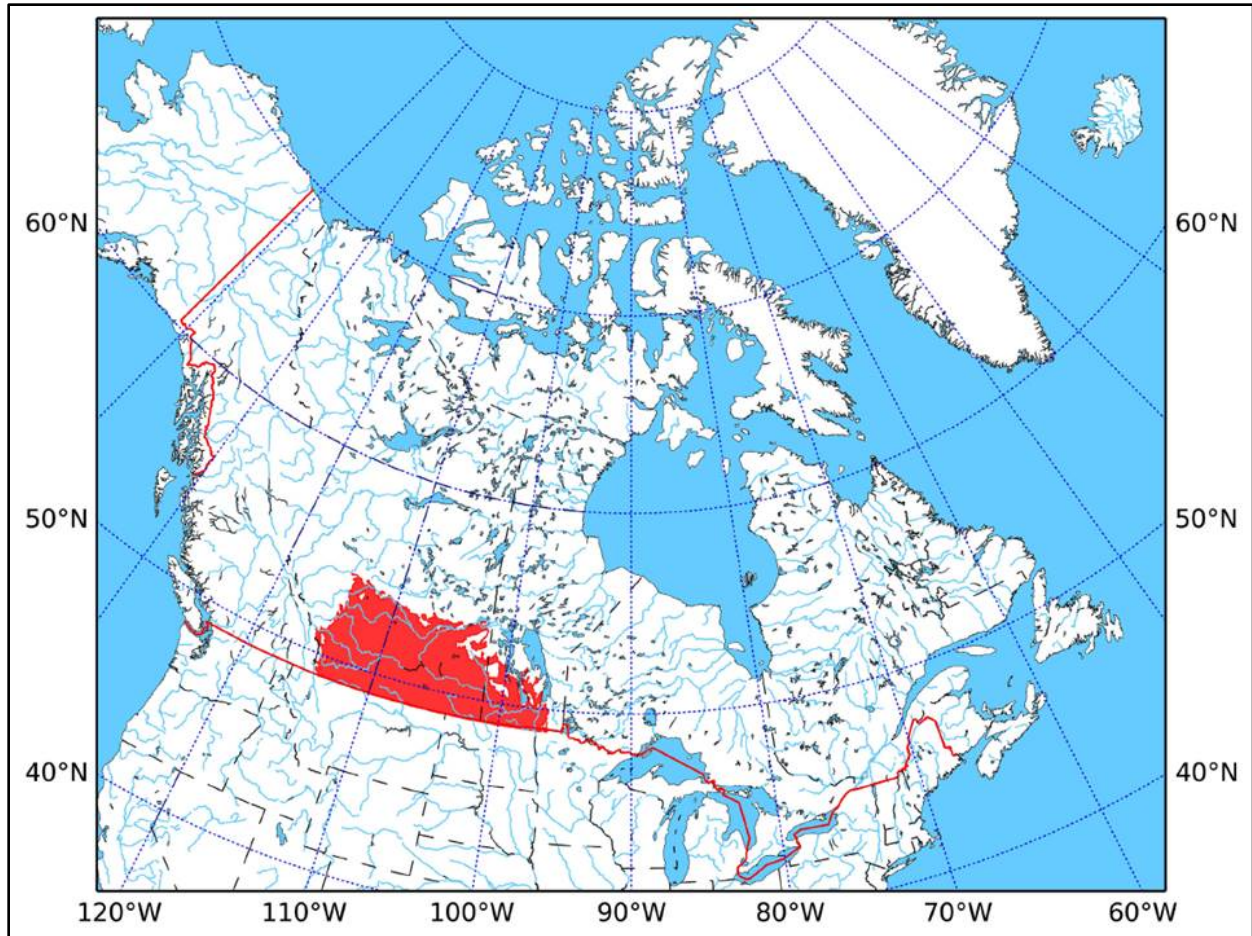


Figure R-6. The Prairie Ecozone as delineated in SLC3.2.

In the course of checking the integrity of the data contained in SLC3.2 for use in this study, it became apparent that there are some areas of Canada where the soil database is not complete. For example, three of the four Atlantic provinces (NS, PE, NL) show significant missing data for certain soil properties. To illustrate, Fig. R-7 shows a map of the Atlantic region generated within the Python program, where the SLC3.2 data for dry bulk density (D_b) in each polygon have been loosely transcribed on the map. It is clear that there are no useable D_b data in NS, PE or NL, although there are undeciphered 'codes' (0, 1, 2, or 3) in the polygons in those three provinces. Conversely, most polygons in NB have useable D_b data.

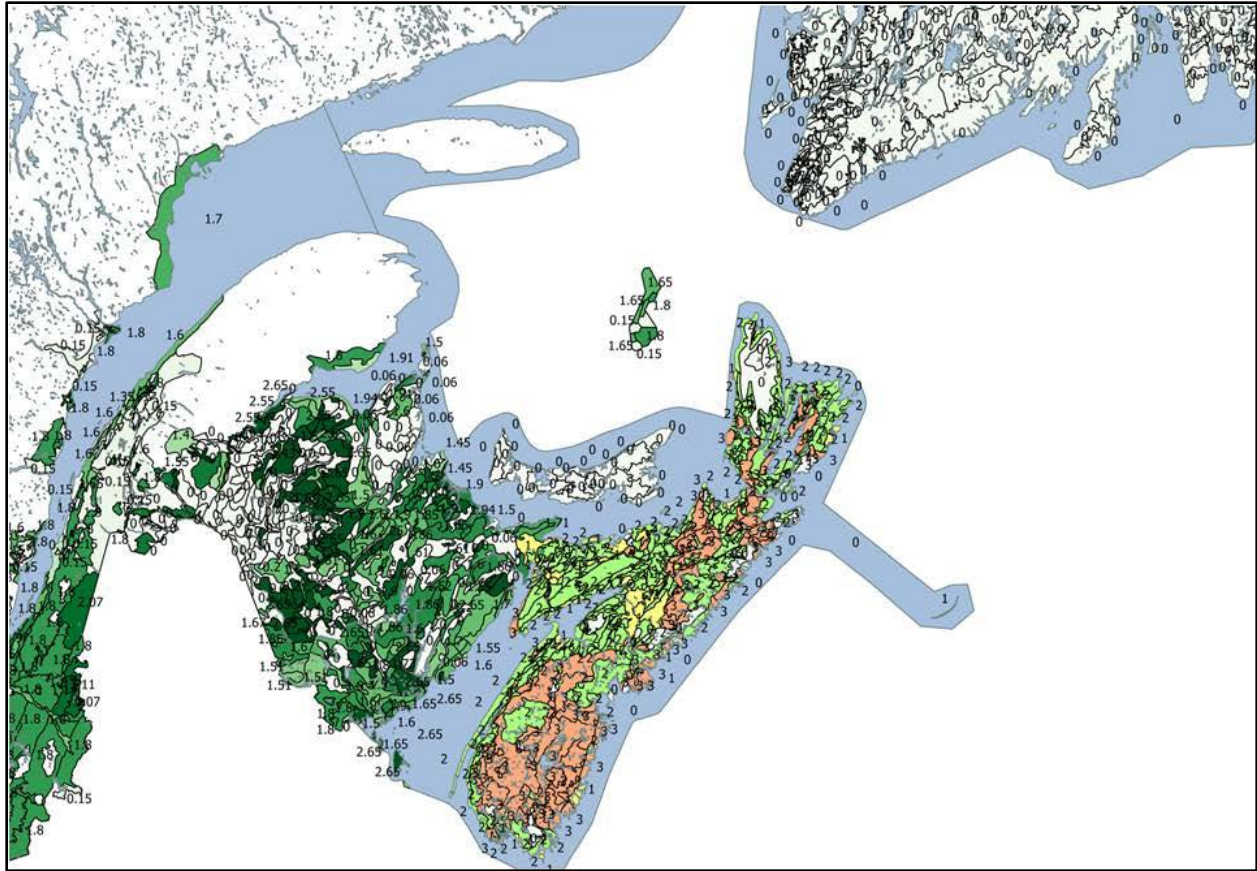


Figure R-7. A GIS map showing the distribution of *Db* data for soils in the four Atlantic provinces, as available in the SLC3.2 database. Only values other than 0, 1, 2 or 3 ('undeciphered' codes) are useable *Db* data (Mg m^{-3}), and these are found only in New Brunswick.

References (Appendix R)

Agriculture and Agri-Food Canada (AAFC). 2013a. Soil Landscapes of Canada (SLC). Available at: <http://sis.agr.gc.ca/cansis/nsdb/slc/index.html> (verified Oct. 6, 2014)

Agriculture and Agri-Food Canada (AAFC). 2013b. National Agri-environmental Health Analysis and Reporting Program (NAHARP). Available at: <http://www.agr.gc.ca/eng/?id=1295378375770> (verified Oct. 6, 2014)

Eilers, W., R. MacKay, L. Graham and A. Lefebvre (eds.). 2010. Environmental Sustainability of Canadian Agriculture: Agri-environmental Indicator Report Series - Report #3. Agriculture and Agri-Food Canada, Ottawa, ON. 249 pp. Available at: <http://www.agr.gc.ca/eng/?id=1295901472640> (verified Oct. 6, 2014)

Environment Canada. 2014. Canadian Environmental Sustainability Indicators. Available at: <http://www.ec.gc.ca/indicateurs-indicators/> (verified Oct. 6, 2014)

Konrad, J.-M. 1999. Frost susceptibility related to soil index properties. *Can. Geotech. J.* 36:403-417.

Lefebvre, A., W. Eilers and B. Chunn (eds.). 2005. Environmental Sustainability of Canadian Agriculture: Agri-environmental Indicator Report Series - Report #2. Agriculture and Agri-Food Canada, Ottawa, ON. 232 pp. Available at: <http://www.ecomatters.com/NAHARFull.pdf> (verified Oct. 6, 2014)

Python Software. 2014. Python 3.4.1 programming language. Available at: <https://www.python.org/> (verified Oct. 6, 2014)

Schut, P., S. Smith, W. Fraser and D. Xiaoyuan Geng. 2011. Soil Landscapes of Canada: building a national framework for environmental information. *Geomatica* 65(3):293-309.

APPENDIX S

Variation of Regional Geoclimatic Conditions across Southern Canada



Variation of Regional Geoclimatic Conditions across Southern Canada

1. Preface

Canada is a continental-scale country with wide variations in regional geoclimatic conditions (i.e., macro-climate, soils). The 'Terrestrial Ecozones' map of Canada (Fig. S-1) shows this variation in physiography and ecology at a nation-wide scale, and singles out the Prairie Ecozone as a particular region of interest in this study.

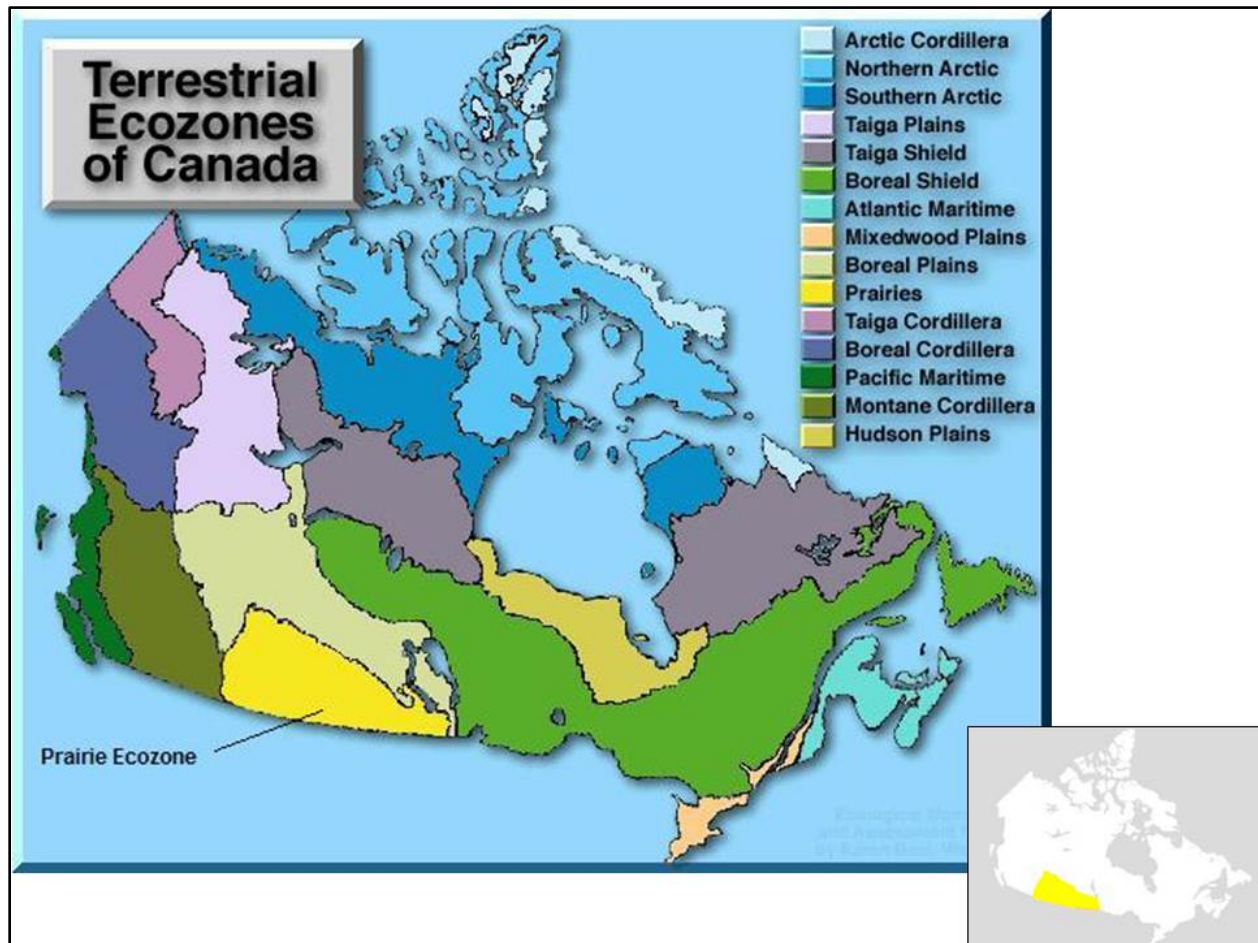


Figure S-1. A map of Terrestrial Ecozones of Canada, with the Prairie Ecozone highlighted in yellow (insert). (source: Environment Canada).

2. Macro-climate

The first geoclimatic factor to consider is macro-climate (Fig. S-2). The 'Prairie Ecozone' is characterized as a 'semi-arid' region (Fig. S-3), while the remainder of southern Canada is 'humid, temperate' and/or 'humid, continental' and/or 'humid, maritime'. The key climatic descriptor in these regions is 'humid', which implies that there is ample and well distributed precipitation, and modest evapotranspirational deficits during the growing season (May - September).

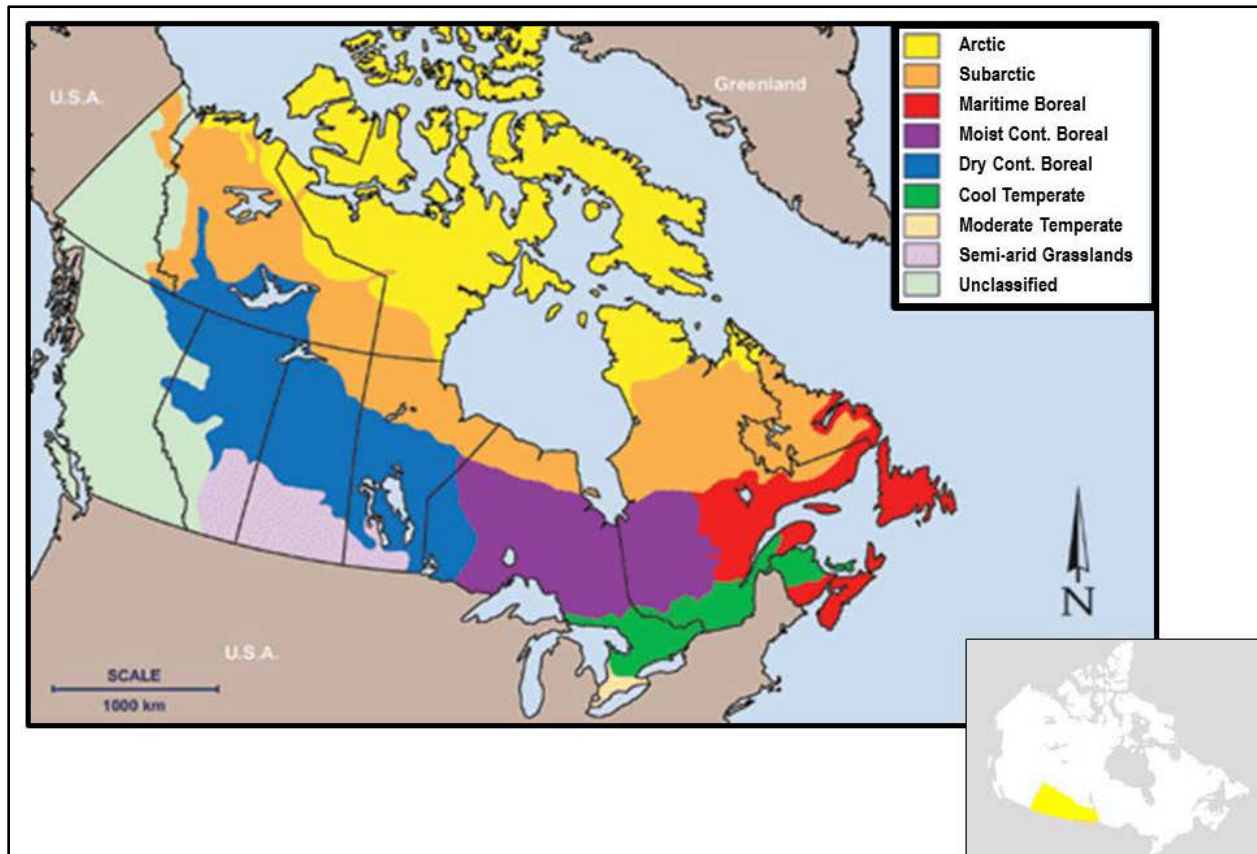


Figure S-2. A map of Ecoclimate Zones of Canada, with the Prairie Ecozone highlighted in yellow (insert). (source: Environment Canada).

This distinction between the Prairie Ecozone macro-climate and that of remainder of southern Canada has significant implications for the 'soil water regime' across the country, and therefore the frost heave risk. Figure S-4 shows two contrasting sets of measured groundwater table depth data (see Appendix Q). The upper graph is from southern Saskatchewan (van der Kamp *et al.*, 2003), and is representative of the seasonal soil water regime in the 'semi-arid' Prairie Ecozone. This graph shows groundwater tables fluctuating seasonally between about 1.5 m and 4 m below the surface. The lower graph is from southern Ontario (Mackintosh & van der Hulst, 1978), and is representative of the seasonal soil water regime in the 'humid, temperate /continental/ maritime' macro-climatic regions of southern Canada. This graph shows groundwater tables fluctuating seasonally between 0 m and about 2 m below the surface, depending on the internal soil drainage class of the soil.

To illustrate the implications on frost heave risk for abandoned transmission pipelines, Figure S-4 also shows pipelines superimposed on the graphs. The example used here is a 60-cm diameter pipeline positioned with the top of the pipe at 1 m below the surface. It is the soil's ability to supply water to growing ice lenses around a pipeline that largely determines the risk of frost heave (Groenevelt & Grant, 2013). For the southern Saskatchewan case, the pipeline would clearly be positioned above the groundwater table virtually year-round (including the winter season), so it is the 'unsaturated soil hydraulic conductivity' (K_{unsat}) that will drive the frost heave process around the pipeline in this instance. For the southern Ontario case, the pipeline would clearly be (all or in part) positioned below the groundwater table during the winter season (even

for the well-drained case), so it is the 'saturated soil hydraulic conductivity' (K_{sat}) that will drive the frost heave process around the pipeline in this instance.

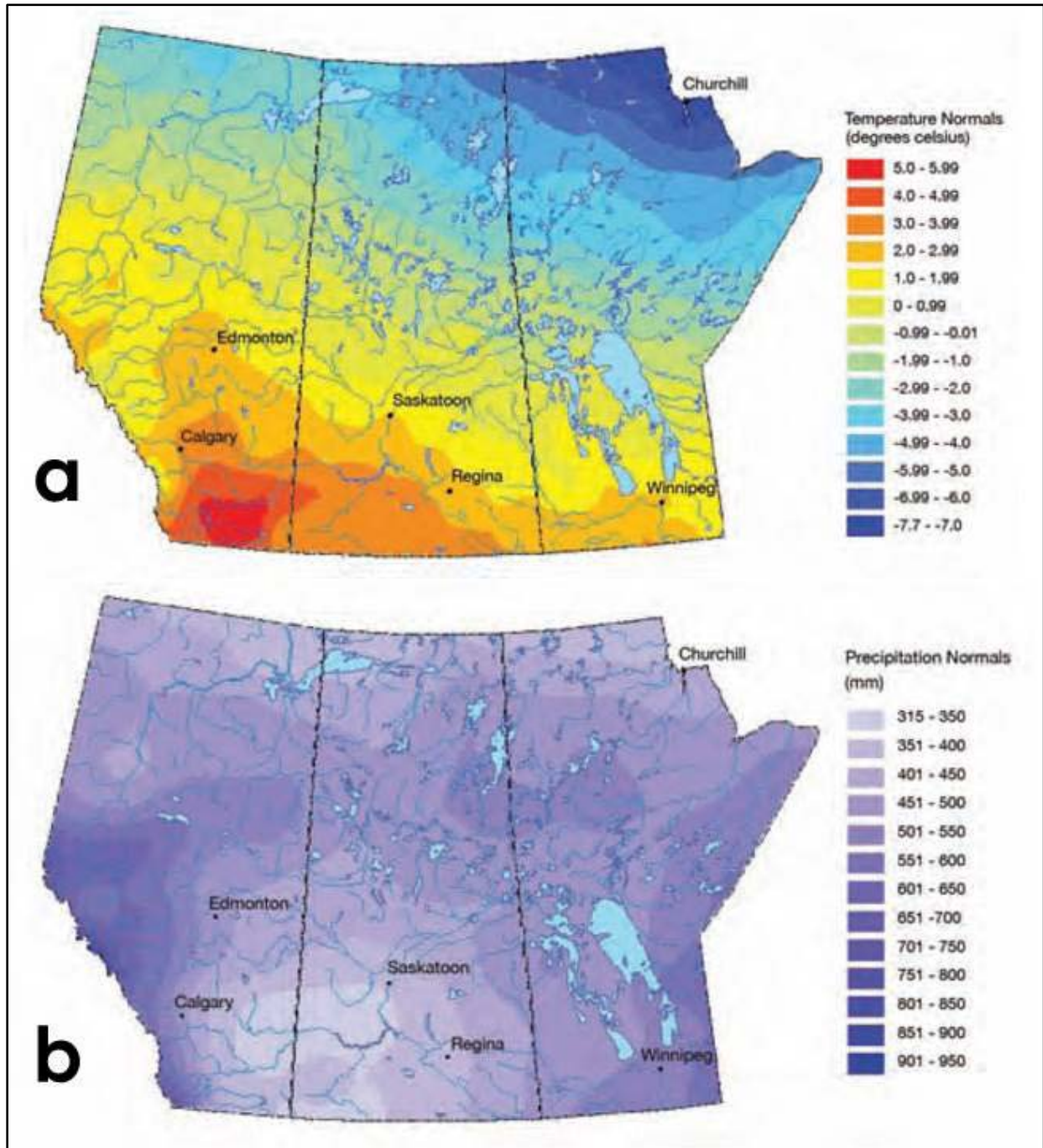


Figure S-3. Long-term climatic normals (1961-1990) for the three Prairie provinces, where a) is mean annual air temperature ($^{\circ}\text{C}$), and b) is total annual precipitation (mm). (after Sauchyn & Kulshreshtha, 2008).

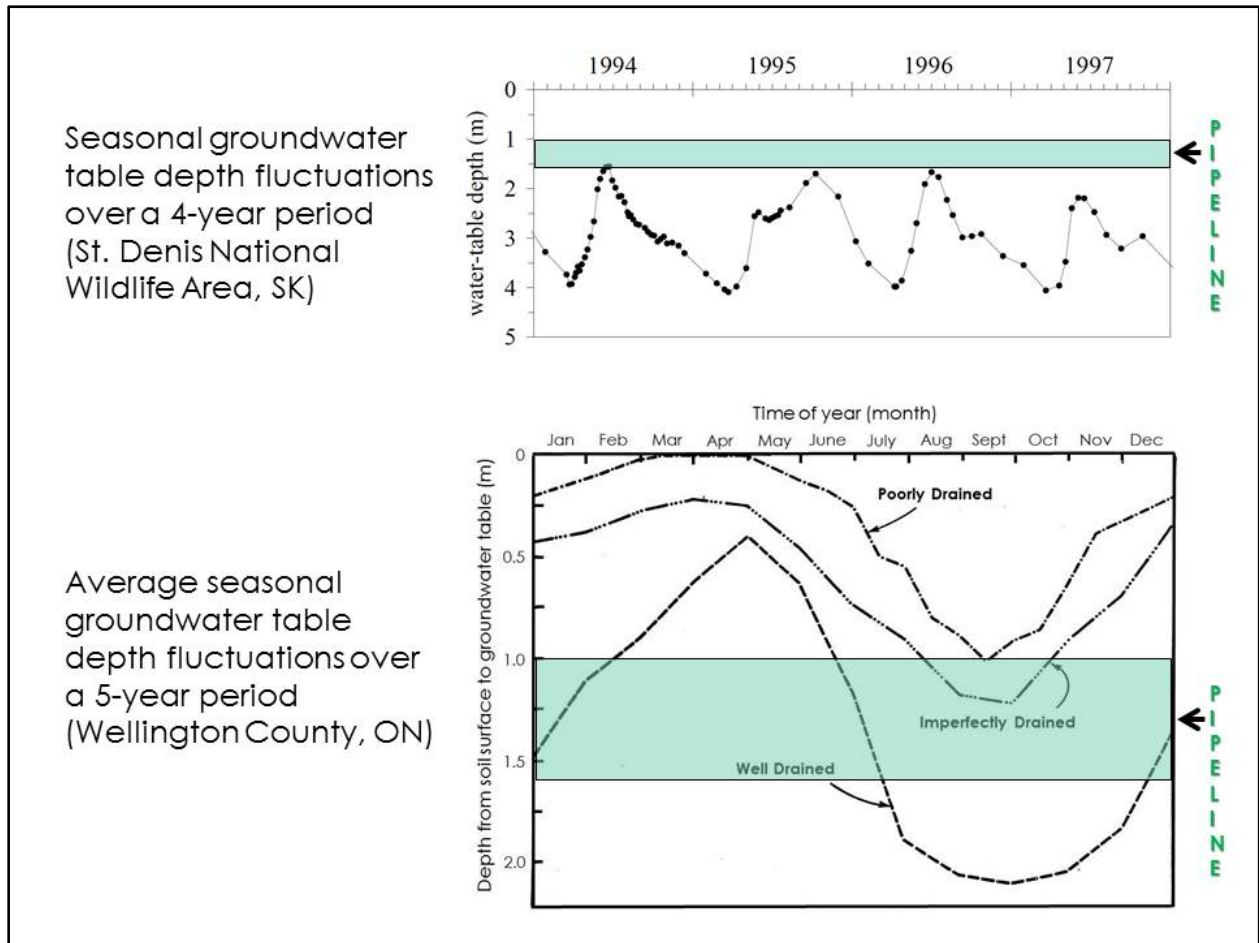


Figure S-4. Two contrasting sets of measured groundwater table depth data, with transmission pipelines superimposed (shown in green).

3. Soils

The second geoclimatic factor to consider is soils. Many soil physical and engineering properties are sensitive to the nature of the clay minerals present. In Canada, soil clay fractions with a significant component of expanding clay minerals (i.e., smectites) are found largely in the Prairie Ecozone, whereas soils characterized by non-expanding clay minerals (i.e., clay mica [illite], chlorite) are found in the remainder of the country (Kodama, 1979).

Figure S-5 shows the distribution of soil orders across the Canadian prairie provinces, including the Prairie Ecozone. The Prairie Ecozone is characterized by soils that exhibit varying degrees of shrink-swell behaviour. This behaviour can be extreme in clay-rich soils, and is caused by the presence of clay minerals that expand in the presence of free water. Some of the chernozemic and salt-affected soils shown in Fig. S-5 will shrink and swell, but it is the vertisolic soils where this behaviour can be extreme (Anderson, 2010). Figure S-6 shows photos of the Sceptre soil association in southern Saskatchewan, which is a Vertisol. It exhibits many of the classic shrink-swell features of Vertisols seen in other parts of the world (e.g. patterned ground, deep cracking, self-mulching, and slickensides).

Soils with vertic properties (i.e., shrink-swell behaviour) are found in the Red River Valley of Manitoba, the Regina Plains, the Eston and Rosetown plains of southwestern Saskatchewan, and the Drumheller Plain northeast of Calgary (Anderson, 2010).

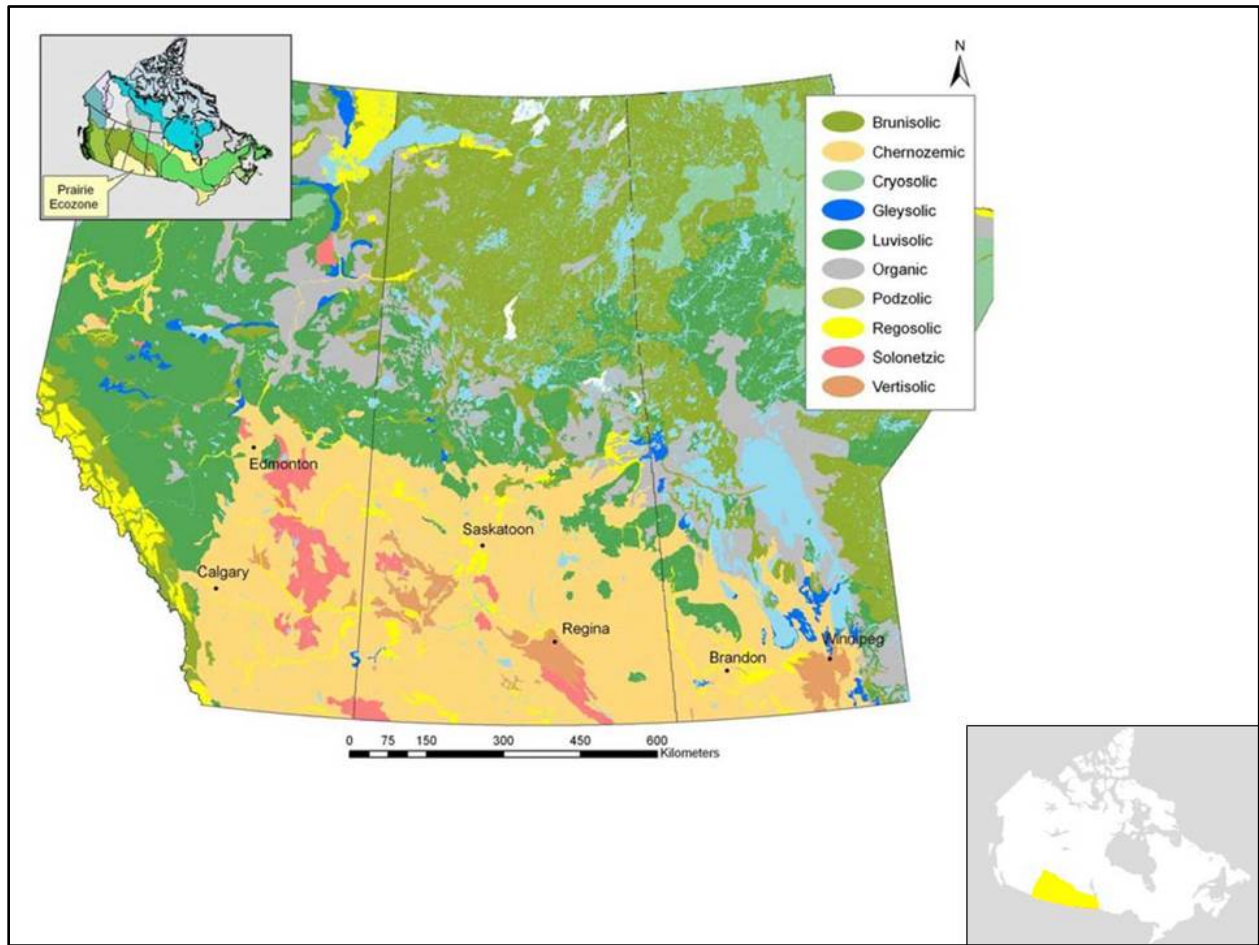


Figure S-5. Soil order map of the prairie provinces, showing the major areas of Chernozemic and Vertisolic soils, as per the Soil Landscapes of Canada (SLC3.2) mapping. The Prairie Ecozone is highlighted in yellow (insert). (after Anderson, 2010).

Vertisol (Sceptre Soil Association, Saskatchewan)



Vertic Properties of the Sceptre Soil Association (Saskatchewan)



Patterned Ground



Deep Cracking, Self-mulching



Slickensides

Figure S-6. Photos of the vertisolic Sceptre soil association in southern Saskatchewan. (after Anderson, 2010).

References (Appendix S)

Anderson, D. 2010. Vertisolic soils of the prairie region. *Prairie Soils and Crops Journal* 3(5):29-36. Available at: <http://www.prairiesoilsandcrops.ca/articles/volume-3-5-screen.pdf> (verified Oct. 6, 2014).

Groenevelt, P.H. and C.D. Grant. 2013. Heave and heaving pressure in freezing soils: A unifying theory. *Vadose Zone J.* 12(1). 11 pp.

Kodama, H. 1979. Clay minerals in Canadian soils: their origin, distribution and alteration. *Can. J. Soil Sci.* 59:37-58.

Mackintosh, E.E. and J. van der Hulst. 1978. Soil drainage classes and soil water table relations in medium and coarse textured soils in southern Ontario. *Can. J. Soil Sci.* 58:287-301.

Sauchyn, D. and S. Kulshreshtha. 2008. Prairies. p. 275-328. In D.S. Lemmen, F.J. Warren, J. Lacroix and E. Bush (eds.) *From Impacts to Adaptation: Canada in a Changing Climate 2007*. Government of Canada, Ottawa, ON.

van der Kamp, G., M. Hayashi and D. Gallen. 2003. Comparing the hydrology of grassed and cultivated catchments in the semi-arid Canadian prairies. *Hydrological Processes* 17:559-575.

APPENDIX T

Pipeline Segments Abandoned-in-Place (Variable Diameter & Length)

Pipeline Segments Abandoned-in-Place (Variable Diameter & Length)

1. Preface

Pipelines may be segmented during abandonment, with portions left in place as short or long pipe segments (DNV, 2010; Swanson *et al.*, 2010). At the inception of this study, PARSC requested that the pipe segment length and diameter issue be given some consideration vis-à-vis frost heave risk. No length specifications were provided by PARSC for 'short' and 'long' pipe segments, but two pipe diameter (o.d.) ranges of interest were specified as follows:

- 'medium' pipe diameter (305 - 610 mm [12 "- 24"] o.d.)
- 'large' pipe diameter (>610 mm [>24"] o.d.)

2. Case study of pipeline abandonment-in-place in Alberta (Swanson *et al.*, 2010)

Figure T-1 shows segments of an abandoned 1925 natural gas pipeline being excavated and removed during 2006-07 in southern Alberta (i.e., pipe diameter = 273 cm [10.75"] o.d.). About 1/3 of the 33-km long pipeline was removed over a period of a few years, and the remainder was abandoned-in-place as segments of varying length (Swanson *et al.*, 2010). A more complete overview of this case study can be found in Section 7 (Volume 1).

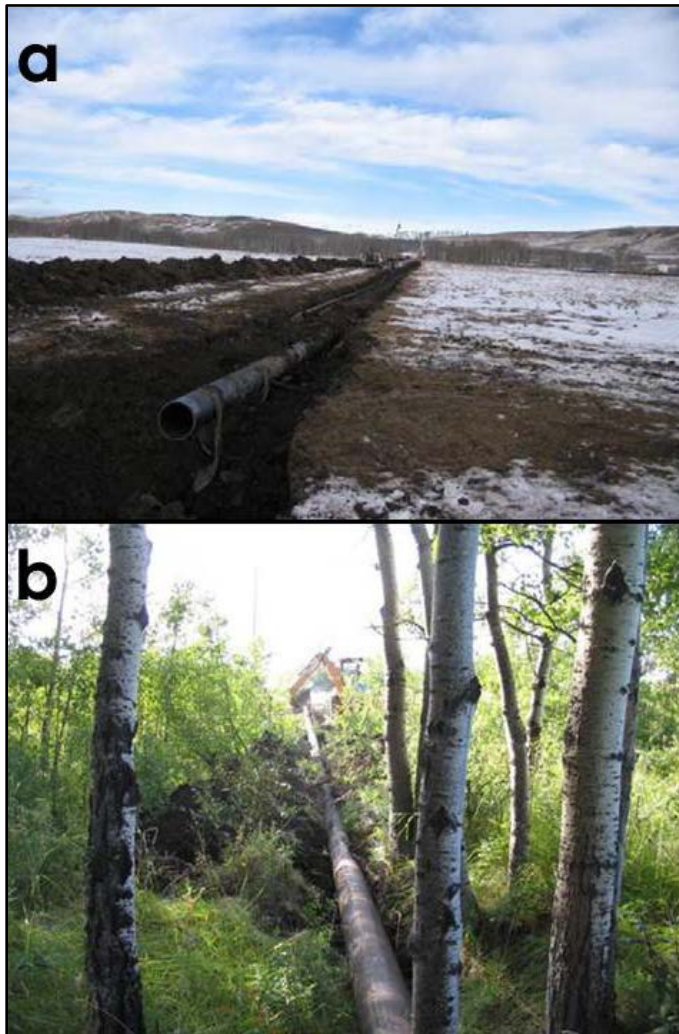
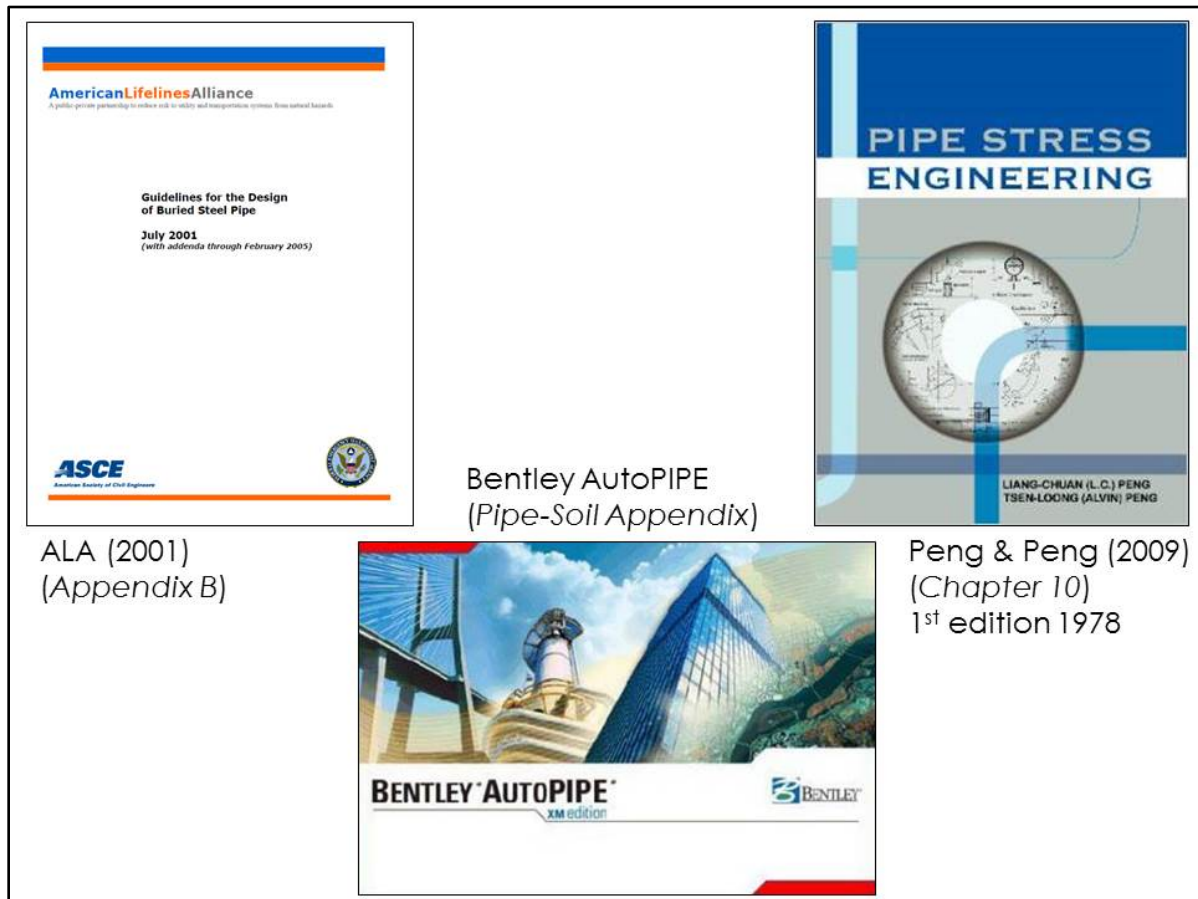


Figure T-1. Removal of segments of an abandoned 1925 natural gas pipeline from a) an open field in 2006, and b) a woodlot area in 2007, south of Calgary, AB. (after Swanson *et al.*, 2010).

3. Determination of soil restraint properties for buried pipelines

Pipeline design engineers need reliable information on pipe-soil interaction in order to predict the behaviour of onshore pipelines that are buried in soil (Tian, 2011). The most widely recognized and applied method for calculating pipe-soil interactions is the ALA method (ALA, 2001), but the Bentley AutoPIPE method (Bentley Systems, Inc., 2013) and the Peng method (Peng & Peng, 2009) are also used by pipeline design engineers (Fig. T-2). The ALA and AutoPIPE methods are generally thought to be the most reliable of the three options because they are based on laboratory and field experimentation, whereas the Peng method is based mostly on theoretical soil mechanics principles (Tian, 2011). The Caesar II pipe stress analysis software (Intergraph Corp., 2014) uses elements of the Peng and the ALA methods in its basic and advanced soil modeling sub-routines, respectively (Tian, 2011).



ALA (2001)
(Appendix B)

Bentley AutoPIPE
(Pipe-Soil Appendix)

Peng & Peng (2009)
(Chapter 10)
1st edition 1978

Figure T-2. The three most established and widely used methods for assessing pipe-soil interactions. (after Tian, 2011).

Soil restraint properties provide information on the relationship between soil resistance and movement of an onshore pipeline. A range of soil and pipe properties (e.g., soil shear strength parameters, pipe diameter, depth of soil cover) can be input into any of the three computational methods (Fig. T-2) to define the 'elastic-plastic soil springs' in the longitudinal, transverse, vertical upward and vertical downward directions around a buried pipeline (Fig. T-3a). Plots can be generated (Fig. T-3b) for each of these four directions such that a 'soil stiffness' parameter (i.e., slope $[K_1]$) and an 'ultimate soil resistance' parameter (P_1) can be determined (Tian, 2011).

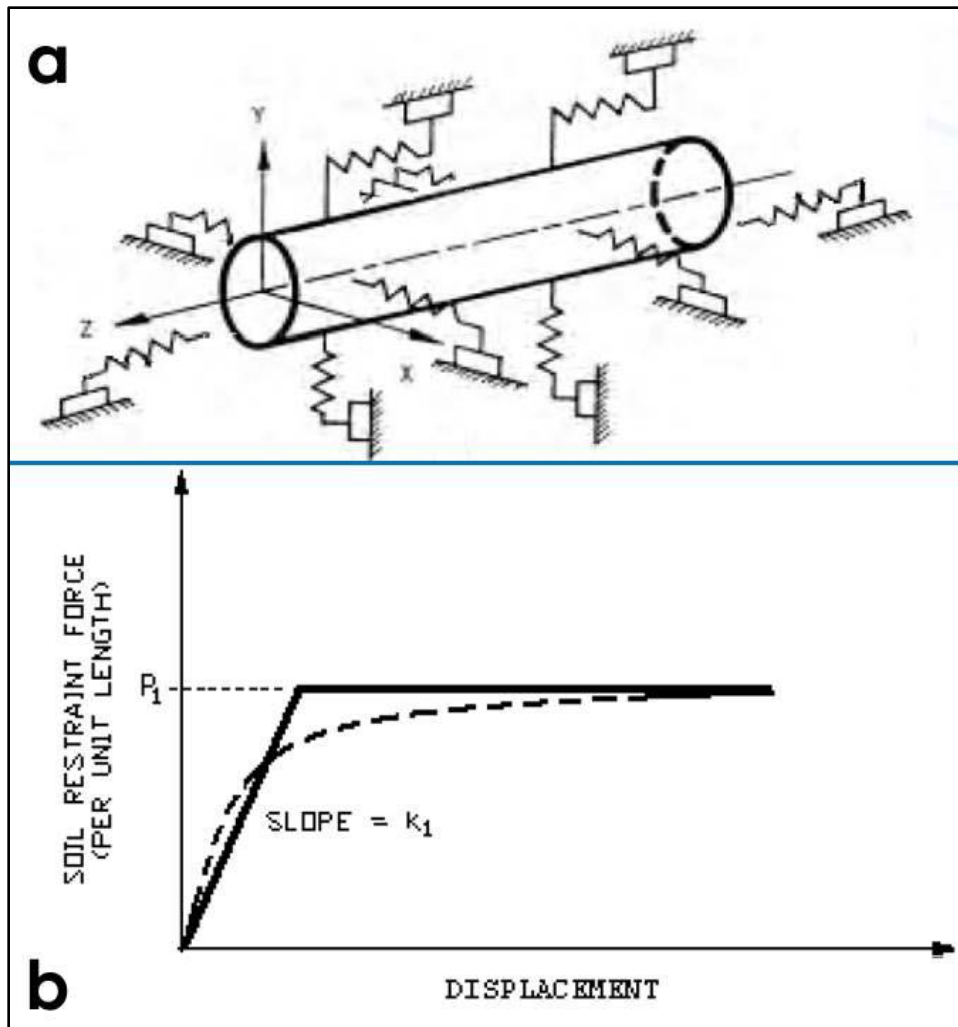


Figure T-3. Illustration of a) the 'elastic-plastic soil springs' concept around a buried pipeline, and b) a generalized plot of soil restraint force (per unit length) vs. pipe displacement, where the actual and idealized relationships are represented by a broken line and a solid line, respectively. (after Tian, 2011).

Tian (2011) carried out example calculations for a 'soft clay' soils in order to contrast the performance of the three computational methods (Fig. T-2). Only the results for the vertically upward direction will be discussed here since frost heave is the main focus of this study. For example, it is known that frost heave can impose loads on operating pipelines or on pipe segments abandoned-in-place that can cause deformations well into the plasticity range of the pipe material (Mohareb *et al.*, 2001). It is also known that 'differential' frost heave is a very spatially and temporally variable thermodynamic process, and particularly so at pipeline road crossings during the operating lifespan of a pipeline (Ferris, 2009). Little is known about differential frost heave risk after pipeline abandonment.

Figure T-4 shows typical values for the three engineering soil properties required to generate plots similar to Fig. T-3b. Tian (2011) used the 'soft clay' material for the example calculations since it represents the worst design case of the six soil types shown (i.e., low shear strength). Soft clay has low dry unit weight, low undrained cohesion and low angle of shearing resistance (Fig. T-4).

Figure T-5 shows the computed results for the vertical upward resistance case, which will reflect the resistance of the pipe to upward jacking by the frost heave process. It was assumed that the pipe diameter was 1000 mm o.d., and the depth of soil cover was 120 cm (Tian, 2011). It is evident that the three computational methods produced very different results. The ALA method (ALA, 2001) was by far the most conservative of the three methods for this particular case, producing an 'ultimate soil resistance' (P_1) of about 25 kN m⁻¹ (circled in red in Fig. T-5). The Bentley AutoPIPE method (Bentley Systems, Inc., 2013) and the Peng method (Peng & Peng, 2009) were as much as 2- to 3-fold higher.

Soil Type	Soft Clay	Normal Clay	Stiff Clay	Loose Sand	Medium Sand	Dense Sand
Dry Unit Weight (kg/m ³)	1600	1800	2000	1600	1800	2000
Undrained Shear Strength (kPa)	5	25	100	0	0	0
Internal Friction Angle (°)	0	0	0	25	30	40

Figure T-4. Typical engineering soil properties for each of six broad categories of unconsolidated material. (after Tian, 2011).

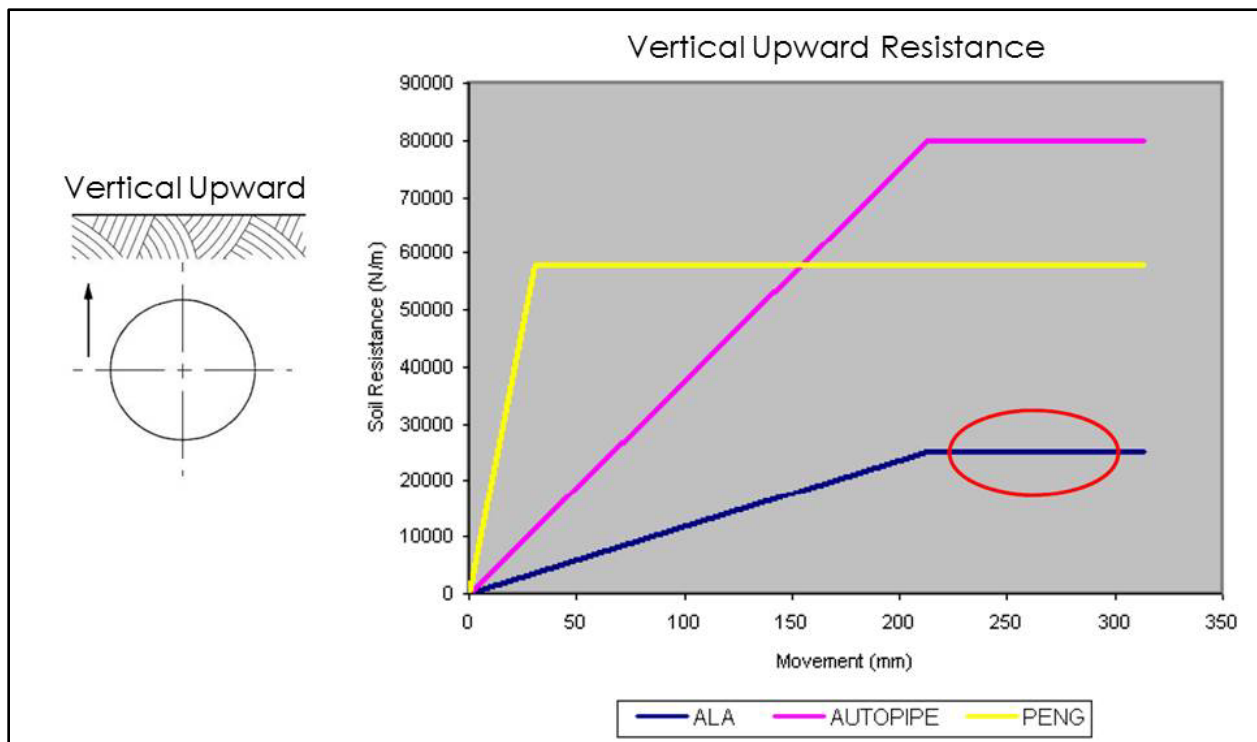


Figure T-5. Plot of soil restraint force (per unit length) vs. pipe displacement for a soft clay using the three established computational methods. (after Tian, 2011).

4. Calculation of virtual anchor lengths for buried pipelines

Pipeline design engineers estimate the 'virtual anchor length' (L_a) in order to determine the risk of a pipe section moving relative to the soil near a directional change (e.g., a bend or a tee) or a 'physical anchor' (e.g., an A/G-U/G transition, natural gas compressor station) in an operating pipeline. Hence, the L_a variable can be regarded as the distance from a bend (Fig. T-6), a tee or an A/G-U/G transition to the point where pipe axial strain is completely suppressed by the soil (Tian, 2011). In the context of pipeline segments abandoned-in-place, however, the L_a variable can be thought of as a buried length of pipe that is sufficiently long so that the axial friction along its length prevents any load or displacement at one end from translating to the other end.

An equation used to estimate L_a is shown as Eqn. T-1 in Figure T-6, and involves the following variables:

- Elastic factor
- Stress - thermal expansion
- Stress - pressure elongation
- Longitudinal soil resistance
- Cross-sectional area of the buried pipe (A)
- Hoop stress (or circumferential stress) (S_{HP})

Clearly, the L_a parameter is sensitive to pipe diameter via the 'A' parameter (Eqn. T-1). This should enable the two pipe diameter ranges of interest to PARSC ('medium' and 'large' [see Section 1 above]) to be accounted for in L_a parameter estimations with Eqn. T-1.

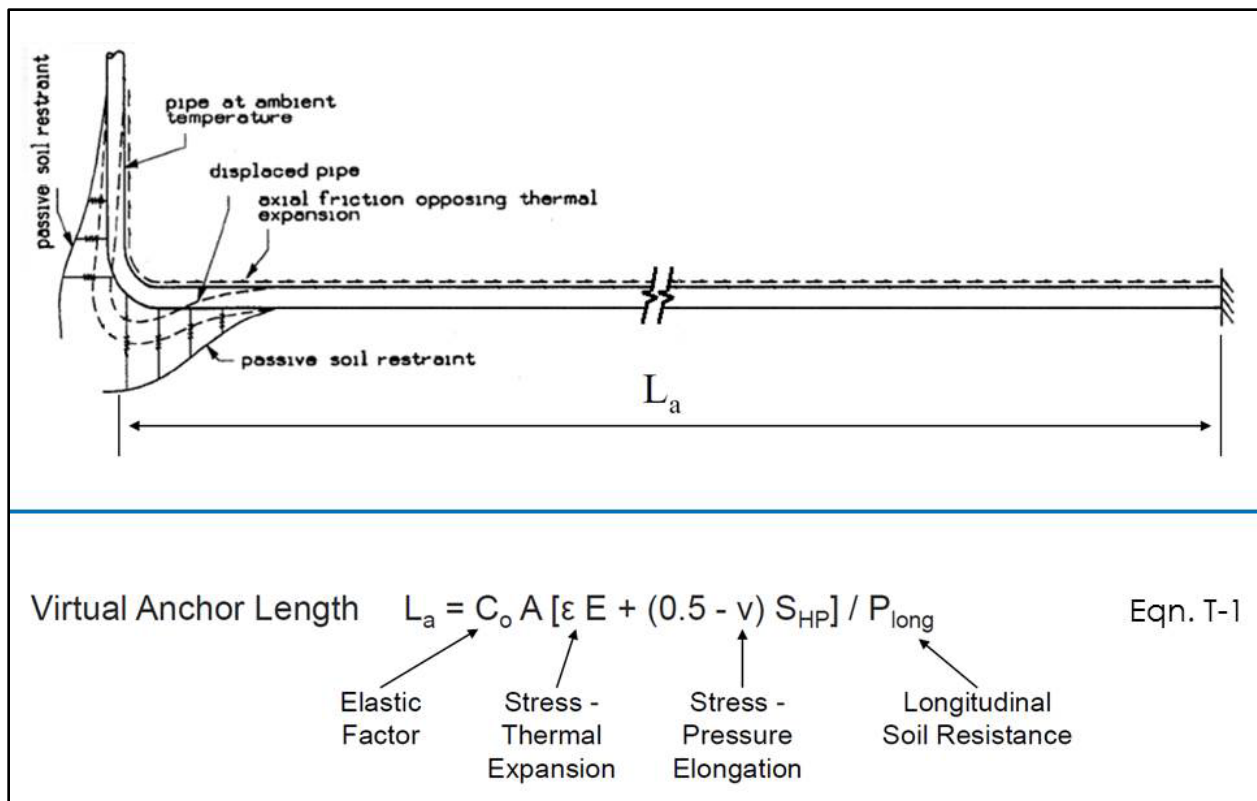


Figure T-6. Estimation of the virtual anchor length (L_a) for a buried onshore pipeline. (after Tian, 2001).

Using all six of the soil types shown in Fig. T-4, Tian (2011) estimated the L_a parameter using the three established computational methods (Fig. T-2). For this trial, it was assumed that the pipe diameter was 1000 mm o.d., the depth of soil cover was 120 cm, the design temperature was 55°C and the design pressure was 10.2 MPaG (Tian, 2011). Figure T-7 shows that the influence of soil type on L_a is very significant, with the 'soft clay' and 'loose sand' soil types (i.e., low strength, low dry unit weight) exhibiting much higher L_a values (range of ~400 m to ~1 km) than the other four soil types. Conversely, the 'stiff clay' soil type (i.e., high strength, high dry unit weight) showed consistently low L_a values of 50 m or less. However, it is also clear that there is a wide disparity in the handling of the soft clay/loose sand soil types by the three established computational methods. Figure T-7 shows a very wide variation in the estimates of the L_a parameter for those two soil types, based on the particular set of pipe-soil input parameters noted above.

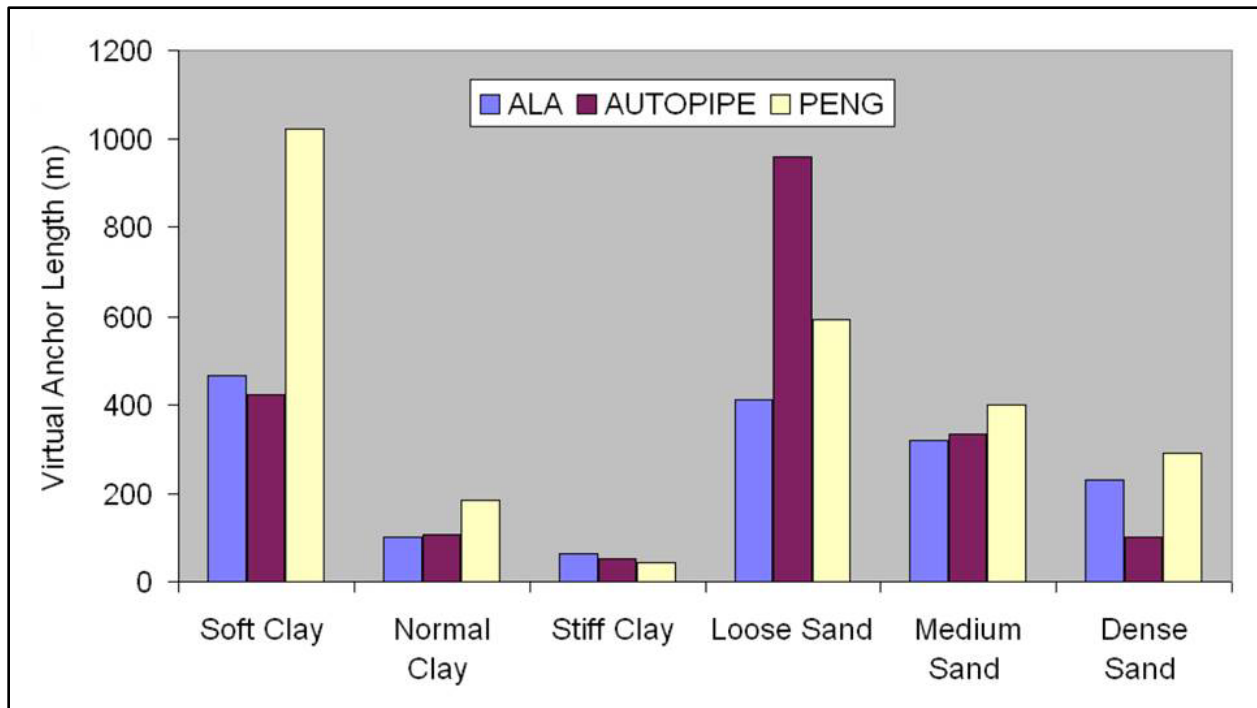


Figure T-7. Histogram of estimated virtual anchor lengths under different soil conditions, and using the three established computational methods. (after Tian, 2011).

5. Summary (Appendix T)

PARSC requested that the pipe segment length and diameter issue be given some consideration in the PARSC - 003 study of frost heave risk to pipelines abandoned-in-place. The information contained in this appendix suggests that the 'virtual anchor length' (L_a) concept may be useful in guiding recommendations on minimum lengths of abandoned pipe segments in order to improve long-term positional stability and diminish the risk of frost heave. Further, the L_a parameter is sensitive to pipe diameter, so minimum length recommendations could vary for 'medium' and 'large' diameters. Unfortunately, the three established computational methods do show significant inconsistency in estimating i) soil restraint force (per unit length) vs. pipe displacement relationships, and ii) the virtual anchor length (L_a) parameter in low strength/low density soils. This aspect requires further investigation so that a preferred computational method with acceptable reliability can be identified for this abandoned pipeline application.

References (Appendix T)

American Lifelines Alliance (ALA). 2001. Guideline for the design of buried steel pipe. July, 2001 (with addenda through February 2005). FEMA and ASCE. 76 pp.

Bentley Systems, Inc., 2013. Piping design and analysis software. AutoPIPE Version 8i. Bentley Systems, Inc., Exton, PA.

Det Norske Veritas (DNV). 2010. Pipeline abandonment scoping study. A report prepared for the National Energy Board (NEB). 85 pp. Available at: <http://www.neb-one.gc.ca/clf-nsi/rthnb/pblcprtctn/pplnbndnmnt/pplnbndnmntscpngstd.pdf> (verified Oct. 6, 2014)

Ferris, G. 2009. Differential frost heave at pipeline-road crossings. p. 68-78. *In* H.D. Mooers and J. Hinzmann (eds.). Cold Regions Engineering 2009: Cold Regions Impacts on Research, Design and Construction. 14th Conference on Cold Regions Engineering, Duluth, MN. Aug. 31 - Sept. 2, 2009.

Intergraph Corporation. 2014. Caesar II - pipe stress analysis software. Available at: <http://www.intergraph.com/products/ppm/caesarii/> (verified Oct. 6, 2014)

Mohareb, M., G.L. Kulak, A. Elwi and D.W. Murray. 2001. Testing and analysis of steel pipe segments. *J. Transportation Engineering* 127(5):408-417.

Peng, L.C. and A. Peng. 2009. Pipe stress engineering. ASME Int'l. Press. First published in 1978. 496 pp.

Swanson, J.M., T. Kunicky and P. Poohkay. 2010. Environmental considerations for pipeline abandonment: a case study from abandonment of a southern Alberta pipeline. Proceedings 8th Intl. Pipeline Conference (IPC2010 - ASME), Calgary, AB. Sept. 27-Oct. 1, 2010. 7 pp.

Tian, D. 2011. Determination of soil restraint properties and calculation of virtual anchor lengths in buried pipelines. KBR. Inc. Gas Speak Colloquium 2011. Sept. 12-14, 2011, Canberra, Australia.